UKD Universitätsklinikum Düsseldorf

hhu Heinrich Heine Universität Düsseldorf

Investigation of bilirubin-induced neurologic dysfunction and cerebral malaria using human iPSC-derived 2D and 3D neuronal models

Inaugural-Dissertation

Zur Erlangung des Doktorgrades
der Mathematisch-Naturwissenschaftlichen Fakultät
der Heinrich-Heine-Universität Düsseldorf

vorgelegt von

Abida Islam Pranty

aus Dhaka, Bangladesch

Düsseldorf, Mai 2024

Aus dem Institut für Stammzellforschung und Regenerative Medizin
der Heinrich-Heine-Universität Düsseldorf

Gedruckt mit der Genehmigung der
Mathematisch-Naturwissenschaftlichen Fakultät der
Heinrich-Heine-Universität Düsseldorf

Berichterstatter:

1. Prof. Dr. James Adjaye

2. Prof. Dr. Matias Zurbriggen

Tag der mündlichen Prüfung: 27/01/2025

Die vorliegende Arbeit ist eine kumulative Dissertation
gemäß § 6 (3) der Promotionsordnung der
Mathematisch-Naturwissenschaftlichen Fakultät
der Heinrich-Heine-Universität Düsseldorf vom 15.08.2018
zur Verleihung des Grades „Doctor rerum naturalium“

Acknowledgements

I have been longing to achieve this very special academic goal of my life of having a doctoral degree for a long time. A lot of people have inexplicable contribution on this journey of mine and thanking them will not be enough. Hence, I would like to express my heartiest gratitude to those people who have guided, helped, and supported me throughout my PhD journey.

Firstly, my humble gratitude towards my supervisor and mentor Prof. Dr. James Adjaye, who did not only give me the chance to pursue a doctoral degree in his lab, but also groomed me as a scientist. He always believed in me and his training and vision about me made me feel confident as a scientist. He trained me doing “scratch to end” of a scientific project and his guidance helped me greatly to develop my scientific skills with creative and critical thinking, planning, troubleshooting, executing, analyzing, and writing. Moreover, he has always been open to discuss, guide, and support my future scientific career. I have experienced a beautiful, honest, and transparent journey with my supervisor, and this credit utterly goes to him for allowing and giving me the access to experience the best possibilities as his PhD student. Additionally, I am very grateful and thankful to Prof. Dr. Matias Zurbriggen for accepting my request to co-supervise me during my doctoral studies.

My heartfelt appreciation towards my colleagues, especially Dr. Nina Graffmann for always attending to my uncountable and never-ending questions and discussions. She also helped me markedly with critical thinking by giving regular feedback on my work, which is a great support any scientist would feel grateful for. I would like to thank my two other colleagues and friends Dr. Lisa Nguyen and Christiane Loerch for tolerating and supporting all my bad and good moments in the lab and personal life during my PhD, and for being so supportive thoroughly. I am very grateful to my entire wonderful team Dr. Claus Kordes, Dr. Wasco Wruck, Martina Bohndorf, Silke Wehrmeyer, Leon-Phillip Szepanowski, Vanessa Cristina Meira de Amorim, Rabea Hokamp, Marina Jovanovic, and Chantelle Thimm. They are a dream team to work with and anybody will flourish having such cooperative, happy, and healthy work environment.

Next, I want to express my deepest gratitude towards my constant and ultimate support system, my family - my parents A.B.M. Nurul Islam and Shanaz Begum, my siblings Nahida Islam, Amir Saiful Islam, Ahmed Rusho, and my husband Andreas Weßelmann. Leaving the home country to pursue my dream was the most difficult sacrifice my family and I had to make.

However, their constant support, love, and understanding towards my wishes and goals made it possible for me to stand where I am today. They held me on my worst days and did not let me go through frustration. Not belonging to the same career line and still being so understanding towards my work is a great gesture which they are consistently showing. I would not have been able to do the PhD the same way if my husband was not by my side. He helped me manage those late working hours, non-stop stress, and weekend work and never complained about my hectic work schedule. He listened to me, cheered me, and always encouraged me to achieve my academic goals with the best possible outcome. All my achievements and success are dedicated to my family. I will also thank my whole family in Germany, especially my mother-in-law Alexandra Weßelmann for always loving me and being supportive. My profound appreciation towards my friend, mentor, and another sister Gladiola Goranci-Buzhala for being my family and a great part of my entire scientific journey so far.

Lastly, I would like to extend my heartfelt thanks towards my best friends Tonny, Warafta, Insha, and Nijhum, who have always supported me and wished for my dreams to come true. They have been my lifelong cheerleaders with their love and faith upon me, and always stayed by my side despite of being 8000 miles apart. There were times when I was questioning myself on how much I can accomplish, but these people and my family never had any doubts on me. Their unconditional love and consistent support have always been my biggest diving force and that will be continued to be so.

My doctoral studies will come to end with this thesis, and I will be forever thankful for this opportunity to grow myself as a person and a scientist. I have learnt a beautiful and different point of view of seeing and solving problems along with being more flexible and acquiring a broader mindset. The science journey will just start taking a new path after completing the PhD and I am very much looking forward to keep improving myself and my research to contribute to the science community and humankind.

Table of Contents

Table of Figures

Abbreviations

Abbreviations	Definition
2D	Two-dimensional
3D	Three-dimensional
AD	Alzheimer's disease
ATM	Ataxia telangiectasia mutated
ATR	Ataxia telangiectasia and Rad3-related protein
AZI2	5-azacytidine induced 2
BBB	Blood-brain barrier
BCL2	B-cell lymphoma 2
BDNF	Brain-derived neurotrophic factor
BF	Free bilirubin
BIND	Bilirubin-induced neurologic dysfunction/ Bilirubin induced neurological damage
BP	Biological process
BIRC	Baculoviral IAP repeat containing
c-MYC/c-Myc	MYC Proto-Oncogene
CB	Conjugated bilirubin
CHEK	Checkpoint kinase
CM	Cerebral malaria
CNS	Crigler-Najjar syndrome
CNS[#]	Central nervous system
DCX	Doublecortin

DJS	Dubin-Johnson syndrome
ER	Endoplasmic reticulum
ESC	Embryonic stem cell
GO	Gene Ontology
GS	Gilbert syndrome
hiPSC	Human induced pluripotent stem cell
HMZ	Hemozoin
ICAM-1	Intercellular adhesion molecule 1
IFL	Inner fibrillary layer
IFN-γ	Interferon-gamma
IL	Interleukin
IL-1ra	IL-1 receptor antagonist
iPSC	Induced pluripotent stem cell
ISVZ	Inner subventricular zone
JAK2	Janus kinase 2
KEGG	Kyoto encyclopedia of genes and genomes
KLF4/Klf4	Kruppel-like transcription factor 4
MAP2	Microtubule-associated protein 2
MAPK	Mitogen-activated protein kinase
MCP-1	Monocyte chemotactic protein-1
MDM2	Mouse double minute 2 homolog
MIF	Macrophage migration inhibitory factor
MSC	Mesenchymal stem cell

MyD88	Myeloid differentiation primary response protein
NADP	Nicotinamide adenine dinucleotide phosphate
NFκB	Nuclear factor kappa B
NLRP3	NLR family pyrin domain-containing 3
NPC	Neural progenitor cell
NSC	Neural stem cell
OCT4/Oct4	Octamer-binding protein 4
OFL	Outer fibrillary layer
oRG	Outer radial glia
OSVZ	Outer subventricular zone
p53	Tumor protein p53
PDGFB	Platelet derived growth factor subunit B
PECAM-1	Platelet and endothelial cell adhesion molecule 1
PI3K	Phosphatidylinositol 3-kinase
PSC	Pluripotent stem cell
RBC	Red blood cell
RS	Rotor syndrome
SOX2/Sox2	SRY-box transcription factor 2
STAT	Signal transducers and activators of transcription
SVZ	Subventricular zone
TNF-α/TNFA	Tumor necrosis factor-α
TNFSF12	TNF superfamily member 12
TRAF	TNF receptor-associated factors

TUJ1	Beta-3-tubulin
UCB	Unconjugated bilirubin
UGT1A1	Uridine diphosphate glucuronosyltransferase family 1 member A1
UGTs	Uridine-diphosphoglucuronate glucuronosyltransferases
VACM-1	Vascular cell adhesion molecule 1
VZ	Ventricular zone
XIAP	X-linked inhibitor of apoptosis protein

Abstract

The neurological disorders named Crigler-Najjar syndrome (CNS) and cerebral malaria (CM) manifest encephalopathy as a clinical phenotype. Bilirubin-induced neurological damage (BIND) is a repercussion of impaired UGT1A1 activity in CNS, while encephalopathy is manifested in CM as a consequence of *Plasmodium falciparum* infection. Due to interspecies divergence and limited recapitulation of the human system, the existing experimental models (rodent models, organotypic cultures, primary and immortalized cell lines) for CNS and CM research need to be improved for further understanding of such brain dysfunctions. In this thesis, the first human induced pluripotent stem cell (hiPSC)-derived 3D brain organoids and 2D neuronal cultures of CNS and CM are employed to further investigate the etiology and mechanisms of free bilirubin (BF)- and hemozoin (HMZ)-induced encephalopathy *in vitro*.

The first study includes a detailed overview of the existing BIND experimental systems, urge for developing a new human-based model, current state of the art of BIND research, advancements, drawbacks, and the prospective applications of stem cell-derived 3D organoids in research, drug testing, regenerative medicine, and other future clinical applications.

Following that, the first available 3D-cortical organoid model of CNS was established in the second study using healthy individual and patient derived iPSCs. BIND was induced in the CNS model with BF exposure and the effects were assessed by analysing gene and protein expression, transcriptome, secretome, KEGG pathways, and cell death. BF treatment instigated inflammatory response in the patient organoids earlier (at 24 h) than in the healthy organoids (at 72 h) and it decreased then at 72 h. Furthermore, the healthy organoids showed apoptotic cell death and DNA damage-repair related gene expression at 24 h post-BF treatment and the activation of inflammation-related pathways at 72 h. Overall, the key findings from this study demonstrated BF-induced neuro-inflammation in this CNS model, while healthy and patient organoids adopted distinct gene regulation, associated Gene Ontologies, and pathways at the analysed time points. These changes resulted in inflammation, DNA damage-repair, or cell death as a response to BF-induced cellular stress.

In the third study, CM was modelled using hiPSC-derived 2D neuronal cultures which were stimulated with the malaria toxin HMZ to investigate particularly HMZ-induced effects in the neurons. Secretome, transcriptome, and metascape based enrichment cluster analyses

confirmed the pathways associated with malaria, inflammatory processes, MAPK cascade, and pro- and anti-inflammatory chemo- and cytokines were activated after HMZ treatment. The findings from this study revealed that HMZ induced inflammatory response and DNA damage in neuronal populations.

Comprehensively, these studies demonstrated a profound inflammatory environment in the central nervous system upon BF and HMZ exposure, while revealing genes, their associated Gene Ontologies and molecular pathways involved in CNS-BIND and CM. In conclusion, these three investigations have exhibited the application of human iPSC-derived 3D brain organoid and 2D neuronal culture models as prospective platforms for understanding the cellular and molecular mechanisms associated with the etiology underlying BIND and CM and furthermore emphasize the potential application for future toxicological studies and drug screening.

Zusammenfassung

Verschiedene neurologische Erkrankungen wie z.B. Crigler-Najjar-Syndrom (CNS) und zerebrale Malaria (cerebral malaria, CM) weisen Enzephalopathie als gemeinsamen klinischen Phänotyp auf. In CNS sind Bilirubin-induzierte neurologische Schäden (BIND) die Folge einer gestörten UGT1A1-Aktivität, während sich die Enzephalopathie bei CM als Folge einer *Plasmodium falciparum*-Infektion manifestiert. Die bestehenden experimentellen Modelle (Nagetiermodelle, organotypische Kulturen, primäre und immortalisierte Zelllinien) sind für die Erforschung von CNS- und CM-assoziierter Enzephalopathie aufgrund der Spezies-Unterschiede und der begrenzten Nachahmung des menschlichen Systems nicht ausreichend, um solche Hirnfunktionsstörungen zu verstehen. In dieser Arbeit werden daher erstmals aus humanen induzierten pluripotenten Stammzellen (hiPSCs) gewonnene 3D-Gehirnorganoide und 2D neuronale Kulturen verwendet, um CNS und CM zu modellieren und um die Ätiologie und die Mechanismen der durch freies Bilirubin (BF) oder durch das Malariatoxin Hämozoin (HMZ) induzierten Enzephalopathie *in vitro* zu untersuchen.

Die erste Studie gibt einen detaillierten Überblick über die bestehenden experimentellen BIND-Systeme, die Notwendigkeit der Entwicklung eines human basierten Modells und den aktuellen Stand der BIND-Forschung. Fortschritte, Nachteile und die voraussichtlichen Anwendungen von aus Stammzellen gewonnenen 3D-Organoiden in der Forschung, der Arzneimittelprüfung, der regenerativen Medizin und anderen zukünftigen klinischen Anwendungen werden diskutiert.

In der zweiten Studie wurde das erste verfügbare 3D-kortikale Organoidmodell für CNS unter Verwendung von iPSCs gesunder Individuen und von Patienten erstellt. BIND wurde im CNS-Modell durch BF-Einwirkung induziert. Die Auswirkungen wurden anhand von Transkriptom- und Sekretomdaten, Gen- und Proteinexpression, KEGG-Signalwegen, und Zelltodassays analysiert. Die BF-Behandlung löste in den Organoiden der Patienten schon nach 24 Stunden eine Entzündungsreaktion aus, die nach 72 Stunden abnahm, während diese Reaktion in den Organoiden der Gesunden erst nach 72 Stunden auftrat. Darüber hinaus wurde in den gesunden Organoiden 24 Stunden nach der BF-Behandlung Apoptose und eine Steigerung der DNA-Reparatur-assoziierten Genexpression nachgewiesen. Insgesamt zeigten die wichtigsten Ergebnisse dieser Studie, dass BF in diesem CNS-Modell Neuroinflammation auslöst, wobei gesunde und kranke Organoide zu den untersuchten Zeitpunkten unterschiedliche

Regulationen der Genexpression, assoziierten Gen-Ontologien und Signalwege aufwiesen. Diese Veränderungen führten zu Entzündungen, zur Reparatur von DNA-Schäden oder zum Zelltod als Reaktion auf BF-induzierten zellulären Stress.

In der dritten Studie wurde CM unter Verwendung von hiPSC-abgeleiteten 2D neuronalen Kulturen modelliert. Diese wurden mit HMZ stimuliert, um dessen Effekte zu untersuchen. Sekretom-, Transkriptom- und Metascape-basierte Enrichment-Cluster-Analysen bestätigten, dass Signalwege die mit Malaria, Entzündungsprozessen, der MAPK-Kaskade, sowie mit pro- und anti-inflammatorischen Chemo- und Zytokinen assoziiert sind nach der HMZ-Behandlung aktiviert wurden. Die Ergebnisse dieser Studie zeigten, dass HMZ eine Entzündungsreaktion und DNA-Schäden in der neuronalen Population auslöste.

Insgesamt zeigten diese drei Studien die Entwicklung eines tiefgreifend entzündlichen Umfelds im zentralen Nervensystem nach BF- und HMZ-Exposition. Sie zeigten Gene, ihre zugehörigen Gene Ontologien und molekulare Wege auf, die an CNS-BIND und CM beteiligt sind. Zusammenfassend lässt sich sagen, dass von menschlichen iPSC-abgeleitete 3D-Gehirnorganoid- und 2D neuronale Kulturmodelle als Plattformen für die Analyse der zellulären und molekularen Mechanismen, die mit der Ätiologie von BIND und CM verbunden sind, geeignet sind und darüber hinaus für die potenzielle Anwendung in toxikologischen Studien und für das Wirkstoff-Screening interessant sind.

1. Introduction

1.1 Human brain and neurological disorders

The human brain is highly complex, and this organ system is divided into three basic units named forebrain, midbrain, and hindbrain. The forebrain is the largest region of the brain containing the entire cerebrum, thalamus, and hypothalamus, while the cerebrum consists of an outer layer (gray matter) and an inner layer (white matter). The outer layer is also known as cortex, which contains four lobes named as: frontal lobe, parietal lobe, temporal lobe, and occipital lobe (Jawabri & Sharma, 2024). During neurogenesis, neuroepithelial cells (neural stem cells) can differentiate into the essential building blocks of the human central nervous system (CNS[#]) called neurons and glia cells. Neuroepithelial cells further form the neuroepithelium. During the cell cycle, the nuclei of these cells migrate upward and downward of the apical-basal axis (apical surface of ventricular zone- basal lamina) giving it a pseudostratified layered outlook (Gotz & Huttner, 2005). Neuroepithelium expansion is required during the mammalian brain development to generate radial glia stem cells, which play a crucial role in human cortex development. The radial glia stem and/or neural progenitor cells (NPCs) can generate neurons and glia cells along with having a scaffolding capacity for cortex architecture and neuron migration (Beattie & Hippenmeyer, 2017). Neurogenesis takes place at the apical surface within the ventricular zone (VZ), which is the proliferative zone for radial glia cells to divide (Figure 1) (Lancaster et al., 2013; Zecevic et al., 2005). Radial glia cells can generate intermediate progenitors and further differentiate into neurons. Intermediate progenitors or neural progenitor cells reside at the VZ-adjacent area known as subventricular zone (SVZ) maintaining the neural stem cell niche, while the neurons migrate to form specific cortical layers of the human cortex (Figure 1) (Lancaster et al., 2013). The progenitor zone organization is more elaborate and precise in human brain compared to rodents or other species. Human brain uniquely includes multiple specific zones in SVZ with an inner fibrillary layer (IFL), an inner SVZ (ISVZ), an outer SVZ (OSVZ), and an outer fibrillary layer (OFL) where neural progenitor cells, intermediate progenitors, and a unique stem cell subset termed outer radial glia (oRG) are located (Fietz et al., 2010; Hansen et al., 2010; Lancaster et al., 2013; Zecevic et al., 2005).

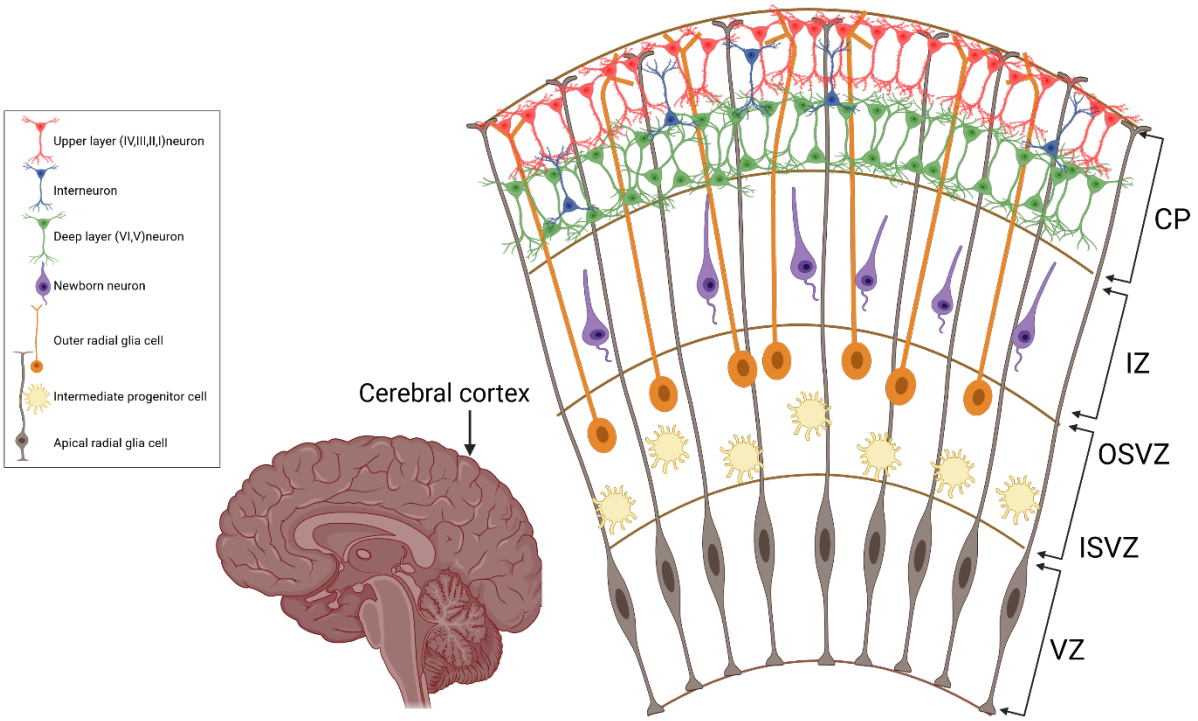

Figure 1. Human cerebral cortex development. Depiction of neurogenesis with generation and amplification of radial glia cells, intermediate stages, and differentiation into neurons during development of the human cerebral cortex. VZ- ventricular zone, ISVZ- inner subventricular zone, OSVZ- outer subventricular zone, IZ- intermediate zone, CP- cortical plate. (Created with BioRender.com)

Since the human brain holds a complex architecture and function, abnormalities in the brain can lead to severe neurological and psychiatric disorders. Due to the complexity and limited access to the human brain, it is challenging to understand neurodevelopment and mechanisms of different brain disorders. Patient-derived biopsy samples and fetal tissue from terminated pregnancies are primary materials which represent the end point of the disease, and access to the earlier stages is limited. Contrarily, potential animal models such as rodent or other mammalian model organisms hold great evolutionary differences with human brain complexity (Sidhaye & Knoblich, 2021). Therefore, pluripotent stem cell (PSC) derived neuronal cultures such as two-dimensional (2D) neurons and three-dimensional (3D) brain organoids provide a potential platform to study human brain development, function, and disease, which closely mimic the human cortex and also reduce ethical controversy.

There are various neurological disorders that affect the structure or function of the brain or cause encephalopathy, a form of brain dysfunction. Different factors such as infection, injury, blood clots, age associated degeneration, cancer, autoimmune dysfunction, and birth defects can cause brain dysfunction (*Encephalopathy*, 2023; Erkkinen & Berkowitz, 2019). In this

thesis, Crigler-Najjar syndrome (CNS) and cerebral malaria (CM) were investigated, where brain encephalopathy is one of the common clinical manifestations observed, but the causal factors of the diseases resulting in encephalopathy are different. CNS is an autosomal recessive disorder caused by an inherited genetic defect in the bilirubin conjugation mechanism, which results in bilirubin-induced neurologic dysfunction (BIND) (Bhandari et al., 2024; Memon et al., 2016). On the other hand, CM is caused by infection with *Plasmodium falciparum* (Albrecht-Schgoer et al., 2022; Dunst et al., 2017).

1.2 Bilirubin-induced neurologic dysfunction (BIND)

1.2.1 Bilirubin

Bilirubin is the final breakdown product of hemoglobin, which is often used to diagnose liver and blood diseases and has a complicated metabolism (Fevery, 2008). Primarily, bilirubin is derived from the erythrocyte hemoglobin breakdown in the reticuloendothelial system, while a smaller portion of bilirubin is originated from breakdown of other heme proteins and failed erythropoiesis in the bone marrow (Figure 2) (London et al., 1950; Memon et al., 2016).

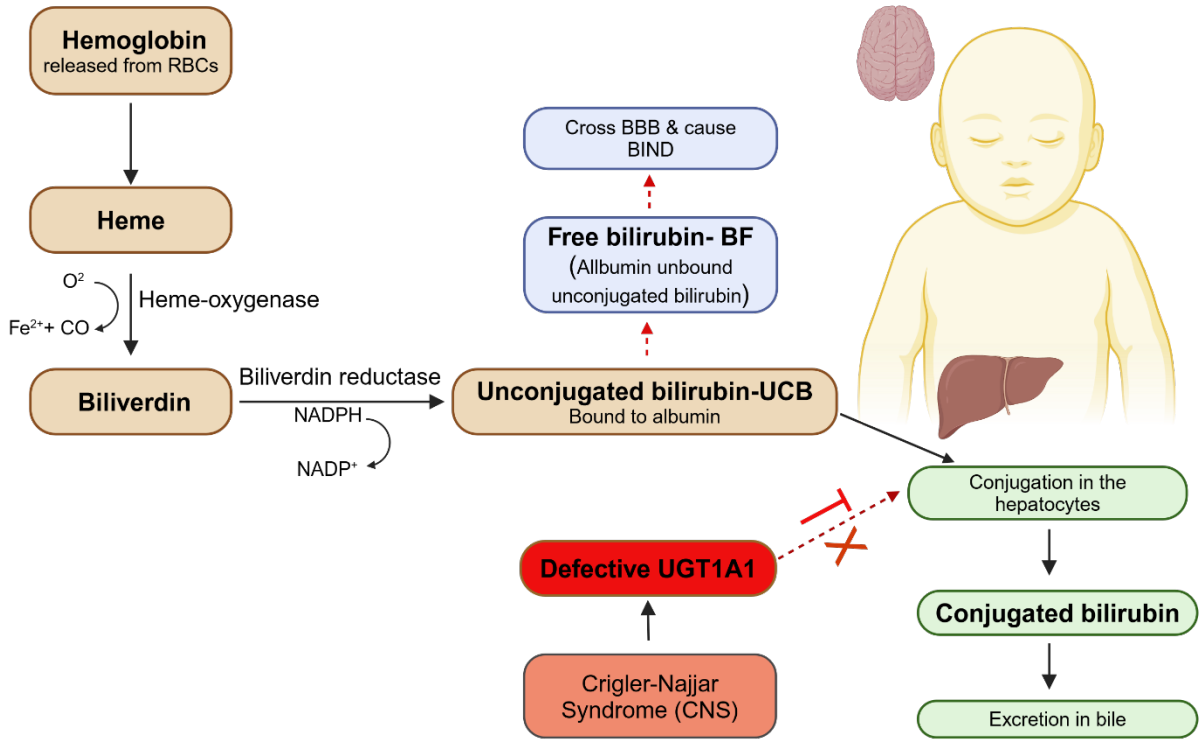

Figure 2. Bilirubin formation and metabolism. Representation of bilirubin formation by heme catabolism. Heme, released from RBCs, is oxidized to biliverdin by heme oxygenase. Eventually, biliverdin is reduced by biliverdin reductase to bilirubin. UCB, which is usually bound to serum albumin, is then transported to the liver, where it is conjugated by UGT1A1 to increase its solubility in water and excretion in bile. Defective UGT1A1 results in partial or incomplete bilirubin conjugation, allowing BF to accumulate in serum, cross the BBB, and cause BIND. RBCs- red blood cells/erythrocytes, CO- carbon monoxide, NADP+- nicotinamide adenine dinucleotide phosphate; (NADPH, the reduced form of NADP+), UGT1A1- uridine diphosphate glucuronyl transferase 1A1, BBB- blood–brain barrier, BIND- bilirubin induced neurologic dysfunction. (Created with BioRender.com)

Bilirubin is generated from heme in several steps. First, heme-oxygenase enzyme catalyses a cleavage at the α carbon bridge of the heme ring and forms biliverdin IXα along with carbon monoxide (Fevery, 2008). Biliverdin IXα is reduced to unconjugated bilirubin (UCB) IXα by the cytosolic enzyme biliverdin reductase (Figure 2). Cleavage at non- α sites is possible to a minor extent, resulting in formation of other isomers such as IXβ and IXγ. These isoforms can be detected in body fluids under special conditions in a very small amount (Aziz et al., 2001; Fevery, 2008; Fevery et al., 1977). Additionally, isomer IIIα and isomer XIIIα may arise from bilirubin-IXα by dipyrrole exchange (Heirwegh, 1976; McDonagh & Assisi, 1972). But these two isomers have not been detected in biological fluids (Fevery et al., 1977; Heirwegh, 1976; Kuenzle, 1970; McDonagh & Assisi, 1972). Consequently, bilirubin conjugation studies in normal mammals are focused largely on bilirubin-IXα isomer (Fevery et al., 1977).

1.2.2 Forms of Bilirubin

Total bilirubin is the sum of three forms of bilirubin, namely direct bilirubin, indirect bilirubin, and delta bilirubin. The direct bilirubin, which is also referred as conjugated bilirubin (CB), and indirect bilirubin referred as unconjugated bilirubin (UCB), are the two main forms of bilirubin (Figure 2). The metabolism of bilirubin takes place predominantly in the liver (Tietze, 2012). Indirect bilirubin or UCB is the immediate breakdown product of hemoglobin, and it is lipophilic in nature (Tietze, 2012). UCB enters the liver where it gets conjugated with glucuronic acid which increases its water-solubility and allows its excretion in the bile (Figure 2) (Singh & Jialal, 2021). Direct bilirubin is post-hepatic CB, which increases bilirubin solubility, simplifies bilirubin excretion process, and reduces its toxicity (Tietze, 2012). It is reported to be increased in biliary disease (such as extrahepatic bile duct obstruction and impaired bile transport) and some liver disease (e.g., hepatitis, cirrhosis, hepatic neoplasm) (Memon et al., 2016; Mohamad Fawzi Mahomoodally, 2022; Tietze, 2012). The non-water soluble UCB attaches to the carrier protein albumin for transport in the blood (Fevery, 2008; Singh & Jialal, 2021). Small amounts of unbound-UCB exist in equilibrium with bound-UCB in the circulation. This albumin unbound, circulating UCB, is known as free bilirubin (BF), which is neurotoxic and associated with acute bilirubin encephalopathy that can progress to more permanent and devastating chronic bilirubin encephalopathy, also known as kernicterus (Figure 2) (Brites, 2012; Memon et al., 2016; Vitek & Ostrow, 2009; Watchko & Tiribelli, 2013). Under normal physiological conditions, hepatocytes uptake UCB rapidly and selectively, then

the bilirubin gets conjugated into bilirubin-glucuronide conjugates becoming water-soluble, and finally is secreted into bile (Memon et al., 2016).

1.2.3 UGT1A1 in bilirubin conjugation

Bilirubin goes through four major steps of hepatic clearance, which includes 1) uptake and storage of UCB by hepatocytes, 2) conjugation of bilirubin, 3) excretion of CB into bile, and 4) reuptake of CB (Memon et al., 2016). Since bilirubin (UCB) is normally bound to serum albumin during circulation, at the first step of bilirubin`s hepatic clearance, it dissociates from albumin before entering hepatocytes (Figure 2). It is not clear whether the initial uptake of free bilirubin is carrier-mediated or by passive diffusion (Sorrentino & Berk, 1988). After entering into hepatocytes, bilirubin attaches to ligandin, which is a cytoplasmic transport protein with much higher bilirubin-affinity than albumin, therefore facilitating bilirubin accumulation and storage inside the hepatocytes (Erlinger et al., 2014; Memon et al., 2016). After binding to ligandin, bilirubin is transported to the smooth endoplasmic reticulum (ER) where the conjugation (second step) takes place. The conjugating enzyme, uridine diphosphate glucuronosyltransferase family 1 member A1 (UGT1A1) is localized at the smooth ER. Uridine-diphosphoglucuronate glucuronosyltransferases (UGTs) are an enzyme family, which is catalysing glucuronidation of various lipophilic endogenous and exogenous compounds to facilitate their excretion in the bile (Kadakol et al., 2000). The *UGT1* gene consists of thirteen variable exons (containing thirteen unique promoters and first exons) and four common exons (exon 2, 3, 4, 5) (Figure 3) (Memon et al., 2016; Ritter et al., 1991; Sticova & Jirsa, 2013). During transcription, each variable first exon with its associated promoter is spliced to the four common exons, which results in 13 possible variants that can be encoded. Among those 13 possible genes, exclusively the one containing variable exon A1 is taking part in bilirubin conjugation (Kadakol et al., 2000; Memon et al., 2016; Sticova & Jirsa, 2013). After leaving the ER, CB (bilirubin glucuronide) is immediately transported into the cytoplasm and efficiently secreted into bile (Figure 2). Interestingly, a substantial fraction of bilirubin glucuronide is re-uptaken into the hepatocytes via enterohepatic circulation (the movement of bile acid molecules from liver to small intestine and back to the liver) (Cai & Chen, 2014; Memon et al., 2016). As UGT1A1 is the only enzyme contributing to bilirubin conjugation in hepatocytes, mutations in this gene lead to partial or complete impairment in bilirubin conjugation and excretion (Figure 2).

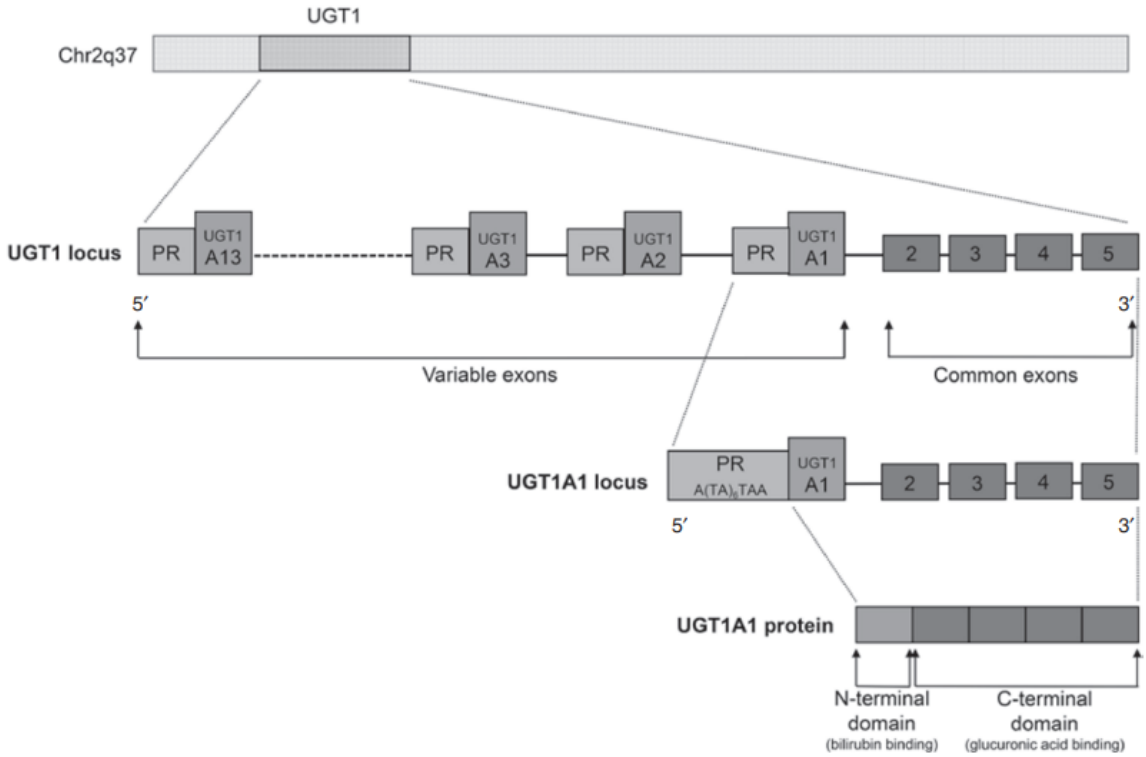

Figure 3. Representation of the UGT1 gene locus and the UGT1A1 protein. Chr- chromosome; PR- promoter regions; UGT- uridine diphosphate glucuronosyltransferase. Illustration reproduced with friendly permission from the publisher. (Memon, N.; Weinberger, B.I.; Hegyi, T.; Aleksunes, L.M. Inherited disorders of bilirubin clearance. Pediatr Res 2016, 79, 378-386, doi:10.1038/pr.2015.247.).

1.2.4 (Unconjugated) Hyperbilirubinemia

Neonatal jaundice is a common clinical problem encountered in the first week of post-natal life, while 8% to 11% of neonates end up developing hyperbilirubinemia (Bhutani et al., 2013; "Practice parameter: management of hyperbilirubinemia in the healthy term newborn. American Academy of Pediatrics. Provisional Committee for Quality Improvement and Subcommittee on Hyperbilirubinemia," 1994). When elevated serum or plasma bilirubin level crosses the laboratory reference range (3 mg/dL) due to deviated bilirubin metabolism, then it is characterized as hyperbilirubinemia or jaundice (Singh & Jialal, 2021). The existing form of bilirubin in serum determines the type of hyperbilirubinemia, which is normally classified as unconjugated (indirect) or conjugated (direct) (Singh & Jialal, 2021). Jaundice in newborns is normally mediated by unconjugated hyperbilirubinemia, which can be a result of some major conditions such as elevated bilirubin production, impaired bilirubin uptake, and reduced bilirubin conjugation (Fargo et al., 2017; Memon et al., 2016; Singh et al., 2021). Among these three major causes, impaired or deficient bilirubin conjugation leads to unconjugated hyperbilirubinemia in neonates, diagnosed as jaundice (Memon et al., 2016). However,

extreme hyperbilirubinemia can lead to kernicterus or bilirubin encephalopathy when the total serum bilirubin level ranges between 25 to 30 mg/dL. Yellow stain of bilirubin deposition in neural cells is characterized as kernicterus (Singh & Jialal, 2021). Hepatic immaturity and inefficient UGT1A1 activity during post-birth days 2 to 5, are the most common causes to develop jaundice in neonates. However, several inherited disorders, such as Gilbert syndrome (GS) or Crigler-Najjar syndromes (CNS) type I and II can also result in impaired bilirubin conjugation, as those disease conditions consist in a partial or complete loss of UGT1A1 enzymatic activity, leading into inefficient bilirubin conjugation with glucuronic acid (Radlovic, 2014; Ramakrishnan et al., 2024; Singh & Jialal, 2021).

1.2.5 Crigler-Najjar syndrome (CNS)

Impaired bilirubin conjugation or transport are manifested by several inherited disorders, leading to impaired bilirubin metabolism and ultimately resulting in various degrees of hyperbilirubinemia of either the predominantly unconjugated or conjugated type. Hereditary hyperbilirubinemias include four different syndromes: GS, CNS, Dubin-Johnson syndrome (DJS), and Rotor syndrome (RS). GS and CNS are characterized by impaired bilirubin conjugation resulting in unconjugated hyperbilirubinemia, while the DJS and RS are characterized by conjugated hyperbilirubinemia (impaired bilirubin transport) (Carey & Balisteri, 2011; Radlovic, 2014; Sticova & Jirsa, 2013; Strassburg, 2010). CNS, DJS and RS are exceptionally rare hereditary conditions, but GS occurs in 2%-10% of the general population (Carey & Balisteri, 2011; Radlovic, 2014; Radu & Atsmon, 2001; Sticova & Jirsa, 2013). Despite being an inherited disorder, GS is associated with presence of 50% UGT enzymatic activity, therefore exhibited as mild unconjugated hyperbilirubinemia or as asymptomatic in young adults (Auclair et al., 1976; Memon et al., 2016). Depending on the degree of UGT1A1 deficiency, the most severe inherited form of unconjugated hyperbilirubinemia- CNS is categorized into two exceptionally rare (only affecting one in a million individuals) autosomal recessive disorder types I and II (Labrune et al., 1994). The clinical expressions and the lethality also vary based on type I and II CNS (Radlovic, 2014). Both types contain defective UGT1A1 activity due to mutations in the coding region of the *UGT1A1* gene, thus resulting in complete or partial inactivation of the UGT1A1 enzyme, and in both cases the bilirubin metabolism in the liver gets disrupted (Figure 2) (Memon et al., 2016). The more severe type, CNS-I, is characterized by total deficiency of the UGT1A1 enzyme, while CNS-II is more subtle due to the partial UGT1A1 deficiency (Canu et al., 2013). Such decrease in or loss of UGT1A1 activity

due to hereditary defects in UGT1A1 hinders bilirubin conjugation, causing free bilirubin to accumulate in serum, cross the BBB, and eventually get deposited in the basal ganglia or cerebellum, thereby resulting in bilirubin-induced neurological dysfunction (BIND) (Figure 2) (Memon et al., 2016; Singh & Jialal, 2021). This can result in acute or chronic bilirubin encephalopathy, known as kernicterus, which includes short- and long-term neurodevelopmental disabilities (Brites, 2012; Canu et al., 2013; Memon et al., 2016). In cases where the kernicterus is developed, almost 70% of newborns die within one week and the other 30% suffer irreversible brain damages (Bortolussi & Muro, 2020). Basal ganglia, cerebellum, brainstem nuclei, peripheral and central auditory pathway, and hippocampus are the brain areas which are reported to be damaged by bilirubin deposition due to CNS-I and II (Amin et al., 2019; Gazzin & Tiribelli, 2011; Singh & Jialal, 2021). The injured brain regions lack an efficient intracellular defence mechanism and this impairment leads to the primary brain damage (Gazzin & Tiribelli, 2011). In this circumstance, the bilirubin accumulation in the brain disrupts the neurodevelopmental process and co-morbid developmental disorders in the CNS[#] occur (Amin et al., 2019). The clinical signs and symptoms vary depending on the affected brain region. For example, movement disorders and athetosis (slow, involuntary, and writing movements of the limbs, tongue, face, neck, and other muscle groups) and abnormal tone were observed when the basal ganglia and cerebellum area were damaged. On the other hand, hearing loss and auditory dysregulation were reported as the symptoms due to the damage in auditory brain nuclei and inferior colliculi (Gazzin & Tiribelli, 2011).

1.2.6 Pathophysiology of BIND

The pathophysiology underlying high bilirubin neurotoxicity is not well understood. Generally, total serum bilirubin consists of both CB and UCB. However, in neonates total serum bilirubin is mostly composed of albumin-bound UCB. UCB is nonpolar and insoluble in water at neutral pH, unless bound to albumin. When the albumin's binding capacity for UCB is exceeded or when the binding sites are competed or occupied with other substances such as sulphonamides, then unbound-UCB or BF has the ability to enter the brain tissue and cause neurotoxicity (Gourley, 1997; Levine et al., 1985; Shapiro, 2003). Albumin plays a protective role toward bilirubin accumulation in the brain, which means low serum albumin increases the risk of developing neurological sequelae even at total serum bilirubin levels under established risk thresholds. In preterm infants the serum albumin is low, which also correlates with the observed neurological sequelae caused by BF in those infants (Gazzin et al., 2023).

Jaundice is the primary visible manifestation of bilirubin accumulation in the tissue and an indication of potential toxicity to the brain (Gazzin et al., 2023). Bilirubin-induced neurotoxicity involves a wide range of pathological mechanisms, which include damage in most brain cell types, for instance neurons, glial cells, and oligodendrocytes (Amin et al., 2019; Brites, 2011). It impairs the development and maturation of neuronal cells along with disrupting crucial brain functions (Brites, 2011). BF induced neurotoxicity selectively damages the CNS[#] and it is more prominent in neurons (rather than the glial cells), which has been also observed in the regional topography of neuronal injury in basal ganglia, cochlear and oculomotors nuclei environment (Ahdab-Barmada, 2000; Ahdab-Barmada & Moossy, 1984; Shapiro, 2003; Watchko, 2006). In CNS, BF`s toxic challenge shows a preference for distinct brain areas including the basal ganglia, cerebellum, brainstem nuclei, peripheral and central auditory pathways, and hippocampus (Ahdab-Barmada & Moossy, 1984; Amin et al., 2019; Gazzin et al., 2023; Volpe, 1981). By accumulating in those areas, BF may disrupt multiple neuro-developmental processes including neurogenesis, myelination, and synaptogenesis during early human brain development (Brites, 2011; Volpe, 1981). Clinical evidences from different studies suggest that there is a possibility of BIND spectrum to overlap with different neurodevelopmental disorders such as cognitive delay, attention deficit hyperactivity disorder, specific learning disorder, autism spectrum disorder, and/or language disorder (Amin et al., 2009; Amin et al., 2019; Brites & Fernandes, 2015; Hyman et al., 1969; Johnson & Bhutani, 2011). To be noted, the correlation of those neurodevelopmental disorders with BIND are not yet completely known or proven. The clinical manifestations of BIND extend in the patients depending on the involved and affected brain region and its corresponding specific integral part of various circuits or loops that influence cognition, learning, behaviour, sensory, and language (Amin et al., 2019). Multiple parameters are also involved in manifesting such developmental disorders of the BIND spectrum in neonates which includes repair capacity and inherent brain plasticity during early brain development; timing, degree and exposure duration of BF; susceptibility of a particular brain region at the time of hyperbilirubinemic condition; and other co-morbidities which could influence the local CNS[#] environment (Amin et al., 2019).

Furthermore, due to neurons being more susceptible towards bilirubin induced neurotoxicity, the molecular pathogenesis of bilirubin-induced neuronal cell injury is demanded to be investigated. Although the molecular pathogenesis is incompletely understood, it is likely that

the presence and accumulation of bilirubin on plasma, mitochondrial, and/ or ER membranes might cause membrane perturbations, which can lead to neuronal excitotoxicity, mitochondrial energy failure, or increased intracellular calcium [Ca2+] concentration (Watchko, 2006). Autopsies of hyperbilirubinemic brains have shown bilirubin localization within neurons and microglia resulting in the loss of neurons, demyelination, and gliosis (Brites, 2012). *In vitro* studies indicated early-staged neurons to be more susceptible to bilirubin-induced neuronal injury, as bilirubin disrupts the dynamics of the neuronal network by inducing oxidative stress in cortical neurons (Vaz et al., 2011). Studies have also reported impaired neuronal growth and alterations in neurogenesis, neuritogenesis, and axonal cytoskeleton dynamics induced by BF which might be relevant to long-term neurodevelopmental disabilities and synaptic plasticity associated abnormalities (Brites, 2012). Based on *in vivo*, *in vitro*, organotypic brain culture, and cell culture data, the involved mechanism underlying BF induced neurotoxicity include oxidative stress, antioxidant response, necrosis, apoptosis, bilirubin oxidase/P450, DNA damage, ER stress, inflammation, autophagy, glutamate release, and signalling pathways (Gazzin et al., 2023).

Even though there are animal models (Gunn rat, transgenic mice) and cellular models, such as primary neuronal cultures and co-cultures of different neuronal cells for investigating BIND, there are still some open questions regarding the mechanisms underlying BIND, which include:

1. Which pathophysiological mechanism is underlying BIND and how it can be modulated?

2. What are the molecular reasons for the higher susceptibility of neurons towards BF compared to other neuronal cell types such as astrocytes?

3. Which timing, degree, and exposure duration of BF in the CNS[#] correlates to the pathological symptoms?

4. Which stages of hyperbilirubinemia or impaired bilirubin conjugation associated conditions are exerting which specific manifestation of BIND spectrum?

Such open questions regarding the BIND mechanism and pathology in the human brain emphasize the importance of establishing a human cell-derived model system to provide more insights into the molecular basis of the disease.

1.2.7 Treatment

Depending on the amount of serum or plasma bilirubin levels and extent of the disease condition, the treatment and therapies for various bilirubin-associated conditions are applied. For example, mild neonatal jaundice resolves by itself within a few weeks, therefore no treatment is necessary at this condition. Phototherapy is applied for moderate to severe jaundice, in which the infant's skin is exposed to light in the blue-green spectrum (460-490 nm) (Kato et al., 2020). The phototherapy is effective as the UV exposure/radiation irreversibly photo-alters bilirubin into lumirubin. Lumirubin is a less dangerous and more water-soluble isomer of bilirubin, which can increase the elimination of this toxic substance in bile, urine, and stool, resulting in reduction of bilirubin-induced toxicity (Ennever et al., 1987; Hansen et al., 2020; Singh & Jialal, 2021). In case of severe neonatal jaundice, transfusion exchange might also be considered as an option, especially when the other treatments do not function properly (Flaherman et al., 2012). Moving from jaundice to GS, the management and care crucially depend on the diagnosis and prognosis of the GS. Regular liver function tests, elevated bilirubin levels, and genetic testing are required to confirm the GS and its further prognosis (Ramakrishnan et al., 2024). Phenobarbital has been shown to normalize bilirubin levels in GS patients by enhancing bilirubin clearance with increased bilirubin conjugation through activation of the phenobarbital module of the UGT1A1 promoter sequence. CNS-II patients also respond quite well to the phenobarbital, whereas CNS-I patients do not. Since CNS-II is milder, phenobarbital can effectively reduce plasma bilirubin levels in CNS-II patients by 25% (Singh & Jialal, 2021). To be noted, the goal for the patients is to sustain total serum bilirubin level below 15 mg/dL, therefore routine monitoring is required. In general, CNS patients (especially CNS-I) rely on 10-12 h of intensive daily phototherapy treatment, to reduce the plasma bilirubin level and prevent further progression to bilirubin encephalopathy (Singh & Jialal, 2021). The UV radiation used during phototherapy can evoke various pathological changes including inflammatory skin diseases. Several mechanisms such as induction of apoptosis, modification of the cytokine milieu, and immunosuppression can be involved during this process. The efficacy of phototherapy is dose and light intensity dependant; however, it is influenced by factors such as age, thickness of the skin, and exposed body surface area. Phototherapy is being used safely and successfully for numerous dermatological disorders over 40 years, nevertheless, this therapy includes short- and long-term complications (Newman et al., 2018; Singh & Jialal, 2021; Torres et al., 2021). Conversely,

skin thickening decreases therapeutic efficiency, even though it is obtained from the phototherapy itself. Furthermore, aggressive phototherapy may cause potential toxicity to the extremely low-birth-weight newborns (Morris et al., 2008). Intravenous immune globulin therapy is another approach to control hyperbilirubinemia and prevent kernicterus (Watchko & Tiribelli, 2013). Phenobarbital, calcium (infusions), ursodeoxycholic acid, metalloporphyrins, chlorpromazine, and cholestyramine are the commonly prescribed medications for the treatment of CNS-I patients (Singh & Jialal, 2021). Orally ingested calcium phosphate can serve as a valuable ancillary to phototherapy in CNS-I patients by interrupting the enterohepatic circulation of bilirubin (Van Der Veere et al., 1996). Plasma bilirubin levels can be reduced with the treatment of heme oxygenase inhibitors (tin-mesoporphyrin, metallophyrins). However, the long-term usage of these compounds leads to severe side effects, which limits prescribing these medications for longer periods (Evans, 2007). Ursodeoxycholic acid can also reduce the total serum bilirubin by increasing the bile-flow and eliminating the bile into the gastrointestinal tract (Honar et al., 2016). The Tetracycline antibiotic- Minocycline has also been reported to show protective affects against bilirubin induced neurotoxicity in Gunn rats. Plasmapheresis is another employed therapeutic intervention, where the unwanted toxins or plasma components are removed from the blood, and then plasma gets replaced before transfusing blood back into the patient (Strauss et al., 2020). Finally, in CNS-I patients, liver transplantation remains as the effective and definite form of treatment for this life-threatening disease. Moreover, this transplantation should be performed before the neurologic damage onset (Labrune & Odievre, 1992; Memon et al., 2016; Schauer et al., 2003; Sticova & Jirsa, 2013). Transplantation of hepatocytes could also be an alternative to liver transplantation, as these cells are the hub of the bilirubin conjugation mechanism (Ambrosino et al., 2005). Another CNS treatment approach which is being investigated is gene therapy. In this approach replacement of the defective UGT1A1 with a normal one or genetic modification with partial replacement of the UGT1A1 is considered, as this gene is responsible for glucuronosyltransferase activity in the patients (Birraux et al., 2009; Singh & Jialal, 2021).

1.2.8 Existing BIND and CNS disease models

Over the span of time researchers have developed different *in vitro*, *ex vivo,* and *in vivo* model systems to closely recapitulate the main characteristics of BIND, neonatal hyperbilirubinemia, and CNS, ranging from cell cultures to engineered mouse models (Figure 4). In those available models BF commonly showed the ability to target and disrupt critical steps in brain

development including cell division, differentiation, migration, synaptogenesis, and myelination (Bortolussi & Muro, 2020; Gazzin et al., 2023).

To trace the bilirubin-induced disease progression and to understand the key mechanism in the CNS, it is essential to generate and study model systems that closely recapitulate the main characteristics of BIND. In the following subsections (1.2.8.1, 1.2.8.2, and 1.2.8.3), the existing models and the associated data will be mentioned which have been studied so far to understand the pathophysiology of CNS and BIND (Figure 4).

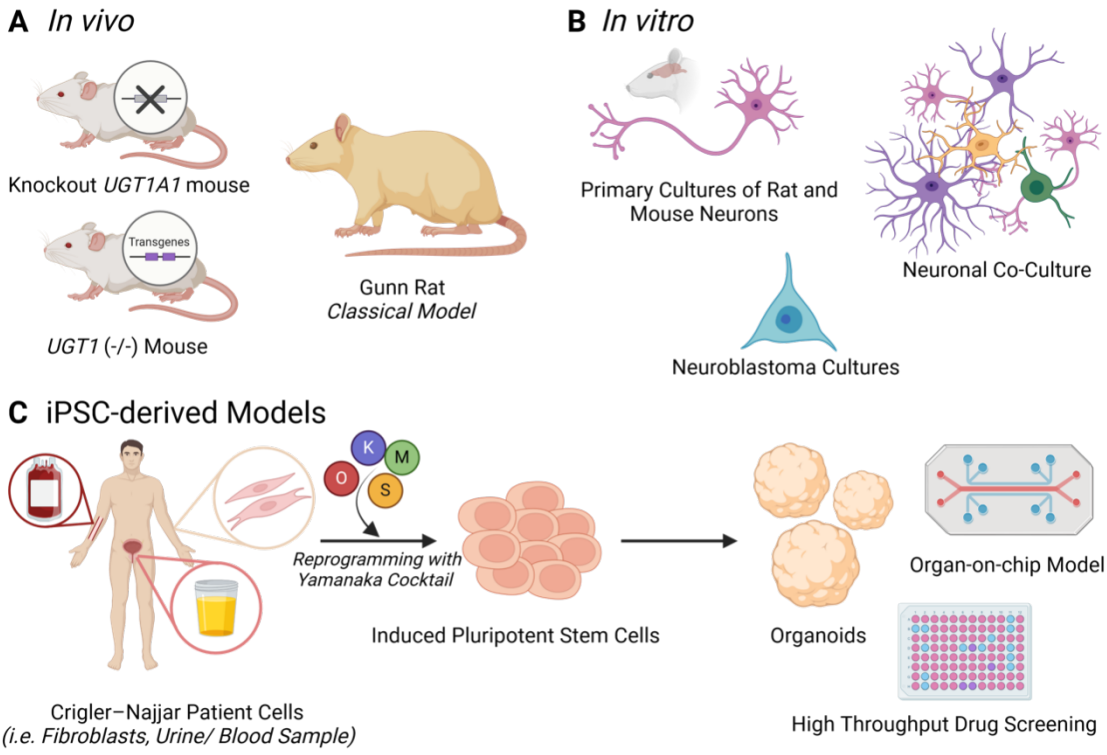

Figure 4. Existing and emerging CNS and BIND models. (A) Existing in vivo models: classical Gunn rat model, knockout and transgenic mouse lines; (B) in vitro models: primary cultures, mixed neuronal co-cultures, and neuroblastoma cultures. (C) Emerging iPSC-derived cultures such as organoid cultures, organ-on-chip to model CNS and its application for high throughput drug screenings specific to the patient's needs. Image obtained from Pranty, A.I., Shumka, S. and Adjaye, J., 2022. Bilirubin-induced neurological damage: current and emerging iPSC-derived brain organoid models. Cells, 11(17), p.2647, as licensed under an open access Creative Common Attribution 4.0 license (https://creativecommons.org/licenses/by/4.0/).

1.2.8.1 Animal Models

In vitro models cannot completely recapitulate the phenotypes of the diseases which are manifested in patients, therefore animal models often work as a bridge to fill those gaps and help revealing the *in vivo* mechanism of the disease. The *in vivo* models can be categorized in

two groups: (1) genetic *in vivo* models of severe hyperbilirubinemia and (2) pharmacologically induced *in vivo* models. The first group can be further sub-categorized into naturally occurring or induced mutations (Bortolussi & Muro, 2020).

Gunn rat is the broadly used model to study hyperbilirubinemia and impaired bilirubin conjugation associated diseases such as CNS. A one-base deletion of exon 4 was spontaneously developed in the UGT1 locus of this strain of Wister rats *(CRIGLER-NAJJAR SYNDROME*; Yueh et al., 2017). This inherent mutation resulted an in-frame premature stop codon, which then translated into a truncated protein, ultimately causing deficiency of all UGT1A1 iso-enzymes members. Having the complete absence of UGT1A1 enzymatic activity in hyperbilirubinemic condition, this Gunn rat model was used as the first animal model to mimic CNS-I and investigate bilirubin metabolism and toxicity *in vivo* (Bortolussi & Muro, 2020; Gunn, 1944). Untreated homozygous Gunn rats show cerebellum-associated abnormalities and hearing impairments similar to the respective human CNS-I phenotype, but still reach the adulthood and contain their fertility without treatment, unlike the human patients. As these untreated Gunn rats recapitulate only a mild phenotype of human CNS-I, different pharmacological compounds such as hemolytic drugs or albumin-bilirubin displacers (i.e., phenylhydrazine, sulfadimethoxine) have been applied to them to induce hyperbilirubinemia with acute CNS$^{\#}$ dysfunction (Bortolussi & Muro, 2020).

Inducing mutations in the animal genome with the help of genetic tools and technologies has made it possible to generate constitutive and conditional knockout, knock-in, and transgenic strains of mice. These genetic manipulations in the mouse model have revealed more key aspects of the diseases (Bortolussi & Muro, 2020; Rice & Shapiro, 2008; Schiavon et al., 2018). For example, UGT1A1-null mice show more severe neurological damages than the Gunn rats and terminate in premature death (Bortolussi et al., 2014; Bortolussi et al., 2012; Nguyen et al., 2008). The reasons behind the phenotypic differences between these rat and mouse models are not clear, while the survival ability and susceptibility towards bilirubin might be specific depending on the strain and species (Bortolussi et al., 2014; Bortolussi & Muro, 2020). The most straightforward and successfully applicable procedure to increase the bilirubin level in the animal models without any genetic modification, is to directly administer UCB (Bortolussi & Muro, 2020; Huang et al., 2017; Song et al., 2014). Even though such bilirubin administration through injections is easily performable in the labs in a dose and time dependent manner to investigate BIND, the induced phenotypes are either transient or

partially mimicking the disease in the human. Animal models have contributed undeniably to understand the mechanisms underlying severe neonatal hyperbilirubinemia. Nevertheless, mechanism and pathology in the human brain still stay unique and is not always comparable with the animal models, which emphasizes the need for a human cell-derived model system to provide more insights into the molecular basis of the disease.

1.2.8.2 In vitro models

In vitro experiment and modelling is considered as an essential tool in basic biology and also in clinical applications. Two major groups of *in vitro* cell cultures have extensively been used in BIND studies, one of which is immortalized cell lines, and the other is primary cultures. Human neuroblastoma cell lines, HeLa cells, Hepa 1c1c7 mouse hepatoma cells, and human U87 astrocytoma cells are some commonly used immortalized cells lines to test bilirubin toxicity (Bortolussi & Muro, 2020; Calligaris et al., 2009; Qaisiya et al., 2017; Rawat et al., 2018; Seubert et al., 2002). On the other hand, primary cultures reflect the original *in vivo* situation better than immortalized cells and also provide key information regarding the disease condition, even though they lack the whole tissue complexity. For instance, bilirubin treatment induced disrupted axons and dendritic processes for neurons and increased pro-inflammatory cytokine release from microglia and astrocytes (Brites, 2012; Fernandes et al., 2009; Fernandes et al., 2006; Fernandes et al., 2004). Additionally, rat and mouse-isolated primary neurons of different regions, astrocytes, microglia, oligodendrocytes, endothelia cells, and embryonic fibroblast cultures have contributed in investigating bilirubin induced toxicity (Bortolussi & Muro, 2020; Brites, 2012; Calligaris et al., 2006). Hippocampal neurons responded with impaired neuronal arborization, increased cell death, mitochondrial dysfunction, and oxidation, when exposed to bilirubin. These neurons also overexpressed active transporters, detoxification pathways, pro survival mechanism, and inflammatory markers as protective mechanisms, which makes this cell type one of the most common and potent cellular models to study bilirubin-induced responses in CNS[#] (Bortolussi & Muro, 2020; Brites, 2012). Moreover, newly differentiated neuronal cell types or younger neuronal cell types that are less differentiated display higher sensitivity compared to mature differentiated neurons (Rodrigues et al., 2002). The observed morphological, biochemical/metabolic, and molecular responses reflect the *in vivo* situation upon bilirubin exposure (Bortolussi & Muro, 2020; Brito et al., 2013). Another important cell type of the CNS[#] named oligodendrocytes, responsible for myelinating the axons of the neurons, also showed susceptibility towards

bilirubin. Decreased myelin basic protein production was observed after bilirubin insult, which led to impaired myelin sheet formation and neuronal axonal function (Brites & Fernandes, 2015). Bilirubin affects not only the neurons and oligodendrocytes, but also astrocytes and microglia. These glial cells released pro-inflammatory mediators tumor necrosis factor-α (TNF- α), interleukin-1β (IL-1β), IL-6, nuclear factor kappa B (NFκB), and activated mitogen-activated protein kinase (MAPK) pathways (p38, JNK1/2, and ERK1/2) upon bilirubin treatment (Bortolussi & Muro, 2020; Brites, 2012).

Co-culture with heterotypic neural population also provides a good platform to study bilirubin induced responses between different neural cell types. For example, astrocytes showed a protective response towards neurons, while bilirubin exposure was detrimental on the neurons (Bortolussi & Muro, 2020; Falcao et al., 2013). Even though these heterotypic cultures explore the crosstalk between different neural cell types, they also might change the cell-cell interactions along with alterations in morphological and physiological properties. Additionally, potential contamination, different life span of cells, different culture medium, and conditions are also some of the disadvantages of this system.

1.2.8.3 Ex vivo models

When a model contains a part or entire tissue isolated from an organism and is cultured *in vitro* under optimal conditions, which are supposed to mimic partially or transiently the physiological condition, then it is called an *ex vivo* model (Bortolussi & Muro, 2020). Culturing brain slices from a specific region or from the entire brain has been used to study bilirubin induced neurotoxicity. These *ex vivo* cultures transiently preserve *in vivo* structure, cellular toxicity, organ heterogeneity, connection, and architecture of the brain. Such organotypic culture studies enabled demonstrating impaired synaptic plasticity and microglia involvement in the BF induced neurotoxicity by using hippocampal slices (Chang et al., 2009). It was also possible to map the regional damaged area by bilirubin and demonstrate multifactorial toxic effects of bilirubin using these cultures (Dal Ben et al., 2017). For instance, hippocampal slices showed more bilirubin susceptibility compared to the inferior and superior colliculus or cerebellum (Dani et al., 2019). Nevertheless, the *ex vivo* data can be very different than *in vivo* or *in vitro* models derived data based on the different experimental conditions, developmental stages of the donor brains, culture duration prior to use, applied bilirubin concentrations, bilirubin- albumin ratio, or BF calculations in the culturing media (Bortolussi & Muro, 2020; Dani et al., 2019). Based on these information drug's efficacy can be evaluated, which have a

potential applicability for the protection of the newborn brains from bilirubin induced toxicity (Dal Ben et al., 2017).

1.3 Cerebral Malaria (CM)

CM is an acute neurological complication of severe malaria infection caused by *Plasmodium falciparum*. The life-cycle of *Plasmodium* species exhibits three stages named: gametocytes, sporozoites, and merozoites. Gametocytes develop into sporozoites within a mosquito ("Plasmodium," 2024). Malaria infection initiates with the bite of an infected female Anopheles mosquito into the skin. The mosquito inoculates 5 to 50 sporozoites to the bloodstream, which further migrate to the liver (Figure 5) (Amino et al., 2005; Renia et al., 2012). Sporozoites multiply inside liver parenchymal cells and generate thousands of liver merozoites. The erythrocytic stage of the infection starts when the erythrocytes (RBCs) are infected by the release of merozoites into the blood stream. The invading merozoites mature and divide rapidly into a multinucleated schizont. Rapid multiplication disrupts the erythrocytes and schizonts, while rupture of each schizont releases 4 to 16 merozoites into the bloodstream, resulting in new infected erythrocytes. A subpopulation of merozoites may develop into gametocytes, which can be taken up by a feeding mosquito, beginning the life cycle over again (Renia et al., 2012). The erythrocytic phase of the infection is responsible for the disease pathology (Figure 5). High fever, muscle aches, and chills are some of the common malaria symptoms which are usually developed 10-15 days after being bitten (Renia et al., 2012). Although malaria infection is curable in many cases, severe malaria can lead to a wide array of pathologies, such as metabolic alterations, renal failure, liver and lung dysfunctions, anemia, and CM (Renia et al., 2012; "Severe falciparum malaria. World Health Organization, Communicable Diseases Cluster," 2000).

CM is defined as a life-threatening cerebrovascular encephalopathy which is commonly characterized by unarousable (unable to localize a painful stimulus) coma (Hadjilaou et al., 2023; "Severe malaria," 2014). Clinical manifestations of CM include coma with seizure onset, brain swelling, brainstem alterations, intracranial hypertension, retinopathy, abnormalities in posture, pupil size and reaction, ocular movements, or abnormal respiratory patterns (Idro et al., 2010; Renia et al., 2012).

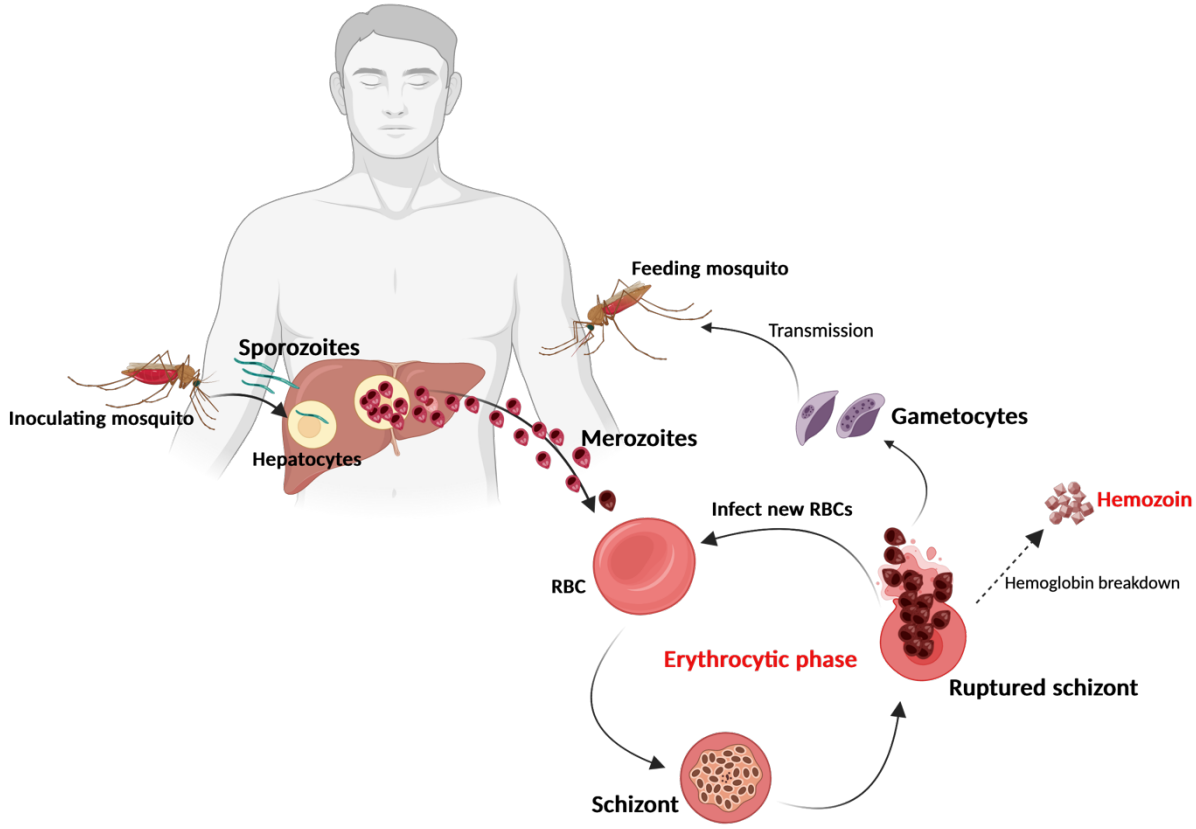

Figure 5. Pathophysiology of Cerebral malaria. Illustration depicting different stages of malaria parasite`s life cycle and infection. Infected Anopheles mosquito bite into the skin begins the infection with the inoculation of sporozoites which migrate to hepatocytes, where sporozoites multiply and generate merozoites. Release of mature merozoites into blood stream infects the RBCs and initiates the disease causing erythrocytic phase. Rapid division and maturation of merozoites forms multinucleated schizont, which gradually gets ruptured resulting in infecting new RBCs, hemozoin formation, and also developing into gametocytes which can be transmitted into new feeding mosquito. RBCs- red blood cells/ erythrocytes (Created with BioRender.com)

Besides causing death, CM is considered as a cause of resulting neurological dysfunction in the patients. The mortality rate in cerebral malaria is high (20% of the infected patients), while surviving patients may sustain cerebral dysfunction along with long-term neuro-cognitive impairments such as ataxia, partial blindness, central hypotonia, epilepsy, motor function, cognition, and behavioural impairments (Carter et al., 2005; Hadjilaou et al., 2023; Idro et al., 2010; John et al., 2008; Newton & Krishna, 1998; van Hensbroek et al., 1997). According to the reports, 1% of *P. falciparum* infected children develop cerebral malaria. Despite of developing at any age, children below 5 years old are the highest risk group for CM (Hadjilaou et al., 2023).

1.3.1 Hemozoin

Of all the human infecting *Plasmodium*, *P. falciparum* is the most virulent and severe anemia or CM development are it`s characteristic pathological manifestations (Olivier et al., 2014). In the infected erythrocytes, the hemoglobin is digested by the parasite as their source of nutrition and energy. As a result, heme is produced as a byproduct (Francis et al., 1997; Olivier et al., 2014; Pandey & Tekwani, 1996). Since heme is highly toxic for the parasite and cannot be excreted by the parasite, it aggregates heme molecules into an insoluble crystal form called hemozoin (HMZ). HMZ and other hemoglobin byproducts are released into the plasma from the infected erythrocytes which promote the release of merozoites resulting in triggering osmotic fragility and destruction of erythrocytes at an accelerated rate (Figure 5) (Mehra et al., 2021; Moore et al., 2006).

1.3.2 Pathophysiology of CM

The pathophysiology of CM in the CNS[#] of humans is not clearly known due to the difficulty in obtaining brain samples. Mouse models and brain autopsy tissue have been used as the source of the investigation of CM. Post-mortem biopsy tissues from patient`s brain showed presence of malaria pigment HMZ in the cerebral cortex, while cerebral edema was observed in the white matter of the brain. Immunohistochemistry staining showed damage in the endothelium and in BBB along with thickened capillaries (Gillrie & Ho, 2017; Mishra & Newton, 2009; Postels & Birbeck, 2013; Renia et al., 2012; Valentim, 2018). CM pathology is a result of aggravated cytoadherence complex formation of RBCs with the endothelial lining of the BBB and results in a disrupted BBB, which is manifested with cell apoptosis, vascular dysfunction, and tissue damage. The impact and role of HMZ during this phenomenon remains unclear (Mehra et al., 2021). Rupture of the BBB may lead to hemorrhages resulting in neurological alterations (Renia et al., 2012). The pathogenesis of CM can be affected or regulated based on the response of the parasite and host. Some key events which define the pathogenesis of CM include leakage in BBB, endothelial cell activation and apoptosis, nitric oxide bioavailability, platelet activation and apoptosis, oxidative stress, and neuro-inflammation (Hora et al., 2016; Medana et al., 2002; Medana & Turner, 2006; Miranda et al., 2013; Percario et al., 2012; van der Heyde et al., 2006; van Veelen et al., 1978). These disrupted or disturbed events may cause neuronal cell death, axonal injury, interrupted neurogenesis, and impaired neuroplasticity, which may lead to cognitive disorders along with short- and long-term neurological sequelae (Medana et al., 2002).

1.3.3 Treatment for CM

CM requires urgent intervention within the intensive care unit, regular monitoring, surveillance, and supporting treatment (Misra et al., 2011; Ndreu et al., 2016; Valentim, 2018; Wah et al., 2016). Antimalarial compounds such as artemisinin derivatives, artesunate, and quinine are preferred to be administered intravenously to treat CM, where artesunate performs better to reduce mortality (34.7%) compared to quinine. Quinine acts only in the last stages of the parasitic erythrocyte cycle, while artesunate has activity in all stages. Artesunate reduces convulsive episodes, coma, and hypoglycemia, while quinine induces hypoglycemia and rapid administration leads to hypotension (Mishra & Newton, 2009; Misra et al., 2011). To shorten the treatment duration and prevent resistance, artesunate and quinines are prescribed in combination (Mishra & Newton, 2009). Additionally, the neurological complications due to malaria can be affiliated with other organ system`s dysfunctions such as: severe anemia, hypoglycemia, imbalanced electrolytes, convulsions, acute renal failure, liver failure, and coagulation disorders, which also should be treated accordingly (Mishra & Newton, 2009). For instance, exchange transfusion is recommended for severe anemia. Corticosteroids, deferoxamine, erythropoietin, and N-acetylcysteine are reported to be used as adjuvant treatment without showing efficacy (Mishra & Newton, 2009; Misra et al., 2011; Valentim, 2018).

1.3.4 Existing models for CM

Unavailability of brain tissue created a hindrance in obtaining pathophysiological data in human CNS[#] and further assessment of CM pathogenesis. Post-mortem brain tissue provides only the late stages of the disease and the consequence of the infection, rather than the ongoing disease progression while the patient is alive. Therefore, despite markedly different histopathological features, CM studies are conducted predominantly in murine models (Adams & Jensen, 2022; Idro et al., 2010; White et al., 2010). CB57BL/6 mice, which are infected with *P.berghei* ANKA, is one of the widely used murine models of CM. The inflammation is characterized with diffuse or no intracerebral sequestration of parasitized erythrocytes, while in humans there is an intracerebral sequestration observed (White et al., 2010). Studies in non-human primates such as *P. falciparum infection in Aotus* and *Saimiri* monkeys and chimpanzees, and *P. coatneyi* and *P. fragile* infections in macaque monkeys were executed, nevertheless the cerebral sequestration was not prominently observed in those models compared to human (Adams & Jensen, 2022; Fujioka et al., 1994; Kawai et al., 1993;

Tongren et al., 2000). Nowadays, modelling CM ranges from single-cell monolayer cultures to multicellular BBB organoids and hiPSC-derived cerebral organoids (Harbuzariu et al., 2019; Pais & Penha-Goncalves, 2023; Urich et al., 2013; Weksler et al., 2005). Along with isolated brain vessel culture, different primary and immortalized endothelial and astrocyte cell lines are commercially available for CM studies, such as the immortalized human cerebral microvascular endothelial cell lines- hCMEC/D3, HBEC-5i, the astrocyte cell line- M059K, co-culture of human astrocytes and neurons, and so on (Adams & Jensen, 2022; Dorovini-Zis et al., 1991; Eugenin et al., 2019; Pais & Penha-Goncalves, 2023; Weksler et al., 2005). iPSC-derived cerebral organoids have also been used to test the heme-induced cortical brain injury associated with CM (Harbuzariu et al., 2019). Due to a huge difference between human CM with CM in other animals, modelling CM requires a suitable human recapitulating system to study the CM pathogenesis in human and also to investigate the toxicology and therapeutics.

1.4 Stem cells in CNS-BIND and CM modelling

The crucial step of investigating the mechanism and molecular events of any specific neurological disorder is establishing a model that can reflect and recapitulate the condition as in the disease. The most commonly used BIND and CM models are mouse models or post-mortem tissue. The mouse models exhibit a very different pathogenesis than humans, while the post-mortem tissues reveal only the final stage phenotype of the disease (Adams & Jensen, 2022; Idro et al., 2010; Marchetto et al., 2011; McKinney, 2017; White et al., 2010). Stem cells create a scope for investigating neurological disease mechanisms and involved developmental disorders, which are more closely relevant to human. Stem cells are defined as cells that can self-renew and have the potency to differentiate into mature functional cells (Tian et al., 2023). These cells are remarkable with their ability to develop into many different cell types in the body during embryonic, fetal, and adult stages of life. Pluripotent stem cells (PSCs) contain germline competency and function assessments, thus holding great promises to be used in understanding human biology and for future toxicological studies, regenerative therapies, drug screening, and personalized medicine. Induced PSC research has increasingly revealed the multifaceted potential of these cells for studying disease progression from early progenitor state to mature state, which enables modelling of a wide range of neurological diseases *in vitro* (Figure 6) (Drews et al., 2012; Imaizumi & Okano, 2014; Logan et al., 2019; Marchetto et al., 2011; McKinney, 2017).

1.4.1 Definition and classification of stem cells

Depending on the source and type of the stem cells, the properties or the stemness of the cells may vary. Stem cells can be classified based on differentiation potential or based on the origin of the cells. Based on the differentiation potency, stem cells can be categorized into five groups, named as totipotent or omnipotent, pluripotent, multipotent, oligopotent, and unipotent (Kolios & Moodley, 2013; Tsang & Sharma, 2018).

Totipotent or omnipotent cells are the most undifferentiated cells and harbour the greatest developmental potency. An oocyte after fertilization and the early stage blastomeres, which are the cells of first two divisions, are totipotent cells (Kolios & Moodley, 2013; Xu et al., 2022). These cells have the potential to differentiate into both embryonic and extraembryonic tissue components. In blastocyst stage totipotent cells differentiate and generate epiblast, trophoectoderm, and primitive endoderm (Frankenberg et al., 2016; Rossant & Tam, 2009). The stem cells derived from epiblast, trophectoderm, and primitive endoderm are respectively, pluripotent stem cells, trophoblast stem cells, and extraembryonic endoderm cells. These blastocyst-derived stem cells have the lineage-restricted differentiation and development capacity, as there is the embryonic and extraembryonic lineage boundaries (Xu et al., 2022). Therefore, totipotent cells are superior in terms of differentiation potency than those cells and have great research interest, as totipotent cells can generate both embryonic (embryo) and extraembryonic tissue (placenta) components, which means an ability to create an entire individual *in vivo*.

PSCs are the cells derived from the epiblast or inner cell mass of the blastocyst, thus being able to proliferate indefinitely and differentiate into all three germ layers- ectoderm, endoderm, and mesoderm. Gradually, further distinct differentiation from these three lineages forms all tissues and develops the organs. PSCs can be divided into two groups depending on the source (from where or how) they are derived, and both of those cell types share similar characteristics. One subtype is called embryonic stem cells (ESCs), which are derived from the inner cell mass of the blastocyst, while another type is iPSCs, which are reprogrammed from somatic cells (explained in paragraph 1.4.2) (Evans & Kaufman, 1981; Kolios & Moodley, 2013; Takahashi & Yamanaka, 2006; Thomson et al., 1998). PSCs have created a great platform for research in human developmental biology, drug discovery, and transplantation medicine, and also for cell therapies for various diseases and injuries. Despite the potential applications of human PSCs, use of ESCs remains ethically controversial due to

their derivation from early embryos, which can be substituted by human iPSCs (de Wert & Mummery, 2003).

Multipotent cells are germ layer specific stem cells or the cells which can differentiate into several cell types of a single germ layer to form different tissue and organs of that specific germ layer, such as neural stem cells (NSCs) and mesenchymal stem cells (MSCs) (Ratajczak et al., 2012). These cells can differentiate further into multiple cell lineages of the corresponding germ layer. For instance, NSCs can differentiate into neurons, astrocytes, and oligodendrocytes (Figure 6) (Canals et al., 2021; "Erratum," 2015; Wang et al., 2018). MSCs can differentiate into osteoblasts, chondrocytes, myoblasts, adipocytes, and fibroblasts (Hwang et al., 2009; Sierra-Sanchez et al., 2018). Oligopotent stem cells are the type of stem cell which can self-renew and differentiate into two or more cell lineages within a specific tissue. For instance, hematopoietic stem cells are able to differentiate into both lymphoid and myeloid lineages (Bozhilov et al., 2023). Unipotent is the last type of cells in this group, which can self-renew and differentiate into only one specific cell type and form a single lineage, such as a germ line stem cells producing only sperm or oocytes, respectively (Kolios & Moodley, 2013).

Based on the origin of the stem cells, they can be grouped into 4 categories, named as ESCs, iPSCs, fetal, and adult stem cells. Among those- ESCs and iPSCs are pluripotent, whereas adult stem cells are multi-, oligo-, or unipotent (Kolios & Moodley, 2013). As mentioned above, ESCs and iPSCs both share similar characteristics and the main difference is, ESCs are derived from the inner cell mass of the blastocyst, while iPSCs are reprogrammed from somatic cells. On the other hand, fetal stem cells are stem cells isolated from fetal tissues, such as fetal blood, bone marrow, kidney, liver, etc. At the end, adult tissue derived stem cells are called adult stem cells or somatic stem cells (Kolios & Moodley, 2013).

1.4.2 Induced pluripotent stem cells (iPSCs)

PSCs create a great scope in regenerative medicine having indefinite self-renewal and differentiation capacity into somatic cell types. The derivation process and application of ESCs is often inconvenient and ethically controversial, therefore using iPSCs is the suitable and best possible alternative for future regeneration therapies and personalized medicine. In 2006/2007 Shinya Yamanaka and Kazutoshi Takahashi established the protocol to induce PSCs from mouse embryonic and/or adult human fibroblasts by introducing four defined factors:

OCT4, SOX2, c-MYC, and KLF4 (Takahashi et al., 2007; Takahashi & Yamanaka, 2006). This protocol has been further optimized by another research group to improve the efficiency by reprogramming the human somatic cells with another four-factor combination of OCT4, SOX2, NANOG, and LIN28 (Yu et al., 2007). The cell source, transcription factor combination, and delivery system to induce the pluripotency with the transcription factors are diverse and continuously being improved. Different integrating and non-integrating delivery systems are being used to introduce the pluripotency factors in the human somatic cells to generate iPSCs. Retrovirus and lentivirus are the most common integrating delivery systems, while adenovirus, sendai virus, pSin plasmid, episomal plasmids, and minicircle DNA are the non-integrating systems (Abu-Dawud et al., 2018; Fusaki et al., 2009; Takahashi & Yamanaka, 2006; Wang & Adjaye, 2011; Zhou & Freed, 2009). Fibroblasts from skin biopsy, human keratinocytes, or fetal foreskin fibroblasts are some somatic cell sources for generating iPSCs, while peripheral blood cells and renal progenitor cells from urine are also being used lately as popular and easily obtainable sources to generate iPSCs (Bohndorf et al., 2017; Graffmann et al., 2021; Takahashi & Yamanaka, 2006). Overall, iPSCs are morphologically identical to ESCs and share the similar pluripotency and differentiation capacity. They are easily accessible regarding generation of patient-specific or disease-specific cell lines. Thus, one can study a specific disease condition, phenotype, mutation, and also can develop customized medication and therapy. iPSCs-derived neural cells have been employed to investigate disease mechanisms and treatment for multiple neurological disorders such as Alzheimer's disease (AD), Parkinson's, multiple sclerosis, amyotrophic lateral sclerosis, Huntington's, spinal muscular atrophy, motor neuron diseases, autism, and rare CNS[#] diseases (Chang et al., 2011; Juopperi et al., 2012; Liu et al., 2023; Riemens et al., 2020; Russo et al., 2015; Sarasua et al., 2014; Stoddard-Bennett & Reijo Pera, 2019; Zhang et al., 2016).

1.4.3 Organoids

2D *in vitro* cultures have been extensively employed to understand the cellular response and bioactivities for decades (Duval et al., 2017). Despite being invaluable, mono-layered mono- or co-culture 2D systems lack cell-cell interaction, morphological, and physiological properties of the whole tissue and resemblance with the *in vivo* responses, which emerged an advanced and potential platform of 3D culture to enhance the cytoarchitectural complexity by employing another dimension around 2D cells with the extracellular matrix (Bortolussi & Muro, 2020). Presence of divergent cell types, cell-cell interaction, and cellular responses

upon stress inducer or toxins make this model a more closely *in vivo*-mimicking system (Simian & Bissell, 2017; Yoon et al., 2019). The attempt of *in vitro* organ regeneration has been demonstrated over a century ago. Dissociation and reaggregation experiments have revealed the self-organizing capacity of vertebrate cells to regenerate an organ system (Corro et al., 2020; Tung & Ku, 1944; Weiss & Taylor, 1960; Wilson, 1907). Later on, stem cell research began to thrive in 1981 which eventually developed further and made significant impact to stem cell and organoid research (Corro et al., 2020; Evans, 1981; Li et al., 1987). By using scaffold or scaffold-free techniques, suspension cultures can turn into 3D culture systems (Corro et al., 2020). This self-organizing capacity of PSCs has made a revolutionary advancement in transforming 2D cell culture to 3D *in vitro* models such as organoids.

Organoids are generated from stem cells (PSCs, fetal, or adult) or isolated organ specific progenitor cells, which are differentiated into a simple tissue-engineered cell-based organ-like intact tissue with multiple cell types and self-patterned spatial organization along with reflecting some function of the system (Lancaster & Knoblich, 2014; Zhao et al., 2022). The goal of this *in vitro* model is to generate a remarkably similar human *in vivo*-like system, recapitulating the endogenous developmental processes and being suitable for implementation in diagnostics, disease modelling, drug discovery, and personalized medicine (Lancaster & Knoblich, 2014; Zhao et al., 2022). Organoid models are being widely used in fundamental and dynamic development and mechanistic studies along with regeneration and repair mechanisms in human tissues upon trauma or injury (Logan et al., 2019; Zhao et al., 2022). By employing organ precursor specific combinations of growth factors and nutrients that are necessary to drive the cells towards a specific tissue identity, organoids from distinct organ systems have been generated, including intestinal, pancreatic islet, kidney, brain, lung, and retinal organoids (Almeqdadi et al., 2019; Lancaster & Knoblich, 2014; Lancaster et al., 2013; Nguyen et al., 2022; Sakaguchi et al., 2015; Xia et al., 2014; Zhong et al., 2014). Organoids derived from healthy and diseased donors can be used to investigate diseases from various organ systems which are not easily accessible such as brain and kidney, or to study genetic disorders by implying gene modification (Lancaster et al., 2013; Pomeshchik et al., 2023). Organoid technology bridges the gap between classical cell culture and *in vivo* models, however there are still limitations of the current system and the extent of similarity with the *in vivo* situation remains to be determined in many cases. For instance, lack of surrounding stromal cells, immune cells, and endothelial cells, batch to batch variability and heterogeneity,

a low degree of functionality, necrotic core formation due to tissue degeneration, limited reproducibility, and minimum reporting standards are some of the drawbacks of the model that need to be optimized and improved (Andrews & Kriegstein, 2022; Corro et al., 2020; Zhao et al., 2022). Nevertheless, these models hold great therapeutic promises with their potential in tissue regeneration and as a means to study biology of common, rare and infectious disease, for drug discovery/testing and development studies, biomarker research, and precision medicine application.

1.4.4 Brain organoids

3D brain organoids are composed of highly divergent neural cell types and subtypes, providing complex cytoarchitecture and cellular interplays with spatial organization. This model recapitulates fundamental mammalian neurodevelopmental mechanisms and characteristics of human brain development. hiPSC-derived brain organoids contain functioning neurons, astrocytes, oligodendrocytes, and to some extent microglia (Lancaster et al., 2013; Pasca et al., 2015; Yoon et al., 2019; Zhang et al., 2023). Additionally, some epigenetic and transcriptomic hallmarks of brain organoids resemble those of the fetal human brain and to some degree with those of early postnatal brain maturation stages (Camp et al., 2015; Gordon et al., 2021; Luo et al., 2016; Zhang et al., 2023).

There are multiple protocols to generate neural organoids, therefore choosing the generation process should depend on the purpose of the study and the application of the model. Researchers generated iPSC-derived self-patterned cerebral organoids containing forebrain, midbrain, hindbrain, and choroid plexus (Lancaster et al., 2013). By manipulating specific cellular identity-determining factors, individual brain-region and feature specific brain organoids have been successfully generated such as: oligodendrocyte organoids, BBB organoids, choroid plexus organoids with cerebrospinal fluid secretion, microglial organoids, retinal organoids, hippocampal organoids, striatum organoids, and organoids with functional neurons and astrocytes (Afanasyeva et al., 2021; Bergmann et al., 2018; Ciarpella et al., 2021; Marton et al., 2019; Miura et al., 2020; Ormel et al., 2018; Pellegrini et al., 2020; Pomeshchik et al., 2023; Sloan et al., 2018). Such diverse incorporation of brain features in brain organoids help this model to resemble and mimic human CNS[#] environment much better compared to other *in vitro* models along with facilitating the understanding of disease pathology, drug mechanism, and customized medication (Edmondson et al., 2014; Giandomenico et al., 2021; Liu et al., 2018; Martins et al., 2022; Nascimento et al., 2019).

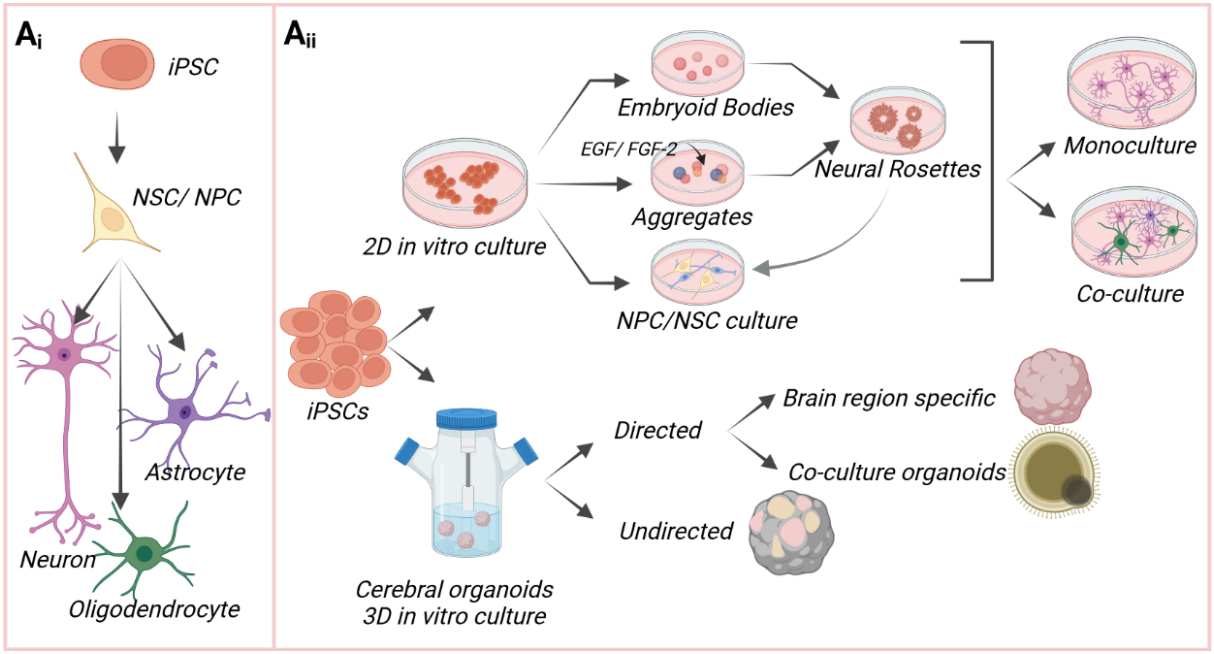

Figure 6. iPSC-derived in vitro 2D and 3D neuronal cultures. (Ai) Schematic representation of iPSCs differentiation into neuronal cells. iPSC-derived NPCs can differentiate into mature neuronal cells such as neurons, astrocytes, and oligodendrocytes. (Aii) NPC generation methods: from 2D mono-layered iPSCs cultured as embryoid bodies, cell aggregation in suspension via neural rosettes formation, or by direct induction from iPSCs to NPCs in 2D. NPCs generated in both approaches can be used for mono- or co-culture of distinct types of neuronal cells. Generation of iPSC-derived 3D organoid culture in a directed or non-directed manner, depending on their application purpose. iPSC- induced pluripotent stem cells, NSC- neural stem cells, NPC- neural progenitor cells. Illustration obtained from Pranty, A.I., Shumka, S. and Adjaye, J., 2022. Bilirubin-induced neurological damage: current and emerging iPSC-derived brain organoid models. Cells, 11(17), p.2647, as licensed under an open access Creative Common Attribution 4.0 license (https://creativecommons.org/licenses/by/4.0/).

Additionally, merging co-culture systems in organoid technology increases the model complexity and depicts human brain development and neuro-pathological conditions (Figure 6) (Kim & Jiang, 2021; Ormel et al., 2018; Zhang et al., 2023). However, it is challenging to create a suitable environment for co-culture organoids as different cell type have different proliferation rates and different neurotropic factors requirements, which might result insufficient cell number of specific types and affect the organoid maturation and culture duration (Frohlich, 2018; Zahmatkesh et al., 2021). Despite having some limitations of organoid technology, iPSC derived brain organoid models serve as a valuable tool by providing insights into human brain development and by modelling neurological disorders such as microcephaly, AD, Parkinson's, cerebellar diseases, cerebral malaria, Timothy syndrome, and Nijmegen breakage syndrome, as well as brain tumors such as gliomas and medulloblastoma (Bras et al., 2022; Goranci-Buzhala et al., 2020; Harbuzariu et al., 2019; Karmirian et al., 2023; Lancaster et al., 2013; Martins et al., 2022; Sidhaye & Knoblich, 2021; Smits et al., 2019; van Essen et al., 2024).

2. Aims and Objectives

The aim of this thesis was to model Crigler-Najjar syndrome (CNS) and cerebral malaria (CM) manifested encephalopathy using iPSC-derived *in vitro* neuronal cultures to imply the advanced application of iPSCs on disease modelling. A subsequent objective was to investigate the cellular and molecular response of the neuronal population (particularly neurons) in hiPSC-derived 2D and 3D brain models upon external challenges, such as free bilirubin (BF) and hemozoin (HMZ) exposure.

The first goal of the study was to model CNS, an autosomal recessive disorder, which has been only investigated in rodents, organotypic cultures, primary and immortalized cellular models. Therefore, the focus was to establish an optimized protocol of brain organoid generation using healthy and CNS patient derived iPSCs and to investigate further bilirubin induced neurologic dysfunction (BIND) in this model. The self-organization and whole tissue formation capacity of iPSCs have evolved a great advancement from 2D to 3D *in vitro* models. Healthy and CNS patient-derived iPSC can be differentiated into 3D brain organoids and then employed as a potential *in vitro* CNS model. Associated BIND and the molecular basis of the detrimental effects of BF in the developing human brain can be further investigated using this CNS model. Generating brain organoids from patient`s cells which contained the disease-causing mutation (UGT1A1) also allows to investigate the effect of the mutation and its subsequent phenotypic manifestation. The second objective was to model a different causal factor driven encephalopathy, manifested in CM using hiPSCs. The specific role of the known malaria toxin-HMZ in CM is unknown. Therefore, the aim was to investigate HMZ-induced effects on the iPSC-derived 2D neuronal cultures. Different BF and HMZ dosages, timing, frequency, and exposure conditions can be applied on these 3D organoids and 2D neurons to optimize the experimental conditions, which allow then exploration of multiple molecular aspects of the disease conditions. Neuronal cultures and brain organoids also hold the potential application for future BIND- and CM- associated toxicological studies, drug screening, and treatments.

The overall goal of this thesis was to establish iPSC derived CNS and CM *in vitro* models to improve the existing encephalopathy models regarding brain dysfunction investigation *in vitro*. Additionally, this study intended to provide insights into a human iPSC-derived 3D-brain organoid model and neuronal cultures to serve as prospective platforms for studying the etiology of BIND- kernicterus and CM.

Structure of the Thesis

In this thesis three publications are presented, which address the potential application of iPSC-derived 2D and 3D neuronal cultures to model and investigate CNS and CM manifested encephalopathy *in vitro*.

1. Pranty, A.I., Shumka, S. and Adjaye, J., 2022. **Bilirubin-induced neurological damage: current and emerging iPSC-derived brain organoid models**. Cells, 11(17), p.2647. (review article)

2. Pranty, A.I., Wruck, W. and Adjaye, J., 2023. **Free Bilirubin Induces Neuro-Inflammation in an Induced Pluripotent Stem Cell-Derived Cortical Organoid Model of Crigler-Najjar Syndrome.** *Cells*, *12*(18), p.2277. (original research)

3. Pranty, A.I., Szepanowski, L.P., Wruck, W., Karikari, A.A., and Adjaye, J., 2024. **Hemozoin induces Malaria via activation of DNA damage, p38 MAPK and Neurodegenerative Pathways in a Human iPSC-derived Neuronal Model of Cerebral Malaria.** Under revision at *Scientific Reports* journal (original research)

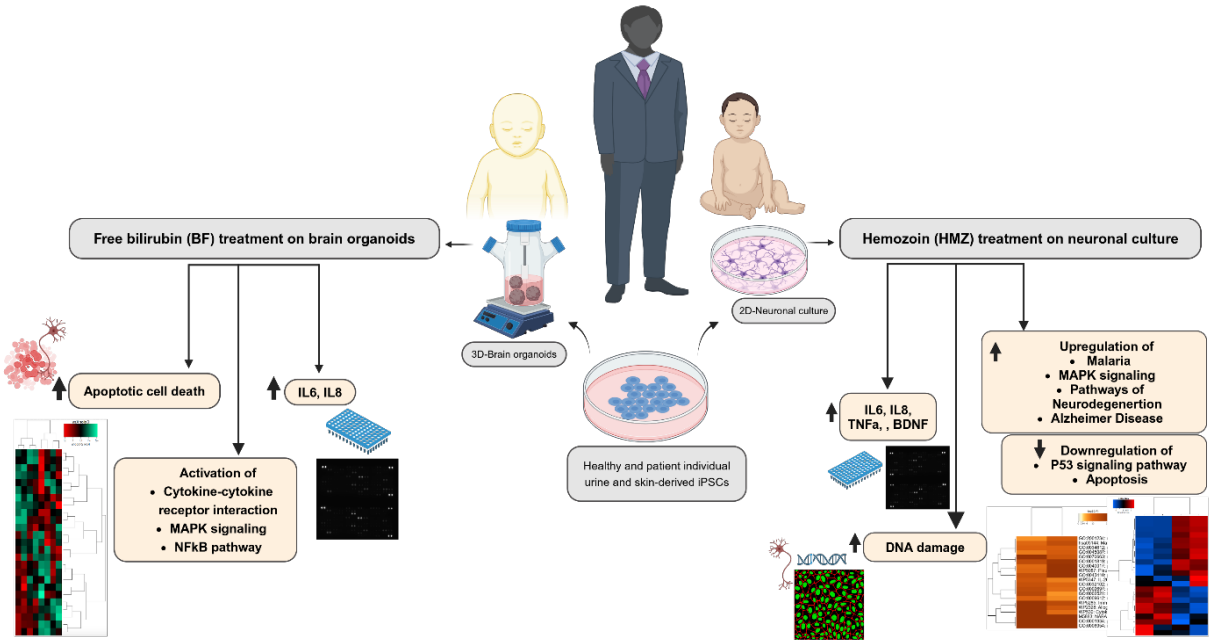

Figure 7. Synopsis of the publications and key observations. Modelling encephalopathy using hiPSC-derived 2D neuronal cultures and 3D brain organoids. (Created with BioRender.com)

3. Publications

3.1 Bilirubin-Induced Neurological Damage: Current and Emerging iPSC-Derived Brain Organoid Models

Abida Islam Pranty, Sara Shumka and James Adjaye

Cells 2022, Volume 11, Issue 17, Article Number 2647

Abstract:

Bilirubin-induced neurological damage (BIND) has been a subject of studies for decades, yet the molecular mechanisms at the core of this damage remain largely unknown. Throughout the years, many in vivo chronic bilirubin encephalopathy models, such as the Gunn rat and transgenic mice, have further elucidated the molecular basis of bilirubin neurotoxicity as well as the correlations between high levels of unconjugated bilirubin (UCB) and brain damage. Regardless of being invaluable, these models cannot accurately recapitulate the human brain and liver system; therefore, establishing a physiologically recapitulating in vitro model has become a prerequisite to unveil the breadth of complexities that accompany the detrimental effects of UCB on the liver and developing human brain. Stem-cell-derived 3D brain organoid models offer a promising platform as they bear more resemblance to the human brain system compared to existing models. This review provides an explicit picture of the current state of the art, advancements, and challenges faced by the various models as well as the possibilities of using stem-cell-derived 3D organoids as an efficient tool to be included in research, drug screening, and therapeutic strategies for future clinical applications.

Authors Contribution: 80 %

A.I.P. wrote, formulated tables, and edited the manuscript.

Status: Published in *Cells* (doi.org/10.3390/cells11172647).

cells

MDPI

Review

Bilirubin-Induced Neurological Damage: Current and Emerging iPSC-Derived Brain Organoid Models

Abida Islam Pranty, Sara Shumka and James Adjaye *

Institute for Stem Cell Research and Regenerative Medicine, Faculty of Medicine, Heinrich-Heine University, Moorenstrasse 5, 40225 Dusseldorf, Germany
* Correspondence: James.Adjaye@med.uni-duesseldorf.de

Abstract: Bilirubin-induced neurological damage (BIND) has been a subject of studies for decades, yet the molecular mechanisms at the core of this damage remain largely unknown. Throughout the years, many in vivo chronic bilirubin encephalopathy models, such as the Gunn rat and transgenic mice, have further elucidated the molecular basis of bilirubin neurotoxicity as well as the correlations between high levels of unconjugated bilirubin (UCB) and brain damage. Regardless of being invaluable, these models cannot accurately recapitulate the human brain and liver system; therefore, establishing a physiologically recapitulating in vitro model has become a prerequisite to unveil the breadth of complexities that accompany the detrimental effects of UCB on the liver and developing human brain. Stem-cell-derived 3D brain organoid models offer a promising platform as they bear more resemblance to the human brain system compared to existing models. This review provides an explicit picture of the current state of the art, advancements, and challenges faced by the various models as well as the possibilities of using stem-cell-derived 3D organoids as an efficient tool to be included in research, drug screening, and therapeutic strategies for future clinical applications.

Keywords: BIND; kernicterus; UCB; iPSCs; organoids

Citation: Pranty, A.I.; Shumka, S.; Adjaye, J. Bilirubin-Induced Neurological Damage: Current and Emerging iPSC-Derived Brain Organoid Models. *Cells* **2022**, *11*, 2647. https://doi.org/10.3390/cells11172647

Academic Editor: Alexander E. Kalyuzhny

Received: 23 June 2022
Accepted: 17 August 2022
Published: 25 August 2022

1. Introduction

Bilirubin is an endogenous toxin that results as a by-product of hemoglobin breakdown. It is often used to diagnose liver and blood diseases and has a complicated metabolism, which is significant in relation to various drug metabolism pathways [1]. Bilirubin is metabolized in the liver by the enzyme encoded by the uridine diphosphate glucuronosyltransferase 1A1 gene (UGT1A1), which conjugates bilirubin to glucuronic acid, making it water-soluble [2]. Being lipophilic, unconjugated bilirubin (UCB) cannot take part in the physiological elimination process and starts accumulating. Conjugation of bilirubin is required for increasing its solubility in plasma, thereby enhancing bilirubin elimination from the body. Furthermore, the high level of UCB can become dangerous and cause various complications.

When bilirubin levels in plasma or serum cross the laboratory reference range due to bilirubin metabolism irregularities, it is diagnosed as hyperbilirubinemia, which can be further categorized as conjugated or unconjugated hyperbilirubinemia (UHB) [3]. Clinical jaundice, for instance, which is caused by neonatal UHB, is a commonly occurring, transitional condition that affects about 85% of newborns in their first week of postnatal life [4–6]. UHB is a condition regulated by the albumin-bound UCB. As a consequence, there is enhanced UCB production, reduced conjugation and dysfunctional hepatic uptake [3]. On the other hand, at mildly elevated concentrations, bilirubin has a protective antioxidant-like effect on the body [7,8]. It can neutralize reactive oxygen species (ROS), prevent oxidative damage, and is even necessary for newborns when they face high concentrations of oxygen in the air for the first time [9–12]. It has been shown that UCB also possesses potent anti-oxidant properties, and modest hyperbilirubinemia may even have health benefits [1].

However, high levels of UCB can pose serious threats, such as severe brain injury, with the possibility of progressing into chronic bilirubin encephalopathy (also referred to as kernicterus) in one in every 100,000 cases, if not treated immediately [6,7]. In cases where it does develop into kernicterus, almost 70% of newborns die within the week and the other 30%, suffer irreversible brain damage [13].

Apart from being an adverse effect of spontaneous neonatal hyperbilirubinemia, BIND may also result from a genetic disorder known as Crigler–Najjar Syndrome (CNS). This life-threatening disorder is caused by the mutation in *UGT1A1*, which causes a complete or partial defect that prevents the liver from metabolizing bilirubin. This hinders bilirubin conjugation, causing UCB to accumulate in serum and eventually cross the blood–brain barrier, proceeding to deposit in the basal ganglia or cerebellum, thereby resulting in BIND [2,3]. Table 1 offers a comprehensive overview of various clinical indications related to hyperbilirubinemia and the respective targets in the brain.

BIND is not only temporarily disabling but also permanent, and it is usually accompanied by movement disorders as well as hearing loss [4,6]. The targeted damage to the central nervous system reflects the regional topography of bilirubin-induced neuropathology, involving the globus pallidus, subthalamic nucleus, metabolic sector of the hippocampus, hippocampal Cornu Ammonis (CA2) neurons, and Purkinje's cells of the cerebellar cortex and the brainstem, as well as the oculomotor and ventral cochlear nuclei [14–16]. However, the key cellular mechanisms accounting for this well-defined regional topography of bilirubin sensitivity are still unclear. One probable reason could be the lack of efficient and suitable in vitro and in vivo models with consistent and comparable findings [12]. Advanced stem-cell-based studies offer great opportunity to establish 3D in vitro model systems to study neurological complications [17–20]. On that account, human-induced pluripotent stem cell (iPSC)-derived 2D neuronal cell cultures along with 3D brain organoids present convenient and efficient models to enable deciphering the molecular mechanisms underlying BIND.

Table 1. Overview of bilirubin-related diseases and clinical manifestations in the brain.

Clinical Indication	Brain Target	Clinical Symptoms	Reference
Bilirubin-induced cerebral cortex injury	• Cortical neurons • Astrocytes • Oligodendrocytes	• Reduction in neurite extension and dendritic and axonal arborization • Increased cell death by apoptosis • Cognitive disorders	[5,21,22]
Basal ganglia injury	• Subthalamus • Globus pallidus • Striatum	• Attention deficit hyperactivity disorder (ADHD) • Specific learning disability (SLD) • Cognitive and behavioral symptoms	[21,23,24]
Bilirubin-induced cerebellar injury	• Cerebellum	• Oxidative stress • Endoplasmic reticulum (ER) stress • Autism spectrum disorder (ASD) • ADHD	[21]
Bilirubin-induced hippocampal injury	• Dendrites and axons of hippocampus	• Adverse synaptic plasticity • Specific learning disabilities	[5,21,25]
Bilirubin-induced auditory nervous system injury	• Brainstem auditory structure	• Language disorders	[26,27]

Table 1. *Cont.*

Clinical Indication	Brain Target	Clinical Symptoms	Reference
Crigler–Najjar Syndrome Type I	• Entire brain • Particularly: • basal ganglia • cerebellum • brainstem nuclei • peripheral and central auditory pathway • hippocampus	• Mild to severe jaundice • Kernicterus	[3]
Crigler–Najjar Syndrome Type II	• Entire brain • Particularly: • basal ganglia • cerebellum • brainstem nuclei • peripheral and central auditory pathway • hippocampus	• Mild jaundice • Kernicterus (rarely)	[3]

1.1. UGT1A1

Glucuronidation is a conjugation reaction in which glucuronic acid, which is produced from the cofactor UDP-glucuronic acid, is covalently bound to a nucleophilic functional group on a substrate [28]. The *UGT1A1* gene, or uridine diphosphate glucuronosyltransferase 1A1 gene, is part of the UGT1 locus, which encodes the enzymes that glucoronidate a variety of substrates. This gene plays a crucial role in the glucuronidation pathway by converting bilirubin from an unconjugated (toxic) state to a conjugated (nontoxic) state [2]. Bilirubin is formed as a by-product of the heme catabolic pathway. After hemoglobin is broken down into heme, it is then transformed into biliverdin (BLV) and subsequently into bilirubin. *UGT1A1* particularly encodes the enzyme that has the ability to convert small lipophilic molecules such as bilirubin into hydrophilic (water-soluble) molecules that can be easily excreted [29,30]. During bilirubin glucuronidation, glucuronic acid is attached (conjugated) to bilirubin through a bilirubin-UDP-glucuronosyltransferase (B-UGT) enzyme-dependent reaction, as B-UGT1 is the only enzyme capable of glucoronating bilirubin [2]. The glucuronidation process takes place in the liver; therefore, liver cells are the primary source of the B-UGT1 enzyme. Thereafter, the water-soluble conjugated version of bilirubin is dissolved in bile and excreted from the body with solid waste.

UGT1A1 was initially cloned by Ritter et al. in 1991 and is located on chromosome 2q37 [30,31]. The UGT1 locus has 13 unique promoters and alternate first exons, followed by four common exons, designated 2, 3, 4 and 5. Before transcription, one of the first exons and its promoter are spliced to the four common exons. This results in 13 different UDP-glucuronosyltransferases being expressed; however, out of 13 possible genes that can be encoded, the only one responsible for bilirubin conjugation is the one containing the alternate exon A1 [2,30].

Reduced expression and partial or total impairment of the B-UGT1 enzyme is caused by mutations in the *UGT1A1* gene's common or bilirubin-specific domains. This can result in inherited unconjugated bilirubinemia disorders, with the most common ones being Gilbert syndrome, Crigler–Najjar syndrome type I (CNS-I) and Crigler–Najjar syndrome type II (CNS-II), also known as Arias syndrome (Table 1) [4,29,30]. The nature of these mutations varies, resulting in phenotypes that range from moderate, in the case of Gilbert syndrome, to severe in CNS-I [4,29,32,33].

In 2000, Kadakol et al. tabulated more than 50 genetic lesions of *UGT1A1* that engender CNS-I and II and presented a correlation of structure to function of *UGT1A1* [29]. Building upon that research, almost a decade later, Canu et al. published an explicit list of Gilbert and CNS disease, causing mutations including more than 130 cases. Single-nucleotide

changes were liable for around 70% of these alterations, whereas deletions, insertions, and polymorphisms attributed for the remaining 30% of alterations [32]. As *UGT1A1* is the crucial player in these diseases, being able to alter its expression in customizable in vitro models could help provide more insights into possible translational treatments.

1.2. Crigler–Najjar Syndrome Type I and II

The most serious form of inherited UHB is Crigler–Najjar syndrome Type-I (CNS-I) [34–36]. It is the outcome of the complete aberration of *UGT1A1*, a very rare autosomal recessive disease, only affecting one in a million individuals [37]. The aberration of *UGT1A1* leads to high bilirubin plasma levels and severe jaundice in neonates [2]. Increased bilirubin availability in plasma may result in bilirubin accumulation in the brain, turning into a life-threatening condition known as bilirubin encephalopathy. Crigler–Najjar Syndrome Type-II (CNS-II) and Gilbert syndrome are two milder versions of CNS-I, where *UGT1A1* is either partially deficient or altered, resulting in a less severe phenotypic manifestation [37].

To lower the plasma bilirubin level and prevent bilirubin encephalopathy, CNS patients rely on 10–12 h of intensive phototherapy treatment every day. Numerous dermatological disorders have been safely and successfully treated with phototherapy for over 40 years [38]. This treatment uses UV radiation to counteract the pathological changes that characterize inflammatory skin diseases through several mechanisms, such as induction of apoptosis, modification of the cytokine milieu, and immunosuppression. Phototherapy is so effective because through UV radiation, bilirubin is irreversibly photo-altered into lumirubin, a structural isomer that is more water-soluble, less dangerous and can be expelled with bile and urine [38,39]. However, the efficiency of the phototherapy can decrease depending on multiple factors, such as age, thickness of the skin, etc. Conversely, skin thickening is one of the effects obtained from the phototherapy itself, which later decreases the therapeutic efficiency. Additionally, extremely low-birth-weight newborns might face potential toxicity due to aggressive phototherapy [40]. A hemolytic process is indicated with the enhancement of total serum bilirubin level despite intensive phototherapy. Exchange transfusions have also been used to control hyperbilirubinemia at a hazardous level and lower the risk of kernicterus. However, phototherapy has greatly reduced the necessity and demand for exchange transfusion [6]. Another approach to control hyperbilirubinemia and prevent acute bilirubin encephalopathy is intravenous immune globulin therapy. Despite the mechanism being unclear, the immune globulin therapy seems to have biological activity against immune-mediated hemolytic diseases associated with the lowering effect of the immune globulin present on the total serum bilirubin level [6]. Pharmacological compounds may provide a direct protection to the neurons from bilirubin toxicity. CNS-II patients respond quite well to the pharmacological therapies, such as treatment with phenobarbital, whereas CNS-I patients do not. Bilirubin conjugation is increased by the activated phenobarbital enhancer module of the *UGT1A1* promoter sequence, thus resulting in enhancement in bilirubin clearance. On the other hand, heme oxygenase inhibitors, such as metallophyrins, can be employed to reduce bilirubin production [41]. Minocycline, which is a tetracycline antibiotic, has shown protective effects in Gunn rat pups against bilirubin-induced neurotoxicity, including neuromotor dysfunction, abnormalities in the auditory pathway and cerebellar hypoplasia [6,42]. Finally, liver transplantation remains the only effective treatment for this life-threatening disease (Table 2) [2,36,43].

Table 2. Existing treatments and therapies for CNS.

Treatment	Advantages	Disadvantages	Reference
Phototherapy	• Non-Invasive • Relatively easy to administer • Inexpensive	• Time consuming/exhausting for the patient (10–12 h/day) • Less effective as patients age • Thickens patients' skin which makes therapy less efficient	[6,44]
Exchange transfusion	• Rapid treatment (in emergency cases lifesaving)	• Thrombocytopenia • Portal vein thrombosis • Necrotizing enterocolitis • Sepsis	[44]
Intravenous immune globulin therapy	• Removes need for exchange transfusions	• Fever • Allergic reactions • Rebound hemolysis • Fluid overload	[6,41]
Liver transplantation	• Most effective	• Does not reverse or alleviate pre-existing neurological damage	[2,44,45]
Phenobarbital	• Increased bilirubin clearance	• Not applicable for CNS-I patients	[6]
Metallophyrins	• Reduce bilirubin production	• Photosensitivity • Iron deficiency • Affect hematopoiesis (the formation of blood cellular components)	[41,46,47]
Minocycline	• Protective effects against neuromotor dysfunction, abnormalities in auditory pathway and cerebellar hypoplasia	• Unsafe for newborns • Affect bone and dentition development	[6]

2. Unravelling the Mechanisms Underlying BIND

To increase our meagre knowledge of BIND, we must understand the pathophysiology underlying high bilirubin neurotoxicity at the molecular level. The brain is a highly specialized and compartmentalized organ with divergent cell populations consisting of neurons and glia, which comprises astrocytes, oligodendrocytes and microglia [48]. Therefore, the location, source and causal agents of BIND are the primary areas worth investigating, along with the cascade of molecular and cellular events that lead to severe damage.

Autopsy results of jaundiced neonates showed disperse yellow spots in the majority of brain areas, except the basal ganglia and medulla oblongata, while intense coloring was observed in those particular areas [49]. These observations indicate that UCB binds to specific types of neurons compared to others and has distinct sensitivities amongst neurons and glia [50]. Microscopic observations of jaundiced brain sections revealed the presence of bilirubin within neurons, neuronal processes and microglia; however, the contribution of individual neuronal cell types and cell-dependent sensitivity towards bilirubin toxicity are still not clarified [48]. In vitro studies have revealed the mechanisms associated with UCB neurotoxicity [48,50]. An increased impairment of cell function has been observed in astrocytes upon high UCB exposure, while neurons show higher susceptibility to cell death [50]. Astrocytes and microglia also seem to play key roles in activating oxidative stress and inflammatory responses. Investigation into intracellular processes of astrocyte and microglia showed that TNF-alpha and IL-1beta pathways as well as MAPK and NF- κB pathways play a key role in cytokine production and cytotoxicity upon UCB stimulation, resulting in UCB-induced neurotoxicity [5,51]. In vivo and in vitro data indicate oxidative stress to play a major role in cytotoxicity upon highly concentrated (toxic) UCB exposure,

while increases in oxidative stress and cytotoxicity were observed in synaptic vesicles, tissue culture cells, and primary cell culture of neurons, astrocytes and oligodendrocytes [5,52,53].

The creation and elimination of bilirubin both result from a sequence of metabolic reactions; therefore, there are distinct ways of limiting the production and degradation of UCB [7]. The heme catabolic pathway primarily regulates bilirubin conjugation, as UCB is the consecutive end-product and UCB is endogenously produced by following this pathway within the majority of cells [54]. Briefly, heme is converted into BLV by heme oxygenase enzyme 1 and 2 (HMOX1, HMOX2), and then BLV reductase (BLVR) converts BLV into UCB. Both HMOX1 and HMOX2 reside in mitochondria, endoplasmic reticulum (ER) and caveolae (membrane micro-domains observed at the interface with the extracellular environment), which might have a correlation with BIND-induced neurocytotoxicity, as various molecular pathways become activated in the course of BIND neurotoxicity. These pathways include inflammation, mitochondrial damage and oxidative stress to ER [5,54,55]. The disturbances in mitochondria and ER usually lead to several additional sequelae, such as neuronal excito-toxicity (a complex process triggered by glutamate receptor activation resulting in dendrite degeneration and cell death), mitochondrial energy failure, increased intracellular calcium concentration and deoxyribonucleic acid (DNA) damage (Figure 1) [16,56,57]. All of these factors may subsequently contribute to neuronal death and bilirubin encephalopathy, leading to kernicterus [5,7,16].

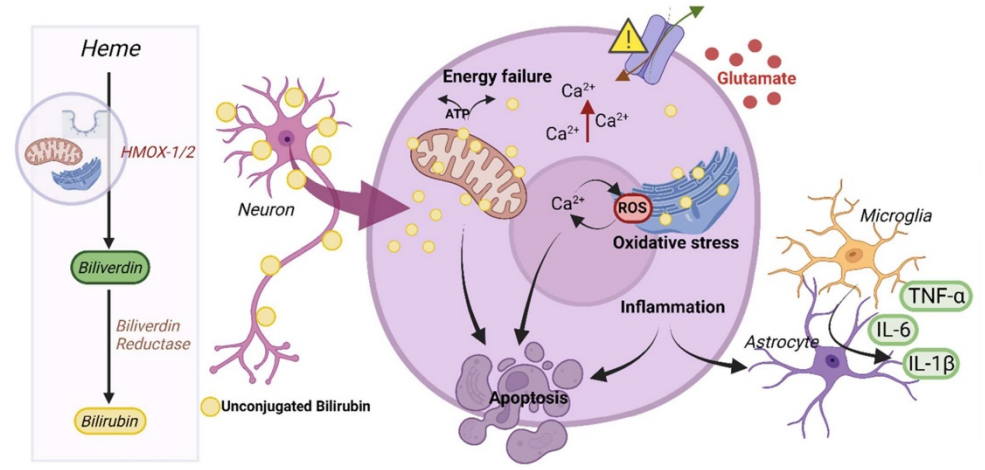

Figure 1. Schematic of the mechanisms involved in BIND induced neurotoxicity. **Left**: Metabolic pathway leading to unconjugated bilirubin (UCB) production. Heme is converted into biliverdin by heme oxygenase (HMOX-1 and 2), located in mitochondria, endoplasmic reticulum and caveolae. Biliverdin is then converted into unconjugated bilirubin by biliverdin reductase. **Right**: Neurons are depicted in this scheme to represent the toxic effects of UCB in brain cells. Neurons are known to be the most affected cell type in UCB toxicity, which involves multiple pathways leading to distinct toxic events, including disruption of the mitochondrial energetic breakdown, ionic imbalance, extracellular accumulation of glutamate, release of inflammatory cytokines by glial cells (here depicted as microglia and astrocytes), as well as increase in reactive oxygen species (ROS) production and oxidative stress. This UCB-induced cytotoxicity can result in apoptosis (the different cell type sizes are not depicted to scale, but rather schematically to simplify the view of the mechanisms) (Created with BioRender.com, accessed on 23 August 2022).

During moderate to severe neonatal jaundice, pre-term newborns show an accelerated susceptibility to UCB toxic effects, which makes prematurity a significant abrasive factor

for UCB encephalopathy [58,59]. The first week of postnatal life might be sensitive due to an increased chance of higher amounts of UCB availability in the circulation due to several factors. Consequently, the conjugation probability of UCB is suppressed and the unbound fraction of UCB (free bilirubin) increases [60]. The entry of UCB in the brain is restricted by the blood–brain barrier (BBB), as BBB is composed of tightly jointed microvascular endothelial cells, forming elaborate junctional complexes and providing unique properties by strictly regulating the ions, molecules and cell movement between blood and brain [60,61]. Lower UCB binding capacity and the higher UCB availability facilitate the entrance of free bilirubin by passive or facilitated diffusion into the brain, thus causing a condition of mild or severe hyperbilirubinemia. Further research is required to increase our meagre understanding of bilirubin entrance into the brain and the resulting cytotoxicity [59].

2.1. Bilirubin-Induced Oxidative Stress

Bilirubin plays a dual role depending on the physiological level of its unconjugated form. At very low levels, it acts beneficially as an antioxidant; however, after attaining a given threshold, it becomes toxic [5,62]. The neuroprotective role of bilirubin within a certain range of concentrations has been known for more than two decades to protect neurons from H_2O_2-induced toxicity [62]. Furthermore, the role of bilirubin as an anti-inflammatory agent and a scavenger of ROS have been intensively studied for a long time [54,63–67]. With the help of nicotinamide adenine dinucleotide phosphate (NADPH) oxidase, bilirubin prevents the generation of superoxides, inhibits ROS production and regulates redox homeostasis. This implies that at lower concentrations, bilirubin is potentially involved in several important cellular signaling pathways, such as cell proliferation, apoptosis, inflammation, and immune system upkeep. Moreover, bilirubin has also been proven to be a powerful signaling molecule that can help guard against a variety of disorders linked to elevated levels of oxidative stress [54,68,69].

On the other hand, bilirubin itself is the cause of oxidative stress. Increased oxidative stress activates transcription factor NF- κB and also increases phosphorylation of mitogen-activated protein kinases (MAPKs), therefore resulting in cytokine production and cell toxicity [70]. It is also clear that neurons are more susceptible to oxidative damage than other cell types in the brain such as astrocytes [71]. Bilirubin-induced DNA damage was found to be significantly increased in vitro, when neuronal and non-neuronal cells were exposed to 140 nM of free bilirubin. As potential adaptive responses to repair the damage, bilirubin therapy triggered primary DNA repair pathways through homologous recombination (HR) and nonhomologous end joining (NHEJ) [7]. These findings add to our understanding of the mechanisms underlying bilirubin toxicity and may have implications for newborns with severe hyperbilirubinemia because DNA damage and oxidative stress may be another significant element causing neuronal death and bilirubin encephalopathy. Studies in Gunn rats and UGT −/− mice have additionally shown high levels of lipid peroxidation by sulfadimethoxine-induced hyperbilirubinemia, as well the activation of key oxidative stress markers [70,72–74]. We anticipate further therapeutic discoveries concerning the role of bilirubin in diseases related to oxidative stress, as the breadth of all its biological functions have yet to be fully uncovered.

2.2. Effects of UCB on the Brain

Autopsies of hyperbilirubinemic brains have shown UCB to be localized within neurons and microglia, which results in the loss of neurons, demyelination, and gliosis (Figure 1). On the other hand, along with inducing oxidative stress in cortical neurons, UCB also disrupts the dynamics of the neuronal network in hippocampal neurons or in immature developing neurons, making these early-staged neurons more susceptible to UCB-induced injury [75]. In isolated cell cultures, UCB impairs neuronal arborization and induces the release of pro-inflammatory cytokines from microglia and astrocytes. However,

cell-dependent sensitivity to UCB toxicity and the role of each neural cell type are not yet understood [5].

Clinical manifestations of hyperbilirubinemia indicate higher selectivity of bilirubin towards damaged brain regions, which particularly includes its preference for basal ganglia, cerebellum, brainstem nuclei, peripheral and central auditory pathways, and hippocampus [12,21]. The increased selectivity towards these injured brain areas has been well-known to closely correlate with the clinical signs of hyperbilirubinemia. However, it is the impairment of intracellular defense mechanisms in these areas, rather than the accumulation of UCB itself, that plays the primary role in brain damage [12]. As a result, bilirubin may disrupt developmental processes while incorporating multiple overlap and co-morbid neurodevelopmental disorders [21]. The damage to the basal ganglia and cerebellum correlates with movement disorders, athetosis (slow, involuntary, and writhing movements of the limbs, tongue, face, neck, and other muscle groups) and abnormal tone; the damage to the auditory brain nuclei and inferior colliculi is correlated to the auditory dysfunctions and hearing loss; and the damage to the brainstem and hippocampus correlates with the impaired oculomotor brainstem response and impairments in memory and learning (Table 1) [12].

Barateiro and his colleagues [76] used a kernicterus mouse model to display axonal damage as well as myelination deficits and glial activation in brain regions that usually accompany the neurological sequelae observed in severe hyperbilirubinemia such as the pons, medulla oblongata, and cerebellum. The observations from the study indicate the cerebellum as the most affected area, displaying greater myelination impairment and glia burden, as well as a loss of Purkinje cells and a reduced arborization of the remaining ones. The increase in astroglial and microglial reactivity possibly emerges as a response to myelination injury. It has also been hypothesized that excessive accumulation of total serum bilirubin (TSB) in the early neonatal period may promote the activation of the gene responsible for myelin basic protein (*MBP*). The increase in MBP seems to correlate with the inhibition or lack of myelin sheath formation. This may occur in response to inflammatory insults that affected the brain in the first place, leading to the production of ROS, or it may be a compensatory response to the lack of functional MBP due to the damage [76].

The Brites lab demonstrated that neuronal growth impairment and cell death caused by UCB is mediated by nitric oxide (NO) and glutamate, modulated by microglia, and prevented by glycoursodeoxycholic acid and interleukin-10 (IL-10) [77]. In another study, Falcao et al., created a model where astrocytes abrogated the well-known UCB-induced neurotoxic effects by preventing the loss of cell viability, dysfunction, and death by apoptosis, as well as the impairment of neuronal outgrowth [78]. UCB-induced alterations on neurogenesis, spinogenesis, neuritogenesis and axonal cytoskeleton dynamics indicate the relevance of UCB in synaptic plasticity abnormalities and the long-term neurodevelopmental disabilities, thereby making pre-term infants more vulnerable towards BIND [5]. Ultimately, the critical dual role of UCB in the brain raises questions, such as (1) which exact mechanisms and physiological switches lead to this beneficial–toxic threshold and (2) how can we regulate this duality of UCB to our advantage for future clinical applications? Having a BIND model as close to the clinical manifestation as possible may help to answer these questions by allowing us to investigate the cellular and pathophysiological mechanisms caused by UCB entry and its further effects in the brain.

2.3. Epigenetic Alterations Due to Bilirubin-Induced Neurotoxicity

Epigenetic studies have shown bilirubin neurotoxicity to affect vital regulatory mechanisms by significant modulation of gene expression [79]. Epigenetic processes involve DNA methylation, RNA methylation, histone post-translational modifications, and non-coding RNAs (ncRNAs), among which histone acetylation plays a vital role in gene modulation for several neuro-biological processes, including synaptic plasticity, brain development, differentiation, maintenance, and survival [80–82]. Apart from affecting cell fate and behavior, the acetylation/de-acetylation-mediated changes in gene expression induce excitotoxicity,

oxidative stress, increased calcium load, inflammation, and apoptosis [83,84] (Figure 1). The observed induced mechanisms indicate a probable link between epigenetic impairment in neurodevelopmental processes and the hyperbilirubinemic phenotype [79]. Following these leads, Vianello et al. used developing and adult Gunn rats to track histone 3 lysine 14 acetylation (H3K14Ac) level in the cerebellum and observed age-dependent alteration of H3K14Ac in hyperbilirubinemic conditions. Gene ontology analysis of H3K14Ac-linked chromatin also revealed 45% of genes to be involved in CNS development. This finding suggests that epigenetic modulation during development and maturation of the brain structure is one of the causes of cerebellum hypoplasia in hyperbilirubinemic Gunn rats. On the other hand, histone acetylation plays a role in controlling oligodendrocyte differentiation and myelin production, and the down-regulation of myelin-associated glycoprotein (*Mag*) is one of the known repercussions of bilirubin-induced disturbances of oligodendrocyte maturation [81,85]. Studies have reported down-regulation of *Mag* in vitro along with other BIND models, including in pre-term infants [76,79]. This indicates that oligodendrocyte maturation and myelination can be affected by altered histone acetylation due to bilirubin-induced neurotoxicity, both in physiological CNS development and post-demyelinated repair processes. Remarks from these studies confirm that epigenetically impaired neurodevelopmental processes in hyperbilirubinemia may have a correlation in bilirubin neurotoxicity [79].

3. BIND and CNS Disease Models

Generating and studying model systems that closely recapitulate the main characteristics of BIND and severe UHB, is of high importance for developing effective clinical treatments and therapies to gain a better understanding of the pathophysiological mechanisms underlying this condition. Figure 2 illustrates a general overview of the most common in vivo and in vitro models of BIND and CNS (Figure 2A,B), as well as why having a CNS patient-derived iPSC model would be a better option (Figure 2C).

3.1. Animal Models

Animal models are often able to bridge the gap that in vitro models fail to recapitulate, as they much better resemble the disease features manifested in patients. Bortolussi and Muro rigorously reviewed animal models used to study bilirubin neurotoxicity and metabolism as well as the in vivo mechanisms of hyperbilirubinemia [13]. The most widely used amongst these models is the Gunn rat. This strain of Wistar rats spontaneously developed a one-base deletion of exon 4 in the *UGT1* locus, thereby creating an in-frame premature stop codon. Since this codon is translated into a truncated protein lacking the transmembrane domain, it results in the deficiency of all members of the UGT1A1 iso-enzymes. The complete deficiency of UGT1A1 enzymatic activity causes hyperbilirubinemia in the Gunn rat, making it the first hyperbilirubinemia animal model to mimic the CNS-I syndrome. This model has enabled scientists to gather a considerable amount of knowledge on bilirubin metabolism and toxicity in vivo [4,86].

Despite having a mild phenotype, Gunn rats display life-long non-hemolytic UHB, which is an important feature of human CNS-I. In order to develop acute central nervous system dysfunction and recapitulate hyperbilirubinemia more precisely, Gunn rats are often treated with hemolytic drugs or albumin–bilirubin displacers, such as sulphonamides or erythrocyte-lysing agents such as phenylhydrazine. An application of this method to induce hyperbilirubinemia is direct administration of sulfadimethoxine, a displacer of bilirubin from albumin binding sites. This increases the fraction of free bilirubin migrating towards lipophilic tissues such as the brain and is accompanied by a drop of systemic bilirubin [13]. If left untreated, homozygous Gunn rats display abnormalities in the cerebellum and hearing impairments just like the respective human CNS-I phenotype; however, unlike the patient-manifested features, these rats reach adulthood and are fertile.

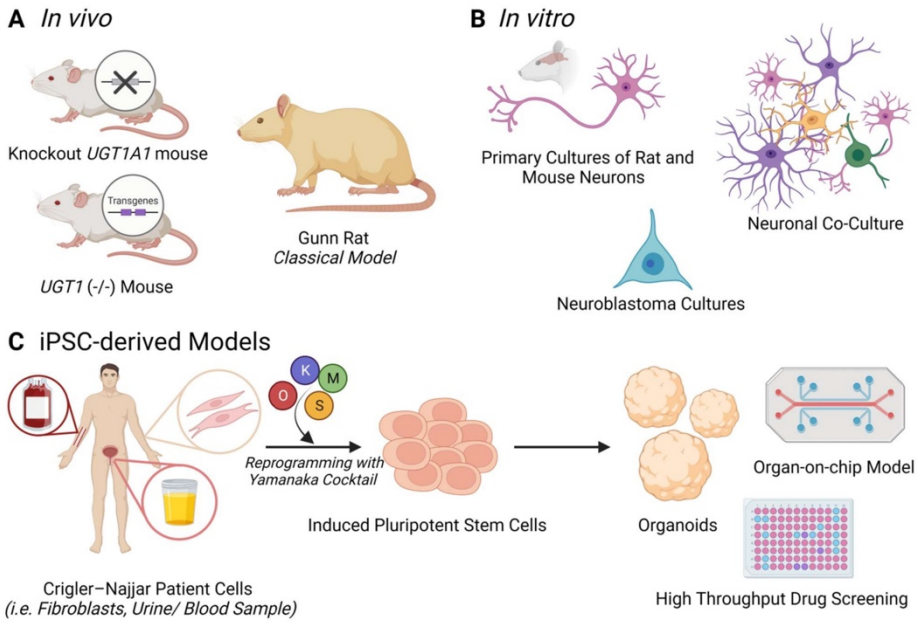

Figure 2. Overview of current models of BIND and Crigler–Najjar Syndrome. (**A**) In vivo models include the classical Gunn rat model, as well as knockout and transgenic mouse lines; (**B**) Some examples of in vitro models are primary cultures, mixed neuronal co-cultures as well as neuroblastoma cultures; (**C**) iPSCs can be generated by reprogramming of distinct types of human cells, such as fibroblasts, blood and urine-derived cells. The cells can be reprogrammed using the Yamanaka transcription factors (OCT4, SOX2, KLF4 and cMYC). A Crigler–Najjar Syndrome patient-derived iPSC model will enable future personalized medicine applications such as organoid cultures, organ-on-chip models and can be used for high throughput drug screenings specific to the patient's needs (Created with BioRender.com, accessed on 21 August 2022).

The *UGT1A*-null mouse is another popular in vivo model, which presents a much more severe phenotype than the Gunn rat, with aggravated neurological damage and consecutive death [87].

Using genetic tools and technologies enable the creation of the mutation. Constitutive and conditional knockout, knock-in and transgenic strains of mice have been generated by manipulating the mouse genome and have allowed for the further exploration of key aspects of this disease. With the disruption of *UGT1* exon 4 by neomycin cassette, scientists were able to generate the first bioengineered mouse model of severe UHB. Mutant mice are a good model to study CNS-I, as they do not express *UGT1A1* and display neonatal hyperbilirubinemia. However, these mice die within 11 days after birth, which makes the model inconvenient for broad-spectrum investigations and reproducibility.

These invaluable animal models have provided an undeniable contribution in understanding the mechanisms underlying severe neonatal hyperbilirubinemia. Nevertheless, they still leave an open question regarding the mechanism and pathology in the human brain, which emphasizes the establishment of a human cell-derived model system to provide more insights into the molecular basis of the disease.

3.2. In Vitro Models

Cell types of different origins are also used to model several aspects of bilirubin toxicity and its main sequelae such as oxidative stress, ER stress and DNA damage. In vitro cultures are being applied extensively to study bilirubin neurotoxicity. These cultures mainly include immortalized cell lines such as human neuroblastoma cell lines, HeLa cells, Hepa 1c1c7 mouse hepatoma cells and human U87 astrocytoma cells, as well as primary cultures of rat and mouse neurons, astrocytes, microglia, oligodendrocytes, endothelial cells, and embryonic fibroblasts (Figure 2). Even though these 2D systems do not mimic the in vivo cell–cell interactions nor the morphological and physiological complexities of the whole tissue, they still display various properties of the in vivo situation. Exposing different types of cells to different concentrations of UCB is one of the key methods in exploring BIND [13].

Hippocampal neurons are the most frequently used cell type for testing the response of neuronal cells to bilirubin. When exposed to bilirubin, these cells exhibit a reduction in axons and dendritic processes, increased cell death, oxidation, and mitochondrial dysfunction, as well as overexpression of protection mechanisms. Moreover, newly differentiated neuronal cell types that are less differentiated display higher sensitivity compared to mature differentiated neurons. Similarly, oligodendrocytes also display high bilirubin susceptibility. Oligodendrocytes downregulate MBP production with the consequent impairment of myelin sheath formation and neuronal axonal function.

Organotypic cultures are another form of ex vivo model that can be used to study bilirubin toxicity; however, there are limited studies exploiting these models, particularly using hippocampal slices. These models were able to demonstrate the impairment of synaptic plasticity due to bilirubin toxicity as well as the involvement of microglia in the UCB-induced neurotoxicity. Thus, 2D cultures have been employed as in vitro models for decades to study the cellular response in biochemical and biophysical directions and have contributed towards the significant advancement in understanding cell behavior and bioactivities [88]. Despite of being well accepted, it cannot be denied that the cell bioactivities and interactions in 2D cultures deviate remarkably compared to the in vivo responses. Considering the urge of having a model that more efficiently mimics in vivo conditions, 3D culture models such as spheroids or organoids have emerged as a potential platform to study different physiological and pathological processes. Employing another dimension around 2D cells with the extracellular matrix (ECM) markedly impacts the cellular fate with respect to proliferation, differentiation, mechano-response, and cell viability [88,89].

3.3. IPSCs and Organoids as Tools for Disease Modeling

Creating a model that properly recapitulates the molecular events underlying a specific neurological disorder is not an easy task. The majority of studies attempting to model BIND and CNS rely primarily on either mouse models, which poorly represent the human pathogenesis and phenotype, or post-mortem tissues, which usually only reflect the final stages of the disease [20,90]. Embryonic stem cells (ESCs) have indefinite self-renewal capacity and plasticity to differentiate into somatic cell types in the embryo, which makes this cell type valuable for studying the mechanisms involved in specialized cells and organ development. ESCs offer a great opportunity for regenerative medicine by generating specialized cells based on different degenerative diseases and replace those with the damaged tissues [91]. However, derivation and application of ESCs remain ethically controversial, as the derivation process involves the use of human inner-cell-mass cells isolated from blastocysts [92,93]. Moreover, it is not always convenient to obtain samples, and the reproducibility of results is affected. These concerns can be side-lined by using human-induced pluripotent stem cells (hiPSCs), as these cells hold great promise for increasing our fundamental understanding of human biology during early development and pave the way for future regeneration therapies and personalized medicine. Recent advancements in gene editing technologies such as clustered regularly inter-spaced short palindromic repeats

(CRISPR) have also made it possible to introduce genetic variants, for example through inducible gene knockout, thus opening new doors for in vitro disease modeling [94–99].

Further expansions in iPSC research have increasingly revealed the multifaceted use of these cells in modeling various diseases in vitro [17–20,100]. With the development of iPSCs, researchers have been able to replicate many diseases, including Parkinson's disease, Nijmegen Breakage Syndrome, and Alzheimer's disease, all by generating different types of cells that mimic the in vivo environment very closely [19,101–109]. For instance, deriving iPSCs from patients with genetic-based neurological conditions and differentiating them into neurons opens up more possibilities to closely observe the pathological mechanisms underlying the disease in vitro [106,110–112].

Shinya Yamanaka and Kazutoshi Takahashi introduced four defined factors; OCT3/4, SOX2, c-MYC, and KLF4, and established the pioneering protocol of generating iPS cells by reprogramming adult human fibroblasts [113,114]. Afterwards, Junying Yu et al. demonstrated another efficient combination of factors with OCT4, SOX2, NANOG, and LIN28 for reprogramming human somatic cells, which specifically exclude c-MYC [92]. Moreover, numerous studies have emerged in recent years, demonstrating the successful generation of iPSCs from different human somatic cells using integrating (retrovirus, lentivirus) and non-integrating (adenovirus, sendai virus, pSin plasmid, episomal plasmids, minicircle DNA) delivery systems [113,115–119]. With the other somatic cell (e.g., blood, urine cells)-derived iPSCs, it has been possible to avoid the invasive approach of skin biopsy, yet some methylation profile differences are still present between iPSCs and ESCs [120–124]. Nevertheless, iPSCs are ethically approved and considered identical regarding cell morphology, proliferation, and differentiation capacity, which also make it possible to generate large quantities of neuronal cultures for disease modeling, drug screening and therapy [19,92,125–127]. Additionally, iPSCs enable studying patient-specific disease conditions by reprogramming the cells obtained directly from the patient and therefore increase the scope to attain customized medication and therapy.

The iPSC-derived 2D monolayer model is the classical approach for obtaining specific neural cell types to enable the investigation of cellular and molecular mechanism associated with healthy and disease states. Neural stem cells (NSCs) or neural progenitor cells (NPCs) have a self-renewing capacity and can differentiate into the neuronal lineage, resulting in multiple types of brain cells during mammalian developmental and adult stage (fetal to postnatal, through adulthood) [128–130]. However, NSCs show heterogeneity and high regional specificity in adults, while the newly differentiated neurons derived from the primary progenitors migrate and intermingle with specific brain regions [130,131]. The type of generated neurons is determined by the neuroepithelial origin of NSCs, which is linked to NSC localization and developmental timing regions [131]. There are various established protocols for generating NSCs derived from iPSCs (Figure 3). Adherent iPSCs are used to generate embryoid bodies (EBs) and these are then with specific growth factors such as epidermal growth factor (EGF), fibroblast growth factor 2 (FGF-2) along with B27 (without retinoic acid) and N2 in the medium to achieve neural rosettes. Afterwards, these neural rosettes can be re-plated in a monolayer culture to obtain NSCs [132,133]. On the other hand, neural rosettes can also be generated without EB formation by using ESC and iPSC colonies, which are detached and then treated with EGF and FGF-2 to grow as cell aggregates. These cell aggregates have the potential to form neural rosettes and are able to differentiate into a range of both central and peripheral neural lineages [132,134–137]. However, the NSCs obtained from neural rosettes may provide a heterogeneous and inconsistent proportion of differentiated cells, which can be avoided by deriving pure cultures of specific types of brain cells from iPSCs with specific inductors [138–141]. Overall, neural rosette formation and differentiating into specific cell types can be employed as a potent in vitro system to study human neurological diseases by uncovering molecular pathways. Nonetheless, some major limitations include distinction among different iPSC lines, batch-to-batch variability, and growth of rosettes in an irregular and non-coordinated manner. Even though it is possible to characterize and measure the quality of individual rosettes using different assays

to some extent, the understanding of the dynamics from monolayer cells to a developed rosette is presently limited [137,142]. Conversely, generating 2D monolayered homogenous neuronal cultures by directed differentiations are financially and technically feasible, along with high-resolution cell morphology and great reproducibility. Guided differentiation to specific neuronal subtypes holds the potential for cell therapy or personalized medicine to treat neurodegenerative diseases [143,144]. However, the non-identical cellular age of the cells and the differences in differentiation, culture and maintenance procedure may also affect the comparability of the results [145].

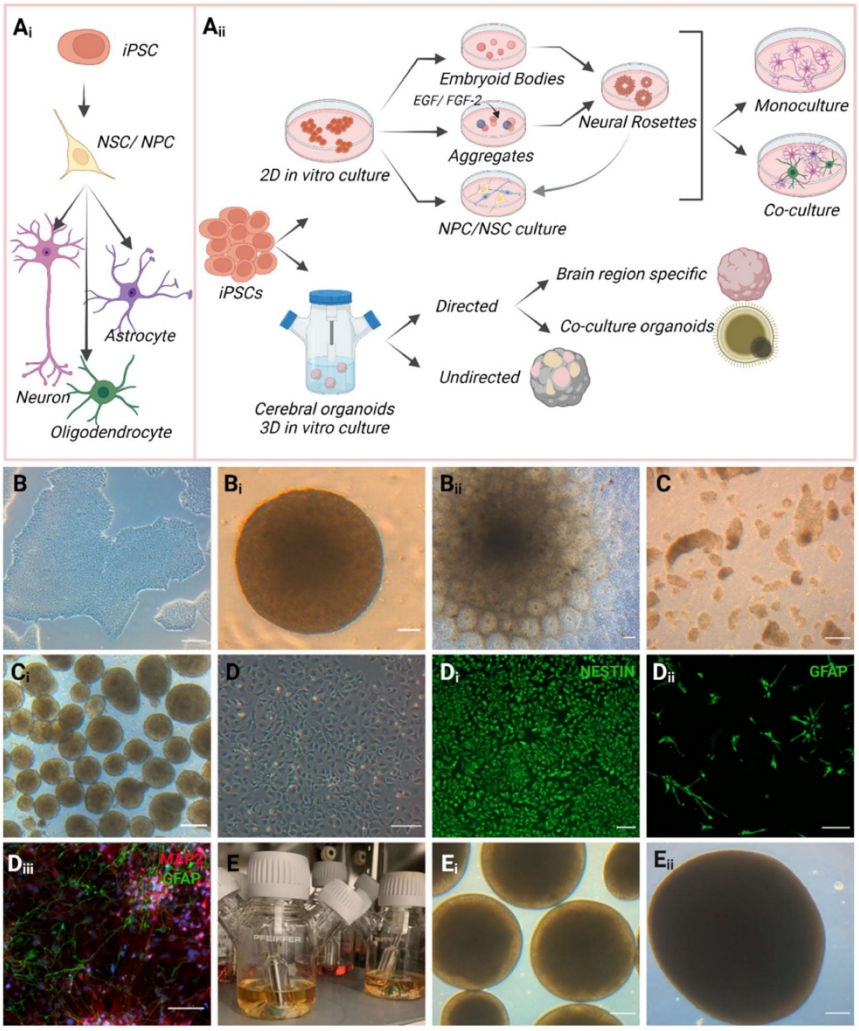

Figure 3. An overview of iPSC-derived 2D and 3D in vitro model generation with examples. Various protocols are available for generating iPSC-derived 2D and 3D in vitro models. (**Ai**) Schematic of iPSCs differentiation into neuronal cells. iPSC-derived neural progenitor cells (NPCs) have the capacity

to differentiate into mature neuronal cells such as neurons, astrocytes, and oligodendrocytes. (**Aii**) NPCs can be obtained from 2D mono-layered iPSCs cultured as embryoid bodies (EBs) or cell aggregation in suspension via neural rosettes formation, or by direct induction from iPSCs to NPCs in 2D. NPCs generated in both approaches can be used for mono- or co-culture of distinct types of neuronal cells. Three-dimensional organoid cultures can be generated in a directed or non-directed manner, depending on their application purpose. (**B**) CNS-I patient-derived iPSCs 2D monolayer culture. (**Bi**) EBs generated from CNS-I patient-derived iPSCs. (**Bii**) Neural rosettes formation by replating EBs in 2D. (**C**) iPSCs are dissociated from the 2D culture to generate aggregates. (**Ci**) Cell aggregates generate spheroids in a shaking incubator. (**D**) Monolayered NPC culture. Immunofluorescence staining shows. (**Di**) Nestin-positive NPC cultures. (**Dii**) GFAP positive astrocytes. (**Diii**) MAP2-positive neurons (red) and GFAP-positive astrocytes (green) co-culture. (**E**) iPSC-derived 3D organoid culture in spinner flask. (**Ei**,**Eii**) Organoids at different time points of culturing. (Scales in 100 μm, bright-field and immunofluorescent staining images are taken from unpublished work in our lab) (Created with BioRender.com, accessed on 21 August 2022).

The self-organizing capacity of hiPSCs to form whole tissues of various organ systems have evolved as a great advancement from 2D to 3D in vitro models [146–148]. In vivo methods provide complex and three-dimensional spatial arrangement to the cells, where circulating molecules, neighboring cell and the extracellular matrix are surrounding them [149]. Mono-layered mono- or co-culture systems lack this in vivo physiological relevance, which has a vital effect on cellular and physiological responses. In this regard, a three-dimensional system offers more physiological resemblance with respect to structural complexity. hiPSC-derived three-dimensional brain organoids recapitulate the key aspects of neurodevelopment along with reflecting some function of the system [150]. Three-dimensional organoids contain highly divergent cell types and subtypes, providing complex architecture and interplays with spatial organization. Being an intact tissue with spatial organization, organoid models offer the opportunity to observe the dynamic growth and development of the system over time [19]. Genetic mutations affect cell type, cell behavior, their interactions, neuronal network, and components of the various neurodevelopmental and physiological processes. iPSC-derived brain organoids afford studying these genetic mutations and multi-faceted brain diseases [108,148,151–153]. Moreover, being cultured in vitro, organoids provide easy accessibility genetically and for live assays [154].

Generally, cerebral organoids are composed of functioning neurons, astrocytes, oligodendrocytes and to some extent microglia [148]. Lancaster et al. established the protocol to generate self-patterned cerebral organoids containing forebrain, midbrain, hindbrain, and choroid plexus identity (non-directed differentiation) [148,155]. They used iPSCs to form EBs, which were gradually directed towards the neuroectodermal lineage, and then maintained these neuroectodermal tissues with extracellular matrix support in a spinning bioreactor to provide nutrition and a three-dimensional environment. With this approach, neural identity can be obtained in 8–10 days, resulting in defined brain regions by 20–30 days of culture, and the organoids can be cultivated for longer period to study later stages of neurodevelopment [154]. As the non-directed protocol relies on the cells' differentiation and self-organization capacity without providing any inductive signals, it is considered as intrinsic and a non-manipulated system [156]. Cerebral organoid research has significantly expanded within the last decade with the introduction of more complexity and specificity [157]. Relying on small molecules, individual brain-region-specific organoids can be generated by growth-factor-based manipulation, which consequently determine the cellular identities such as cerebral organoids with choroid plexus, hippocampus, retina and striatum [158–161]. The generation of organoids by co-culturing different cells is another advanced and innovative approach to enhance the model complexity and to investigate the cell–cell and cell–matrix interplays in a 3D environment during human brain development and disease [162–164]. The co-culture systems in organoid technology reveals the mechanism of stem cell interactions, which might be useful in regenerative medicine study [165]. For example, iPSC-derived microglia (cells or assembloids) can be integrated into the

midbrain organoids (generated from iPSCs), and then neurodegenerative and neuroinflammatory diseases can be investigated using this model. In contrast, microglia differentiation medium lacks neurotrophic factors, which are required for promoting dopaminergic neuron differentiation, resulting in lower numbers of dopaminergic neurons [166]. Consequently, the incompatibility between the small molecules in the medium might interact and affect the quantity and quality of existing cell types. Therefore, it is challenging to compose a perfect culture medium for co-culture organoids, as these comprise different cell types, where individual cell types require distinct medium compositions [165]. Additionally, a major drawback includes different proliferation rates of the co-cultured cells in the system, which might affect the maturity of the organoids and limit the long-term culture. On the other hand, release of paracrine factors by one cell type might affect the other cells either positively or negatively in this system [167,168]. Since both directed and non-directed organoid generation processes have benefits and drawbacks, the application of each should be determined according to the purpose of the study (Figure 3).

Considering various incorporated features in cerebral organoids, these models are closer to the developing human brain and mimic the neural environment much better compared to other in vitro models. This facilitates the understanding of disease pathology, drug mechanism and customized medication [108,153,169–171]. Cerebral organoids represent a higher degree of maturation and developmental dynamics mimicking the early second trimester of the fetal brain tissue; nevertheless, the accurate human brain equivalent age of the organoids still remains an unanswered question [172]. Furthermore, the organoid model shows high batch-to-batch variability in common with other iPSC-based models and requires sophisticated methods [19]. During slow development of the organoids, a tissue-degenerated necrotic core tends to form in the center due to the lack of optimal diffusion of nutrients and metabolites. Although the culture medium is oxygenated in the bioreactors, this is not enough to support culture for a longer period [148]. Despite the limitations, iPSC-derived brain organoids are a promising tool for 3D in vitro model systems, as they display functions and circuitry comparable to the human brain [148]. Even though they do not fully recapitulate the complexities of the human brain, they can still be a valuable study tool, as they are composed of distinct neural cell types important for the central nervous system [173]. Furthermore, human brain organoids have revealed useful insights into human brain development and successfully helped to model a variety of neurological disorders such as microcephaly, Timothy syndrome, and Nijmegen Breakage Syndrome, as well as brain tumors such as gliomas [108,148,174–178]. All of these models offer a solid platform for future of brain organoids as a valid tool for studying neurological disorders affecting the human brain [179].

UHB is an ailment observed in the first postnatal week, which can lead to acute or chronic UCB encephalopathy. The neonates show vulnerability towards UCB and have an increased risk associated with particular conditions, such as premature birth, sepsis, and hypoxia. Pre-term and low-birth-weight infants are even more vulnerable towards BIND due to neurodevelopmental immaturity, when sepsis or infection is incorporated [5,180,181]. Since brain organoids recapitulate key aspects of neurodevelopment and reflect certain functions of the system, they can therefore be exposed to UCB for modeling BIND. Both the immature and mature stage of cerebral organoids can be exposed to UCB for shorter (4–5 h) and longer (72 h–several days) periods to mimic the acute and chronic effect of UCB in the CNS. As UCB is a lipophilic compound, it should be able to penetrate the organoids. Additionally, iPSCs derived from CNS-I patients can be used to generate brain organoids, which will model the disease more precisely due to defective *UGT1A1*, and these organoids can be exposed to UCB to mimic the hyperbilirubinemic condition in the CNS [112]. As autopsy revealed the presence of UCB in neurons, astrocytes, neuronal process and so on, divergent cell types containing organoids will help us to understand the pathophysiology of BIND. Neurons are known to be more susceptible to UCB than astrocytes and generally demonstrate a higher level of ROS, protein oxidation and lipid peroxidation upon UCB exposure [71,182]. On the other hand, astrocytes cause morphological changes in

mitochondria and ER when affected by high concentrations of UCB, leading to oxidative stress and cell death [183,184]. Furthermore, high levels of ROS produced by neurons upon UCB exposure results in oxidative stress in microglia [185]. Overall, UCB exposure affects the redox status of neurons and glial cells and induce inflammation with increased ROS, thus resulting in cell death in the CNS [71,182]. As cerebral organoids are composed of neuronal cell types and subtypes with some functionality and network complexity, it is possible to recapitulate the altered redox status induced by UCB toxicity and consecutive inflammatory responses using this model. However, it should be noted that bilirubin might also be considered as a neuroprotective compound when the concentration is below 100 nM [5,62]. In this regard, a kill curve should be performed to identify the suitable concentration for UCB, which can be used to mimic the hyperbilirubinemic condition in the CNS.

Furthermore, co-morbidity along with the degree and timing of UHB can affect an infant to develop one or multiple defects from the BIND spectrum. Therefore, studying the independent correlation of UHB with each neurodevelopmental disorder individually is not sufficient. Appropriate statistical analyses and power can be applied to evaluate possible co-morbidities of multiple neurodevelopmental disorders within the BIND spectrum, which may help us to define the association of each neurodevelopmental disorder with bilirubin-induced neurotoxicity [21,186,187]. Some of the parameters of bilirubin-induced neurotoxicity measurement include assessment of oxidative stress, DNA and RNA damage, post-transcriptional modifications, bilirubin accumulation in the brain and transporters, ER stress, inflammation and autophagy, which are also possible to study in the cerebral organoid model [13,70]. For instance, after UCB exposure to cerebral organoids, oxidative stress or impaired redox status can be monitored by glutathione (GSH) and oxidized glutathione (GSSG) measurements, where a lower ratio of [GSH]/[GSSG] indicates an increased oxidative state [70]. From transcriptome analysis of the treated organoids, bilirubin-induced ER responses can be observed by altered gene expression and regulation of ER stress-related genes (e.g., CHOP, ATF3, FAS) [74]. Gene ontology analysis can also reveal the connection between ER and inflammatory responses through distinct but relevant pathways (e.g., activation of p-ERK, NF-κB pathways) [70,188]. Moreover, assessment of pro-inflammatory mediators such as IL-6, IL-8, TNF-α, IL-1β by cytokine array or ELISA, can help uncover bilirubin-mediated inflammation [189,190]. UCB induced increased oxidative stress and ER stress, and neurodegeneration-mediated inflammation leads to apoptotic cell death, which can be detected by deoxynucleotidyl transferase-mediated deoxyuridine nick-end labeling (TUNEL) assay [70].

4. Concluding Remarks

To date, there are very few effective treatment options for CNS-I. To lower plasma bilirubin levels and prevent bilirubin encephalopathy, patients undergo daily phototherapy treatments, which inevitably become less effective as the patients age. Exchange transfusion is also sometimes used as an emergency treatment for neonates to rapidly lower serum bilirubin concentrations; however, this approach has been associated with serious complications, such as thrombocytopenia, portal vein thrombosis, necrotizing enterocolitis, and sepsis [44]. Liver transplantation remains the only effective treatment for this life-threatening disease, even though it does not reverse or alleviate pre-existing neurological damage [2,36,43–45].

Severe neonatal jaundice and hyperbilirubinemia remain a cause of devastating neurological damage in infants. Although this occurrence is rare, it can be completely avoided if the neonates receive treatment on time and the medical professionals prevent early discharge [12]. Currently, there is a clear gap in the knowledge we possess on the molecular mechanisms underlying this neurological damage. Therefore, creating a model of BIND based on genetically inherited disorders of the *UGT1A1* gene, such as CNS Type I and II, can help us further understand these mechanisms.

Possible therapeutic approaches include anti-inflammatory-based medicines, gene manipulation and albumin infusion. Some other promising approaches include the modulation of nuclear receptors, cytochromes or BLVR activity, to control bilirubin production or to stimulate alternative bilirubin-disposal pathways. However, further research is needed before these techniques can be applied clinically. To shed light on human biology and health, a thorough understanding of the molecular pathways leading to bilirubin neurotoxicity is critical.

Other potential therapies include hepatocyte transplantation, during which about 5–15% of the liver is replaced by transplanted hepatocytes, as well as gene therapy. Injections of naked plasmid DNA and adeno-associated virus gene therapies are currently being investigated, as preclinical models have been quite promising [44]. The constant hope with new emerging iPSC-derived 3D brain organoid models is that they can help shed light onto developing more effective ways of handling BIND and inherited unconjugated bilirubinemia disorders in the near future. Eventually, this model will enhance our understanding of the etiology underlying BIND and its pathology in the human CNS. This knowledge will aid in the development of drugs and future clinical applications.

Author Contributions: A.I.P. wrote, formulated tables and edited the manuscript. S.S. wrote, edited and helped with the figures. J.A. conceptualized the work, edited the manuscript, acquired funding and supervised the study. All authors have read and agreed to the published version of the manuscript.

Funding: J.A. acknowledges funding from the Medical Faculty of Heinrich Heine University, Duesseldorf, Germany.

Informed Consent Statement: Not applicable.

Acknowledgments: The authors would like to acknowledge Leon-Phillip Szepanowski for providing some of the immunofluorescence images used in this work.

Conflicts of Interest: The authors declare no conflict of interest.

References

1. Fevery, J. Bilirubin in clinical practice: A review. *Liver Int.* **2008**, *28*, 592–605. [CrossRef] [PubMed]
2. Memon, N.; Weinberger, B.I.; Hegyi, T.; Aleksunes, L.M. Inherited disorders of bilirubin clearance. *Pediatr. Res.* **2016**, *79*, 378–386. [CrossRef] [PubMed]
3. Singh, A.; Jialal, I. Unconjugated Hyperbilirubinemia. In *StatPearls*; StatPearls Publishing LLC.: Treasure Island, FL, USA, 2021.
4. Bortolussi, G.; Muro, A.F. Advances in understanding disease mechanisms and potential treatments for Crigler–Najjar syndrome. *Exp. Opin. Orphan Drugs* **2018**, *6*, 425–439. [CrossRef]
5. Brites, D. The evolving landscape of neurotoxicity by unconjugated bilirubin: Role of glial cells and inflammation. *Front. Pharmacol.* **2012**, *3*, 88. [CrossRef]
6. Watchko, J.F.; Tiribelli, C. Bilirubin-induced neurologic damage–mechanisms and management approaches. *N. Engl. J. Med.* **2013**, *369*, 2021–2030. [CrossRef]
7. Rawat, V.; Bortolussi, G.; Gazzin, S.; Tiribelli, C.; Muro, A.F. Bilirubin-Induced Oxidative Stress Leads to DNA Damage in the Cerebellum of Hyperbilirubinemic Neonatal Mice and Activates DNA Double-Strand Break Repair Pathways in Human Cells. *Oxid. Med. Cell Longev.* **2018**, *2018*, 1801243. [CrossRef]
8. Stocker, R.; Ames, B.N. Potential role of conjugated bilirubin and copper in the metabolism of lipid peroxides in bile. *Proc. Natl. Acad. Sci. USA* **1987**, *84*, 8130–8134. [CrossRef]
9. Bulmer, A.C.; Blanchfield, J.T.; Toth, I.; Fassett, R.G.; Coombes, J.S. Improved resistance to serum oxidation in Gilbert'ss syndrome: A mechanism for cardiovascular protection. *Atherosclerosis* **2008**, *199*, 390–396. [CrossRef]
10. Jangi, S.; Otterbein, L.; Robson, S. The molecular basis for the immunomodulatory activities of unconjugated bilirubin. *Int. J. Biochem. Cell Biol.* **2013**, *45*, 2843–2851. [CrossRef]
11. Vitek, L.; Ostrow, J.D. Bilirubin chemistry and metabolism; harmful and protective aspects. *Curr. Pharm. Des.* **2009**, *15*, 2869–2883. [CrossRef]
12. Gazzin, S.; Tiribelli, C. Bilirubin-induced neurological damage. *J. Matern. Fetal. Neonatal. Med.* **2011**, *24* (Suppl. 1), 154–155. [CrossRef]
13. Bortolussi, G.; Muro, A.F. Experimental models assessing bilirubin neurotoxicity. *Pediatr. Res.* **2020**, *87*, 17–25. [CrossRef] [PubMed]

14. Ahdab-Barmada, M.; Moossy, J. The neuropathology of kernicterus in the premature neonate: Diagnostic problems. *J. Neuropathol. Exp. Neurol.* **1984**, *43*, 45–56. [CrossRef] [PubMed]
15. Dal Ben, M.; Bottin, C.; Zanconati, F.; Tiribelli, C.; Gazzin, S. Evaluation of region selective bilirubin-induced brain damage as a basis for a pharmacological treatment. *Sci. Rep.* **2017**, *7*, 41032. [CrossRef] [PubMed]
16. Watchko, J.F. Kernicterus and the molecular mechanisms of bilirubin-induced CNS injury in newborns. *Neuromolecular Med.* **2006**, *8*, 513–529. [CrossRef]
17. Drews, K.; Jozefczuk, J.; Prigione, A.; Adjaye, J. Human induced pluripotent stem cells–from mechanisms to clinical applications. *J. Mol. Med.* **2012**, *90*, 735–745. [CrossRef]
18. Kunkanjanawan, T.; Noisa, P.; Parnpai, R. Modeling neurological disorders by human induced pluripotent stem cells. *J. Biomed. Biotechnol.* **2011**, *2011*, 350131. [CrossRef]
19. Logan, S.; Arzua, T.; Canfield, S.G.; Seminary, E.R.; Sison, S.L.; Ebert, A.D.; Bai, X. Studying Human Neurological Disorders Using Induced Pluripotent Stem Cells: From 2D Monolayer to 3D Organoid and Blood Brain Barrier Models. *Compr. Physiol.* **2019**, *9*, 565–611. [CrossRef]
20. Marchetto, M.C.; Brennand, K.J.; Boyer, L.F.; Gage, F.H. Induced pluripotent stem cells (iPSCs) and neurological disease modeling: Progress and promises. *Hum. Mol. Genet.* **2011**, *20*, R109–R115. [CrossRef]
21. Amin, S.B.; Smith, T.; Timler, G. Developmental influence of unconjugated hyperbilirubinemia and neurobehavioral disorders. *Pediatr. Res.* **2019**, *85*, 191–197. [CrossRef]
22. Jew, J.Y.; Sandquist, D. CNS changes in hyperbilirubinemia. Functional implications. *Arch. Neurol.* **1979**, *36*, 149–154. [CrossRef] [PubMed]
23. Aron, A.R.; Poldrack, R.A. Cortical and subcortical contributions to Stop signal response inhibition: Role of the subthalamic nucleus. *J. Neurosci.* **2006**, *26*, 2424–2433. [CrossRef] [PubMed]
24. Frank, M.J.; Loughry, B.; O'Reilly, R.C. Interactions between frontal cortex and basal ganglia in working memory: A computational model. *Cogn. Affect Behav. Neurosci.* **2001**, *1*, 137–160. [CrossRef] [PubMed]
25. Burgess, N.; Maguire, E.A.; O'Keefe, J. The human hippocampus and spatial and episodic memory. *Neuron* **2002**, *35*, 625–641. [CrossRef]
26. Amin, S.B.; Prinzing, D.; Myers, G. Hyperbilirubinemia and language delay in premature infants. *Pediatrics* **2009**, *123*, 327–331. [CrossRef]
27. Amin, S.B. Clinical assessment of bilirubin-induced neurotoxicity in premature infants. *Semin. Perinatol.* **2004**, *28*, 340–347. [CrossRef]
28. King, C.D.; Rios, G.R.; Green, M.D.; Tephly, T.R. UDP-glucuronosyltransferases. *Curr. Drug. Metab.* **2000**, *1*, 143–161. [CrossRef]
29. Kadakol, A.; Ghosh, S.S.; Sappal, B.S.; Sharma, G.; Chowdhury, J.R.; Chowdhury, N.R. Genetic lesions of bilirubin uridine-diphosphoglucuronate glucuronosyltransferase (UGT1A1) causing Crigler-Najjar and Gilbert syndromes: Correlation of genotype to phenotype. *Hum. Mutat.* **2000**, *16*, 297–306. [CrossRef]
30. Owens, I.S.; Basu, N.K.; Banerjee, R. UDP-glucuronosyltransferases: Gene structures of UGT1 and UGT2 families. *Methods Enzymol.* **2005**, *400*, 1–22. [CrossRef]
31. Ritter, J.K.; Crawford, J.M.; Owens, I.S. Cloning of two human liver bilirubin UDP-glucuronosyltransferase cDNAs with expression in COS-1 cells. *J. Biol. Chem.* **1991**, *266*, 1043–1047.
32. Canu, G.; Minucci, A.; Zuppi, C.; Capoluongo, E. Gilbert and Crigler Najjar syndromes: An update of the UDP-glucuronosyltransferase 1A1 (UGT1A1) gene mutation database. *Blood Cells Mol. Dis.* **2013**, *50*, 273–280. [CrossRef] [PubMed]
33. Skierka, J.M.; Kotzer, K.E.; Lagerstedt, S.A.; O'Kane, D.J.; Baudhuin, L.M. UGT1A1 genetic analysis as a diagnostic aid for individuals with unconjugated hyperbilirubinemia. *J. Pediatr.* **2013**, *162*, 1146–1152. [CrossRef] [PubMed]
34. Crigler, J.F., Jr.; Najjar, V.A. Congenital familial nonhemolytic jaundice with kernicterus. *Pediatrics* **1952**, *10*, 169–180. [PubMed]
35. Ritter, J.K.; Yeatman, M.T.; Ferreira, P.; Owens, I.S. Identification of a genetic alteration in the code for bilirubin UDP-glucuronosyltransferase in the UGT1 gene complex of a Crigler-Najjar type I patient. *J. Clin. Investig.* **1992**, *90*, 150–155. [CrossRef]
36. Sticova, E.; Jirsa, M. New insights in bilirubin metabolism and their clinical implications. *World J. Gastroenterol.* **2013**, *19*, 6398–6407. [CrossRef]
37. Labrune, P.; Myara, A.; Hadchouel, M.; Ronchi, F.; Bernard, O.; Trivin, F.; Chowdhury, N.R.; Chowdhury, J.R.; Munnich, A.; Odievre, M. Genetic heterogeneity of Crigler-Najjar syndrome type I: A study of 14 cases. *Hum. Genet.* **1994**, *94*, 693–697. [CrossRef]
38. Torres, A.E.; Lyons, A.B.; Hamzavi, I.H.; Lim, H.W. Role of phototherapy in the era of biologics. *J. Am. Acad. Dermatol.* **2021**, *84*, 479–485. [CrossRef]
39. Vreman, H.J.; Wong, R.J.; Stevenson, D.K. Phototherapy: Current methods and future directions. *Semin. Perinatol.* **2004**, *28*, 326–333. [CrossRef] [PubMed]
40. Morris, B.H.; Oh, W.; Tyson, J.E.; Stevenson, D.K.; Phelps, D.L.; O'Shea, T.M.; McDavid, G.E.; Perritt, R.L.; Van Meurs, K.P.; Vohr, B.R.; et al. Aggressive vs. conservative phototherapy for infants with extremely low birth weight. *N. Engl. J. Med.* **2008**, *359*, 1885–1896. [CrossRef]
41. Schulz, S.; Wong, R.J.; Vreman, H.J.; Stevenson, D.K. Metalloporphyrins - an update. *Front. Pharmacol.* **2012**, *3*, 68. [CrossRef]

42. Lin, S.; Wei, X.; Bales, K.R.; Paul, A.B.; Ma, Z.; Yan, G.; Paul, S.M.; Du, Y. Minocycline blocks bilirubin neurotoxicity and prevents hyperbilirubinemia-induced cerebellar hypoplasia in the Gunn rat. *Eur. J. Neurosci.* **2005**, *22*, 21–27. [CrossRef] [PubMed]
43. Labrune, P.; Odievre, M. Toward a treatment of Crigler-Najjar syndrome? *Arch. Fr. Pediatr.* **1992**, *49*, 467–468. [PubMed]
44. Dhawan, A.; Lawlor, M.W.; Mazariegos, G.V.; McKiernan, P.; Squires, J.E.; Strauss, K.A.; Gupta, D.; James, E.; Prasad, S. Disease burden of Crigler-Najjar syndrome: Systematic review and future perspectives. *J. Gastroenterol. Hepatol.* **2020**, *35*, 530–543. [CrossRef] [PubMed]
45. Fitzpatrick, E.; Mtegha, M.; Dhawan, A. Crigler-Najjar syndrome: Therapeutic options and consequences of mutations in the UGT1A1 complex. *Expert Rev. Endocrinol. Metab.* **2008**, *3*, 725–737. [CrossRef]
46. Maines, M.D.; Trakshel, G.M. Tin-protoporphyrin: A potent inhibitor of hemoprotein-dependent steroidogenesis in rat adrenals and testes. *J. Pharmacol. Exp. Ther.* **1992**, *260*, 909–916.
47. Kappas, A.; Drummond, G.S.; Galbraith, R.A. Prolonged clinical use of a heme oxygenase inhibitor: Hematological evidence for an inducible but reversible iron-deficiency state. *Pediatrics* **1993**, *91*, 537–539. [CrossRef]
48. Brites, D. Bilirubin injury to neurons and glial cells: New players, novel targets, and newer insights. *Semin. Perinatol.* **2011**, *35*, 114–120. [CrossRef]
49. Hansen, T.W. Pioneers in the scientific study of neonatal jaundice and kernicterus. *Pediatrics* **2000**, *106*, E15. [CrossRef]
50. Brites, D.; Fernandes, A.; Falcao, A.S.; Gordo, A.C.; Silva, R.F.; Brito, M.A. Biological risks for neurological abnormalities associated with hyperbilirubinemia. *J. Perinatol.* **2009**, *29*, S8–S13. [CrossRef]
51. Fernandes, A.; Falcao, A.S.; Abranches, E.; Bekman, E.; Henrique, D.; Lanier, L.M.; Brites, D. Bilirubin as a determinant for altered neurogenesis, neuritogenesis, and synaptogenesis. *Dev. Neurobiol.* **2009**, *69*, 568–582. [CrossRef]
52. Genc, S.; Genc, K.; Kumral, A.; Baskin, H.; Ozkan, H. Bilirubin is cytotoxic to rat oligodendrocytes in vitro. *Brain Res.* **2003**, *985*, 135–141. [CrossRef]
53. Deganuto, M.; Cesaratto, L.; Bellarosa, C.; Calligaris, R.; Vilotti, S.; Renzone, G.; Foti, R.; Scaloni, A.; Gustincich, S.; Quadrifoglio, F.; et al. A proteomic approach to the bilirubin-induced toxicity in neuronal cells reveals a protective function of DJ-1 protein. *Proteomics* **2010**, *10*, 1645–1657. [CrossRef] [PubMed]
54. Gazzin, S.; Vitek, L.; Watchko, J.; Shapiro, S.M.; Tiribelli, C. A Novel Perspective on the Biology of Bilirubin in Health and Disease. *Trends Mol. Med.* **2016**, *22*, 758–768. [CrossRef] [PubMed]
55. Dudau, M.; Codrici, E.; Tanase, C.; Gherghiceanu, M.; Enciu, A.M.; Hinescu, M.E. Caveolae as Potential Hijackable Gates in Cell Communication. *Front. Cell Dev. Biol.* **2020**, *8*, 581732. [CrossRef]
56. Choi, D.W. Excitotoxicity: Still Hammering the Ischemic Brain in 2020. *Front. Neurosci.* **2020**, *14*, 579953. [CrossRef]
57. Mattson, M.P. Excitotoxicity. In *Stress: Physiology, Biochemistry, and Pathology*; Academic Press: Cambridge, MA, USA, 2019; pp. 125–134.
58. Dennery, P.A.; Seidman, D.S.; Stevenson, D.K. Neonatal hyperbilirubinemia. *N. Engl. J. Med.* **2001**, *344*, 581–590. [CrossRef]
59. Gourley, G.R. Bilirubin metabolism and kernicterus. *Adv. Pediatr.* **1997**, *44*, 173–229.
60. Cardoso, F.L.; Brites, D.; Brito, M.A. Looking at the blood-brain barrier: Molecular anatomy and possible investigation approaches. *Brain Res. Rev.* **2010**, *64*, 328–363. [CrossRef]
61. Daneman, R.; Prat, A. The blood-brain barrier. *Cold Spring Harb. Perspect. Biol.* **2015**, *7*, a020412. [CrossRef]
62. Doré, S.; Takahashi, M.; Ferris, C.D.; Zakhary, R.; Hester, L.D.; Guastella, D.; Snyder, S.H. Bilirubin, formed by activation of heme oxygenase-2, protects neurons against oxidative stress injury. *Proc. Natl. Acad. Sci. USA* **1999**, *96*, 2445–2450. [CrossRef]
63. Brito, M.A.; Brites, D.; Butterfield, D.A. A link between hyperbilirubinemia, oxidative stress and injury to neocortical synaptosomes. *Brain Res.* **2004**, *1026*, 33–43. [CrossRef] [PubMed]
64. Asad, S.F.; Singh, S.; Ahmad, A.; Khan, N.U.; Hadi, S.M. Prooxidant and antioxidant activities of bilirubin and its metabolic precursor biliverdin: A structure-activity study. *Chem. Biol. Interact.* **2001**, *137*, 59–74. [CrossRef]
65. Dani, C.; Martelli, E.; Bertini, G.; Pezzati, M.; Filippi, L.; Rossetti, M.; Rizzuti, G.; Rubaltelli, F.F. Plasma bilirubin level and oxidative stress in preterm infants. *Arch. Dis. Child Fetal. Neonatal. Ed.* **2003**, *88*, F119–F123. [CrossRef] [PubMed]
66. Dani, C.; Poggi, C.; Pratesi, S. Bilirubin and oxidative stress in term and preterm infants. *Free Radic. Res.* **2019**, *53*, 2–7. [CrossRef] [PubMed]
67. Midan, D.A.R.; Bahbah, W.A.; Bayomy, N.R.; Ashour, N.M. Clinical Assessment of Neuroinflammatory Markers and Antioxidants in Neonates with Hyperbilirubinemia and Their Association with Acute Bilirubin Encephalopathy. *Children* **2022**, *9*, 559. [CrossRef]
68. Vitek, L. Bilirubin as a signaling molecule. *Med. Res. Rev.* **2020**, *40*, 1335–1351. [CrossRef]
69. Droge, W. Free radicals in the physiological control of cell function. *Physiol. Rev.* **2002**, *82*, 47–95. [CrossRef]
70. Yueh, M.F.; Chen, S.; Nguyen, N.; Tukey, R.H. Developmental onset of bilirubin-induced neurotoxicity involves Toll-like receptor 2-dependent signaling in humanized UDP-glucuronosyltransferase1 mice. *J. Biol. Chem.* **2014**, *289*, 4699–4709. [CrossRef]
71. Brito, M.A.; Rosa, A.I.; Falcao, A.S.; Fernandes, A.; Silva, R.F.; Butterfield, D.A.; Brites, D. Unconjugated bilirubin differentially affects the redox status of neuronal and astroglial cells. *Neurobiol. Dis.* **2008**, *29*, 30–40. [CrossRef]
72. Daood, M.J.; Hoyson, M.; Watchko, J.F. Lipid peroxidation is not the primary mechanism of bilirubin-induced neurologic dysfunction in jaundiced Gunn rat pups. *Pediatr. Res.* **2012**, *72*, 455–459. [CrossRef]

73. Bortolussi, G.; Codarin, E.; Antoniali, G.; Vascotto, C.; Vodret, S.; Arena, S.; Cesaratto, L.; Scaloni, A.; Tell, G.; Muro, A.F. Impairment of enzymatic antioxidant defenses is associated with bilirubin-induced neuronal cell death in the cerebellum of Ugt1 KO mice. *Cell Death Dis.* **2015**, *6*, e1739. [CrossRef] [PubMed]
74. Vodret, S.; Bortolussi, G.; Jasprova, J.; Vitek, L.; Muro, A.F. Inflammatory signature of cerebellar neurodegeneration during neonatal hyperbilirubinemia in Ugt1 (-/-) mouse model. *J. Neuroinflamm.* **2017**, *14*, 64. [CrossRef] [PubMed]
75. Vaz, A.R.; Silva, S.L.; Barateiro, A.; Falcão, A.S.; Fernandes, A.; Brito, M.A.; Brites, D. Selective vulnerability of rat brain regions to unconjugated bilirubin. *Mol. Cell Neurosci.* **2011**, *48*, 82–93. [CrossRef]
76. Barateiro, A.; Chen, S.; Yueh, M.F.; Fernandes, A.; Domingues, H.S.; Relvas, J.; Barbier, O.; Nguyen, N.; Tukey, R.H.; Brites, D. Reduced Myelination and Increased Glia Reactivity Resulting from Severe Neonatal Hyperbilirubinemia. *Mol. Pharmacol.* **2016**, *89*, 84–93. [CrossRef]
77. Silva, S.L.; Vaz, A.R.; Diogenes, M.J.; van Rooijen, N.; Sebastiao, A.M.; Fernandes, A.; Silva, R.F.; Brites, D. Neuritic growth impairment and cell death by unconjugated bilirubin is mediated by NO and glutamate, modulated by microglia, and prevented by glycoursodeoxycholic acid and interleukin-10. *Neuropharmacology* **2012**, *62*, 2398–2408. [CrossRef] [PubMed]
78. Falcao, A.S.; Silva, R.F.; Vaz, A.R.; Silva, S.L.; Fernandes, A.; Brites, D. Cross-talk between neurons and astrocytes in response to bilirubin: Early beneficial effects. *Neurochem. Res.* **2013**, *38*, 644–659. [CrossRef] [PubMed]
79. Vianello, E.; Zampieri, S.; Marcuzzo, T.; Tordini, F.; Bottin, C.; Dardis, A.; Zanconati, F.; Tiribelli, C.; Gazzin, S. Histone acetylation as a new mechanism for bilirubin-induced encephalopathy in the Gunn rat. *Sci. Rep.* **2018**, *8*, 13690. [CrossRef] [PubMed]
80. Lilja, T.; Heldring, N.; Hermanson, O. Like a rolling histone: Epigenetic regulation of neural stem cells and brain development by factors controlling histone acetylation and methylation. *Biochim. Biophys. Acta* **2013**, *1830*, 2354–2360. [CrossRef]
81. Fagiolini, M.; Jensen, C.L.; Champagne, F.A. Epigenetic influences on brain development and plasticity. *Curr. Opin. Neurobiol.* **2009**, *19*, 207–212. [CrossRef]
82. Ma, L.H.; Yan, J.; Jiao, X.H.; Zhou, C.H.; Wu, Y.Q. The Role of Epigenetic Modifications in Neurotoxicity Induced by Neonatal General Anesthesia. *Front. Mol. Neurosci.* **2022**, *15*, 877263. [CrossRef]
83. Shein, N.A.; Shohami, E. Histone deacetylase inhibitors as therapeutic agents for acute central nervous system injuries. *Mol. Med.* **2011**, *17*, 448–456. [CrossRef] [PubMed]
84. Covington, H.E., 3rd; Maze, I.; Sun, H.; Bomze, H.M.; DeMaio, K.D.; Wu, E.Y.; Dietz, D.M.; Lobo, M.K.; Ghose, S.; Mouzon, E.; et al. A role for repressive histone methylation in cocaine-induced vulnerability to stress. *Neuron* **2011**, *71*, 656–670. [CrossRef] [PubMed]
85. Brito, M.A.; Zurolo, E.; Pereira, P.; Barroso, C.; Aronica, E.; Brites, D. Cerebellar axon/myelin loss, angiogenic sprouting, and neuronal increase of vascular endothelial growth factor in a preterm infant with kernicterus. *J. Child Neurol.* **2012**, *27*, 615–624. [CrossRef] [PubMed]
86. Gunn, C.K. Hereditary Acholuric Jaundice in the Rat. *Can. Med. Assoc. J.* **1944**, *50*, 230–237. [PubMed]
87. Nguyen, N.; Bonzo, J.A.; Chen, S.; Chouinard, S.; Kelner, M.J.; Hardiman, G.; Belanger, A.; Tukey, R.H. Disruption of the ugt1 locus in mice resembles human Crigler-Najjar type I disease. *J. Biol. Chem.* **2008**, *283*, 7901–7911. [CrossRef]
88. Duval, K.; Grover, H.; Han, L.H.; Mou, Y.; Pegoraro, A.F.; Fredberg, J.; Chen, Z. Modeling Physiological Events in 2D vs. 3D Cell Culture. *Physiology* **2017**, *32*, 266–277. [CrossRef]
89. Bonnier, F.; Keating, M.E.; Wróbel, T.P.; Majzner, K.; Baranska, M.; Garcia-Munoz, A.; Blanco, A.; Byrne, H.J. Cell viability assessment using the Alamar blue assay: A comparison of 2D and 3D cell culture models. *Toxicol. In Vitro* **2015**, *29*, 124–131. [CrossRef]
90. McKinney, C.E. Using induced pluripotent stem cells derived neurons to model brain diseases. *Neural Regen. Res.* **2017**, *12*, 1062–1067. [CrossRef]
91. Vazin, T.; Freed, W.J. Human embryonic stem cells: Derivation, culture, and differentiation: A review. *Restor. Neurol. Neurosci.* **2010**, *28*, 589–603. [CrossRef]
92. Yu, J.; Vodyanik, M.A.; Smuga-Otto, K.; Antosiewicz-Bourget, J.; Frane, J.L.; Tian, S.; Nie, J.; Jonsdottir, G.A.; Ruotti, V.; Stewart, R.; et al. Induced pluripotent stem cell lines derived from human somatic cells. *Science* **2007**, *318*, 1917–1920. [CrossRef]
93. Sun, Q.; Zhang, Z.; Sun, Z. The potential and challenges of using stem cells for cardiovascular repair and regeneration. *Genes Dis.* **2014**, *1*, 113–119. [CrossRef] [PubMed]
94. Chen, Y.; Cao, J.; Xiong, M.; Petersen, A.J.; Dong, Y.; Tao, Y.; Huang, C.T.; Du, Z.; Zhang, S.C. Engineering Human Stem Cell Lines with Inducible Gene Knockout using CRISPR/Cas9. *Cell Stem Cell* **2015**, *17*, 233–244. [CrossRef] [PubMed]
95. Waddington, S.N.; Privolizzi, R.; Karda, R.; O'Neill, H.C. A Broad Overview and Review of CRISPR-Cas Technology and Stem Cells. *Curr. Stem Cell Rep.* **2016**, *2*, 9–20. [CrossRef] [PubMed]
96. Ferreccio, A.; Mathieu, J.; Detraux, D.; Somasundaram, L.; Cavanaugh, C.; Sopher, B.; Fischer, K.; Bello, T.; A, M.H.; Levy, S.; et al. Inducible CRISPR genome editing platform in naive human embryonic stem cells reveals JARID2 function in self-renewal. *Cell Cycle* **2018**, *17*, 535–549. [CrossRef]
97. Lane, A.; Jovanovic, K.; Shortall, C.; Ottaviani, D.; Panes, A.B.; Schwarz, N.; Guarascio, R.; Hayes, M.J.; Palfi, A.; Chadderton, N.; et al. Modeling and Rescue of RP2 Retinitis Pigmentosa Using iPSC-Derived Retinal Organoids. *Stem Cell Rep.* **2020**, *15*, 67–79. [CrossRef]
98. Dell' Amico, C.; Tata, A.; Pellegrino, E.; Onorati, M.; Conti, L. Genome editing in stem cells for genetic neurodisorders. *Prog. Mol. Biol. Transl. Sci.* **2021**, *182*, 403–438. [CrossRef]
99. Nishiga, M.; Qi, L.S.; Wu, J.C. CRISPRi/a Screening with Human iPSCs. *Methods Mol. Biol.* **2021**, *2320*, 261–281. [CrossRef]

100. Spitzhorn, L.S.; Kordes, C.; Megges, M.; Sawitza, I.; Gotze, S.; Reichert, D.; Schulze-Matz, P.; Graffmann, N.; Bohndorf, M.; Wruck, W.; et al. Transplanted Human Pluripotent Stem Cell-Derived Mesenchymal Stem Cells Support Liver Regeneration in Gunn Rats. *Stem Cells Dev.* **2018**, *27*, 1702–1714. [CrossRef]
101. Israel, M.A.; Yuan, S.H.; Bardy, C.; Reyna, S.M.; Mu, Y.; Herrera, C.; Hefferan, M.P.; Van Gorp, S.; Nazor, K.L.; Boscolo, F.S.; et al. Probing sporadic and familial Alzheimer's disease using induced pluripotent stem cells. *Nature* **2012**, *482*, 216–220. [CrossRef]
102. Hossini, A.M.; Megges, M.; Prigione, A.; Lichtner, B.; Toliat, M.R.; Wruck, W.; Schroter, F.; Nuernberg, P.; Kroll, H.; Makrantonaki, E.; et al. Erratum: Induced pluripotent stem cell-derived neuronal cells from a sporadic Alzheimer's disease donor as a model for investigating AD-associated gene regulatory networks. *BMC Genom.* **2015**, *16*, 433. [CrossRef]
103. Halevy, T.; Akov, S.; Bohndorf, M.; Mlody, B.; Adjaye, J.; Benvenisty, N.; Goldberg, M. Chromosomal Instability and Molecular Defects in Induced Pluripotent Stem Cells from Nijmegen Breakage Syndrome Patients. *Cell Rep.* **2016**, *16*, 2499–2511. [CrossRef] [PubMed]
104. Flamier, A.; El Hajjar, J.; Adjaye, J.; Fernandes, K.J.; Abdouh, M.; Bernier, G. Modeling Late-Onset Sporadic Alzheimer's Disease through BMI1 Deficiency. *Cell Rep.* **2018**, *23*, 2653–2666. [CrossRef]
105. Pomeshchik, Y.; Klementieva, O.; Gil, J.; Martinsson, I.; Hansen, M.G.; de Vries, T.; Sancho-Balsells, A.; Russ, K.; Savchenko, E.; Collin, A.; et al. Human iPSC-Derived Hippocampal Spheroids: An Innovative Tool for Stratifying Alzheimer Disease Patient-Specific Cellular Phenotypes and Developing Therapies. *Stem Cell Rep.* **2020**, *15*, 256–273. [CrossRef] [PubMed]
106. Martins, S.; Muller-Schiffmann, A.; Erichsen, L.; Bohndorf, M.; Wruck, W.; Sleegers, K.; Van Broeckhoven, C.; Korth, C.; Adjaye, J. IPSC-Derived Neuronal Cultures Carrying the Alzheimer's Disease Associated TREM2 R47H Variant Enables the Construction of an Abeta-Induced Gene Regulatory Network. *Int. J. Mol. Sci.* **2020**, *21*, 4516. [CrossRef] [PubMed]
107. Graffmann, N.; Ncube, A.; Martins, S.; Fiszl, A.R.; Reuther, P.; Bohndorf, M.; Wruck, W.; Beller, M.; Czekelius, C.; Adjaye, J. A stem cell based in vitro model of NAFLD enables the analysis of patient specific individual metabolic adaptations in response to a high fat diet and AdipoRon interference. *Biol. Open* **2021**, *10*. [CrossRef]
108. Martins, S.; Erichsen, L.; Datsi, A.; Wruck, W.; Goering, W.; Chatzantonaki, E.; de Amorim, V.C.M.; Rossi, A.; Chrzanowska, K.H.; Adjaye, J. Impaired p53-Mediated DNA Damage Response Contributes to Microcephaly in Nijmegen Breakage Syndrome Patient-Derived Cerebral Organoids. *Cells* **2022**, *11*, 802. [CrossRef]
109. Mlody, B.; Wruck, W.; Martins, S.; Sperling, K.; Adjaye, J. Nijmegen Breakage Syndrome fibroblasts and iPSCs: Cellular models for uncovering disease-associated signaling pathways and establishing a screening platform for anti-oxidants. *Sci. Rep.* **2017**, *7*, 7516. [CrossRef]
110. Yamanaka, S. Patient-specific pluripotent stem cells become even more accessible. *Cell Stem Cell* **2010**, *7*, 1–2. [CrossRef]
111. Yap, M.S.; Nathan, K.R.; Yeo, Y.; Lim, L.W.; Poh, C.L.; Richards, M.; Lim, W.L.; Othman, I.; Heng, B.C. Neural Differentiation of Human Pluripotent Stem Cells for Nontherapeutic Applications: Toxicology, Pharmacology, and In Vitro Disease Modeling. *Stem Cells Int.* **2015**, *2015*, 105172. [CrossRef]
112. Graffmann, N.; Martins, S.; Ljubikj, T.; Matte, J.C.; Bohndorf, M.; Wruck, W.; Adjaye, J. Generation of a Crigler-Najjar Syndrome Type I patient-derived induced pluripotent stem cell line CNS705 (HHUUKDi005-A). *Stem Cell Res.* **2021**, *51*, 102167. [CrossRef]
113. Takahashi, K.; Yamanaka, S. Induction of pluripotent stem cells from mouse embryonic and adult fibroblast cultures by defined factors. *Cell* **2006**, *126*, 663–676. [CrossRef] [PubMed]
114. Takahashi, K.; Tanabe, K.; Ohnuki, M.; Narita, M.; Ichisaka, T.; Tomoda, K.; Yamanaka, S. Induction of pluripotent stem cells from adult human fibroblasts by defined factors. *Cell* **2007**, *131*, 861–872. [CrossRef] [PubMed]
115. Abu-Dawud, R.; Graffmann, N.; Ferber, S.; Wruck, W.; Adjaye, J. Pluripotent stem cells: Induction and self-renewal. *Philos. Trans. R. Soc. Lond. B Biol. Sci.* **2018**, *373*, 20170213. [CrossRef] [PubMed]
116. Fusaki, N.; Ban, H.; Nishiyama, A.; Saeki, K.; Hasegawa, M. Efficient induction of transgene-free human pluripotent stem cells using a vector based on Sendai virus, an RNA virus that does not integrate into the host genome. *Proc. Jpn. Acad. Ser. B Phys. Biol. Sci.* **2009**, *85*, 348–362. [CrossRef]
117. Wang, Y.; Mah, N.; Prigione, A.; Wolfrum, K.; Andrade-Navarro, M.A.; Adjaye, J. A transcriptional roadmap to the induction of pluripotency in somatic cells. *Stem Cell Rev. Rep.* **2010**, *6*, 282–296. [CrossRef]
118. Zhou, W.; Freed, C.R. Adenoviral gene delivery can reprogram human fibroblasts to induced pluripotent stem cells. *Stem Cells* **2009**, *27*, 2667–2674. [CrossRef]
119. Yu, J.; Hu, K.; Smuga-Otto, K.; Tian, S.; Stewart, R.; Slukvin, I.I.; Thomson, J.A. Human induced pluripotent stem cells free of vector and transgene sequences. *Science* **2009**, *324*, 797–801. [CrossRef]
120. Deng, J.; Shoemaker, R.; Xie, B.; Gore, A.; LeProust, E.M.; Antosiewicz-Bourget, J.; Egli, D.; Maherali, N.; Park, I.H.; Yu, J.; et al. Targeted bisulfite sequencing reveals changes in DNA methylation associated with nuclear reprogramming. *Nat. Biotechnol.* **2009**, *27*, 353–360. [CrossRef]
121. Kim, K.; Doi, A.; Wen, B.; Ng, K.; Zhao, R.; Cahan, P.; Kim, J.; Aryee, M.J.; Ji, H.; Ehrlich, L.I.; et al. Epigenetic memory in induced pluripotent stem cells. *Nature* **2010**, *467*, 285–290. [CrossRef]
122. Bohndorf, M.; Ncube, A.; Spitzhorn, L.S.; Enczmann, J.; Wruck, W.; Adjaye, J. Derivation and characterization of integration-free iPSC line ISRM-UM51 derived from SIX2-positive renal cells isolated from urine of an African male expressing the CYP2D6 *4/*17 variant which confers intermediate drug metabolizing activity. *Stem Cell Res.* **2017**, *25*, 18–21. [CrossRef]

123. Nguyen, L.; Wruck, W.; Erichsen, L.; Graffmann, N.; Adjaye, J. Correction: Nguyen et al. The Nephrotoxin Puromycin Aminonucleoside Induces Injury in Kidney Organoids Differentiated from Induced Pluripotent Stem Cells. *Cells* **2022**, *11*, 635, Erratum in: *Cells* **2022**, *11*, 1980. [CrossRef] [PubMed]
124. Paulitschek, C.; Schulze-Matz, P.; Hesse, J.; Schmidt, T.; Wruck, W.; Adjaye, J.; Schrader, J. Generation and characterization of two iPSC lines from human epicardium-derived cells. *Stem Cell Res.* **2017**, *20*, 50–53. [CrossRef] [PubMed]
125. Takahashi, K.; Okita, K.; Nakagawa, M.; Yamanaka, S. Induction of pluripotent stem cells from fibroblast cultures. *Nat. Protoc.* **2007**, *2*, 3081–3089. [CrossRef] [PubMed]
126. Bai, X.; Yan, Y.; Canfield, S.; Muravyeva, M.Y.; Kikuchi, C.; Zaja, I.; Corbett, J.A.; Bosnjak, Z.J. Ketamine enhances human neural stem cell proliferation and induces neuronal apoptosis via reactive oxygen species-mediated mitochondrial pathway. *Anesth. Analg.* **2013**, *116*, 869–880. [CrossRef]
127. Kikuchi, C.; Bienengraeber, M.; Canfield, S.; Koopmeiner, A.; Schafer, R.; Bosnjak, Z.J.; Bai, X. Comparison of Cardiomyocyte Differentiation Potential Between Type 1 Diabetic Donor- and Nondiabetic Donor-Derived Induced Pluripotent Stem Cells. *Cell Transplant.* **2015**, *24*, 2491–2504. [CrossRef]
128. Temple, S. The development of neural stem cells. *Nature* **2001**, *414*, 112–117. [CrossRef]
129. Behnan, J.; Stangeland, B.; Langella, T.; Finocchiaro, G.; Tringali, G.; Meling, T.R.; Murrell, W. Identification and characterization of a new source of adult human neural progenitors. *Cell Death Dis.* **2017**, *8*, e2991. [CrossRef]
130. Kriegstein, A.; Alvarez-Buylla, A. The glial nature of embryonic and adult neural stem cells. *Ann. Rev. Neurosci.* **2009**, *32*, 149–184. [CrossRef]
131. Obernier, K.; Tong, C.K.; Alvarez-Buylla, A. Restricted nature of adult neural stem cells: Re-evaluation of their potential for brain repair. *Front. Neurosci.* **2014**, *8*, 162. [CrossRef]
132. Elkabetz, Y.; Panagiotakos, G.; Al Shamy, G.; Socci, N.D.; Tabar, V.; Studer, L. Human ES cell-derived neural rosettes reveal a functionally distinct early neural stem cell stage. *Genes Dev.* **2008**, *22*, 152–165. [CrossRef]
133. Yuan, T.; Liao, W.; Feng, N.H.; Lou, Y.L.; Niu, X.; Zhang, A.J.; Wang, Y.; Deng, Z.F. Human induced pluripotent stem cell-derived neural stem cells survive, migrate, differentiate, and improve neurologic function in a rat model of middle cerebral artery occlusion. *Stem Cell Res. Ther.* **2013**, *4*, 73. [CrossRef] [PubMed]
134. Falk, A.; Koch, P.; Kesavan, J.; Takashima, Y.; Ladewig, J.; Alexander, M.; Wiskow, O.; Tailor, J.; Trotter, M.; Pollard, S.; et al. Capture of neuroepithelial-like stem cells from pluripotent stem cells provides a versatile system for in vitro production of human neurons. *PLoS ONE* **2012**, *7*, e29597. [CrossRef]
135. Ebert, A.D.; Shelley, B.C.; Hurley, A.M.; Onorati, M.; Castiglioni, V.; Patitucci, T.N.; Svendsen, S.P.; Mattis, V.B.; McGivern, J.V.; Schwab, A.J.; et al. EZ spheres: A stable and expandable culture system for the generation of pre-rosette multipotent stem cells from human ESCs and iPSCs. *Stem Cell Res.* **2013**, *10*, 417–427. [CrossRef] [PubMed]
136. Nemati, S.; Hatami, M.; Kiani, S.; Hemmesi, K.; Gourabi, H.; Masoudi, N.; Alaei, S.; Baharvand, H. Long-term self-renewable feeder-free human induced pluripotent stem cell-derived neural progenitors. *Stem Cells Dev.* **2011**, *20*, 503–514. [CrossRef]
137. Townshend, R.F.; Shao, Y.; Wang, S.; Cortez, C.L.; Esfahani, S.N.; Spence, J.R.; O'Shea, K.S.; Fu, J.; Gumucio, D.L.; Taniguchi, K. Effect of Cell Spreading on Rosette Formation by Human Pluripotent Stem Cell-Derived Neural Progenitor Cells. *Front. Cell Dev Biol.* **2020**, *8*, 588941. [CrossRef]
138. Qi, Y.; Zhang, X.J.; Renier, N.; Wu, Z.; Atkin, T.; Sun, Z.; Ozair, M.Z.; Tchieu, J.; Zimmer, B.; Fattahi, F.; et al. Combined small-molecule inhibition accelerates the derivation of functional cortical neurons from human pluripotent stem cells. *Nat. Biotechnol.* **2017**, *35*, 154–163. [CrossRef]
139. Roybon, L.; Lamas, N.J.; Garcia, A.D.; Yang, E.J.; Sattler, R.; Lewis, V.J.; Kim, Y.A.; Kachel, C.A.; Rothstein, J.D.; Przedborski, S.; et al. Human stem cell-derived spinal cord astrocytes with defined mature or reactive phenotypes. *Cell Rep.* **2013**, *4*, 1035–1048. [CrossRef]
140. Douvaras, P.; Wang, J.; Zimmer, M.; Hanchuk, S.; O'Bara, M.A.; Sadiq, S.; Sim, F.J.; Goldman, J.; Fossati, V. Efficient generation of myelinating oligodendrocytes from primary progressive multiple sclerosis patients by induced pluripotent stem cells. *Stem Cell Rep.* **2014**, *3*, 250–259. [CrossRef]
141. Abud, E.M.; Ramirez, R.N.; Martinez, E.S.; Healy, L.M.; Nguyen, C.H.H.; Newman, S.A.; Yeromin, A.V.; Scarfone, V.M.; Marsh, S.E.; Fimbres, C.; et al. iPSC-Derived Human Microglia-like Cells to Study Neurological Diseases. *Neuron* **2017**, *94*, 278–293.e279. [CrossRef]
142. Sabitha, K.R.; Shetty, A.K.; Upadhya, D. Patient-derived iPSC modeling of rare neurodevelopmental disorders: Molecular pathophysiology and prospective therapies. *Neurosci. Biobehav. Rev.* **2021**, *121*, 201–219. [CrossRef]
143. Han, F.; Hu, B. Stem Cell Therapy for Parkinson's Disease. *Adv. Exp. Med. Biol.* **2020**, *1266*, 21–38. [CrossRef] [PubMed]
144. Kim, T.W.; Koo, S.Y.; Studer, L. Pluripotent Stem Cell Therapies for Parkinson Disease: Present Challenges and Future Opportunities. *Front. Cell Dev. Biol.* **2020**, *8*, 729. [CrossRef] [PubMed]
145. Unterholzner, J.; Millischer, V.; Wotawa, C.; Sawa, A.; Lanzenberger, R. Making Sense of Patient-Derived iPSCs, Transdifferentiated Neurons, Olfactory Neuronal Cells, and Cerebral Organoids as Models for Psychiatric Disorders. *Int. J. Neuropsychopharmacol.* **2021**, *24*, 759–775. [CrossRef] [PubMed]
146. Eiraku, M.; Watanabe, K.; Matsuo-Takasaki, M.; Kawada, M.; Yonemura, S.; Matsumura, M.; Wataya, T.; Nishiyama, A.; Muguruma, K.; Sasai, Y. Self-organized formation of polarized cortical tissues from ESCs and its active manipulation by extrinsic signals. *Cell Stem Cell* **2008**, *3*, 519–532. [CrossRef]

147. Eiraku, M.; Takata, N.; Ishibashi, H.; Kawada, M.; Sakakura, E.; Okuda, S.; Sekiguchi, K.; Adachi, T.; Sasai, Y. Self-organizing optic-cup morphogenesis in three-dimensional culture. *Nature* **2011**, *472*, 51–56. [CrossRef]
148. Lancaster, M.A.; Renner, M.; Martin, C.A.; Wenzel, D.; Bicknell, L.S.; Hurles, M.E.; Homfray, T.; Penninger, J.M.; Jackson, A.P.; Knoblich, J.A. Cerebral organoids model human brain development and microcephaly. *Nature* **2013**, *501*, 373–379. [CrossRef]
149. Simian, M.; Bissell, M.J. Organoids: A historical perspective of thinking in three dimensions. *J. Cell Biol.* **2017**, *216*, 31–40. [CrossRef]
150. Yoon, S.J.; Elahi, L.S.; Pasca, A.M.; Marton, R.M.; Gordon, A.; Revah, O.; Miura, Y.; Walczak, E.M.; Holdgate, G.M.; Fan, H.C.; et al. Reliability of human cortical organoid generation. *Nat. Methods* **2019**, *16*, 75–78. [CrossRef]
151. Gabriel, E.; Ramani, A.; Karow, U.; Gottardo, M.; Natarajan, K.; Gooi, L.M.; Goranci-Buzhala, G.; Krut, O.; Peters, F.; Nikolic, M.; et al. Recent Zika Virus Isolates Induce Premature Differentiation of Neural Progenitors in Human Brain Organoids. *Cell Stem Cell* **2017**, *20*, 397–406.e395. [CrossRef]
152. Pasca, A.M.; Sloan, S.A.; Clarke, L.E.; Tian, Y.; Makinson, C.D.; Huber, N.; Kim, C.H.; Park, J.Y.; O'Rourke, N.A.; Nguyen, K.D.; et al. Functional cortical neurons and astrocytes from human pluripotent stem cells in 3D culture. *Nat. Methods* **2015**, *12*, 671–678. [CrossRef]
153. Qian, X.; Nguyen, H.N.; Song, M.M.; Hadiono, C.; Ogden, S.C.; Hammack, C.; Yao, B.; Hamersky, G.R.; Jacob, F.; Zhong, C.; et al. Brain-Region-Specific Organoids Using Mini-bioreactors for Modeling ZIKV Exposure. *Cell* **2016**, *165*, 1238–1254. [CrossRef] [PubMed]
154. Giandomenico, S.L.; Sutcliffe, M.; Lancaster, M.A. Generation and long-term culture of advanced cerebral organoids for studying later stages of neural development. *Nat. Protoc.* **2021**, *16*, 579–602. [CrossRef]
155. Lancaster, M.A.; Knoblich, J.A. Generation of cerebral organoids from human pluripotent stem cells. *Nat. Protoc.* **2014**, *9*, 2329–2340. [CrossRef] [PubMed]
156. Hong, Y.J.; Do, J.T. Neural Lineage Differentiation From Pluripotent Stem Cells to Mimic Human Brain Tissues. *Front. Bioeng. Biotechnol.* **2019**, *7*, 400. [CrossRef] [PubMed]
157. Kelava, I.; Lancaster, M.A. Dishing out mini-brains: Current progress and future prospects in brain organoid research. *Dev. Biol.* **2016**, *420*, 199–209. [CrossRef] [PubMed]
158. Pellegrini, L.; Albecka, A.; Mallery, D.L.; Kellner, M.J.; Paul, D.; Carter, A.P.; James, L.C.; Lancaster, M.A. SARS-CoV-2 Infects the Brain Choroid Plexus and Disrupts the Blood-CSF Barrier in Human Brain Organoids. *Cell Stem Cell* **2020**, *27*, 951–961.e955. [CrossRef] [PubMed]
159. Ciarpella, F.; Zamfir, R.G.; Campanelli, A.; Ren, E.; Pedrotti, G.; Bottani, E.; Borioli, A.; Caron, D.; Di Chio, M.; Dolci, S.; et al. Murine cerebral organoids develop network of functional neurons and hippocampal brain region identity. *iScience* **2021**, *24*, 103438. [CrossRef]
160. Afanasyeva, T.A.V.; Corral-Serrano, J.C.; Garanto, A.; Roepman, R.; Cheetham, M.E.; Collin, R.W.J. A look into retinal organoids: Methods, analytical techniques, and applications. *Cell Mol. Life Sci.* **2021**, *78*, 6505–6532. [CrossRef]
161. Miura, Y.; Li, M.Y.; Birey, F.; Ikeda, K.; Revah, O.; Thete, M.V.; Park, J.Y.; Puno, A.; Lee, S.H.; Porteus, M.H.; et al. Generation of human striatal organoids and cortico-striatal assembloids from human pluripotent stem cells. *Nat. Biotechnol.* **2020**, *38*, 1421–1430. [CrossRef]
162. Ormel, P.R.; Vieira de Sa, R.; van Bodegraven, E.J.; Karst, H.; Harschnitz, O.; Sneeboer, M.A.M.; Johansen, L.E.; van Dijk, R.E.; Scheefhals, N.; Berdenis van Berlekom, A.; et al. Microglia innately develop within cerebral organoids. *Nat. Commun.* **2018**, *9*, 4167. [CrossRef]
163. Kim, H.; Jiang, P. Generation of human pluripotent stem cell-derived fused organoids with oligodendroglia and myelin. *STAR Protoc.* **2021**, *2*, 100443. [CrossRef] [PubMed]
164. Shaker, M.R.; Pietrogrande, G.; Martin, S.; Lee, J.H.; Sun, W.; Wolvetang, E.J. Rapid and Efficient Generation of Myelinating Human Oligodendrocytes in Organoids. *Front. Cell Neurosci.* **2021**, *15*, 631548. [CrossRef] [PubMed]
165. Zahmatkesh, E.; Khoshdel-Rad, N.; Mirzaei, H.; Shpichka, A.; Timashev, P.; Mahmoudi, T.; Vosough, M. Evolution of organoid technology: Lessons learnt in Co-Culture systems from developmental biology. *Dev. Biol.* **2021**, *475*, 37–53. [CrossRef] [PubMed]
166. Cukier, J.; Batzofin, J.H.; Conner, J.S.; Franklin, R.R. Genital tract reconstruction in a patient with congenital absence of the vagina and hypoplasia of the cervix. *Obstet. Gynecol.* **1986**, *68*, 32S–36S. [PubMed]
167. Frohlich, E. Comparison of conventional and advanced in vitro models in the toxicity testing of nanoparticles. *Artif. Cells Nanomed. Biotechnol.* **2018**, *46*, 1091–1107. [CrossRef]
168. Kook, Y.M.; Jeong, Y.; Lee, K.; Koh, W.G. Design of biomimetic cellular scaffolds for co-culture system and their application. *J. Tissue Eng.* **2017**, *8*, 2041731417724640. [CrossRef]
169. Nascimento, J.M.; Saia-Cereda, V.M.; Sartore, R.C.; da Costa, R.M.; Schitine, C.S.; Freitas, H.R.; Murgu, M.; de Melo Reis, R.A.; Rehen, S.K.; Martins-de-Souza, D. Human Cerebral Organoids and Fetal Brain Tissue Share Proteomic Similarities. *Front. Cell Dev. Biol.* **2019**, *7*, 303. [CrossRef]
170. Liu, C.; Oikonomopoulos, A.; Sayed, N.; Wu, J.C. Modeling human diseases with induced pluripotent stem cells: From 2D to 3D and beyond. *Development* **2018**, *145*, dev156166. [CrossRef]
171. Edmondson, R.; Broglie, J.J.; Adcock, A.F.; Yang, L. Three-dimensional cell culture systems and their applications in drug discovery and cell-based biosensors. *Assay Drug Dev. Technol.* **2014**, *12*, 207–218. [CrossRef]

172. Krencik, R.; Ullian, E.M. A cellular star atlas: Using astrocytes from human pluripotent stem cells for disease studies. *Front. Cell Neurosci.* **2013**, *7*, 25. [CrossRef]
173. van den Hurk, M.; Bardy, C. Single-cell multimodal transcriptomics to study neuronal diversity in human stem cell-derived brain tissue and organoid models. *J. Neurosci. Methods* **2019**, *325*, 108350. [CrossRef] [PubMed]
174. Goranci-Buzhala, G.; Mariappan, A.; Gabriel, E.; Ramani, A.; Ricci-Vitiani, L.; Buccarelli, M.; D'Alessandris, Q.G.; Pallini, R.; Gopalakrishnan, J. Rapid and Efficient Invasion Assay of Glioblastoma in Human Brain Organoids. *Cell Rep.* **2020**, *31*, 107738. [CrossRef] [PubMed]
175. Birey, F.; Andersen, J.; Makinson, C.D.; Islam, S.; Wei, W.; Huber, N.; Fan, H.C.; Metzler, K.R.C.; Panagiotakos, G.; Thom, N.; et al. Assembly of functionally integrated human forebrain spheroids. *Nature* **2017**, *545*, 54–59. [CrossRef] [PubMed]
176. Xiang, Y.; Tanaka, Y.; Patterson, B.; Kang, Y.J.; Govindaiah, G.; Roselaar, N.; Cakir, B.; Kim, K.Y.; Lombroso, A.P.; Hwang, S.M.; et al. Fusion of Regionally Specified hPSC-Derived Organoids Models Human Brain Development and Interneuron Migration. *Cell Stem Cell* **2017**, *21*, 383–398.e387. [CrossRef] [PubMed]
177. Pasca, S.P. Building three-dimensional human brain organoids. *Nat. Neurosci.* **2018**, 1. [CrossRef]
178. Sidhaye, J.; Knoblich, J.A. Brain organoids: An ensemble of bioassays to investigate human neurodevelopment and disease. *Cell Death Differ* **2021**, *28*, 52–67. [CrossRef]
179. Koo, B.; Choi, B.; Park, H.; Yoon, K.J. Past, Present, and Future of Brain Organoid Technology. *Mol. Cells* **2019**, *42*, 617–627. [CrossRef]
180. Bhutani, V.K.; Johnson, L.H.; Shapiro, S.M. Kernicterus in sick and preterm infants (1999–2002): A need for an effective preventive approach. *Semin. Perinatol.* **2004**, *28*, 319–325. [CrossRef]
181. Moll, M.; Goelz, R.; Naegele, T.; Wilke, M.; Poets, C.F. Are recommended phototherapy thresholds safe enough for extremely low birth weight (ELBW) infants? A report on 2 ELBW infants with kernicterus despite only moderate hyperbilirubinemia. *Neonatology* **2011**, *99*, 90–94. [CrossRef]
182. Conforti, L.; Adalbert, R.; Coleman, M.P. Neuronal death: Where does the end begin? *Trends Neurosci.* **2007**, *30*, 159–166. [CrossRef]
183. Silva, R.F.; Mata, L.M.; Gulbenkian, S.; Brites, D. Endocytosis in rat cultured astrocytes is inhibited by unconjugated bilirubin. *Neurochem. Res.* **2001**, *26*, 793–800. [CrossRef] [PubMed]
184. Higgins, G.C.; Beart, P.M.; Shin, Y.S.; Chen, M.J.; Cheung, N.S.; Nagley, P. Oxidative stress: Emerging mitochondrial and cellular themes and variations in neuronal injury. *J. Alzheimers Dis.* **2010**, *20*, S453–S473. [CrossRef]
185. Floyd, R.A.; Hensley, K. Oxidative stress in brain aging. Implications for therapeutics of neurodegenerative diseases. *Neurobiol. Aging* **2002**, *23*, 795–807. [CrossRef] [PubMed]
186. Johnson, L.; Bhutani, V.K. The clinical syndrome of bilirubin-induced neurologic dysfunction. *Semin. Perinatol.* **2011**, *35*, 101–113. [CrossRef] [PubMed]
187. Wusthoff, C.J.; Loe, I.M. Impact of bilirubin-induced neurologic dysfunction on neurodevelopmental outcomes. *Semin. Fetal Neonatal. Med.* **2015**, *20*, 52–57. [CrossRef] [PubMed]
188. Qaisiya, M.; Brischetto, C.; Jasprova, J.; Vitek, L.; Tiribelli, C.; Bellarosa, C. Bilirubin-induced ER stress contributes to the inflammatory response and apoptosis in neuronal cells. *Arch. Toxicol.* **2017**, *91*, 1847–1858. [CrossRef] [PubMed]
189. Fernandes, A.; Silva, R.F.; Falcao, A.S.; Brito, M.A.; Brites, D. Cytokine production, glutamate release and cell death in rat cultured astrocytes treated with unconjugated bilirubin and LPS. *J. Neuroimmunol.* **2004**, *153*, 64–75. [CrossRef]
190. Fernandes, A.; Falcao, A.S.; Silva, R.F.; Gordo, A.C.; Gama, M.J.; Brito, M.A.; Brites, D. Inflammatory signalling pathways involved in astroglial activation by unconjugated bilirubin. *J. Neurochem.* **2006**, *96*, 1667–1679. [CrossRef]

3.2 Free Bilirubin Induces Neuro-Inflammation in an Induced Pluripotent Stem Cell-Derived Cortical Organoid Model of Crigler-Najjar Syndrome

Abida Islam Pranty, Wasco Wruck and James Adjaye

Cells 2023, Volume 12, Issue 18, Article Number 2277

Abstract:

Bilirubin-induced neurological damage (BIND), which might progress to kernicterus, occurs as a consequence of defects in the bilirubin conjugation machinery, thus enabling albumin-unbound free bilirubin (BF) to cross the blood–brain barrier and accumulate within. A defect in the UGT1A1 enzyme-encoding gene, which is directly responsible for bilirubin conjugation, can cause Crigler–Najjar syndrome (CNS) and Gilbert's syndrome. We used human-induced pluripotent stem cell (hiPSC)-derived 3D brain organoids to model BIND in vitro and unveil the molecular basis of the detrimental effects of BF in the developing human brain. Healthy and patient-derived iPSCs were differentiated into day-20 brain organoids, and then stimulated with 200 nM BF. Analyses at 24 and 72 h post-treatment point to BF-induced neuro-inflammation in both cell lines. Transcriptome, associated KEGG, and Gene Ontology analyses unveiled the activation of distinct inflammatory pathways, such as cytokine–cytokine receptor interaction, MAPK signalling, and NFκB activation. Furthermore, the mRNA expression and secretome analysis confirmed an upregulation of pro-inflammatory cytokines such as IL-6 and IL-8 upon BF stimulation. This novel study has provided insights into how a human iPSC-derived 3D brain organoid model can serve as a prospective platform for studying the etiology of BIND kernicterus.

Authors Contribution: 80 %

A.I.P. designed and performed experiments, analysed the data, wrote, and edited the manuscript.

Status: Published in *Cells* (doi.org/10.3390/cells12182277).

cells

MDPI

Article

Free Bilirubin Induces Neuro-Inflammation in an Induced Pluripotent Stem Cell-Derived Cortical Organoid Model of Crigler-Najjar Syndrome

Abida Islam Pranty [1], Wasco Wruck [1] and James Adjaye [1,2,*]

[1] Institute for Stem Cell Research and Regenerative Medicine, Medical Faculty, Heinrich-Heine University Düsseldorf, 40225 Düsseldorf, Germany; abida.pranty@hhu.de (A.I.P.); wasco.wruck@med.uni-duesseldorf.de (W.W.)
[2] Zayed Centre for Research into Rare Diseases in Children (ZCR), University College London (UCL)—EGA Institute for Women's Health, 20 Guilford Street, London WC1N 1DZ, UK
* Correspondence: james.adjaye@med.uni-duesseldorf.de

Abstract: Bilirubin-induced neurological damage (BIND), which might progress to kernicterus, occurs as a consequence of defects in the bilirubin conjugation machinery, thus enabling albumin-unbound free bilirubin (BF) to cross the blood–brain barrier and accumulate within. A defect in the UGT1A1 enzyme-encoding gene, which is directly responsible for bilirubin conjugation, can cause Crigler–Najjar syndrome (CNS) and Gilbert's syndrome. We used human-induced pluripotent stem cell (hiPSC)-derived 3D brain organoids to model BIND in vitro and unveil the molecular basis of the detrimental effects of BF in the developing human brain. Healthy and patient-derived iPSCs were differentiated into day-20 brain organoids, and then stimulated with 200 nM BF. Analyses at 24 and 72 h post-treatment point to BF-induced neuro-inflammation in both cell lines. Transcriptome, associated KEGG, and Gene Ontology analyses unveiled the activation of distinct inflammatory pathways, such as cytokine–cytokine receptor interaction, MAPK signaling, and NFκB activation. Furthermore, the mRNA expression and secretome analysis confirmed an upregulation of pro-inflammatory cytokines such as IL-6 and IL-8 upon BF stimulation. This novel study has provided insights into how a human iPSC-derived 3D brain organoid model can serve as a prospective platform for studying the etiology of BIND kernicterus.

Keywords: BIND; kernicterus; Crigler–Najjar syndrome; UGT1A1; 3D brain organoid; free bilirubin; neuro-inflammation

Citation: Pranty, A.I.; Wruck, W.; Adjaye, J. Free Bilirubin Induces Neuro-Inflammation in an Induced Pluripotent Stem Cell-Derived Cortical Organoid Model of Crigler-Najjar Syndrome. *Cells* **2023**, *12*, 2277. https://doi.org/10.3390/cells12182277

Academic Editor: Thomas Durcan

Received: 17 July 2023
Revised: 30 August 2023
Accepted: 12 September 2023
Published: 14 September 2023

1. Introduction

Neonatal jaundice is a common occurring transitional condition, caused by unconjugated hyperbilirubinemia, which affects about 85% of newborns in their first week of postnatal life [1,2]. Unconjugated hyperbilirubinemia is normally benign; nevertheless, the protective mechanisms of the brain can be surpassed in the infants when albumin-unbound free bilirubin (BF) starts accumulating and crosses the blood–brain barrier (BBB) due to defective bilirubin conjugation machinery. Elevated bilirubin levels result in severe brain injury including short-term and long-term neurodevelopmental disabilities, which can progress into acute or chronic bilirubin encephalopathy, known as kernicterus, or bilirubin-induced neurological dysfunction (BIND) [3]. Kernicterus is a complex neuropathological ailment, which can lead to acute or chronic neurological disabilities, resulting in BIND [4,5]. A genetic disorder caused by a defective UGT1A1 (UDP glucuronosyltransferase family 1 member A1) enzyme leads to Crigler–Najjar syndrome (CNS) and can also cause BIND [6]. Bilirubin-UGT1 (UGT1A1) is the only isoform of the uridine 5′-diphospho-glucuronosyltransferases (UGTs) enzyme family that specifically contributes to bilirubin conjugation. Therefore, a mutation in the gene encoding UGT1A1 can cause CNS type 1 and 2 by complete or partial inactivation of the enzyme, respectively, which prevents the liver from metabolizing bilirubin [7]. The more severe type (CNS-1) is characterized by

total deficiency of the UGT1A1 enzyme, while CNS-2 (the milder one) is characterized by a partial UGT1A1 deficiency [6]. A decrease in or loss of UGT1A1 activity due to hereditary defects in UGT1A1 hinders bilirubin conjugation, causing BF to accumulate in serum, cross the BBB, and eventually get deposited in the basal ganglia or cerebellum, thereby resulting in BIND [7–9]. The mechanism underlying BIND and the correlation between the BF levels and neurological abnormalities are not well understood.

Neuro-inflammation is one of the key features observed in the distinct model systems of bilirubin-induced brain toxicity. It has been shown that in *UGT1A1* knocked-out mice, Toll-like receptor 2 (TLR2) is required for regulating gliosis, pro-inflammatory mediators, and oxidative stress when neonatal mice are exposed to severe hyperbilirubinemia, but TLR2 also has anti-apoptotic properties. This correlates with the upregulation of tumor necrosis factor alpha (TNF-α), interleukin (IL) 1ß, and IL-6, thus indicative of neuro-inflammation in the CNS [10]. Neuronal damage in distinct neurodegenerative diseases and neuro-inflammatory diseases (such as Alzheimer's disease, Parkinson's disease, and Multiple Sclerosis) are reported to be mediated by various inflammatory and neurotoxic factors, such as IL-6, IL-8, TNF-α, intracellular Ca^{2+} elevation, chemokines, activation of mitogen-activated protein kinases (MAPKs), and nuclear factor kappa B (NFκB) [11]. TNF-α and NFκB are the key mediators of bilirubin-induced inflammatory responses in murine models [12]. Sustained exposure of developing mouse cerebellum with free unconjugated bilirubin induces activation of oxidative stress, endoplasmic reticulum (ER) stress, and inflammatory markers, thus pointing to inflammation as a key contributor of bilirubin-induced damage in conjunction with ER stress in the onset of neurotoxicity [12]. Immature rat neurons also manifested distinct features of oxidative stress and cell dysfunction upon bilirubin exposure by increased ROS production, the disruption of the glutathione redox status, and cell death [13]. Bilirubin-induced apoptosis and necrosis-like cell death leading to neuritic atrophy and astrocyte activation have also been observed in monotypic nerve cell cultures [14,15]. During necrosis, various receptors become activated and the uncontrolled release of cytosolic constituents may induce inflammatory responses in the surrounding tissue [16]. Various stimuli (e.g., cytokines) can cause both apoptosis and necrosis in the same cell population. Furthermore, by modulating signaling pathways (such as death receptors and kinase cascades), it is possible to switch between apoptosis and necrosis [16,17]. Necroptosis is a programmed form of necrosis, or inflammatory cell death, which allows the cell to undergo cellular suicide in a caspase-independent manner in the presence of caspase inhibitors [18]. Elevated bilirubin levels perturb the plasma, mitochondrial, and/or ER membranes of neuronal cells, probably leading to neuronal excitotoxicity, mitochondrial energy failure, or increased intracellular calcium concentration [Ca^{2+}], which are assumed to be linked to the pathogenesis of BIND. Increased [Ca^{2+}] and the following downstream events may activate proteolytic enzymes, apoptotic pathways, and/or necrosis, depending on the intensity and duration of the bilirubin exposure [15].

In this study, we used human-induced pluripotent stem cell (hiPSC)-derived 3D brain organoids as a potential in vitro model system to enhance our understanding of BIND-associated molecular pathogenesis and the breadth of complexities at the cellular and molecular levels that accompany the detrimental effects of free bilirubin to the developing human brain. hiPSC derived from a healthy and a CNS patient were differentiated into day-20 brain organoids and then continuously stimulated with 200 nM BF to observe the possible short-term and long-term BF-induced effects [3,19]. We performed further analyses and observed the induction of neuro-inflammation along with the activation of the cytokine–cytokine receptor interaction, calcium signaling pathway, MAPK signaling pathway, and neuroactive ligand–receptor interaction as processes leading to BIND.

2. Materials and Methods

2.1. Cell Cultivation, Formation of Neural Cortical Organoids, and Bilirubin Treatment on Cortical Organoids

The hiPSC lines derived from the renal progenitor cells isolated from the urine of a 51-year-old healthy male of African origin (UM51) and fibroblast cells from a male Crigler–Najjar syndrome (CNS) patient (i705-C2) were used in this study [20,21] (Table S1). The cells were plated on Matrigel (Corning, New York, NY, USA)-coated culture dishes using mTeSR plus medium (StemCell Technologies, Vancouver, Canada). The cultures were routinely tested for mycoplasma contamination. The cells were dissociated into small aggregates with ReLeSR (StemCell Technologies, Vancouver, Canada) every 5–7 days and split in a 1:5 ratio into fresh Matrigel-coated dishes. Alternatively, the cells were also split as single cells using accutase (Life Technologies, Waltham, MA, USA) while seeding for organoid generation. The protocol described by Gabriel et al., 2016, was employed to differentiate the iPSCs into cortical organoids with minor modifications [22]. Briefly, 20,000 single iPSCs were seeded onto each well of a U-bottom 96-well plate (NucleonTM SpheraTM, Thermo Fisher Scientific, Rockford, IL, USA) to form embryoid bodies (EBs) with mTesR plus medium and 10 µM ROCK inhibitor Y-27632 (Tocris Bioscience, Wiesbaden, Germany). The EBs were cultured on the plate for 5 days with the neural induction medium (StemCell Technologies, Vancouver, Canada) to initiate neural induction. On day 6, the EBs were transferred into a bioreactor (PFIEFFER, Lahnau, Germany) with a differentiation medium consisting of DMEM/F12 and the Neural Basal Medium (in 1:1 ratio), supplemented with 1:200 N2, 1:100 L-glutamine, 1:100 B27 w/o vitamin A, 100 U/mL penicillin, 100 mg/mL streptomycin, 0.05 mM MEM non-essential amino acids (NEAA), 0.05 mM β-mercaptoethanol (all from Gibco, Waltham, MA, USA), and 23 µM insulin (Sigma, Taufkirchen, Germany) (see Table S2). The spinner flasks were coated with anti-adherent rinsing solution (StemCell Technologies, Vancouver, Canada) before transferring the EBs. The transferred EBs were counted as day-0 organoids from this time point (differentiation day 6), as the spheres were transferred into the spinner flask to spontaneously pattern into cortical organoids. From day 9 onward, 0.5 µM of dorsomorphin (Tocris Bioscience, Wiesbaden, Germany) and 5 µM SB431542 (Tocris Bioscience, Wiesbaden, Germany) were added to the differentiation medium, and the medium in the bioreactor was changed once a week. The day-20 cortical organoids were treated up to 72 h with 200 nM free bilirubin (BF), while dimethyl sulfoxide (DMSO) served as the control and the medium was refreshed every 24 h. In brief, free bilirubin (Sigma-Aldrich Chemicals, Taufkirchen, Germany) was used in this study. DMSO was used to dissolve the bilirubin to obtain a stock concentration of 100 mM and further diluted to 200 µM. For the treatment and control conditions, BF and DMSO were diluted (1:1000) in the culture medium, respectively.

Hepatocyte-like cells (HLCs) were derived from the iPSCs following the protocol described by Graffmann et al., 2016 (Figure S1) [23].

2.2. Cryosectioning

The cells (HLCs) were fixed in 4% paraformaldehyde (PFA) (Polysciences, Warrington, FL, USA) for 10 min and the cortical organoids were fixed for 30 min at 37 °C. After washing with PBS, the cells were directly used for staining and the organoids were dehydrated with 30% sucrose in PBS overnight at 4 °C. Then, the organoids were embedded using the Tissue-Tek OCT Compound (embedding medium) (Sakura Finetek, Umkirch, Germany) in cryomolds and snap-frozen in 2-methylbutan (Carl Roth, Karlsruhe, Germany) and dry ice. The embedded organoids were stored at −80 °C. The organoids were sectioned into 15 µm sections using a Cryostat (CM1850, Leica, Nussloch, Germany) and captured in Superfrost plus slides (Thermo Scientific, Waltham, MA, USA). The sectioned organoid slices were stored at −80 °C prior to the immunofluorescence-based analyses.

2.3. Immunocytochemistry

The fixed cells were permeabilized for 10 min with 0.1% Triton X-100 in PBS+Glycine (30 mM Glycine) at room temperature (RT). They were then washed once with PBS and

then the unspecific binding sites were blocked for 2 h at RT with blocking buffer 0.3% BSA in PBS+Glycine. The frozen sections were thawed at RT and PBS was added drop by drop without touching the organoid sections and incubated at RT for 15 min. The Tissue Tek was washed off with PBS and the slide was washed once more with PBS. The sections were permeabilized with 0.7% Triton X-100 + 0.2% Tween 20 in PBS+Glycine for 15 min at RT. After, permeabilization blocking was carried out for 2 h at RT with 0.2% Triton X-100 + 0.3% BSA in PBS+Glycine. For the cells and organoid sections, the primary antibody solution was incubated overnight at 4 °C (see Table S3). After removing the primary antibodies and thorough washing, the secondary antibodies were added for 2 h and incubated at RT. The nuclei were stained with Hoechst. The stained cells and sections were imaged using a Zeiss fluorescence microscope (LSM 700). Particular staining regions were observed under a Zeiss confocal microscope (LSM 700). Individual channel images were processed and merged with ImageJ software version 1.53c.

2.4. TUNEL Assay

Apoptotic cells were detected using the DeadEnd™ Fluorometric TUNEL System (Promega, G3250, Madison, WI, USA) following the manufacturer' s protocol.

2.5. Reverse Transcriptase PCR (RT-PCR)

The cells (HLCs) and cortical organoids were lysed in Trizol to isolate the RNA. In total, 7–8 BF-treated and non-treated organoids were taken for RNA isolation. The RNA was isolated with the Direct-zol™ RNA Isolation Kit (Zymo Research, Freiburg, Germany) according to the user's manual, including the 15 min and 30 min DNase digestion step for cells and organoids, respectively. A total of 500 ng of RNA was reverse-transcribed using the TaqMan Reverse Transcription Kit (Applied Biosystems, Waltham, MA, USA). The primer sequences are shown in Table S4. Real-time PCRs were performed in technical and independent experiment triplicates (n = 3) with Power Sybr Green Master Mix (Life Technologies, Darmstadt, Germany) on a VIIA7 (Life Technologies, Darmstadt, Germany) machine. The mean values were normalized to the ribosomal protein lateral stalk subunit P0 (*RPLP0*) and the fold change was calculated using the indicated controls. The observed fold changes are depicted as mean values with a 95% confidence interval (CI). A statistical analysis of the data was conducted by using Student's unpaired two-sample *t*-test on the basis of the difference between each sample mean compared to the corresponding control mean.

2.6. Human XL Cytokine Assay

The conditioned medium or supernatant of the control and BF-treated cortical organoids from both the 24 and 72 h treatments were stored and used for the proteome profiler antibody array. The relative expression levels of 105 soluble human proteins and cytokines were determined using the Human XL Cytokine Array Kit from R&D Systems. The cytokine array was performed following the manufacturer's guidelines. In brief, the membranes were blocked for 1 h on a rocking platform using the provided blocking buffer and then the samples were prepared by diluting the desired quantity to a final volume of 1.5 mL with the distinct array buffer (array buffer 6). The sample mixtures were pipetted onto the blocked membranes and were incubated overnight at 4 °C on a rocking platform. The membranes were then washed three times with washing buffer for 10 min each at RT. Then, the membranes were incubated with the detection antibody cocktail for 1 h at RT and then washed three times thoroughly. Afterward, Streptavidin-HRP was added onto the membranes, which were incubated for 30 min at RT. The ECL detection reagent (Cytiva, Freiburg, Germany) was used to visualize the spots on the membrane and then detected in a Fusion FX instrument (PeqLab, Erlangen, Germany).

2.7. Image and Data Analysis of the Human XL Cytokine Array

After performing the cytokine array with non-treated and BF-treated organoids, the hybridizations of the cytokine arrays were scanned with the Fusion FX instrument (PeqLab, Erlangen, Germany) and read into the FIJI/ImageJ software version 1.53c, Java 1.8.0_172, where the spots were quantified as described in our previous publication by Wruck et al. [24,25]. The spots were associated with the cytokine identifiers provided by the manufacturer (Proteome Profiler Array from R&D Systems, Human XL Cytokine Array Kit, Catalog Number ARY022B). The integrated densities of the spots as a result of the quantification were read into the R/Bioconductor [26]. The Robust Spline Normalization from the R/Bioconductor package lumi was applied to the data [27]. The expressed and differentially expressed cytokines were determined as described previously [24]. The differential expression was tested via the moderated *t*-test from the Bioconductor package limma, adjusted for the false discovery rate via the method of Benjamini and Hochberg [28,29]. The cytokines expressed in both conditions (detection p value < 0.05) with an adjusted limma differential expression p value < 0.05 were considered upregulated when their ratio was greater than 1.2 (6/5) and downregulated when their ratio was less than 0.8333 (5/6).

2.8. Analysis of Gene Expression Data

The i705-C2 and UM51 organoid samples, untreated and treated with BF, were measured after 24 and 72 h on the Affymetrix Human Clariom S Array at the core facility of the Heinrich-Heine Universität, Düsseldorf (BMFZ: Biomedizinisches Forschungszentrum). Processing of the microarray data was performed in the R/Bioconductor environment [26]. The background correction and normalization with the Robust Multi-array Average (RMA) method was achieved by the Bioconductor package oligo [30]. Using the values of the dedicated background spots on the microarray, a statistic was calculated to determine a detection p value to judge if a probeset was expressed (detection $p < 0.05$) as was described before in Graffmann et al. [23]. The probesets expressed following this criterion were mapped to unique gene symbols according to the annotations provided by Affymetrix and compared in Venn diagrams via the VennDiagram package [31]. The function heatmap.2 from the R gplots package was applied to draw the heatmaps and the associated clustering dendrograms using the Pearson correlation as the similarity measure and color-scaling by Z-scores of rows (genes) [32]. The genes with a detection p value below 0.05 in both conditions were considered upregulated when the ratio was greater than 1.5 or downregulated when the ratio was less than 0.67.

2.9. Analysis of Pathways and Gene Ontologies (GOs)

For the analysis of the KEGG (Kyoto Encyclopedia of Genes and Genomes) pathways, the associations between the genes and pathways were downloaded from the KEGG website on 6 July 2020 [33]. The over-representation of pathways in the gene sets of interest was tested via the R-built in the hypergeometric test. The R package GOstats was applied for calculating over-represented gene ontologies [34]. For the dot plots of the most significantly over-represented pathways, the R package ggplot2 was employed [35].

2.10. Western Blotting

The total proteins from the cortical organoids and HLCs were isolated using the RIPA buffer (Sigma-Aldrich Chemicals, Taufkirchen, Germany), consisting of protease and phosphatase inhibitors (Roche, Mannheim, Germany). Afterward, the Pierce BCA Protein Assay Kit (Thermo Fisher, Waltham, MA, USA) was used to determine the protein concentrations. Approximately 20 µg of the heat-denatured protein lysate of each sample was loaded on a 4–12% SDS-PAGE and then transferred by wet blotting onto a 0.45 µm nitrocellulose membrane (GE healthcare, Solingen, Germany). After 1 h of blocking with 5% milk in TBST, the membranes were stained with anti-P53, anti-γH2AX, anti-UGT1A1, anti-CREB, anti-phospho-CREB, and anti-phospho-P38MAPK antibodies. Incubation with

primary antibodies was performed overnight at 4 °C. After washing the membranes three times with TBST, the secondary antibody incubation was performed for 2 h at RT followed by washing with TBST (Table S3). Anti β-Actin and anti-GAPDH (glyceraldehyde-3-phosphate dehydrogenase) were used as the housekeeping proteins to normalize the protein expression. ECL Western Blotting Detection Reagents (Cytiva, Freiburg, Germany) were used to visualize the stained protein bands and then detected in a Fusion FX instrument (PeqLab, Erlangen, Germany). A band intensity quantification and analysis was performed with Fusion Capt Advance software FX7 16.08 (PeqLab, Erlangen, Germany) and was normalized to the β-Actin band intensity.

2.11. Statistical Analysis

Statistical analyses for the comparison of each sample to their corresponding control were carried using Student's unpaired two-sample *t*-test. The calculations were performed with GraphPad Prism Software version 8.0.2 (263) (GraphPad software, San Diego, CA, USA) and Microsoft Excel. An asterisk depicts significance, which is determined by a p value ≤ 0.05, ** $p < 0.01$ and *** $p < 0.001$. The error bars depict the $\pm$ 95% confidence interval (qRT-PCR data) or mean $\pm$ standard deviation (SD) (IF quantification and WB).

2.12. Measurement of Cytochrome P450 Activity

The P450-GloTM CYP2D6 Assay and P450-GloTM CYP3A4 Assay Luciferin-IPA (Promega) kits were used to measure the Cytochrome P450 2D6 and P450 3A4 activity by employing a luminometer (Lumat LB 9507, Berthold Technologies, Bad Wildbad, Germany).

3. Results

3.1. iPSC-Derived Cortical Organoids Show Typical Cortical Neuronal Features

The hiPSCs derived from the renal progenitor cells isolated from the urine of a 51-year-old healthy male of African origin (UM51) and the fibroblast cells from a Crigler–Najjar syndrome (CNS) male patient (i705-C2) were cultured as colonies and used to generate 3D cortical neuronal organoids in triplicate. The i705-C2 iPSCs-derived HLCs retained defective UGT1A1 expression, as the cells were derived from the Crigler–Najjar syndrome (CNS) patient (Figure S1) [20,21]. The iPSCs were seeded as single cells to form embryoid bodies (EBs) and then transferred into a bioreactor to grow spontaneously as organoids (Figure 1a,b). Similar to previously established cerebral organoids, our generated organoids recapitulated human cortical developmental features with progenitor zone organization and the presence of radial glia stem cells and cortical neurons (Figure 1c) [36]. The self-patterned organoids showed cortical neuronal identity with the expression of the radial glia marker-SRY-box transcription factor 2 (SOX2), neuronal markers Beta III tubulin (TUJ1), microtubule-associated protein 2 (MAP2), and doublecortin (DCX) at day 15 (Figure 1c). These generated cortical organoids were treated with BF for further experimental analysis (Figure 1a).

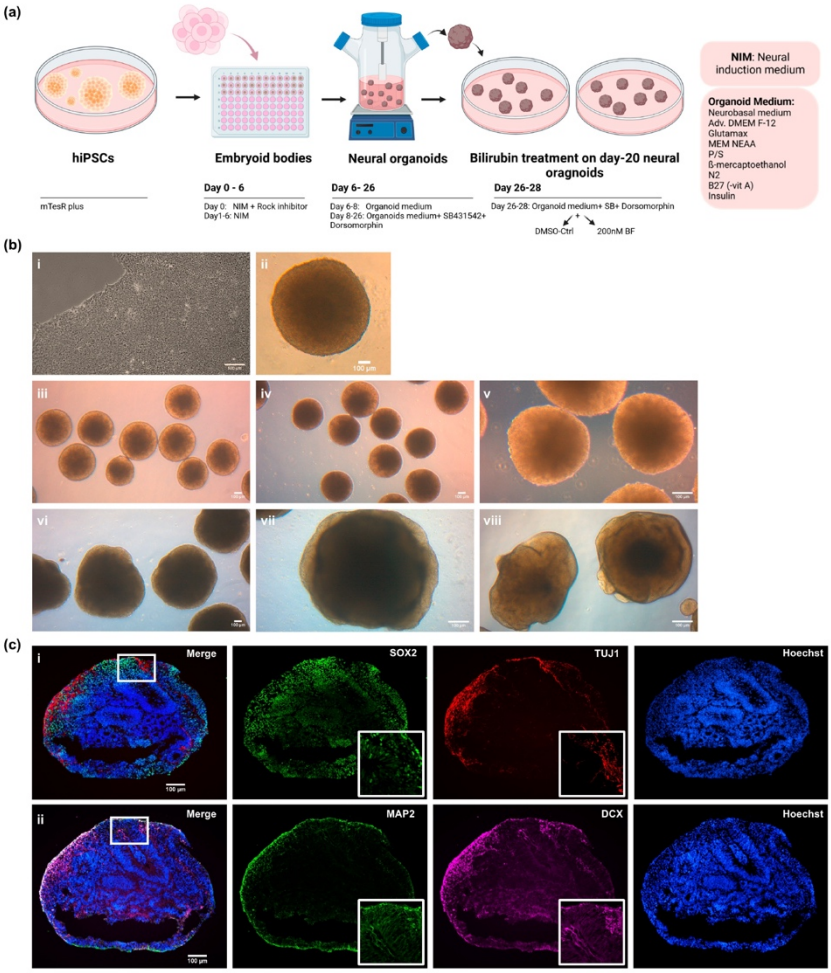

Figure 1. Generation of iPSC-derived cortical brain organoids and treatment with free bilirubin (BF). (**a**) Schematic depiction of the generation of cortical organoids. (Created with BioRender.com, accessed on 10 August 2023). (**b**) Bright-field images show the cortical brain organoid generation from iPSCs to organoids. Scale bars depict 100 µm. (**i**) iPSCs culture from patient-derived iPSC line (i705-C2) (**ii**). EBs were formed after 24 h of seeding in U-bottom 96-well plates. (**iii**, **iv**, **v**) Day-1 organoids (day 7 of differentiation). (**vi**, **vii**, **viii**) Day-20 organoids before BF treatment. (**c**) Neural identity of day-15 cortical organoids was confirmed by the expression of (**i**) the radial glia marker SOX2 (green) and neuronal marker TUJ1 (red), and (**ii**) MAP2 (green) and DCX (magenta), on sections and IF staining. Scale bars depict 100 µm.

3.2. Bilirubin (BF)-Induced Neuro-Inflammation with Elevated Expression of Pro-Inflammatory Cytokines

The day-20 cortical organoids were treated continuously with 200 nM free bilirubin for 72 h in the bioreactor (Figure 1a). The RNA from the UM51 and i705-C2 cortical organoids was isolated in triplicate (n = 3) at the 24 h and 72 h time points of the BF-treated and control conditions to investigate the expression of pro-inflammatory-associated cytokines at the

mRNA level. In parallel, the supernatant was collected at both time points to carry out a further secretome analysis using cytokine arrays (Figure S2a,b). The qRT-PCR analysis from the i705-C2 line showed a 3-fold increase in the *IL-6* and *IL-8* expression at 24 h post-treatment but decreased to 2-fold at 72 h, while the *IL-8* gene expression was enhanced 3-fold also for the UM51 healthy control line (Figure 2a). The *IL-6* mRNA expression was enhanced 1.5-fold only at 72 h post-treatment in the healthy line. On the other hand, the expression of *TNF-α* did not show any change upon BF exposure for the UM51 line, but a slight increase with a 1.5-fold (24 h and 72 h) change was observed in the i705-C2 line. Additionally, a heatmap obtained from the cytokine array-based analysis showed the secretome profile of various cytokines after BF treatment for both cell lines at 24 h and 72 h (Figure 2b) (Figure S2b). The enhanced secretion of the pro-inflammatory cytokines such as IL-6, IL-8, TNF-α, IL1-ß, IL-16, and INF-G was observed along with the anti-inflammatory cytokine interleukin (IL)-1 receptor antagonist (IL1-ra), IL-4, IL-11, and IL-13 secretion (Figure 2b). A number of the major anti-inflammatory cytokines which regulate pro-inflammatory cytokine expression include IL1-ra, IL-4, IL-10, IL-11, and IL-13 [37]. We could see a slight decrease in the IL1-ra, IL-10, IL-11, and IL-13 secretion in the 24 hrs post-treatment condition, while IL-4 expression was slightly increased. On the other hand, at 72 h, the expression of IL-4 decreased whilst that of IL1-ra, IL-10, and IL-13 showed modest increases in the treated condition (Figure S2). The secretome analysis also revealed enhanced vascular endothelial growth factor (VEGF) secretion and reduced sex hormone-binding globulin (SHBG) secretion upon BF treatment for all the conditions, except UM51 at 24 h (Figure 2b) (Figure S2b). The healthy line showed a 2-fold increase in the *VEGF* mRNA expression at 72 h, whilst the patient line showed a 1.4-fold and 1.6-fold increase at 24 and 72 h, respectively (Figure S2c). On the other hand, the *SHBG* expression was slightly decreased by 0.6-fold (UM51) and 0.8-fold (i705-C2) at 72 h post-treatment (Figure S2c). Overall, the increase in both the mRNA expression and protein secretion of IL-6, IL-8, and TNF-α implies the initiation of neuro-inflammation in the cortical organoids upon BF treatment.

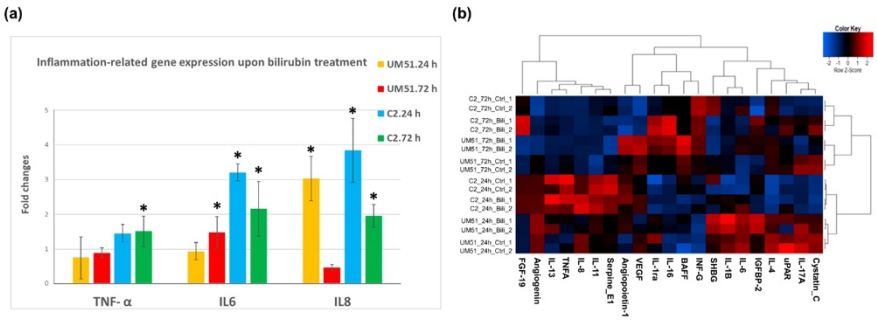

Figure 2. BF enhances the expression of pro-inflammatory cytokines. (**a**) qPCR analysis shows increased mRNA expression of pro-inflammatory cytokines such as *IL-6* and *IL-8* for both cell lines, while *TNF-α* was upregulated only for the patient line. Inflammatory responses were observed at 24 h in the patient line but declined gradually at 72 h, whereas the initiation of inflammatory responses shifted at 72 h for the UM51 line. Depicted values are the mean of three independent (n = 3) experiments. Error bars depict ± 95% confidence interval. Asterisk (*) depicts significance, which is determined by p value ≤ 0.05. Significance was calculated by using Student's unpaired two-sample t-test based on a difference between each sample mean compared to the mean value of the corresponding controls. Values were normalized to *RPLP0* (housekeeping gene) and subsequently to DMSO-treated control organoids. (**b**) Cytokine array-based secretome analysis showed increased IL-6, IL-8, and TNF-α secretion along with other cytokines upon BF exposure, while the healthy control line showed lower IL-6, IL-8, and TNF-α secretion compared to the patient line.

3.3. Distinct Inflammation-Associated Pathways Are Activated by BF in Cortical Organoids

To further investigate the neuro-inflammatory effect of BF on cortical organoids at the molecular level, the RNA was isolated from 24 and 72 h post-treated and untreated (control) UM51 and i705-C2 cortical organoids for a microarray-based transcriptome analysis. The Venn diagrams obtained from the transcriptome analysis revealed that the i705-C2 cortical organoids expressed 14,721 genes in common between the treatment and control and uniquely expressed 906 genes at 24 h post-treatment, whereas at 72 h, 15,317 genes were expressed in common, and 124 genes were uniquely expressed in the i705-C2 organoids (Figure 3a). On the other hand, the UM51 cortical organoids expressed 15,491 and 15,731 common sets of genes, while 289 and 351 genes were uniquely expressed upon BF exposure at 24 h and 72 h, respectively (Figure 3a). The KEGG pathways associated with the uniquely expressed genes at 24 h post-treatment included *TNFSF12* (TNF superfamily member 12), *AZI2* (5-azacytidine induced 2), and *MyD88* (myeloid differentiation primary response protein), and, for example, a cytokine–cytokine receptor interaction was activated in the i705-C2 line, which gradually decreased at 72 h (Figure 3b,c) (Figure S3b) (File S1). Cytokine–cytokine receptor activation was not observed in the healthy UM51 line at 24 h but at 72 h (Figure 3d) (Figure S3c). However, the calcium and MAPK signaling pathways and the neuroactive ligand–receptor interactions were activated at 24 h for the patient line and for both cell lines at 72 h post-BF exposure (Figure 3b–d) (Figure S3a).

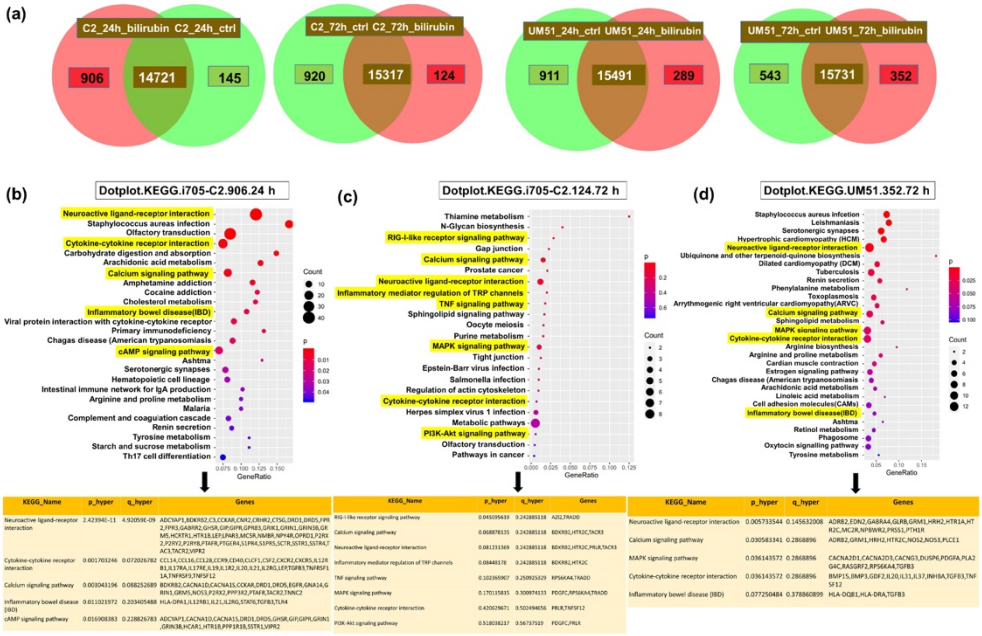

KEGG_Name	p_hyper	q_hyper	Genes
Neuroactive ligand-receptor interaction	2.42394E-11	4.92059E-09	ADCYAP1,BDKRB2,C3,CCKAR,CNR2,CRHR2,CTSG,DRD1,DRD5,FPR2,FPR3,GABRB2,GHSR,GIPR,GPR83,GRM1,GRM3,GRM8,GRM5,HCRTR1,HTR1B,LEP,LPAR3,MC5R,NMBR,NPY4R,OPRD1,P2RX2,P2RY2,P2RY8,PTAFR,PTGER4,S1PR4,S1PR5,SCT R,SSTR1,SSTR4,TAC1,TACR2,VIPR2
Cytokine-cytokine receptor interaction	0.001703246	0.072026782	CCL14,CCL16,CCL28,CCR9,CD40,CLCF1,CSF2,CXCR2,CXCR5,IL12RB1,IL17RA,IL17RE,IL19,IL1R2,IL20,IL21,IL2RG,LEP,TGFB3,TNFRSF11A,TNFRSF13B,TNFSF12
Calcium signaling pathway	0.003043196	0.088252689	BDKRB2,CACNA1D,CACNA1S,CCKAR,DRD1,DRD5,EGFR,GNA14,GRIN3,GRM5,NOS3,P2RX2,PPP3R2,PTAFR,TACR2,TNNC2
Inflammatory bowel disease (IBD)	0.011021972	0.203405488	HLA-DPA1,IL12RB1,IL2,IL2RG,STAT6,TGFB3,TLR4
cAMP signaling pathway	0.011908383	0.228826783	ADCYAP1,CACNA1D,CACNA1S,DRD1,DRD5,GHSR,GIP,GIPR1,GRIN3B,HCAR1,HTR1B,PPP3R2,S1PR1,SSTR1,VIPR2

KEGG_Name	p_hyper	q_hyper	Genes
RIG-I-like receptor signaling pathway	0.045095633	0.242885338	AZI2,TRAF6D
Calcium signaling pathway	0.068878135	0.242885338	BDKRB2,HTR2C,TACR3
Neuroactive ligand-receptor interaction	0.081191369	0.242885338	BDKRB2,HTR2C,PRLR,TACR3
Inflammatory mediator regulation of TRP channels	0.08448178	0.242885338	BDKRB2,HTR2C
TNF signaling pathway	0.102365907	0.250925329	RPS6KA4,TRAD D
MAPK signaling pathway	0.170115835	0.309974333	PDGFC,MPS6KA4,TRAD D
Cytokine-cytokine receptor interaction	0.420029671	0.502494656	PRLR,TMFSF12
PI3K-Akt signaling pathway	0.518038237	0.56737103	PDGFC,PRLR

KEGG_Name	p_hyper	q_hyper	Genes
Neuroactive ligand-receptor interaction	0.005733544	0.145632008	ADRB2,EDN2,GABRA4,GLRB,GRM1,HRH2,HTR1A,HTR2C,MC2R,NPBWR2,PROK1,PTH1R
Calcium signaling pathway	0.030583341	0.2868896	ADRB2,GRM1,HRH2,HTR2C,NOS2,NOS3,PLCE1
MAPK signaling pathway	0.036143572	0.2868896	CACNA2D1,CACNA2D3,CACNG3,DUSP6,PDGFA,PLA2G4C,RASGRF2,RPS6KA4,TGFB3
Cytokine-cytokine receptor interaction	0.036143572	0.2868896	BMP15,IBMP3,IGDF2,IL20,IL31,IL37,JNHBA,TGFB3,TNFSF12
Inflammatory bowel disease (IBD)	0.077250484	0.378860899	HLA-DQB1,HLA-DRA,TGFB3

Figure 3. Overview of distinct activated pathways upon BF treatment in cortical brain organoids. (**a**) Venn diagrams show the uniquely and differentially expressed genes upon bilirubin treatment for UM51 and i705-C2 cell lines for both the 24 h and 72 h time points. Dot plots from KEGG-associated pathways and corresponding genes revealed cytokine–cytokine receptor activation in the patient line at 24 h post-treatment and (**b**), which goes down gradually at 72 h (**c**). This cytokine–cytokine receptor activation was not observed in the UM51 line at 24 h (Figure S3c) but observed at 72 h (**d**). Dot plots show the activation of calcium signaling pathway, MAPK signaling pathway, and neuroactive ligand–receptor interaction for both cell lines at 72 h post-BF exposure.

3.4. BF Treatment Differentially Regulates DNA Damage and Repairs-Related Pathways

The transcriptome analysis of the cortical organoids provided an overview of the GO terms and associated KEGG pathways of the differentially regulated genes (common set of genes) upon BF exposure (Files S1–S4). The KEGG pathways revealed that DNA damage and repair-related pathways such as P53 signaling, homologous recombination, and the Fanconi Anemia pathway were upregulated in the UM51 line and downregulated in the i705-C2 line at 24 h (Figure 4(bii,biii)) (File S2). In parallel, at 24 h, the i705-C2 line showed activation of the NFκB, PI3K, and chemokine signaling pathways, indicating to the initiation of inflammation, while the cellular developmental processes related to the Notch and TGFβ signaling pathways were upregulated (Figure 4(bi)). Interestingly, a number of these inflammatory and development-related pathways (neuroactive ligand–receptor interaction, cAMP signaling pathway, and cytokine–cytokine receptor interaction) were observed to be downregulated at 24 h in the UM51 line (Figure 4(biv)). The mRNA expression of *NLRP3* (NLR family pyrin domain-containing 3) seems to be enhanced only for the i705-C2 line, which is an upstream activator of NFκB signaling and plays a role in inflammation, immune response, and apoptosis. The activation and increased *NLRP3* mRNA expression might indicate NFκB-mediated inflammatory responses upon BF exposure (Figure S3b). UM51 showed a slight increase in both the mRNA (1.2-fold) and protein expression of the cAMP-response element-binding protein (CREB) (1.3-fold) and the protein expression for phospho-CREB (1.13-fold), while the i705-C2 line showed only slightly enhanced mRNA expression (Figures S3b and S4a,b). Moreover, the UM51 line showed slightly enhanced mRNA expression of the DNA damage–repair and apoptosis-related genes at 24 and 72 h such as *P53* (tumor protein P53) (1.24-fold and 1.14-fold), *BCL2* (B-cell lymphoma 2) (1.5-fold and 1.3-fold), *ATM* (ataxia telangiectasia mutated) (1.41-fold), *ATR* (ataxia telangiectasia and Rad3-related protein) (1.3-fold and 1.3-fold), *CHEK1* (checkpoint kinase 1) (1.3-fold and 1.2-fold), and *CHEK2* (1.6-fold) compared to the i705-C2 line (Figure 4(ai)). However, the patient line showed increased *BCL2* (1.3-fold) and *MDM2* (mouse double minute 2 homolog) (1.4-fold) expression at 24 h and increased *P53* (1.6-fold) expression at 72 h post-BF treatment. In addition to that, the Western blot (WB) analysis revealed a 1.64-fold increase in the P53 protein expression at 24 h in the healthy line and with a non-significant 1.1-fold increase at 72 h in the patient line (Figure 4(aii,iii)). Furthermore, the GO terms of the common set of expressed genes revealed neurodevelopmental pathways to be differentially upregulated with the activation of the cellular developmental process, nervous system development, axon development, axon guidance, tight junction, positive regulation of axogenesis, and positive regulation of synapse assembly for both cell lines at 72 h post-BF treatment (Figure S4d) (File S4).

3.5. BF Induces Apoptotic Cell Death in Cortical Organoid

The apoptotic cell death in the BF-treated cortical organoids was evaluated by immunofluorescence and Western blot analysis. Both cell lines exhibited an increased level of cell death based on terminal deoxynucleotidyl transferase dUTP nick end labeling (TUNEL) at 24 h post-treatment (Figure 5a,b). Cleaved caspase 3 (CASP 3) positive cells were observed in the organoid sections, pointing at apoptotic cell death at 24 h post-treatment (Figure 5a,b).

Immunofluorescence-based quantification revealed a 34% increase in the TUNEL and cleaved Caspase 3 positive cells in the UM51 organoid sections, whereas the i705-C2 sections had 22% TUNEL positive and 25% cleaved Caspase 3 positive cells at 24 h (Figure 5c). The γH2AX expression, which indicates both DNA damage or apoptotic cell death, showed an enhanced protein expression of 1.26-fold based on the WB analysis on the healthy line after 24 h of BF exposure, whilst the patient line showed almost no change in the γH2AX expression (1.04-fold increase) (Figure 5d). The immunofluorescence-based staining also showed a 15% increase in the γH2AX expression at 24 h post-BF treatment for the healthy line (Figure S5a,b). A further indication of DNA damage was observed with the upregulation of the P53-mediated signaling pathway in the KEGG

analysis of the UM51 transcriptome at 24 h (Figure 4(biii)). The necroptosis-associated genes shown in the Pearson heatmap derived from our transcriptome analyses revealed that the upregulated expressed genes for the patient organoid (X-linked inhibitor of apoptosis protein (*XIAP*); tumor necrosis factor receptor-associated factors (*TRAF*), *TRAF2* and *TRAF5*; signal transducers and activators of transcription (*STAT*), *STAT1*, *STAT2*, *STAT3*, and *STAT4*; janus kinase 2 (*JAK2*); and baculoviral IAP repeat containing (*BIRC*), *BIRC3*, *BIRC5*, and *BIRC6*) are associated with inflammation, whilst the upregulated genes (*FAS* and *CASP8*) for the healthy organoid are associated with apoptosis (Figure S5c). Regardless of the BF treatment, the transcriptomes of the patient samples were clustered separately in the heatmap from the healthy line, which might also indicate that the observed upregulation is a phenotype of the defective UGT1A1 in the patient line-derived organoids.

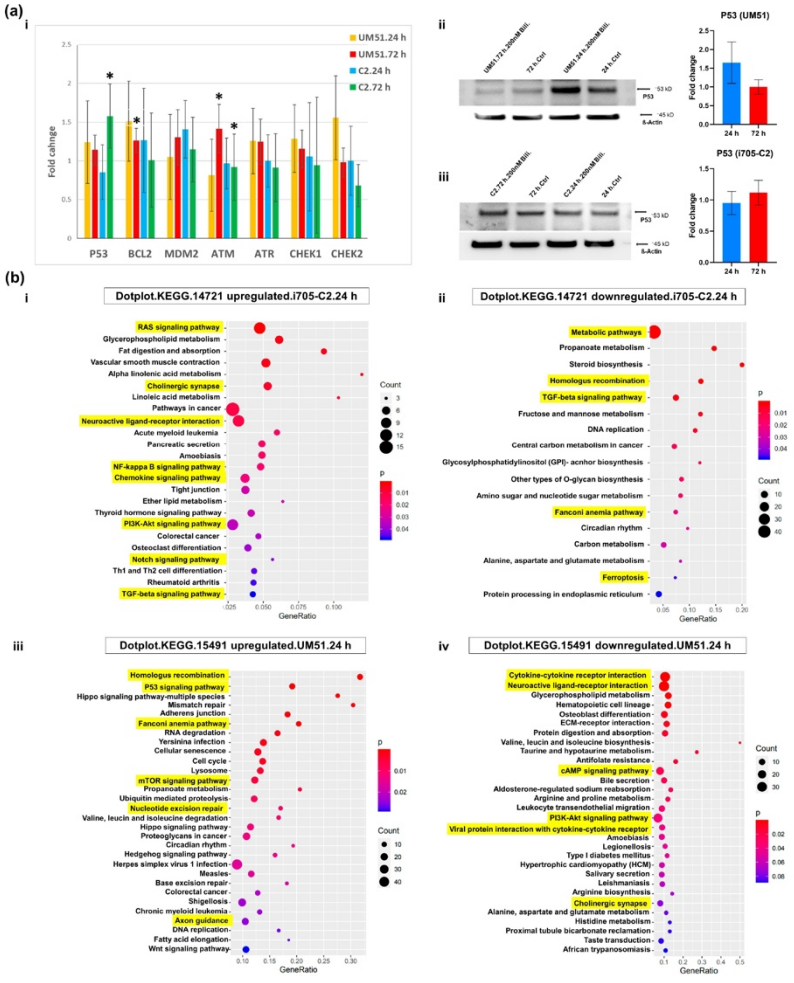

Figure 4. BF treatment differentially regulated DNA damage and repair-related pathways. (**a**) (**i**) qRT-PCR analysis shows DNA damage and repair-related gene (*P53*, *BCl2*, *MDM2*, *ATM*, *ATR*,

CHEK1, *CHEK2*) expression after BF treatment. Depicted values are mean of three independent (n = 3) experiments. Error bars depict ± 95% confidence interval. Asterisk depicts significance, which is determined by p value ≤ 0.05. Significance was calculated by using Student's unpaired two-sample t-test based on the difference between each sample mean compared to the corresponding control mean. Values were normalized to *RPLP0* (housekeeping gene) and subsequently to DMSO-treated control organoids. (**ii**, **iii**) WB analysis shows increased P53 protein expression at 24 h in the healthy line and at 72 h in the patient line, thus implying DNA damage and/or apoptotic cell death. Bar graphs show protein expression in fold change. Depicted values are mean of three independent (n = 3) experiments. Error bars depict mean ± standard deviation (SD). Values were normalized to β-Actin (housekeeping protein) and subsequently to DMSO-treated control organoids. (**b**) Dot plots from KEGG pathways revealed DNA damage and repair-related pathways such as P53 signaling pathway, homologous recombination, Fanconi Anemia pathways to be upregulated in the healthy line at 24 h (**iii**) and downregulated in the patient line (**ii**). Additionally, at 24 h, the patient line showed activation of NFκB, PI3K, and chemokine signaling pathways, thus implying the onset of inflammation (**i**). Cytokine–cytokine receptor interaction, neuroactive ligand–reactor interaction, cAMP signaling pathway were downregulated in the healthy line at 24 h (**iv**).

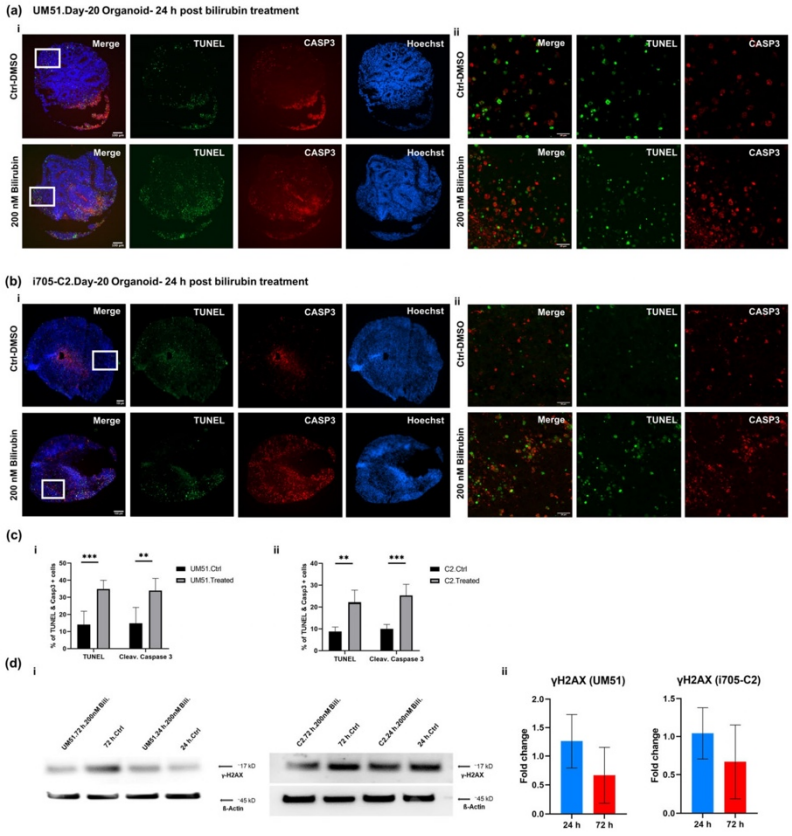

Figure 5. BF treatment initiates apoptotic cell death on cortical neurons. IF staining of day-20 cortical organoid sections after 24 h of BF exposure for the healthy line (**a**) and patient line (**b**). In

panels (**a**) (**i**), (**b**) (**i**), (**c**) (**i, ii**), we see increased apoptotic cell death as confirmed by the presence of TUNEL positive (green) staining and the apoptotic cell death marker-cleaved CASP 3 (red). Scale bars depict 100 µm. (**a**) (**ii**), (**b**) (**ii**) Confocal imaging of the TUNEL (green), cleaved CASP 3 (red) positive cells shows a higher magnification. Scale bars depict 20 µm. (**c**) (**i, ii**) Bar graphs indicate quantification of TUNEL and cleaved CASP3 staining (n = 6). Error bars depict mean ± SD. Asterisk depicts significance, which is determined by p value ≤ 0.05, ** $p < 0.01$ and *** $p < 0.001$. Significance in comparison to control was calculated by using Student's unpaired two-sample *t*-test. (**d**) (**i, ii**) WB analysis showed increased γH2AX expression at 24 h post-BF treatment (n = 3). Bar graphs show the protein expression in fold change. Error bars depict mean ± SD. Values were normalized to β-Actin (housekeeping protein) and subsequently to DMSO-treated control organoids.

4. Discussion

In this study, we generated iPSC-derived 3D cortical organoids to model BIND in vitro and unveil insights into the detrimental effects of BF in the developing human brain at the molecular and protein level. Our in vitro model comprises a healthy iPSC (UM51) and a CNS patient-derived (i705-C2) iPSC, harboring the UGT1A1 mutation [20,21]. Defective UGT1A1 protein expression was confirmed after differentiation of the iPSCs into hepatocyte-like cells (HLCs).

BF can interfere BBB integrity by glutathione disruption and increased endothelial nitric oxide synthase (NOS) by enhanced cytokine release [3,38]. Cytokines play a key role in regulating nerve cell responses during a brain injury [39]. Cytokines might have both beneficial and detrimental effects on neurons depending on their levels of secretion [4,40,41]. The production of pro-inflammatory mediators can cause neuronal apoptosis and neuro-inflammation [42,43]. Even though microglia are the key cell type in the central nervous system which secrete pro-inflammatory cytokines upon stress, bilirubin-treated neurons showed enhanced secretion of IL-6 with decreased secretion of IL-1β [44]. Based on these findings, we analyzed the mRNA expression of several pro-inflammatory cytokines and their secretome profile. The mRNA expression from the control and BF-treated conditions showed a 3-fold increase in the *IL-6* and *IL-8* expression at 24 h post-treatment in the i705-C2 line which then decreased to 2-fold at 72 h. A similar pattern was observed in the secretome analysis for the i705-C2 line with an increased secretion of IL-6 and IL-8 at 24 h post-treatment, which then decreased at 72 h. The secretion of IL-6 can be repressed by IL-10 [37]. The increased secretion levels of the anti-inflammatory proteins IL-10 and IL-13 at 72 h might repress the IL-6 and IL-8 secretions. This observation might imply that inflammatory responses were initiated earlier in the i705-C2 organoids and gradually reverted to normal levels with time as a consequence of the cellular defense mechanisms establishing homeostasis. On the other hand, the UM51 (healthy) line showed 3-fold enhanced *IL-8* mRNA expression only at 24 h, while the IL-8 protein secretion was decreased at this time point. However, the IL-8 protein secretion was increased at 72 h. In parallel, the IL-6 protein secretion was enhanced for both 24 and 72 h post-BF treatment, while the mRNA expression showed a 1.5-fold increase only at 72 h. The *TNF-α* levels did not show any elevation upon BF exposure for the UM51 line but a 1.5-fold change increase in both the secretome and mRNA expression in the i705-C2 line. Fernandes et al. previously reported that bilirubin enhances the tumor necrosis factor receptor 1 (TNFR1) protein level in neural cells (such as astrocytes) along with a time-dependent release of TNF-α, IL-1ß, and IL-6. But neurons secrete merely low levels of IL-6 and even to a lesser extent TNF-α [4]. The correlation of the mRNA and secretome expression observed in our results suggests that mRNA and protein expression might have a slight time shift in their expression as a response to stress to induce inflammation in CNS. For example, the patient organoids showed increased IL1-β secretion only at 24 h, while the IL1-ra secretion was increased at 72 h for both cell lines. IL1-ra is a natural inhibitor of IL1-β, as this receptor competitively binds to the same receptor as IL1-β. Consequently, IL1-β-mediated cellular changes are obstructed, which might be the reason for the observed decrease in IL1-β secretion at 72 h post-BF treatment [37,45,46]. Having the anti-inflammatory effects, increased IL1-ra might

antagonize cytokine-mediated inflammatory responses to re-establish the normal condition at 72 h. These observations point to a variation in the levels and patterns of initiation and responses to inflammation post-BF treatment. The secretome analysis also revealed enhanced VEGF and reduced SHBG secretion upon BF treatment for all conditions, except UM51 at 24 h. Previous studies described low VEGF expression in the adult human brain and upregulated VEGF levels have been observed in chronic neuro-inflammation [47,48]. Increased VEGF expression might be a cause or response to bilirubin treatment, which remains a question because of the multiple roles played by VEGF. On the other hand, SHBG exhibits anti-inflammatory effects in macrophages and adipocytes; however, SHBG expression in the brain is not yet known [49]. A slight reduction in *SHBG* expression by 0.6-fold (UM51) and 0.8-fold (i705-C2) at 72hrs post-BF treatment might indicate a tendency toward the initiation of an anti-inflammatory response. The secretome profile unveiled a pro-inflammatory CNS environment with variable cytokine secretion for both the healthy and disease cell lines at different time points, thus indicating pronounced neuro-inflammation upon BF treatment. Overall, in accord with Brites et al., the increase in mRNA expression and secreted levels of IL-6, IL-8, and TNF-α along with other inflammatory cytokines points to the onset or initiation of neuro-inflammation in the cortical organoids upon BF treatment [3,4,50].

Next, we performed a transcriptome-based microarray analysis to have an overview of the molecular effects of BF on cortical organoids, such as differential gene expression and associated biological processes (GO-BP) and KEGG pathways. Both cell lines showed activation of the cytokine–cytokine receptor interaction, calcium-signaling pathway, MAPK signaling, and neuroactive ligand–receptor interaction, among their uniquely expressed gene sets. In the patient line, cytokine–cytokine receptor activation was activated at both 24 and 72 h in the BF-treated condition, whereas in the healthy line this pathway seemed to be activated at 72 h. The observed GO terms and KEGG-associated pathways did not show activation of any of these mentioned pathways at 24 h in the treated condition in the UM51 line. Activation of GO-BP inflammatory bowel disease was observed in the i705-C2-24 h and UM51-72 h post-treated conditions. These findings point toward a possibility that the patient line shows an accelerated response to initiate inflammatory responses (24 h in this case) than the healthy line. The slightly enhanced mRNA expression of *TNSF12* (1.12-fold in UM51 and 1.6-fold in i705-C2), *AZI2* (1.2-fold in i705-C2), and *MyD88* (1.2-fold in i705-C2) was observed upon BF treatment. The increased expression of these genes points to the initiation of inflammation upon BF treatment [51–55].

The GO-BP terms revealed at 72 h the activation of the positive regulation of NFκB transcription factor activity (*AR*, *TRADD*, and *RPS6KA4*) in the i705-C2 line, while the positive regulation of the CREB transcription factor activity (*RELN* and *RPS6KA4*) and NLRP3 inflammasome complex assembly (*GBP5* and *NLRP3*) was revealed in the UM51 line. The activation and increased *NLRP3* mRNA expression might indicate NFκB-mediated inflammatory responses upon BF exposure. Similar to astrocytes and microglia, bilirubin-induced NFκB activation was observed in neurons as well but at lower levels [11,28]. Based on the cellular context, NFκB plays diverse roles in the central nervous system. The axonal growth of neurons can be implicated with NFκB activation [56,57]. NFκB may also regulate neural development, plasticity, and neurogenesis [4,58,59]. From our observed results, the GO-BP terms of the common set of genes revealed the neurodevelopmental pathways to be upregulated for both cell lines at 72 h post-BF treatment with the activation of nervous system development, axon development, axon guidance, tight junction, positive regulation of axogenesis, and synapse assembly. On the other hand, activation of the MAPK cascade was also observed in both the UM51 and i705-C2 lines upon BF treatment. MAPK signaling pathways were observed to be activated in bilirubin-treated astrocytes as well [4]. A slight enhancement with a 1.25-fold increase in the phospho-P38 protein expression was observed for the patient line post-BF exposure by Western blot analysis.

The KEGG pathways associated with the common set of genes revealed that DNA damage and repair-related pathways such as P53 signaling, homologous recombination,

and Fanconi anemia pathway were upregulated in the UM51 line at 24 h. These pathways were downregulated at 24 h in the i705-C2 line. With respect to DNA damage, P53 induces multiple classes of its target genes, such as metabolic genes, DNA repair genes, cell-cycle arrest, and cell death effectors [60]. The UM51 line showed enhanced mRNA expression of the DNA damage–repair and apoptosis-related genes such as *P53*, *BCl2*, *ATM*, *ATR*, *CHEK1*, and *CHEK2* compared to the i705-C2 line. The P53 protein expression was 1.64-fold upregulated at 24 h in the healthy line and the level decreased at 72 h. Conversely, there was no increase in the P53 protein expression (1.1-fold at 72 h) in the patient line, but an increase in the *P53* mRNA expression (1.6-fold) was observed at 72 h. Interestingly, a number of inflammatory and development-related pathways (neuroactive ligand–receptor interaction and cytokine–cytokine receptor interaction) were downregulated at 24 h in the UM51 line. Indications of inflammatory responses were observed at 72 h, implying a delayed initiation of inflammation in the healthy line. In parallel, at 24 h, the i705-C2 line showed activation of the NFκB, PI3K, and chemokine signaling pathways, thus implying the initiation of inflammation. The expression of *NLRP3* which is known to play a role in inflammation, immune responses, and apoptosis was enhanced 1.9-fold in the i705-C2 line only [61]. The observed activation of the NFκB, MAPK, and calcium signaling pathways along with increased IL-6 and IL-8 expression in our CNS model confirms the initiation of neuro-inflammation after BF treatment in these organoids, as the observed pathways have also been reported to be associated with other neuro-inflammatory diseases [62].

On the other hand, positive regulation of CREB transcription factor activity could be a response to stress or the induction of inflammatory cascades [63]. Zhang et al. described that bilirubin can regulate the Ca^{2+} channel opening [64]. This might have a correlation with the observed activation of calcium signaling upon BF exposure in the KEGG pathway analysis. The Ca^{2+} influx into cortical neurons regulates the expression of nNOS mediated by a CREB transcription factor [64]. The positive regulation of the CREB expression was observed in the UM51 cell line. Of note, CREB is associated with inflammation and apoptotic cell death, while both could be possible effects of BF on the organoids [65]. The UM51 line showed a 1.2-fold increase in both the mRNA and protein expression of CREB and a 1.2-fold increase in phospho-CREB protein expression. Apoptotic cell death was observed in both cell lines at 24 h post-BF exposure. However, the UM51 line showed more than a 30% increase in apoptotic cell death, while the patient line showed around a 20% increase. γH2AX, which can be a marker for both DNA damage and apoptotic cell death, also underwent a 1.4-fold increase in protein expression in the UM51 line [66]. Multiple stages of necroptosis and apoptosis signaling cascades can be regulated by each other. As the necroptosis-associated genes such as *XIAP*, *TRAF2*, *TRAF5*, *STAT1*, *STAT2*, *STAT3*, *STAT4*, *JAK2*, *BIRC3*, *BIRC5*, and *BIRC6* are upregulated in the patient organoids, this might imply reduced apoptosis but increased inflammatory response due to necroptosis compared to the healthy organoids [67–71].

Through all the observed analyses, the UM51 line showed increased apoptotic cell death and DNA damage and repair-related gene expression at 24 h post-BF treatment and then the activation of inflammatory-related pathways at 72 h. On the other hand, the i705-C2 line did not show increased DNA damage and repair-related gene expression at 24 h (*ATM*, *ATR*, *CHEK1*, and *CHEK2*). However, the i705-C2 line leaned toward the initiation of inflammation at 24 h, which then decreased at 72 h. Overall, these observations are indicative of a switch or shift in the initiation of inflammation and cell death-related pathways in these cell lines after treating with BF. Although both cell lines showed inflammatory responses after BF treatment, they seemed to be adopting distinct pathways and time points to respond to the BF-induced stress which results in apoptotic cell death, DNA damage–repair, or inflammation.

5. Conclusions

In summary, this study provides valuable molecular insights into BF-induced neuro-inflammation in iPSC-derived cortical organoids. The global gene expression analyses

provided an overview of the distinct pathways and genes which might be associated with the neuro-inflammatory effects induced by BF. The iPSC-derived cortical organoids employed in this study represent a Crigler–Najjar syndrome model to study defective UGT1A1 and its subsequent phenotypic manifestation and potential application for future BIND-associated toxicological studies and drug screening.

Supplementary Materials: The following supporting information can be downloaded at: https://www.mdpi.com/article/10.3390/cells12182277/s1, Table S1: Information on the iPS cell lines; Table S2: Composition of cortical organoid differentiation medium; Table S3: List of antibodies; Table S4: List of qRT-PCR primers; Figure S1: Generation of UM51 and i705-C2 iPSC-derived HLCs to verify the expression of UGT1A1; Figure S2: Secretome analysis of individual samples using the Human XL Cytokine Array; Figure S3: Selected GO terms with corresponding genes and KEGG pathways from the uniquely expressed genes post-BF exposure; Figure S4: WB analysis and dot plots of upregulated GO-BP terms from the common set of genes at 72 h post-BF treatment; Figure S5: Immunofluorescence staining shows the expression of γH2AX at 24 h post-BF exposure and heatmap shows necroptosis-associated gene expression; Supplementary File S1: Complete lists of KEGG pathways with the associated unique gene sets of bilirubin-treated i705-C2 and UM51 organoids at 24 and 72 h; Supplementary File S2: Complete lists of up- and downregulated KEGG pathways in the common gene set of i705-C2 and UM51 control and bilirubin-treated condition at 24 h; Supplementary File S3: Complete lists of GO terms based on uniquely expressed gene sets of bilirubin-treated i705-C2 and UM51 cortical organoids at 24 and 72 h; Supplementary File S4: Complete list of GO terms based on the upregulated common gene set between i705-C2 and UM51 control and bilirubin-treated condition at 72 h; Supplementary File S5: Uncropped whole blot membranes that were cropped for generating figures.

Author Contributions: A.I.P. designed and performed the experiments, processed and analyzed the data, and wrote and edited the manuscript. W.W. performed the bioinformatic analysis and data curation, helped with the figures, wrote the bioinformatic section in Section 2, and edited the manuscript. J.A. conceptualized and designed the work, edited the manuscript, acquired funding, and supervised the study. All authors have read and agreed to the published version of the manuscript.

Funding: This research received no external funding. J.A. acknowledges the medical faculty of Heinrich Heine University for financial support.

Institutional Review Board Statement: The study was conducted according to the guidelines set by the ethics committee of the medical faculty of Heinrich-Heine University, Germany (protocol code: 5704).

Data Availability Statement: All microarray data generated and analyzed during the current study are available in the GEO repository (https://www.ncbi.nlm.nih.gov/geo/, accessed on 18 July 2023) under the accession number GSE243133.

Conflicts of Interest: The authors declare no conflict of interest.

References

1. Bortolussi, G.; Muro, A.F. Advances in understanding disease mechanisms and potential treatments for Crigler–Najjar syndrome. *Expert Opin. Orphan Drugs* **2018**, *6*, 425–439. [CrossRef]
2. Watchko, J.F.; Tiribelli, C. Bilirubin-Induced Neurologic Damage-Mechanisms and Management Approaches. *N. Engl. J. Med.* **2013**, *369*, 2021–2030. [CrossRef] [PubMed]
3. Brites, D. The Evolving Landscape of Neurotoxicity by Unconjugated Bilirubin: Role of Glial Cells and Inflammation. *Front. Pharmacol.* **2012**, *3*, 88. [CrossRef] [PubMed]
4. Fernandes, A.; Falcão, A.S.; Silva, R.F.M.; Gordo, A.C.; Gama, M.J.; Brito, M.A.; Brites, D. Inflammatory signalling pathways involved in astroglial activation by unconjugated bilirubin. *J. Neurochem.* **2006**, *96*, 1667–1679. [CrossRef] [PubMed]
5. Shapiro, S.M. Definition of the Clinical Spectrum of Kernicterus and Bilirubin-Induced Neurologic Dysfunction (BIND). *J. Perinatol.* **2004**, *25*, 54–59. [CrossRef]
6. Canu, G.; Minucci, A.; Zuppi, C.; Capoluongo, E. Gilbert and Crigler Najjar syndromes: An update of the UDP-glucuronosyltransferase 1A1 (UGT1A1) gene mutation database. *Blood Cells Mol. Dis.* **2013**, *50*, 273–280. [CrossRef]
7. Memon, N.; I Weinberger, B.; Hegyi, T.; Aleksunes, L.M. Inherited disorders of bilirubin clearance. *Pediatr. Res.* **2015**, *79*, 378–386. [CrossRef]
8. Pranty, A.I.; Shumka, S.; Adjaye, J. Bilirubin-Induced Neurological Damage: Current and Emerging iPSC-Derived Brain Organoid Models. *Cells* **2022**, *11*, 2647. [CrossRef]

9. Singh, A.; Jialal, I. Unconjugated Hyperbilirubinemia. In *StatPearls*; StatPearls Publishing LLC.: Treasure Island, FL, USA, 2021.
10. Yueh, M.F.; Chen, S.; Nguyen, N.; Tukey, R.H. Developmental Onset of Bilirubin-induced Neurotoxicity Involves Toll-like Receptor 2-dependent Signaling in Humanized UDP-glucuronosyltransferase1 Mice. *J. Biol. Chem.* **2014**, *289*, 4699–4709. [CrossRef]
11. Gidáli, J.; Poros, A.; Harsányi, V.; Fehér, I.; Mód, A.; Hollán, Z. Granulocyte-macrophage progenitor cells in allogenic bone marrow transplantation: Correlation of progenitor cell content and regeneration in the graft. *Orvosi Hetil.* **1989**, *130*, 2251–2254.
12. Vodret, S.; Bortolussi, G.; Jašprová, J.; Vitek, L.; Muro, A.F. Inflammatory signature of cerebellar neurodegeneration during neonatal hyperbilirubinemia in Ugt1 -/- mouse model. *J. Neuroinflamm.* **2017**, *14*, 1–16. [CrossRef]
13. Vaz, A.R.; Silva, S.L.; Barateiro, A.; Falcão, A.S.; Fernandes, A.; Brito, M.A.; Brites, D. Selective vulnerability of rat brain regions to unconjugated bilirubin. *Mol. Cell. Neurosci.* **2011**, *48*, 82–93. [CrossRef] [PubMed]
14. Falcão, A.S.; Silva, R.F.M.; Vaz, A.R.; Gomes, C.; Fernandes, A.; Barateiro, A.; Tiribelli, C.; Brites, D. Cross-Talk Between Neurons and Astrocytes in Response to Bilirubin: Adverse Secondary Impacts. *Neurotox. Res.* **2013**, *26*, 1–15. [CrossRef] [PubMed]
15. Watchko, J.F. Kernicterus and the Molecular Mechanisms of Bilirubin-Induced CNS Injury in Newborns. *NeuroMol. Med.* **2006**, *8*, 513–530. [CrossRef] [PubMed]
16. Proskuryakov, S.Y.; Konoplyannikov, A.G.; Gabai, V.L. Necrosis: A specific form of programmed cell death? *Exp. Cell Res.* **2003**, *283*, 1–16. [CrossRef] [PubMed]
17. Nirmala, J.G.; Lopus, M. Cell death mechanisms in eukaryotes. *Cell Biol. Toxicol.* **2019**, *36*, 145–164. [CrossRef] [PubMed]
18. Vanden Berghe, T.; Linkermann, A.; Jouan-Lanhouet, S.; Walczak, H.; Vandenabeele, P. Regulated necrosis: The expanding network of non-apoptotic cell death pathways. *Nat. Rev. Mol. Cell Biol.* **2014**, *15*, 135–147. [CrossRef] [PubMed]
19. Doré, S.; Takahashi, M.; Ferris, C.D.; Hester, L.D.; Guastella, D.; Snyder, S.H. Bilirubin, formed by activation of heme oxygenase-2, protects neurons against oxidative stress injury. *Proc. Natl. Acad. Sci. USA* **1999**, *96*, 2445–2450. [CrossRef] [PubMed]
20. Graffmann, N.; Martins, S.; Ljubikj, T.; Matte, J.C.; Bohndorf, M.; Wruck, W.; Adjaye, J. Generation of a Crigler-Najjar Syndrome Type I patient-derived induced pluripotent stem cell line CNS705 (HHUUKDi005-A). *Stem Cell Res.* **2021**, *51*, 102167. [CrossRef]
21. Bohndorf, M.; Ncube, A.; Spitzhorn, L.-S.; Enczmann, J.; Wruck, W.; Adjaye, J. Derivation and characterization of integration-free iPSC line ISRM-UM51 derived from SIX2-positive renal cells isolated from urine of an African male expressing the CYP2D6 *4/*17 variant which confers intermediate drug metabolizing activity. *Stem Cell Res.* **2017**, *25*, 18–21. [CrossRef]
22. Gabriel, E.; Gopalakrishnan, J. Generation of iPSC-derived Human Brain Organoids to Model Early Neurodevelopmental Disorders. *J. Vis. Exp.* **2017**, e55372. [CrossRef]
23. Graffmann, N.; Ring, S.; Kawala, M.-A.; Wruck, W.; Ncube, A.; Trompeter, H.-I.; Adjaye, J. Modeling Nonalcoholic Fatty Liver Disease with Human Pluripotent Stem Cell-Derived Immature Hepatocyte-Like Cells Reveals Activation of PLIN2 and Confirms Regulatory Functions of Peroxisome Proliferator-Activated Receptor Alpha. *Stem Cells Dev.* **2016**, *25*, 1119–1133. [CrossRef] [PubMed]
24. Wruck, W.; Boima, V.; Erichsen, L.; Thimm, C.; Koranteng, T.; Kwakyi, E.; Antwi, S.; Adu, D.; Adjaye, J. Urine-Based Detection of Biomarkers Indicative of Chronic Kidney Disease in a Patient Cohort from Ghana. *J. Pers. Med.* **2022**, *13*, 38. [CrossRef] [PubMed]
25. Schneider, C.A.; Rasband, W.S.; Eliceiri, K.W. NIH Image to ImageJ: 25 Years of image analysis. *Nat. Methods* **2012**, *9*, 671–675. [CrossRef] [PubMed]
26. Gentleman, R.C.; Carey, V.J.; Bates, D.M.; Bolstad, B.; Dettling, M.; Dudoit, S.; Ellis, B.; Gautier, L.; Ge, Y.; Gentry, J.; et al. Bioconductor: Open software development for computational biology and bioinformatics. *Genome Biol.* **2004**, *5*, R80. [CrossRef] [PubMed]
27. Du, P.; Kibbe, W.A.; Lin, S.M. lumi: A pipeline for processing Illumina microarray. *Bioinformatics* **2008**, *24*, 1547–1548. [CrossRef] [PubMed]
28. Abu-Dawud, R.; Graffmann, N.; Ferber, S.; Wruck, W.; Adjaye, J. Pluripotent stem cells: Induction and self-renewal. *Philos. Trans. R. Soc. B Biol. Sci.* **2018**, *373*, 20170213. [CrossRef] [PubMed]
29. Benjamini, Y.; Hochberg, Y. Controlling the False Discovery Rate: A Practical and Powerful Approach to Multiple Testing. *J. R. Stat. Soc. Ser. B Methodol.* **1995**, *57*, 289–300. [CrossRef]
30. Carvalho, B.S.; Irizarry, R.A. A framework for oligonucleotide microarray preprocessing. *Bioinformatics* **2010**, *26*, 2363–2367. [CrossRef]
31. Chen, H.; Boutros, P.C. VennDiagram: A package for the generation of highly-customizable Venn and Euler diagrams in R. *BMC Bioinform.* **2011**, *12*, 35. [CrossRef]
32. Warnes, G.R. *Gplots: Various R Programming Tools for Plotting Data*; ScienceOpen, Inc.: Boston, MA, USA, 2015.
33. Kanehisa, M.; Furumichi, M.; Tanabe, M.; Sato, Y.; Morishima, K. KEGG: New perspectives on genomes, pathways, diseases and drugs. *Nucleic Acids Res.* **2017**, *45*, D353–D361. [CrossRef] [PubMed]
34. Falcon, S.; Gentleman, R. Using GOstats to test gene lists for GO term association. *Bioinformatics* **2006**, *23*, 257–258. [CrossRef] [PubMed]
35. Wickham, H. *Ggplot2: Elegant Graphics for Data Analysis*; Springer: New York, NY, USA, 2009.
36. Lancaster, M.A.; Renner, M.; Martin, C.A.; Wenzel, D.; Bicknell, L.S.; Hurles, M.E.; Homfray, T.; Penninger, J.M.; Jackson, A.P.; Knoblich, J.A. Cerebral organoids model human brain development and microcephaly. *Nature* **2013**, *501*, 373–379. [CrossRef] [PubMed]
37. Zhang, J.M.; An, J. Cytokines, inflammation, and pain. *Int. Anesthesiol. Clin.* **2007**, *45*, 27–37. [CrossRef]

38. Palmela, I.; Cardoso, F.L.; Bernas, M.; Correia, L.; Vaz, A.R.; Silva, R.F.M.; Fernandes, A.; Kim, K.S.; Brites, D.; Brito, M.A. Elevated levels of bilirubin and long-term exposure impair human brain microvascular endothelial cell integrity. *Curr. Neurovascular Res.* **2011**, *8*, 153–169. [CrossRef] [PubMed]
39. Allan, S.M.; Rothwell, N.J. Cytokines and acute neurodegeneration. *Nat. Rev. Neurosci.* **2001**, *2*, 734–744. [CrossRef] [PubMed]
40. Xie, Z.; Smith, C.J.; Van Eldik, L.J. Activated glia induce neuron death via MAP kinase signaling pathways involving JNK and p38. *Glia* **2003**, *45*, 170–179. [CrossRef] [PubMed]
41. Rothwell, N.J. Cytokines—Killers in the brain? *J. Physiol.* **1999**, *514*, 3–17. [CrossRef]
42. Morandi, A.; Hughes, C.G.; Girard, T.D.; McAuley, D.F.; Ely, E.W.; Pandharipande, P.P. Statins and Brain Dysfunction: A Hypothesis to Reduce the Burden of Cognitive Impairment in Patients Who Are Critically Ill. *Chest* **2011**, *140*, 580–585. [CrossRef]
43. Daulatzai, M.A. Dysfunctional Nucleus Tractus Solitarius: Its Crucial Role in Promoting Neuropathogentic Cascade of Alzheimer's Dementia—A Novel Hypothesis. *Neurochem. Res.* **2012**, *37*, 846–868. [CrossRef]
44. Gazzin, S.; Tiribelli, C. Bilirubin-induced neurological damage. *J. Matern. Neonatal Med.* **2011**, *24*, 154–155. [CrossRef] [PubMed]
45. Jeanjean, A.; Moussaoui, S.; Maloteaux, J.-M.; Laduron, P. Interleukin-1β induces long-term increase of axonally transported opiate receptors and substance P. *Neuroscience* **1995**, *68*, 151–157. [CrossRef] [PubMed]
46. Schweizer, A.; Feige, U.; Fontana, A.; Müller, K.; Dinarello, C.A. Interleukin-1 enhances pain reflexes. Mediation through increased prostaglandin E2 levels. *Inflamm. Res.* **1988**, *25*, 246–251. [CrossRef] [PubMed]
47. Li, J.; Chen, S.; Zhao, Z.; Luo, Y.; Hou, Y.; Li, H.; He, L.; Zhou, L.; Wu, W. Effect of VEGF on Inflammatory Regulation, Neural Survival, and Functional Improvement in Rats following a Complete Spinal Cord Transection. *Front. Cell. Neurosci.* **2017**, *11*, 381. [CrossRef] [PubMed]
48. Wang, H.; Wang, Y.; Li, D.; Liu, Z.; Zhao, Z.; Han, D.; Yuan, Y.; Bi, J.; Mei, X. VEGF inhibits the inflammation in spinal cord injury through activation of autophagy. *Biochem. Biophys. Res. Commun.* **2015**, *464*, 453–458. [CrossRef] [PubMed]
49. Yamazaki, H.; Kushiyama, A.; Sakoda, H.; Fujishiro, M.; Yamamotoya, T.; Nakatsu, Y.; Kikuchi, T.; Kaneko, S.; Tanaka, H.; Asano, T. Protective Effect of Sex Hormone-Binding Globulin against Metabolic Syndrome: In Vitro Evidence Showing Anti-Inflammatory and Lipolytic Effects on Adipocytes and Macrophages. *Mediat. Inflamm.* **2018**, *2018*, 3062319. [CrossRef] [PubMed]
50. Brites, D. Bilirubin Injury to Neurons and Glial Cells: New Players, Novel Targets, and Newer Insights. *Semin. Perinatol.* **2011**, *35*, 114–120. [CrossRef]
51. Kim, S.-H.; Kang, Y.-J.; Kim, W.-J.; Woo, D.-K.; Lee, Y.; Kim, D.-I.; Park, Y.B.; Kwon, B.S.; Park, J.-E.; Lee, W.-H. TWEAK Can Induce Pro-Inflammatory Cytokines and Matrix Metalloproteinase-9 in Macrophages. *Circ. J.* **2004**, *68*, 396–399. [CrossRef]
52. Bayer, A.L.; Alcaide, P. MyD88: At the heart of inflammatory signaling and cardiovascular disease. *J. Mol. Cell. Cardiol.* **2021**, *161*, 75–85. [CrossRef]
53. Vorkapic, E.; Lundberg, A.M.; Mäyränpää, M.I.; Eriksson, P.; Wågsäter, D. TRIF adaptor signaling is important in abdominal aortic aneurysm formation. *Atherosclerosis* **2015**, *241*, 561–568. [CrossRef]
54. Fukasaka, M.; Ori, D.; Kawagoe, T.; Uematsu, S.; Maruyama, K.; Okazaki, T.; Kozaki, T.; Imamura, T.; Tartey, S.; Mino, T.; et al. Critical Role of AZI2 in GM-CSF–Induced Dendritic Cell Differentiation. *J. Immunol.* **2013**, *190*, 5702–5711. [CrossRef] [PubMed]
55. Wei, M.; Zheng, Y.; Xu, J.; Sun, Q. AZI2 positively regulates the induction of type I interferon in influenza-trigger pediatric pneumonia. *Pathog. Dis.* **2022**, *80*, ftac016. [CrossRef] [PubMed]
56. Kaltschmidt, B.; Kaltschmidt, C. NF-B in the Nervous System. *Cold Spring Harb. Perspect. Biol.* **2009**, *1*, a001271. [CrossRef] [PubMed]
57. Teng, F.Y.H.; Tang, B.L. NF-κB Signaling in Neurite Growth and Neuronal Survival. *Rev. Neurosci.* **2010**, *21*, 299–314. [CrossRef] [PubMed]
58. Gutierrez, H.; Davies, A.M. Regulation of neural process growth, elaboration and structural plasticity by NF-κB. *Trends Neurosci.* **2011**, *34*, 316–325. [CrossRef] [PubMed]
59. Yakovleva, T.; Bazov, I.; Watanabe, H.; Hauser, K.F.; Bakalkin, G. Transcriptional control of maladaptive and protective responses in alcoholics: A role of the NF-κB system. *Brain Behav. Immun.* **2011**, *25*, S29–S38. [CrossRef]
60. Jiménez, A.; Lu, D.; Kalocsay, M.; Berberich, M.J.; Balbi, P.; Jambhekar, A.; Lahav, G. Time-series transcriptomics and proteomics reveal alternative modes to decode p53 oscillations. *Mol. Syst. Biol.* **2022**, *18*, e10588. [CrossRef] [PubMed]
61. Kelley, N.; Jeltema, D.; Duan, Y.; He, Y. The NLRP3 Inflammasome: An Overview of Mechanisms of Activation and Regulation. *Int. J. Mol. Sci.* **2019**, *20*, 3328. [CrossRef]
62. Bassani, T.B.; Vital, M.A.; Rauh, L.K. Neuroinflammation in the pathophysiology of Parkinson's disease and therapeutic evidence of anti-inflammatory drugs. *Arq. Neuro-Psiquiatria* **2015**, *73*, 616–623. [CrossRef]
63. Wen, A.Y.; Sakamoto, K.M.; Miller, L.S. The Role of the Transcription Factor CREB in Immune Function. *J. Immunol.* **2010**, *185*, 6413–6419. [CrossRef]
64. Zhang, B.; Yang, X.; Gao, X. Taurine protects against bilirubin-induced neurotoxicity in vitro. *Brain Res.* **2010**, *1320*, 159–167. [CrossRef] [PubMed]
65. Wang, L.; Nie, Q.; Gao, M.; Yang, L.; Xiang, J.-W.; Xiao, Y.; Liu, F.-Y.; Gong, X.-D.; Fu, J.-L.; Wang, Y.; et al. The transcription factor CREB acts as an important regulator mediating oxidative stress-induced apoptosis by suppressing αB-crystallin expression. *Aging* **2020**, *12*, 13594–13617. [CrossRef] [PubMed]
66. Sharma, A.; Singh, K.; Almasan, A. Histone H2AX Phosphorylation: A Marker for DNA Damage. *Methods Mol. Biol.* **2012**, *920*, 613–626. [CrossRef] [PubMed]

67. Vucic, D. XIAP at the crossroads of cell death and inflammation. *Oncotarget* **2018**, *9*, 27319–27320. [CrossRef] [PubMed]
68. Shiozaki, E.N.; Chai, J.; Rigotti, D.J.; Riedl, S.J.; Li, P.; Srinivasula, S.M.; Alnemri, E.S.; Fairman, R.; Shi, Y. Mechanism of XIAP-Mediated Inhibition of Caspase-9. *Mol. Cell* **2003**, *11*, 519–527. [CrossRef] [PubMed]
69. Lalani, A.I.; Zhu, S.; Gokhale, S.; Jin, J.; Xie, P. TRAF Molecules in Inflammation and Inflammatory Diseases. *Curr. Pharmacol. Rep.* **2017**, *4*, 64–90. [CrossRef] [PubMed]
70. Perner, F.; Ernst, T.; Heidel, F.H. Roles of JAK2 in Aging, Inflammation, Hematopoiesis and Malignant Transformation. *Cells* **2019**, *8*, 854. [CrossRef]
71. Duodu, P.; Sosa, G.; Canar, J.; Chhugani, O.; Gamero, A.M. Exposing the Two Contrasting Faces of STAT2 in Inflammation. *J. Interf. Cytokine Res.* **2022**, *42*, 467–481. [CrossRef]

3.3 Hemozoin induces Malaria via activation of DNA damage, p38 MAPK and Neurodegenerative Pathways in a Human iPSC-derived Neuronal Model of Cerebral Malaria

Abida Islam Pranty[#], Leon-Phillip Szepanowski[#], Wasco Wruck, Akua Afriyie Karikari and James Adjaye

BioRxiv (2024)

Abstract:

Malaria caused by Plasmodium falciparum infection results in severe complications including cerebral malaria (CM), in which approximately 30% of patients end up with neurological sequelae. Sparse in vitro cell culture-based experimental models which recapitulate the molecular basis of CM in humans has impeded progress in our understanding of its etiology. This study employed healthy human induced pluripotent stem cells (iPSCs) derived neuronal cultures stimulated with hemozoin (HMZ)- the malarial toxin as a model for CM. Secretome, qRT-PCR, Metascape, and KEGG pathway analyses were conducted to assess elevated proteins, genes, and pathways. Neuronal cultures treated with HMZ showed enhanced secretion of interferon-gamma (IFN-γ), interleukin (IL)1-beta (IL-1β), IL-8 and IL-16. Enrichment analysis revealed malaria, positive regulation of cytokine production and positive regulation of mitogen-activated protein kinase (MAPK) cascade which confirm inflammatory response to HMZ exposure. KEGG assessment revealed up-regulation of malaria, MAPK and neurodegenerative diseases-associated pathways which corroborates findings from previous studies. Additionally, HMZ induced DNA damage in neurons. This study has unveiled that exposure of neuronal cultures to HMZ, activates molecules and pathways similar to that observed in CM and neurodegenerative diseases. Furthermore, our model is an alternative to rodent experimental models of CM.

Author Contribution: 50-60%

A.I.P. designed and performed the experiments, processed and analysed the data, and wrote and edited the manuscript.

Status: Submitted to *Scientific reports* Journal (under revision). Pre-print available in the open access pre-print repository *BioRxiv* (doi.org/10.1101/2024.03.08.584068).

Hemozoin induces Malaria via activation of DNA damage, p38 MAPK and Neurodegenerative Pathways in Human iPSC-derived Neuronal Model of Cerebral Malaria.

Abida Islam Pranty[1 #], Leon-Phillip Szepanowski[1 #], Wasco Wruck[1], Akua Afriyie Karikari[3] and James Adjaye[1,2*]

[1]Institute for Stem Cell Research and Regenerative Medicine, Medical Faculty, Heinrich-Heine University, 40225 Düsseldorf, Germany

[2]University College London – EGA Institute for Women's Health, Zayed Centre for Research into Rare Diseases in Children (ZCR), 20 Guilford Street, London WC1N 1DZ

[3]Department of Biomedical Sciences, School of Allied Health Sciences, College of Health and Allied Sciences, University of Cape Coast, Cape Coast, Ghana

[#]Equal contribution

*Correspondence: james.adjaye@med.uni-duesseldorf.de

Abstract

Malaria caused by *Plasmodium falciparum* infection results in severe complications including cerebral malaria (CM), in which approximately 30% of patients end up with neurological sequelae. Sparse in vitro cell culture-based experimental models which recapitulate the molecular basis of CM in humans has impeded progress in our understanding of its etiology. This study employed healthy human induced pluripotent stem cells (iPSCs) derived neuronal cultures stimulated with hemozoin (HMZ)- the malarial toxin as a model for CM. Secretome, qRT-PCR, Metascape, and KEGG pathway analyses were conducted to assess elevated proteins, genes, and pathways. Neuronal cultures treated with HMZ showed enhanced secretion of interferon-gamma (IFN-γ), interleukin (IL)1-beta (IL-1β), IL-8 and IL-16. Enrichment analysis revealed malaria, positive regulation of cytokine production and positive regulation of mitogen-activated protein kinase (MAPK) cascade which confirm inflammatory response to HMZ exposure. KEGG assessment revealed up-regulation of malaria, MAPK and neurodegenerative diseases-associated pathways which corroborates findings from previous studies. Additionally, HMZ induced DNA damage in neurons. This study has unveiled that exposure of neuronal cultures to HMZ, activates molecules and pathways similar to that observed in CM and neurodegenerative diseases. Furthermore, our model is an alternative to rodent experimental models of CM.

Key words: iPSC, neurons, Hemozoin, cerebral malarial, neuro- inflammation, DNA damage.

Introduction

In spite of the significant efforts to combat malaria, the disease remains a public health problem globally. In 2021, there were an estimated 247 million malaria cases in 84 malaria endemic countries, which represents an increase of 2 million cases compared with 2020[1]. Also, the continuous importation of malaria to non-endemic regions consistently challenges elimination efforts, leading to the spread of drug-resistant parasites within and between countries[2]. *Plasmodium falciparum* and *vivax* are the most virulent of the five human parasite species. Nonetheless, *P. falciparum* is the species primarily implicated in severe and fatal forms of clinical malaria[3]. Principal to the pathogenesis of *P. falciparum* is the toxin, hemozoin (HMZ), which is also referred to as the malaria pigment. Falciparum does not infiltrate the brain parenchyma but can cause severe damage to neurons, through the release of HMZ, which

can induce reactive oxygen species (ROS) mediated macromolecular damage and inflammatory response[4,5]. Moreover, *P. falciparum* poses a challenge for experimental malaria investigations, due to its inability to infect species like rodents[6]. A majority of falciparum malaria research is based on clinical studies, which limits access to certain tissues such as the brain. Human derived induced pluripotent stem cells (iPSCs) have emerged as a relevant tool for modelling several diseases *in-vitro*[7,8]. iPSCs can be used for extensive studies related to disease pathogenesis, the impact of exogenous factors and the molecular targets of disease-modulating treatments. With the lack of an appropriate experimental model for *P. falciparum*, and with the difficulty in studying the molecular-basis and mechanisms associated with malaria in human subjects, there is a pressing need for new models of falciparum malaria.

A major complication of falciparum infection is cerebral malaria (CM). Clinically, CM is characterized by lack of consciousness and coma, with high mortality rates[9]. Post-CM survivors sustain brain injuries and neurological sequelae including cognitive impairment, motor skill impairment, cortical blindness, seizures and attention deficit hyperactive disorder[9,10]. To date, the pathogenic mechanisms leading to cerebral malaria remains an enigma as studies have been hampered by limited accessibility to human tissues and brain injury in human post-mortem tissues has provided limited cross-sectional data[11]. In a previous study using pooled transcriptome data from whole blood analysis of *P. falciparum* malaria patients, we discovered that falciparum malaria shared similar biological processes with neurodegenerative diseases[4]. Additionally, in our previous study we employed an iPSC-based model discovering that malaria was a significant pathway in constructing a network of genes associated with late onset Alzheimer's disease (LOAD)[12]. Both mild and severe forms of falciparum malaria have been previously linked to psychiatric disorders such as depression, irritability, anxiety, difficulties with concentration, disorientation and forgetfulness[13]. Deciphering the molecular changes that occur during the disease pathogenesis could unravel the link between falciparum malaria and neurodegenerative diseases.

In this study, we employed two healthy iPSC-line-derived neuronal cultures to characterize molecular changes that occur upon exposure of neuronal cultures to the parasite's most potent toxin- HMZ. After exposure to HMZ, qRT-PCR and secretome analysis revealed an increase in pro-inflammatory molecules and neurotrophins including interleukin-1-beta (IL-1β), IL-16, interferon-gamma (IFN-γ), monocyte chemotactic protein-1 (MCP-1), vascular endothelial growth factor (VEGF) and brain derived neurotrophic factor (BDNF). Pathway enrichment analysis using the Kyoto Encyclopedia of Genes and Genomes (KEGG) network revealed malaria, mitogen-activated protein kinase (MAPK), neurodegenerative and Alzheimer's disease (AD) pathways, as upregulated in HMZ-exposed cells. This corroborates our previous study where neurodegenerative and AD pathways were elevated in falciparum malaria patients. Metascape assessment uncovered malaria, regulation of leukocyte proliferation, positive regulation of cytokine production and positive regulation of MAPK cascade, which are indicative of cellular inflammatory response to HMZ exposure. Furthermore, western blot analysis confirmed DNA damage in UM51-derived neurons, implicating HMZ as genotoxic. Investigations using HMC3 microglia cells revealed a similar pattern of inflammation and cellular injury. Taken together, the findings of this study consolidate the theory that CM and neurodegenerative diseases, such as AD, activate similar cellular mechanisms through inflammation, which could account for the neurological deficits observed in CM patients. It also demonstrates that iPSC-derived neuronal cultures could serve as a valuable model in research regarding CM.

Results

Generation of iPSC-derived neuronal networks to model cerebral malaria

The UM51 line was generated from SIX2-positive renal progenitor cells isolated from the urine of a 51-year-old healthy male of African origin[14], while healthy human fetal foreskin fibroblasts were reprogrammed to generate the B4-iPSC line (HFF1, ATCC, #ATCCSCRC-1041, http://www.atcc.org)[15] (Supplementary Table S1). To obtain neuronal networks, UM51 and B4 iPSCs were seeded as single cells for neural induction, then expanded as neural progenitor cells and further differentiated into neurons (Fig. 1a, Supplementary Fig. 1). A dose-response curve was prepared using ascending concentrations of HMZ on neuronal cultures to determine IC80 (cell survival rate) and the closest lower concentration examined (20 µM) was used for all following experiments (Supplementary Fig. 1). Subsequently, day 16 neuronal cultures from both cell lines were exposed to 20 µM hemozoin (HMZ) for 48 h to observe HMZ- induced effects in central nervous system (CNS) cell populations with the aim of modeling cerebral malaria using iPSC-derived neuronal cultures (Fig. 1a, Supplementary Fig. 1).

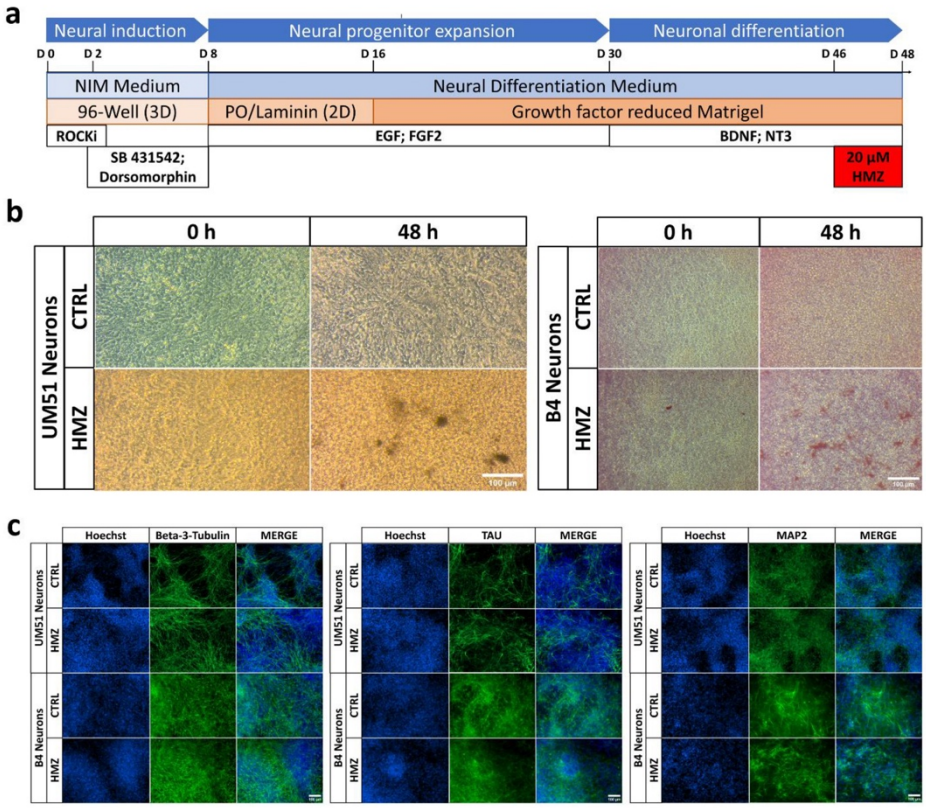

Figure 1. Generation, characterization and utilization of iPSC-derived neuronal cultures for modelling cerebral malaria. (a) Schematic outline of the protocol used to generate iPSC-derived neuronal cultures. **(b)** Representative bright field images of control and HMZ-treated UM51- and B4 iPSC-derived neuronal cultures at 0h and 48 h of exposure. Scale bar 100 µm. **(c)** Representative immunocytochemistry (ICC) images of β3-Tubulin-, TAU- and MAP2-positive cells in UM51- and B4-derived neuronal cultures after 48 h HMZ exposure in comparison to control. Scale bar 100 µm.

Bright field microscopy showed deposition of malaria pigments as brown crystals inside or around the neuronal cultures after 48 h of treatment (Fig. 1b, Supplementary Fig. 1). Neuronal

features were confirmed in both control and HMZ-treated neuronal cultures by expression of neuronal markers Beta III tubulin (β3-Tubulin), tubulin associated unit (TAU), and microtubule-associated protein 2 (MAP2) (Fig. 1c, Supplementary Fig. 1).

HMZ activates inflammatory-associated pathways in iPSC-derived neuronal cultures

Supernatants from UM51 neuronal cultures were used to analyze the secretome profile of both HMZ-treated and control conditions (Supplementary Fig. 2). The resulting secretome profiles were further analyzed utilizing hierarchical clustering analysis (heatmap using Pearson correlation as similarity measure in Fig. 2a), which indicated induction of an inflammatory response upon treatment with 20 µM HMZ for 48 h. Usually pro- and anti-inflammatory cytokines are involved not only in inflammatory response but also in immune-regulatory functions. A number of crucial pro-inflammatory cytokines such as IL-8, IL1-B, IFN-G, IL-16 showed enhanced secretion, while anti-inflammatory cytokines such as IL-4, IL-13 showed reduced secretion (Fig. 2a) (Supplementary Fig. 2).

We further performed a Metascape-based analysis utilizing the list of up- and down-regulated cytokines obtained from the UM51 neuronal culture. The resulting enrichment clusters revealed malaria, positive regulation of cytokine production, positive regulation of MAPK cascade, and inflammatory responses to be activated by HMZ treatment (Fig. 2b). KEGG analysis revealed distinct regulated pathways upon HMZ exposure, which include malaria, (p=1.65 x 10-7, FDR=2.59 x 10-6), MAPK signalling pathway (p=1.21 x 10-9, FDR=2.84 x 10-8), pathways of neurodegeneration (p=0.0325, FDR=0.0588) and Alzheimer disease (p=0.0446, FDR=0.0716) as upregulated pathways, and p53 signalling pathway (p=0.0069, FDR=0.0143) and apoptosis (p=0.0358, FDR=0.0576) as downregulated pathways (Fig. 2c, (Supplementary File 1).

Following the observations from the secretome profile, we performed qRT-PCR analysis to confirm mRNA expression of selected chemo- and cytokines in neuronal cultures of both cell lines (UM51 and B4) from treated and control conditions. Increased *IL-8* and *TNF-α* mRNA expression were observed in both cell lines upon HMZ treatment, while *IL-6* was only up-regulated in UM51 neuronal cultures (Fig. 2b). Furthermore, immune-regulatory, and inflammation-associated chemokines such as monocyte chemoattractant protein-1 (MCP-1) and macrophage migration inhibitory factor (MIF) showed increased secretion upon HMZ treatment (Fig. 2a, Supplementary Fig. 2). Secretion of vascular endothelial growth factor (VEGF) and platelet derived growth factor subunit B (PDGFB), both belonging to the same protein family and reported to be associated with inflammation, were also enhanced [7] (Fig. 2a). Additionally, enhanced mRNA expression and protein secretion of brain derived neurotrophic factor (BDNF) was observed. BDNF has been reported to be involved in modulating neuro-inflammation by providing neuroprotection[16] (Fig. 2a, 2e). Next, we analyzed mRNA expression of selected genes associated with the mentioned pathways. Both UM51 and B4 neuronal cultures showed similar trends upon HMZ treatment in the neuronal cultures with an increase in *BDNF*, *C-C Motif Chemokine Ligand 2* (*CCL2*) expression, while both indicated a decrease in *VEGFA* and *PDGFB* expression (Fig. 2e). However, the decreased mRNA expression and increased protein secretion of VEGF and PDGFB point at additional factors besides transcription playing a role in the secretion of these proteins[17]. *CCL2* and *PECAM1* encode for the MCP-1 and CD31 protein, respectively. Both CCL2 and PECAM1 showed upregulated mRNA expression in both UM51 and B4-derived neuronal cultures after HMZ treatment (Fig. 2e).

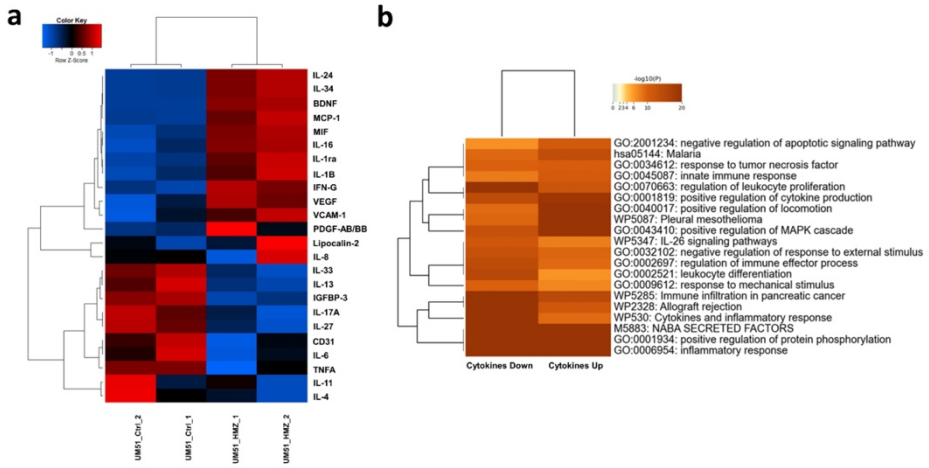

c

KEGG_Name (Upregulated)	p_hyper	q_hyper	Genes
Malaria	1.65E-07	2.59E-06	CCL2,CD40LG,HGF,ICAM1,IFNG,IL1B
MAPK signaling pathway	1.21E-09	2.84E-08	BDNF,CD14,CSF1,EGF,FGF19,FGF7,FLT3LG,HGF,IL1A,IL1B, PDGFA,PDGFB,VEGFA
Pathways of neurodegeneration	0.032533	0.058809507	AGER,BDNF,CSF1,DKK1,IL1A,IL1B
Alzheimer disease	0.044612	0.071617	AGER,CSF1,DKK1,IL1A,IL1B
KEGG_Name (Downregulated)	**p_hyper**	**q_hyper**	**Genes**
p53 signaling pathway	0.006855	0.014347	FAS,IGFBP3,THBS1
Apoptosis	0.0358292	0.057583	FAS,IL3,TNF

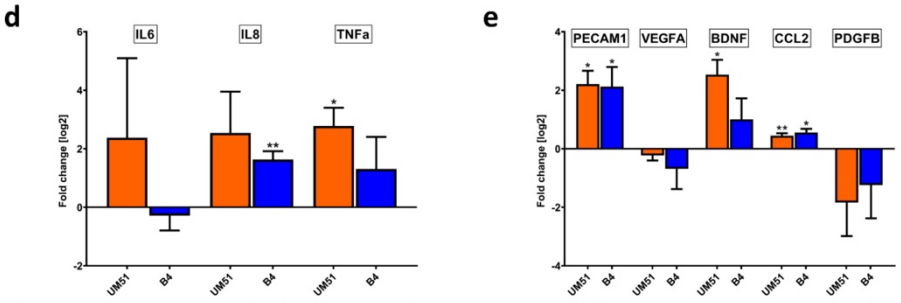

Figure 2. Secretome analysis of neuronal cultures upon HMZ exposure reveals activation of inflammatory response, MAPK-signaling and neurodegenerative pathway. Cytokine array analyses was performed with supernatant derived from the UM51 neuronal cultures. **(a)** Pearson´s heatmap depicting selected chemo- and cytokines regulated in UM51 neuronal cultures after 48 h HMZ exposure in comparison to control. **(b)** Metascape-generated heatmap comparing the sets of up- and downregulated chemo- and cytokines derived from UM51 neuronal cultures after 48 h HMZ exposure reveals a secretome signature involved in i.a. Malaria, response to tumor necrosis factor and positive regulation of MAPK cascade. **(c)** Table depicting selected KEGG pathways including up-regulated malaria, MAPK signalling pathway, pathways of neurodegeneration and Alzheimer disease and down-regulated p53 signalling pathway and apoptosis, as well as associated genes upon HMZ exposure in comparison to control. **(d)** Relative mRNA expression analysis of *IL6, IL8* and *TNFA* in UM51 and B4-

derived neuronal cultures after 48 h HMZ exposure in comparison to control. **(e)** Relative mRNA expression analysis of *PECAM1, VEGFA, BDNF, CCL2* and *PDGFB* in UM51 and B4-derived neuronal cultures after 48 h HMZ exposure in comparison to control. (d,e) UM51 n=3; B4 Ctrl n=2; B4 HMZ n=3; blots depict mean and error bars depict SD of all experiments. Asterisk (*) depicts significance, which is indicated by *p<0.05; **p<0.01.

HMZ exposure induces DNA damage in UM51-derived neuronal cultures

We performed immunocytochemistry (ICC) and western blot (WB) analysis to evaluate the expression of the DNA damage marker- γH2AX (Fig. 3a, 3b). Both cell lines showed a similar trend with increased γH2AX levels in the WB analyses after HMZ exposure compared to the corresponding controls (Fig.3b, 3c).

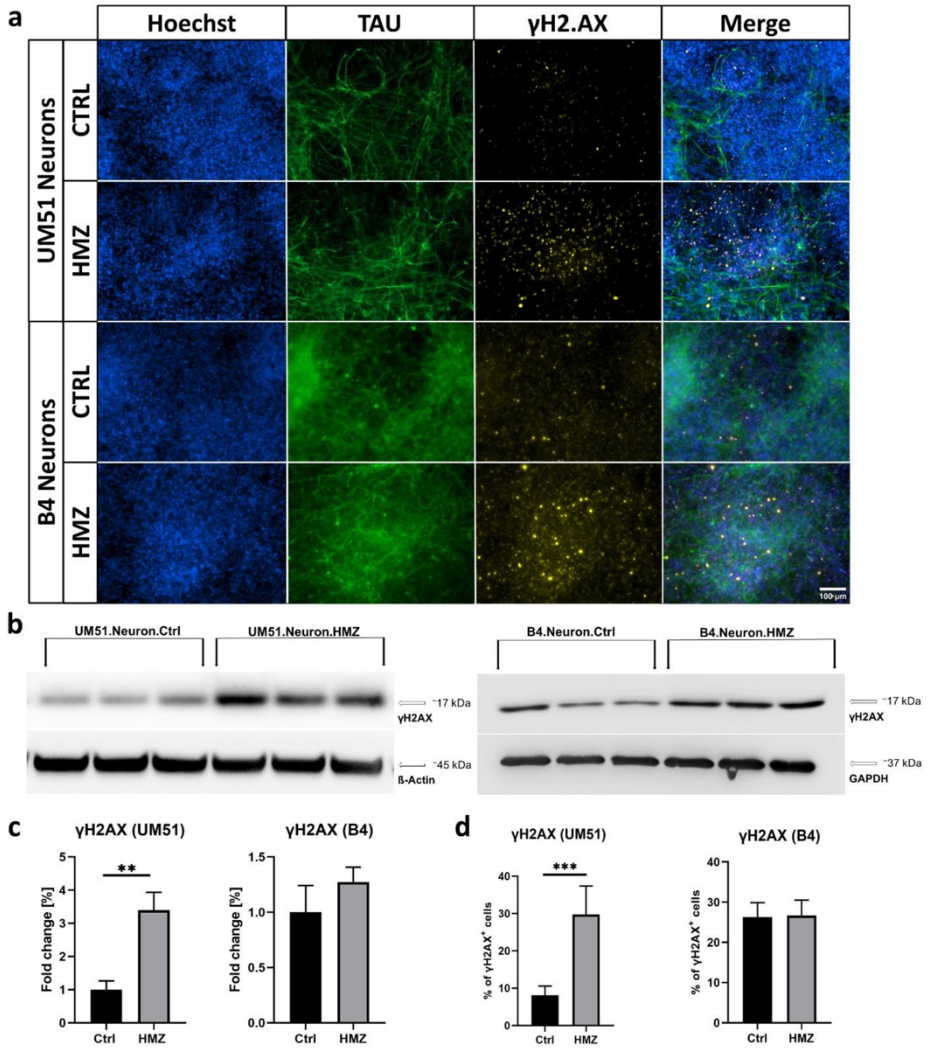

Figure 3. HMZ exposure induces DNA damage in iPSC-derived neuronal cultures. All depicted results were recorded in UM51- and B4-derived neuronal cultures after 48 h HMZ exposure and compared to their corresponding controls. **(a)** Representative ICC images showing TAU- and γH2AX-

positive cells. Scale bar 100 µm. **(b)** WB analysis for γH2AX. **(c)** Bar graphs showing γH2AX protein expression in fold change. Values were normalized to ß-Actin and GAPDH (housekeeping gene) and subsequently to control samples. **(d)** Manual ICC quantification of γH2AX-positive nuclei. (c,d) n=3 for each condition, blots depict mean and error bars depict SD of all experiments. Asterisk (*) depicts significance, which is indicated by **p<0.01; ***p<0.001. Approximately six random fields from three separate differentiations for each condition were manually analysed (d).

Manual counting of nuclei in ICC staining showed 30% γH2AX-positive cells after 48 h of HMZ exposure in the UM51 neuronal culture, while the control condition consisted of 6% γH2AX positive cells (Fig. 3a, 3d). On the contrary, B4 neuronal cultures showed almost no change in ICC staining analysis (Fig. 3a, 3d). Aligning with the observation from ICC, in WB analysis UM51 neurons showed stronger response to HMZ treatment than the B4 neurons with a 3.4-fold increase in γH2AX expression, while the B4 neurons showed only a 1.3-fold increase compared to their corresponding controls (Fig. 3b, 3c).

HMZ potentially activates p38 MAPK and not p53 signalling pathway in iPSC-derived neurons

As HMZ treatment on iPSC-derived neuronal cultures indicated p53 signalling pathway to be downregulated (Fig. 2d), and γH2AX levels were increased (Fig. 3), we investigated selected p53 signalling pathway-associated markers involved in DNA damage response and repair mechanisms (Supplementary Fig 3)[18-20]. First, we analysed mRNA expression of the DNA damage and repair related genes in both UM51 and B4-derived neuronal cultures. We observed p53 and MDM2 to be downregulated and ATM, ATR, CHEK1, CHEK2 to be significantly upregulated compared to the corresponding controls (Fig. 4a, 4b).

In the WB analysis, p53 protein expression of the HMZ treated UM51 sample showed a slight increase, while the other P53 signalling-associated markers MDM2 (in both cell lines) and FAS (in UM51) showed a downregulated expression (Fig. 4c, 4d, 4f). All observations regarding these mentioned p53 signalling pathway-associated gene and protein expressions indicate a more vigorous response of the UM51 neuronal cultures upon HMZ exposure compared to B4 neuronal cultures (Fig. 4). This observation aligns with the observed higher DNA damage in the UM51 neuronal cultures compared to B4 (Fig. 3). Further experiments with immortalized HMC3 microglia-like cells also followed a similar trend with regards to p53 signalling pathway-associated markers and γH2AX expression after 48 h of HMZ exposure (Supplementary Fig. 4). Additionally, the change in total P38MAPK and phospho-P38MAPK protein expression might indicate MAPK signalling pathway activation after HMZ treatment in the iPSC-derived neuronal cultures (Fig. 4e, Fig. 2d).

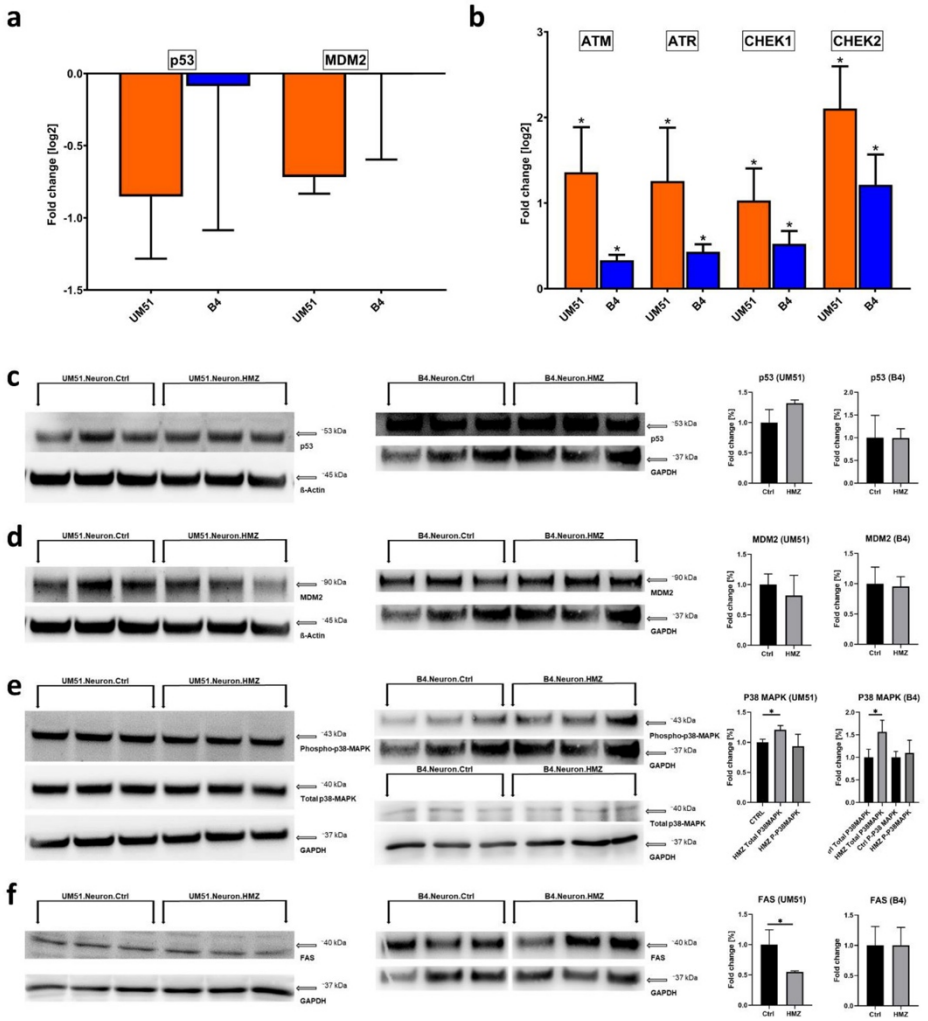

Figure 4. HMZ exposure activates DNA damage responses. All depicted results were performed in UM51- and B4-derived neuronal cultures after 48 h HMZ exposure and compared to their corresponding controls. **(a)** Relative mRNA expression analysis of *p53* and *MDM2*. **(b)** Relative mRNA expression analysis of *ATM, ATR, CHEK1* and *CHEK2*. **(c-f)** WB analyses and quantification of WB analyses for p53, MDM2, total p38, phospho-p38 and FAS. Values were normalized to ß-Actin and GAPDH and subsequently to control samples. (a,b) UM51 n=3; B4 Ctrl n=2; B4 HMZ n=3 (c-f) n=3 for each condition. (a-f) Blots depict mean and error bars depict SD of all experiments. Asterisk (*) depicts significance, which is indicated by *p<0.05.

Discussion

An acute neurological complication of *P. falciparum* infection is CM, which is marked by neurological sequela in some survivors. The molecular mechanisms that underlie CM remain an enigma, which can partly be attributed to the lack of a suitable model that captures the clinical outcomes observed in patients. In this study, we employed neuronal cultures derived from iPSC lines obtained from two healthy ethnically diverse males and HMZ, the malaria toxin, as an *in-vitro* model of CM. TAU, MAP2 and β3-Tubulin- positive neuronal cultures were then

stimulated with 20 µM HMZ for 48 h and deposition of the malarial toxin as brown crystals around neurons was observed. The deposition of HMZ as insoluble crystals into tissues is a common feature reported in both experimental and clinical malaria[21,22]. Indeed, the severity of falciparum infection is often correlated with the deposition of HMZ in organs[23] and HMZ granules have been previously linked to thrombosed micro-vessels in fatal CM induced hemorrhage[24].

Central to the progression of CM is neuro-inflammation. Notable inflammatory markers reported in CM include IL-1β, IL-6, IL-8, IFN-γ, TNF-α, PECAM-1, VCAM-1 and ICAM-1[25-27]. In this investigation, a secretome analysis using neuronal cell culture supernatant from UM51 cell line after HMZ treatment was conducted. Pearson´s heatmap analysis revealed an elevated IL-1β, IL-8 (partly), IL-16 and IFN-γ secretion. On the other hand, the levels of TNF-α, IL-6, IL-4 and IL-13 were lower in the HMZ treated cells. Interestingly, there was also a surge in the inflammatory-associated proteins: PDGFB, MIF, MCP-1 and VCAM-1. The increase in expression of these molecules is indicative of an inflammatory environment driven predominantly by a T helper type 1 (Th1) phenotype. Previous studies in clinical malaria have demonstrated that patients with CM had higher levels of pro-inflammatory Th1 cytokines as compared to severe malarial anemia patients[28,29], which could account in part for the acute injuries observed in CM. In addition, these Th1 cytokines and inflammation associated proteins may be crucial to the development of neurocognitive and psychiatric disorders in CM patients. For instance, IL-8, IL-16 and MCP-1 have been implicated in neurocognitive symptoms in individuals with depression and anxiety[30], and IL-1β and IL-16 were associated with psychiatric symptoms in schizophrenia patients[31]. Again, in neurodegenerative research, IL-16 was reportedly increased in patients with cerebrovascular dementias and AD[32]. Although IL-16 has been associated with psychiatric disorders and AD, this is the first study to implicate the cytokine in an experimental CM model. The cytokine was found to be significantly higher in asymptomatic falciparum patients when compared to individuals infected with Chikungunya virus[33]. Hitherto, there have been no reports on this cytokine in CM studies involving humans, which necessitates further research to understand the relationship between IL-16 and neurological impairment in CM patients. The reduced concentrations of IL-6 and TNF-α could be attributed to a delayed protein synthesis at the time of the assay. The pathogenesis of CM is characterized by persistent up-regulation of Th1 cytokines and inadequate production of anti-inflammatory cytokines including IL-4 and IL-13, which could possibly account for the observed lower levels of IL-4 and IL-13[34]. Instead of anti-inflammatory cytokines, the neurotrophic factor BDNF was elevated, which indicates a cellular response to remedy the highly inflammatory environment. In a study involving Ugandan children, McDonald et al., reported that lower BDNF levels were associated with poor prognosis in patients with CM, whereas higher levels of BDNF resulted in faster recovery from coma[35]. Using iPSC-derived brain organoids, Harbuzariu et al., discovered elevated levels of BDNF in response to heme injury[11]. Moreover, reduced BDNF expression has been linked to inflammation-induced apoptosis in neurons[36], signifying a protective role of this neurotrophin against neuronal damage.

Metascape-based analysis data, obtained from up- and down-regulated proteins identified in the secretome screening, revealed an enrichment of proteins associated with malaria, MAPK cascade and inflammatory processes. The results confirm that HMZ is capable of activating cellular processes involved in malaria infection, even in the absence of the parasite. It also implies that the molecules elevated in our *in-vitro* CM model are relevant in malaria pathogenesis. With reference to the KEGG analysis, there was an up-regulation of pathways associated with malaria, MAPK signalling, neurodegeneration, and AD, whereas p53 signalling and apoptosis pathways were down-regulated. The up-regulated pathways support data from previous studies that identified genes related to neurodegenerative and AD pathways in CM patients[4,37,38]. This signifies that CM and neurodegenerative diseases, especially AD, share

similar cellular mechanisms with a common denominator being inflammation. In contrast, the down-regulated p53 and apoptotic pathways can be attributed to the significant concentration of BDNF in our assay. Indeed, it has been confirmed that BDNF inhibits pro-apoptotic signalling following brain injury[11]. Saba et al., confirmed that BDNF significantly decreased apoptosis in serum deprived astrocytes by reducing p53 and active Caspase-3 expression[39], hence the down-regulation of these pathways in our experiment.

Subsequent to secretome screening, the mRNA expression levels of pro-inflammatory cytokines associated with severe CM (TNF-α, IL-6, IL-8)[28] but had a reduced/marginal protein expression, were examined in both UM51 and B4 neuronal cultures. Our analysis revealed significant upregulation of *TNFA* and *IL-8* in both neuronal cultures, and *IL-6* in only the UM51 neurons. The outcome demonstrates the phenomenon of poor correlation between mRNA and protein synthesis[40], which explains the lower concentration of these cytokines in the secretome analysis, though differences in mRNA levels were significant.

Additionally, we examined the mRNA expression levels of genes associated with the up-regulated KEGG pathways in both cell lines namely: *BDNF*, *CCL2* (MCP-1), *PECAM1*, *PDGFB* and *VEGF*. With the exception of the angiogenic factors, *PDGFB* and *VEGF*, we saw an increase in mRNA expression of the other molecules. It is noteworthy that PDGFB and VEGF were elevated in the secretome analysis, therefore the lower mRNA levels once again demonstrate a poor correlation between mRNA and protein synthesis. Collectively, these experiments provide evidence that CCL2, PECAM1, PDGF and VEGF, which are reported to modify cell junctions, increase endothelial permeability and enhance leukocyte trans-endothelial migration in inflammation[41-44] are key elements to HMZ induced cellular injury in CM. Ultimately, the significant expression of these factors represents inflammation and immune cell extravasation during CM pathogenesis.

A consequence of continuous inflammation is DNA damage. Therefore, in our successive experiments, we measured γH2AX, a reliable marker for DNA double strand breaks[45] in both UM51 and B4 neuronal cultures. Additionally, we examined a selection of molecules involved in DNA damage and repair checkpoints including ATM, ATR, CHEK1 and CHEK2. Our analyses revealed a significant increase in γH2AX level, representing DNA damage in the UM51 neuronal cultures and only a slight increase in B4. This result is the first to confirm that HMZ induces DNA damage in neurons. The DNA checkpoint investigation revealed significant expression of *ATM, ATR, CHEK1* and *CHEK2* in both cultures, but more evident in UM51. Next, we measured downstream targets of the damage response pathway, p53 and p38 MAPK. We found the expression of *p53* transcripts to be lower in both cultures, but the expression of p53 protein to be slightly increased in UM51. We also detected lower protein levels of MDM2 (a negative regulator of p53) and FAS, a downstream target of p53. However, except for FAS, the changes were minimal. These results indicate that p53 pathway was not involved in the stress response in our experiments. On the contrary, we observed an up-regulation of total p38 MAPK in both cell lines, though there was no significantly higher expression of phosphorylated p38 MAPK. This is an indication that p38 pathway was activated in response to stress in our study. Previous research has described an activation of the p38 MAPK pathway in response to DNA damage through ATM, when p53 pathway was deficient or compromised[46,47]. Moreover, p38 MAPK was found to mediate the release of lysozyme and upregulate other pro-inflammatory molecules in an experiment involving human adherent monocytes and natural HMZ[48]. Again, p38 MAPK was up-regulated in peripheral blood mononuclear cells of patients infected with *P. falciparum*[49]. These observations suggest a vital role of p38 MAPK in facilitating cellular response to *P. falciparum* and HMZ.

As a subsequent goal, we examined the effect of HMZ on HMC3 microglia cells. There was an increase in the expression of known microglial activation markers-triggering receptor

expressed on myeloid cells 2 (*TREM2*), ionized calcium binding adaptor molecule 1 (*IBA1*) and *CD45*. Compared to the control group, the level of γH2AX in HMZ treated microglia cells was higher though not significant. With the exception of ATR and CHEK1, there was an up-regulation of the other DNA damage response molecules (ATM, CHEK2) in HMC3 cells. Once more, there was no significant increase in p53 levels in HMZ treated microglia cells. Thus, neurons and microglia cells show a similar response pattern to HMZ stimulation.

A limitation of this study is the lack of complete cellular components characteristic of the brain, which comprise of neurons, glial cells, microglia, oligodendrocytes and vascular units. This would have provided the complexity of varying responses of the different cell types to HMZ exposure in CM pathology. Future experiments using brain organoids could be a suitable approach in this regard.

Conclusion

This study aimed at identifying molecules and pathways that mediate neuronal response to HMZ. Additional to the well-established cytokines identified in CM, we discovered IL-16, which has been implicated in other neurological diseases but not in CM. We also provide evidence for the first time that HMZ induces DNA damage in neurons. In summary, this study has demonstrated that HMZ can potently induce inflammatory responses in a comparable manner to clinical falciparum malaria. In addition, iPSC-derived neuronal cultures may provide a robust model for CM research. Also, given the increasing evidence of a link between neurodegenerative diseases and CM, further studies are required to validate this assertion, specifically with regards to the molecules that drive the pathogenesis and the phenotype of these diseases.

References

1 *World malaria report 2022:* https://www.who.int/teams/global-malaria-programme/reports/world-malaria-report-2022

2 Arisco, N. J., Peterka, C. & Castro, M. C. Imported malaria definition and minimum data for surveillance. *Scientific Reports* **12**, 17982, doi:10.1038/s41598-022-22590-6 (2022).

3 Gilson, R. C. *et al.* Growth of Plasmodium falciparum in response to a rotating magnetic field. *Malaria Journal* **17**, 190, doi:10.1186/s12936-018-2333-2 (2018).

4 Karikari, A. A., Wruck, W. & Adjaye, J. Transcriptome-based analysis of blood samples reveals elevation of DNA damage response, neutrophil degranulation, cancer and neurodegenerative pathways in Plasmodium falciparum patients. *Malaria Journal* **20**, 383, doi:10.1186/s12936-021-03918-5 (2021).

5 Polimeni, M. & Prato, M. Host matrix metalloproteinases in cerebral malaria: new kids on the block against blood-brain barrier integrity? *Fluids Barriers CNS* **11**, 1-1, doi:10.1186/2045-8118-11-1 (2014).

6 Jiménez-Díaz, M.-B., Möhrle, J. J., Angulo-Barturen, I. & Demarta-Gatsi, C. Using Cryopreserved Plasmodium falciparum Sporozoites in a Humanized Mouse Model to Study Early Malaria Infection Processes and Test Prophylactic Treatments. *Microorganisms* **11**, 2209 (2023).

7 Pranty, A. I., Wruck, W. & Adjaye, J. Free Bilirubin Induces Neuro-Inflammation in an Induced Pluripotent Stem Cell-Derived Cortical Organoid Model of Crigler-Najjar Syndrome. *Cells* **12**, doi:10.3390/cells12182277 (2023).

8 Harbuzariu, A. *et al.* Neuregulin-1/ErbB4 signaling modulates Plasmodium falciparum HRP2-induced damage to brain cortical organoids. *iScience* **25**, 104407, doi:10.1016/j.isci.2022.104407 (2022).

9 Schiess, N. *et al.* Pathophysiology and neurologic sequelae of cerebral malaria. *Malaria Journal* **19**, 266, doi:10.1186/s12936-020-03336-z (2020).
10 Idro, R., Marsh, K., John, C. C. & Newton, C. R. Cerebral malaria: mechanisms of brain injury and strategies for improved neurocognitive outcome. *Pediatr Res* **68**, 267-274, doi:10.1203/PDR.0b013e3181eee738 (2010).
11 Harbuzariu, A. *et al.* Modelling heme-mediated brain injury associated with cerebral malaria in human brain cortical organoids. *Scientific Reports* **9**, 19162, doi:10.1038/s41598-019-55631-8 (2019).
12 Martins, S. *et al.* IPSC-Derived Neuronal Cultures Carrying the Alzheimer's Disease Associated TREM2 R47H Variant Enables the Construction of an Aβ-Induced Gene Regulatory Network. *International journal of molecular sciences* **21**, 4516, doi:10.3390/ijms21124516 (2020).
13 Nevin, R. L. & Croft, A. M. Psychiatric effects of malaria and anti-malarial drugs: historical and modern perspectives. *Malaria Journal* **15**, 332, doi:10.1186/s12936-016-1391-6 (2016).
14 Bohndorf, M. *et al.* Derivation and characterization of integration-free iPSC line ISRM-UM51 derived from SIX2-positive renal cells isolated from urine of an African male expressing the CYP2D6 *4/*17 variant which confers intermediate drug metabolizing activity. *Stem Cell Res* **25**, 18-21, doi:10.1016/j.scr.2017.10.004 (2017).
15 Wang, Y. & Adjaye, J. A cyclic AMP analog, 8-Br-cAMP, enhances the induction of pluripotency in human fibroblast cells. *Stem cell reviews and reports* **7**, 331-341, doi:10.1007/s12015-010-9209-3 (2011).
16 Nociti, V. & Romozzi, M. The Role of BDNF in Multiple Sclerosis Neuroinflammation. *Int J Mol Sci* **24**, doi:10.3390/ijms24098447 (2023).
17 Guzman-Hernandez, M. L., Potter, G., Egervari, K., Kiss, J. Z. & Balla, T. Secretion of VEGF-165 has unique characteristics, including shedding from the plasma membrane. *Mol Biol Cell* **25**, 1061-1072, doi:10.1091/mbc.E13-07-0418 (2014).
18 Kanehisa, M., Furumichi, M., Sato, Y., Kawashima, M. & Ishiguro-Watanabe, M. KEGG for taxonomy-based analysis of pathways and genomes. *Nucleic acids research* **51**, D587-D592 (2023).
19 Kanehisa, M. & Goto, S. KEGG: kyoto encyclopedia of genes and genomes. *Nucleic acids research* **28**, 27-30 (2000).
20 Kanehisa, M. Toward understanding the origin and evolution of cellular organisms. *Protein Science* **28**, 1947-1951 (2019).
21 Frita, R., Carapau, D., Mota, M. M. & Hänscheid, T. In Vivo Hemozoin Kinetics after Clearance of Plasmodium berghei Infection in Mice. *Malaria Research and Treatment* **2012**, 373086, doi:10.1155/2012/373086 (2012).
22 Eugenin, E. A., Martiney, J. A. & Berman, J. W. The malaria toxin hemozoin induces apoptosis in human neurons and astrocytes: Potential role in the pathogenesis of cerebral malaria. *Brain research* **1720**, 146317-146317, doi:10.1016/j.brainres.2019.146317 (2019).
23 Pham, T.-T., Lamb, T. J., Deroost, K., Opdenakker, G. & Van den Steen, P. E. Hemozoin in Malarial Complications: More Questions Than Answers. *Trends in Parasitology* **37**, 226-239, doi:https://doi.org/10.1016/j.pt.2020.09.016 (2021).
24 Greiner, J. *et al.* Correlation of hemorrhage, axonal damage, and blood-tissue barrier disruption in brain and retina of Malawian children with fatal cerebral malaria. *Frontiers in Cellular and Infection Microbiology* **5**, doi:10.3389/fcimb.2015.00018 (2015).
25 Newton, C. R. & Krishna, S. Severe falciparum malaria in children: current understanding of pathophysiology and supportive treatment. *Pharmacol Ther* **79**, 1-53, doi:10.1016/s0163-7258(98)00008-4 (1998).
26 Brown, H. *et al.* Cytokine Expression in the Brain in Human Cerebral Malaria. *The Journal of infectious diseases* **180**, 1742-1746, doi:10.1086/315078 (1999).
27 Akide Ndunge, O. B., Kilian, N. & Salman, M. M. Cerebral Malaria and Neuronal Implications of Plasmodium Falciparum Infection: From Mechanisms to Advanced Models. *Advanced Science* **9**, 2202944, doi:https://doi.org/10.1002/advs.202202944 (2022).

28 Mandala, W. L. *et al.* Cytokine Profiles in Malawian Children Presenting with Uncomplicated Malaria, Severe Malarial Anemia, and Cerebral Malaria. *Clinical and Vaccine Immunology* **24**, e00533-00516, doi:doi:10.1128/CVI.00533-16 (2017).

29 Mahittikorn, A. *et al.* Increased interferon-γ levels and risk of severe malaria: a meta-analysis. *Scientific Reports* **12**, 18917, doi:10.1038/s41598-022-21965-z (2022).

30 Pawlowski, T. *et al.* Depression and neuroticism in patients with chronic hepatitis C: correlation with peripheral blood mononuclear cells activation. *J Clin Virol* **60**, 105-111, doi:10.1016/j.jcv.2014.03.004 (2014).

31 Cheng, X. *et al.* Correlation between elevated serum interleukin-1β, interleukin-16 levels and psychiatric symptoms in patients with schizophrenia at different stages. *BMC Psychiatry* **23**, 396, doi:10.1186/s12888-023-04896-5 (2023).

32 Di Rosa, M. *et al.* Chitotriosidase and inflammatory mediator levels in Alzheimer's disease and cerebrovascular dementia. *Eur J Neurosci* **23**, 2648-2656, doi:10.1111/j.1460-9568.2006.04780.x (2006).

33 Lobaloba Ingoba, L. *et al.* Diagnosis of Chikungunya Virus in Febrile Patients From a Malaria Holoendemic Area. *International Journal of Infectious Diseases* **109**, 247-252, doi:10.1016/j.ijid.2021.06.043 (2021).

34 Waknine-Grinberg, J. H., McQuillan, J. A., Hunt, N., Ginsburg, H. & Golenser, J. Modulation of cerebral malaria by fasudil and other immune-modifying compounds. *Experimental Parasitology* **125**, 141-146, doi:https://doi.org/10.1016/j.exppara.2010.01.005 (2010).

35 McDonald, C. R. *et al.* Brain-derived Neurotrophic Factor Is Associated With Disease Severity and Clinical Outcome in Ugandan Children Admitted to Hospital With Severe Malaria. *Pediatr Infect Dis J* **36**, 146-150, doi:10.1097/INF.0000000000001382 (2017).

36 Calabrese, F. *et al.* Brain-derived neurotrophic factor: a bridge between inflammation and neuroplasticity. *Front Cell Neurosci* **8**, 430, doi:10.3389/fncel.2014.00430 (2014).

37 Cabantous, S. *et al.* Understanding Human Cerebral Malaria through a Blood Transcriptomic Signature: Evidences for Erythrocyte Alteration, Immune/Inflammatory Dysregulation, and Brain Dysfunction. *Mediators of Inflammation* **2020**, 3280689, doi:10.1155/2020/3280689 (2020).

38 Thiam, A. *et al.* Gene expression profiling in blood from cerebral malaria patients and mild malaria patients living in Senegal. *BMC Medical Genomics* **12**, 148, doi:10.1186/s12920-019-0599-z (2019).

39 Saba, J. *et al.* Astrocyte truncated tropomyosin receptor kinase B mediates brain-derived neurotrophic factor anti-apoptotic effect leading to neuroprotection. *Journal of Neurochemistry* **146**, 686-702, doi:https://doi.org/10.1111/jnc.14476 (2018).

40 Liu, Y., Beyer, A. & Aebersold, R. On the Dependency of Cellular Protein Levels on mRNA Abundance. *Cell* **165**, 535-550, doi:10.1016/j.cell.2016.03.014 (2016).

41 Bazzari, A. H. & Bazzari, F. H. BDNF Therapeutic Mechanisms in Neuropsychiatric Disorders. *International journal of molecular sciences* **23**, 8417 (2022).

42 Roberts, T. K. *et al.* CCL2 disrupts the adherens junction: implications for neuroinflammation. *Lab Invest* **92**, 1213-1233, doi:10.1038/labinvest.2012.80 (2012).

43 Yao, H., Duan, M. & Buch, S. Cocaine-mediated induction of platelet-derived growth factor: implication for increased vascular permeability. *Blood* **117**, 2538-2547, doi:10.1182/blood-2010-10-313593 (2011).

44 Zhang, Z. G. *et al.* VEGF enhances angiogenesis and promotes blood-brain barrier leakage in the ischemic brain. *J Clin Invest* **106**, 829-838, doi:10.1172/JCI9369 (2000).

45 Mah, L. J., El-Osta, A. & Karagiannis, T. C. γH2AX: a sensitive molecular marker of DNA damage and repair. *Leukemia* **24**, 679-686, doi:10.1038/leu.2010.6 (2010).

46 Roy, S. *et al.* The role of p38 MAPK pathway in p53 compromised state and telomere mediated DNA damage response. *Mutation Research/Genetic Toxicology and Environmental Mutagenesis* **836**, 89-97, doi:https://doi.org/10.1016/j.mrgentox.2018.05.018 (2018).

47 Reinhardt, H. C., Aslanian, A. S., Lees, J. A. & Yaffe, M. B. p53-deficient cells rely on ATM- and ATR-mediated checkpoint signaling through the p38MAPK/MK2 pathway for survival after DNA damage. *Cancer Cell* **11**, 175-189, doi:10.1016/j.ccr.2006.11.024 (2007).
48 Polimeni, M. *et al.* Haemozoin Induces Early Cytokine-Mediated Lysozyme Release from Human Monocytes through p38 MAPK- and NF-kappaB- Dependent Mechanisms. *PLOS ONE* **7**, e39497, doi:10.1371/journal.pone.0039497 (2012).
49 Hu, W.-C. Human immune responses to Plasmodium falciparum infection: molecular evidence for a suboptimal THαβ and TH17 bias over ideal and effective traditional TH1 immune response. *Malaria Journal* **12**, 392, doi:10.1186/1475-2875-12-392 (2013).
50 Hyowon An, J. T. L., Aubrey G. Bailey,James S. Marron,Dirk P. Dittmer "Dr4pl: A Stable Convergence Algorithm for the 4 Parameter Logistic Model.". *The R Journal* **11/2**, 171, doi:10.32614/RJ-2019-003 (2019).
51 Wickham, H. *Ggplot2: elegant graphics for data analysis*. 212 (Springer, 2009).
52 Schneider, C. A., Rasband, W. S. & Eliceiri, K. W. NIH Image to ImageJ: 25 years of image analysis. *Nat Methods* **9**, 671-675, doi:10.1038/nmeth.2089 (2012).
53 Gentleman, R. C. *et al.* Bioconductor: open software development for computational biology and bioinformatics. *Genome Biol* **5**, R80, doi:10.1186/gb-2004-5-10-r80 (2004).
54 Du, P., Kibbe, W. A. & Lin, S. M. lumi: a pipeline for processing Illumina microarray. *Bioinformatics* **24**, 1547-1548, doi:10.1093/bioinformatics/btn224 (2008).
55 Warnes, G. R., Ben Bolker, Lodewijk Bonebakker, Robert Gentleman, Wolfgang Huber Andy Liaw, Thomas Lumley, Martin Maechler, et al. . *Gplots: Various R Programming Tools for Plotting Data.*, <http://CRAN.R-project.org/package=gplots> (2015).
56 Zhou, Y. *et al.* Metascape provides a biologist-oriented resource for the analysis of systems-level datasets. *Nat Commun* **10**, 1523, doi:10.1038/s41467-019-09234-6 (2019).
57 Kanehisa, M., Furumichi, M., Tanabe, M., Sato, Y. & Morishima, K. KEGG: new perspectives on genomes, pathways, diseases and drugs. *Nucleic Acids Res* **45**, D353-D361, doi:10.1093/nar/gkw1092 (2017).

Methods and Materials

Cell culture

- **iPSCs culture and NPC generation**

Two healthy male-derived iPSC lines were used in this study. The UM51-hiPSC line was derived from SIX2-positive renal progenitor cells isolated from the urine of a 51-year-old healthy male of African origin (UM51)[14]. The other iPSC line (B4) was generated from healthy human fetal foreskin fibroblasts (HFF1, ATCC, #ATCCSCRC-1041, http://www.atcc.org)[15] (Supplementary Table S1). iPSCs were plated on Matrigel (Corning, New York, NY, USA)-coated culture dishes using mTeSR Plus medium (StemCell Technologies, Vancouver, Canada). Cultures were routinely tested for mycoplasma contamination. Cells were passaged by dissociation into small aggregates with ReLeSR (StemCell Technologies, Vancouver, Canada) every 5–7 days and split in a 1:5 ratio into fresh Matrigel-coated dishes. For neural progenitor cell (NPC) generation, iPSCs were split as single cells using accutase (Life Technologies, Waltham, MA, USA). In brief, at day 0, iPSC-colonies were dissociated with warm (37°C) accutase, centrifuged at 200 rcf for 5 min, then resuspended in mTESR+ with 10µM of ROCK inhibitor. 20,000 cells in 100 µL cell suspension were seeded per well of a 96 u-bottom well plate (Low attachment, U bottom) to form embryoid bodies (EBs). Seeded iPSCs were spinned down at 110 rcf for 3 min and incubated at 37°C with 5% CO_2 for 24h. At day 1, half of the medium volume was aspirated and replaced with neural induction medium (NIM)

with 10µM of ROCK inhibitor. EBs were culture for 7 days (day 2-8) with NIM supplemented with 10 µM SB431542 and 5 µM Dorsomorphin (10µM of ROCK inhibitor until day 3). Medium was refreshed daily. On day 8, 20-30 EBs were plated per well of a Poly-Ornithine/Laminin (Sigma-Aldrich; Merck KGaA, Darmstadt, Germany) -coated 6-well plate to generate neural rosettes. EBs were cultured in neural differentiation medium (NDM) (Neurobasal A, 1% B27, 1% GlutaMAX, 1% P/S) supplemented with 20 ng/mL EGF and 20 ng/mL FGF2 and incubated at 37°C with 5% CO_2 in static position. The medium was changed daily. At day 16, neural rosettes were selected using STEMdiff™ Neural Rosette Selection Reagent (StemCell Technologies, Vancouver, Canada) for 30 min-1 h at 37°. Warm accutase was used for 30 min at 37°C to dissociate the neural rosettes. NPCs were further cultured in Growth-Factor Reduced (GFR) Matrigel (Corning, New York, NY, USA)-coated plates with NDM supplemented with 20 ng/mL EGF and 20 ng/mL FGF2. Accutase was used for splitting the NPCs. In parallel, early passages of NPCs were frozen in Cryostore CS10 (StemCell Technologies) for later usage.

- **Neuronal differentiation and Hemozoin treatment**

UM51- and B4 iPSC-derived NPCs were used for the neuronal differentiation. To initiate differentiation, NPCs were dissociated with warm accutase and plated on GFR Matrigel (Corning, New York, NY, USA)-coated plates. 500,000 cells/well in a 6-well plate and 80,000 cells/well in a 24 well plate were seeded to produce neuronal cultures. For cell adhesion, NDM supplemented with 20 ng/mL EGF and 20 ng/mL FGF2 was used for 24h, which was then changed to NDM supplemented with 20 ng/mL BDNF and 20 ng/mL NT3 for the rest of the differentiation (Day 2-16). Cells were cultured until day 16 and medium was changed every 2-3 days. At day 16, neuronal cultures were exposed to 20 µM HMZ for 48 h.

Hemozoin (InvivoGen #tlrl-hz) was dissolved in PBS (pH 7.4) to obtain a stock concentration of 4.06 mM (5mg/mL). To obtain a homogenous dispersion of hemozoin, the hemozoin-PBS suspension was sonicated for 5 minutes. For treatment, 20 µM hemozoin (HMZ) was added to the culture medium and incubated for 48 h.

Cell viability assay

To ascertain the appropriate concentration, we performed resazurin assay/alamar blue assay on B4 iPSC-derived neuronal cultures by exposing those to 0, 5 µM, 10 µM, 20 µM, 50 µM, 100 µM, 200 µM HMZ for 48 h. In brief, day 16 neurons were treated with the mentioned HMZ concentrations continuously for 48 h. 2 h before reaching the analysis time point, resazurin solution was added and incubated at 37°C with 5% CO_2. After 2 h, 100 µl supernatant was transferred to a 96-well flat bottom plate in triplicate for each condition. Fluorescence was recorded using a plate reader with a 560 nm excitation/ 590 nm emission filter set. For the resazurin solution, a stock of 0.15 mg/mL resazurin in PBS was prepared, which was further diluted 1:10 with PBS before use. 100 µl diluted resazurin solution was added per well. 3 wells containing culture medium and diluted resazurin were prepared for background subtraction and instrument gain adjustment.

Based on Resazurin measurements of neuronal culture treated with varying doses of HMZ, IC50 plots were generated within the R environment employing the packages dr4pl and ggplot2[50,51] (Supplementary Fig. 1). The dr4pl method was parametrized to use a logistic model, the fitted curve was plotted using values from the model. Additionally, the IC50 was calculated via the logistic model in dr4pl.

Immunocytochemistry

Cells were fixed in 4% paraformaldehyde (PFA) (Polysciences, Warrington, FL, USA) for 10 min at room temperature (RT). After washing with 3 times with PBS, cells were directly used for staining. Fixed cells were permeabilized for 10 min using 0.1% Triton X-100 in PBS+Glycine (30 mM Glycine) at RT. After washing once with PBS, unspecific binding sites were blocked for 2 h at RT with 3% BSA in PBS+Glycine. Primary antibodies were diluted in 3% BSA in PBS+Glycine and incubated overnight at 4°C (Supplementary Table S2). After washing three times with PBS, secondary antibodies diluted in 3% BSA/PBS/Glycine were added for 2 h and incubated at RT. Nuclei were stained with Hoechst 33258. Stained cells were imaged using a Zeiss fluorescence microscope (LSM 700). Individual channel images were processed and merged with ImageJ software version 1.53c (U. S. National Institutes of Health, Bethesda, Maryland, USA). Cell counting was performed using the “Cell counter“ function of ImageJ.

Secretome Analysis

- **Human XL Cytokine Array**

After 48 h of HMZ treatment, the conditioned medium of the control and HMZ-treated neuronal cultures were stored at -20°C. Relative expression levels of 105 soluble human proteins and cytokines were determined using the Human XL Cytokine Array Kit from R&D Systems. The cytokine array was performed following the manufacturer’s guidelines. In brief, the membranes were blocked for 1 h on a rocking platform using the provided blocking buffer. Samples were prepared by diluting the desired quantity to a final volume of 1.5 mL with array buffer (array buffer 6). The sample mixtures were pipetted onto the blocked membranes and incubated overnight at 4°C on a rocking platform. Membranes were washed three times with washing buffer for 10 min each at RT. Then, the membranes were incubated with detection antibody cocktail for 1h at RT and washed three times. Afterwards, Streptavidin-HRP was added onto the membranes, and incubated for 30 min at RT. ECL detection reagent (Cytiva, Freiburg, Germany) was used to visualize bound proteins as spots, which were detected using a Fusion FX instrument (PeqLab, Erlangen, Germany) (Supplementary Fig. 2).

- **Image Analysis of Cytokine Arrays**

Images of the hybridized cytokine assays were scanned and analyzed via the FIJI/ImageJ software[52]. The grid on the cytokine array was detected semi-automatically employing pre-processing via Gaussian blur (size 4) and local maxima finding. The csv file containing the local maxima detected by FIJI/ImageJ was imported into the R programming environment and based on it corners were found and the grid between them interpolated making use of positions found as local maxima. Quantification of the spots at the grid locations was performed by the FIJI Microarray Profile plugin by Bob Dougherty and Wayne Rasband (https://www.optinav.info/MicroArray_Profile.htm, accessed on 21 December 2022), using integrated densities. Cytokine names were taken from proprietary lists of the manufacturer (Proteome Profiler Array from R & D Systems, Human XL Cytokine Array Kit, Catalog Number ARY022B) and assigned to the quantified spots by their grid positions.

- **Cytokine Data Analysis**

The follow-up-processing of the quantified spots within the R/Bioconductor environment started with the Robust Spline Normalization from the R/Bioconductor package lumi[53,54]. The function heatmap.2 from the gplots package was applied to draw heatmaps using Pearson correlation as similarity measure[55]. Based on this cluster analysis via heatmap.2 genes were

split into two clusters associated with up- and down-regulation by HMZ for subsequent analysis.

Metascape Analysis

Comprehensive functional analysis of the clustered gene ontology (GO) biological processes and pathways (KEGG pathways, Reactome Gene Sets, Canonical pathways, and CORUM) of gene-sets based on data derived from the Human XL Cytokine Array was performed using Metascape[56] (http://metascape.org, accessed on 13 October 2023). Lists of up- and downregulated cytokines were treated as gene-sets for analytical purposes.

Pathway analysis

Cytokines were subjected to cluster analysis via the heatmap.2 function from the R package gplots using Pearson correlation as similarity measure and the default setting of hclust as hierarchical clustering method[55]. Cytokines from the two resulting clusters of HMZ-induced up- and down-regulation were analyzed for over-represented KEGG pathways in the follow-up analysis[57]. KEGG pathways were downloaded from the KEGG website in February 2023. The R-builtin hypergeometric test was employed to determine the p-value indicating the significance of the over-represented pathways. Malaria and p53 signaling (KEGG) pathway, shown in the supplementary fig. 3 were taken respectively from https://www.genome.jp/kegg-bin/show_pathway?hsa05144 and https://www.genome.jp/pathway/hsa04115.

Reverse Transcriptase PCR (RT-PCR)

Control and HMZ-treated cells were lysed for 15 min in Trizol. RNA was isolated using the Direct-zol™ RNA Isolation Kit (Zymo Research, Freiburg, Germany) according to the user's manual, including the DNA digestion step. 500 ng of RNA was reverse transcribed using the TaqMan Reverse Transcription Kit (Applied Biosystems, Waltham, MA, USA). The primer sequences are shown in (Supplementary Table S3). Real-time PCRs were performed in technical and independent experiment triplicates (n=3) with Power Sybr Green Master Mix (Life Technologies, Darmstadt, Germany) on a VIIA7 (Life Technologies, Darmstadt, Germany) machine. Mean values were normalized to the ribosomal protein lateral stalk subunit P0 (RPLP0) and fold-change was calculated using the indicated controls. Changes in gene expression were presented in log2-scale. All values are depicted as mean with a 95% confidence interval (CI). Each singular value (Ctrl and HMZ) was compared to the mean of all corresponding control samples. The resulting values were used for statistical analysis. Statistical analysis was performed using Student′s unpaired two-sample t-tests. For ease of reading, only values of the treated condition were presented.

Western Blotting

Total protein from UM51- and B4-derived neuronal cultures was isolated using RIPA buffer (Sigma-Aldrich Chemicals, Taufkirchen, Germany), supplemented with protease and phosphatase inhibitors (Roche, Mannheim, Germany). Afterwards, Pierce BCA Protein Assay Kit (Thermo Fisher, Waltham, MA, USA) was used to determine protein concentration of the samples. 20 µg of the heat-denatured protein lysate of each sample was loaded on a 4–12% SDS-PAGE and then transferred via wet blotting onto a 0.45 µm nitro-cellulose membrane (GE Healthcare, Solingen, Germany). After 1 h of blocking with 5% milk in TBST, the membranes were stained with anti-γH2AX, anti-p53, anti-MDM2, anti-P38MAPK, anti-phospho-P38MAPK, anti-FAS, anti-Caspase 3, and anti-cleaved caspase 3 antibodies in the appropriate buffer (Supplementary Table S2). Incubation with primary antibodies was performed overnight at 4°C.

After washing the membranes three times with TBST, secondary antibody incubation was performed for 2 h at RT followed by washing with TBST (Supplementary Table S2). Anti-β-Actin and anti-GAPDH (glyceralde-hyde-3-phosphate dehydrogenase) were used as housekeeping proteins to normalize protein expression. ECL Western Blotting Detection Reagents (Cytiva, Freiburg, Germany) were used to visualize the stained protein bands and then detected in a Fusion FX instrument (PeqLab, Erlangen, Germany). Band intensity quantification and analysis was performed with Fusion Capt Advance software FX7 16.08 (PeqLab, Erlangen, Germany).

Statistical Analysis

All obtained results were represented as mean ± standard deviation. Statistical analysis (Student's unpaired two-samples t-test) was performed utilizing GraphPad Prism v.8.0.2 (GraphPad Software, Boston, USA). A p-value of <0.05 was considered as statistically significant during analysis.

Acknowledgment

The authors are grateful to Kanehisa Laboratories for the permission to use their figures for Malaria and p53 signalling path for our figures. The figures were taken from https://www.genome.jp/kegg/

Author contributions

A.I.P. and L.P.S. designed and performed the experiments, processed and analyzed the data, and wrote and edited the manuscript. W.W. performed the bioinformatic analysis and data curation, helped with the figures, wrote the bioinformatic section in the Methods and Materials, and edited the manuscript. A.A.K. conceptualized the work, wrote and edited the manuscript. J.A. conceptualized and designed the work, edited the manuscript, acquired funding, and supervised the study. All authors have read and agreed to the submitted version of the manuscript.

Data availability statement

Datasets resulting from the cytokine assay analyses in this study are available in the supplementary materials (Supplementary File 1, 2) data of this work.

Funding

J.A. acknowledges the medical faculty of Heinrich Heine University for financial support.

Conflicts of Interest

The authors declare no conflicts of interest.

4. Discussion

Encephalopathy is a set of conditions that results brain dysfunction. It can be manifested in different disease conditions, caused by divergent causal factors ranging from infection, toxin exposure, stroke, head injury, and tumorigenesis to different underlying rare conditions such as autoimmune or mitochondrial conditions (*Encephalopathy*, 2023). Consequences of encephalopathy can be severe and fatal with permanent brain damage along with long term neurological effects, cognition and developmental disorders and delays, as well as coma. Alike most neurological disorders, there is no cure for encephalopathy. Nevertheless, if diagnosed in the initial stage, the applied treatment might manage the underlying aggravating condition. Therefore, deciphering the etiology of the disease condition is crucial along with investigating the cellular and molecular effects of the pathophysiology in a human recapitulating system.

Bilirubin-induced encephalopathy or bilirubin-induced neurologic dysfunction (BIND) is associated with hyperbilirubinemia in mammalian neonates, in which accumulation of free bilirubin (BF) in different brain regions such as basal ganglia, cerebellum, and brain stem nuclei causes irreversible neurological damages in neonates (Amini et al., 2017; Shapiro, 2003). Clinical manifestations of bilirubin induced encephalopathy include neurological impairments such as motor-development delay, hearing loss, epilepsy, cerebral palsy, mental retardation, lethargy, and poor nutrition. Since no specific therapeutic strategy exists for these patients, this condition may lead to death or permanent nervous system complications (Amini et al., 2017). Crigler-Najjar syndrome (CNS) is a rare disease, which affects 0.6 to 1 in 1 million newborns around the world and is caused by an inherited genetic disorder of bilirubin conjugation mechanism, resulting in BIND (Collaud et al., 2019). The inner mechanisms leading to BIND are still largely unknown, which prompts for more research and suitable models to investigate BIND and its neurological consequences.

Encephalopathy is also clinically manifested in cerebral malaria (CM), caused by the *Plasmodium falciparum* infection. CM causes lesion of the upper motor neurons, resulting in manifestations from headaches to deterioration of the level of consciousness (Mishra & Newton, 2009; Misra et al., 2011; Zapata Zapata & Blair Trujillo, 2003). Cognitive difficulties, language, and behavioural problems are some of the documented observed complications in 24% of children after CM (Mishra & Newton, 2009). CM pathogenesis is unclear due to the difficulty in obtaining brain samples.

To elucidate disease mechanisms for CNS and CM, studies have been conducted mainly on rodent models (*in vivo),* post-mortem brain autopsy tissues (*ex vivo*), and some of the available immortalized cell lines (*in vitro*). Therefore, it is a pre-requisite to establish a suitable model to investigate the mechanisms leading to encephalopathy, such as BIND or CM, which could resemble the human CNS[#] and the neurological consequences caused by the respective disease conditions. Human iPSCs have become an emerging tool to generate healthy and patient specific models, due to their ability to generate 2D and 3D cellular models such as neuron, spheroid, and organoid cultures, facilitating neuroscience research. iPSC-derived 2D and 3D neuronal models are being implied to investigate an array of human brain disorders (Penney et al., 2020). Besides, these models can be used for drug toxicity testing, regenerative therapies, personalized medicine, and therapies, as well as investigating the pathophysiology of various diseases. 3D organoid models particularly mimic cellular diversity, morphological structure, and functions of the target organ. However, iPSC-derived 2D and 3D neural cell cultures hold shortcomings such as lack of vasculature, hormone and sensory stimuli mediated inputs, interregional connectivity, while 3D organoids may also lack adequate oxygen supply, nutrients and metabolite exchange resulting in necrotic core formation after reaching a certain size limit (Tomaskovic-Crook et al., 2021). These cultures may manifest reduced reproducibility due to high inter-donor variability (Hoffman et al., 2017; Tomaskovic-Crook et al., 2021). Opportunely, there are emerging technologies and approaches to overcome such drawbacks. Despite having some limitations, iPSC-derived *in vitro* brain organoid models and 2D neuronal cultures can give deeper insights into the developing human brain along with cellular and molecular responses upon toxin exposure. This enables researchers to investigate BF- and/or HMZ-induced effects in the CNS[#].

The comprehensive aim of this thesis was to model CNS and CM using iPSC-derived neuronal cultures and investigate resulting encephalopathy caused by these disease conditions. In the first part of the thesis, an explicit assessment about the existing CNS models to investigate BIND and the current potential of emerging BIND models was discussed. Following that, the first available hiPSC-derived CNS model of 3D brain organoids was successfully generated, which was employed to model BIND *in vitro*. Thus, it was possible to investigate BF-induced detrimental effects in the developing human brain on the molecular basis. At the end, 2D neuronal cultures obtained from hiPSCs were used to model CM *in vitro* with HMZ exposure. HMZ-induced effects in the CNS[#] were studied to unveil the specific role of HMZ on neurons.

4.1 Assessment of current and emerging BIND models

BIND has been studied for decades, yet the pathophysiology of this encephalopathic condition is poorly understood. Gunn rat is the classic *in vivo* bilirubin encephalopathy model along with transgenic mice (Bortolussi & Muro, 2018; Gunn, 1944; Nguyen et al., 2008). Immortalized cell lines such as human neuroblastoma cell lines and human U87 astrocytoma cells and primary cultures (hippocampal neurons, mouse or rat derived neurons, astrocytes, oligodendrocytes, and microglia) have also been implied to investigate BIND (Bortolussi & Muro, 2020). These existing models have revealed invaluable knowledge about the molecular basis of BIND, nevertheless, those cannot recapitulate the human brain system. PSC-derived brain organoids can be integrated as a potential platform to study BIND. iPSCs can be generated from patients with BIND manifestations, which can further be used to differentiate into brain organoids allowing to study a patient specific model to understand the etiology of the disease condition. As BIND may result from CNS and the primary goal of the thesis was to model CNS leading to BIND, firstly the current state of the art, emerging advancements, as well as the challenges faced by the existing models were explicitly assessed in this review article (paragraph 3.1) along with the possibilities to employ stem cells-derived brain organoid models to study BIND and it`s future clinical applications (Pranty et al., 2022).

Bilirubin, an endogenous toxin, and a by-product of hemoglobin catabolic reaction is metabolized in the liver by the enzyme encoded by the *UGT1A1* gene. The UGT1A1 enzyme conjugates bilirubin and makes it water-soluble, while unconjugated bilirubin (UCB) is lipophilic (Memon et al., 2016). Hyperbilirubinemia (unconjugated) is a condition where the plasma or serum bilirubin levels cross the reference range and can result into clinical jaundice (Bortolussi & Muro, 2018). BIND can be an adverse effect of spontaneous neonatal hyperbilirubinemia, while it may also result from an autosomal recessive disorder- CNS, by complete or partial absence of UGT1A1 activity due to a mutation in the *UGT1A1* encoding gene. Complete deficiency of UGT1A1 enzymatic activity causes CNS type I and partial deficiency causes CNS type II. Due to the hindrance in bilirubin conjugation in CNS patients, UCB accumulates in serum, however, only the albumin-unbound unconjugated bilirubin (free bilirubin-BF) can cross the BBB and be neurotoxic leading to bilirubin encephalopathy (Brites, 2012; Memon et al., 2016; Watchko & Tiribelli, 2013). BF can deposit in various brain regions such as basal ganglia or cerebellum and progress to acute or chronic bilirubin encephalopathy (Memon et al., 2016; Singh & Jialal, 2021).

Gunn rat is the first and classic hyperbilirubinemia model to mimic CNS and BIND as they completely lack UGT1A1 enzymatic activity due to a spontaneous mutation in the UGT1 locus resulting in the deficiency of all UGT1A1 iso-enzymes (Bortolussi & Muro, 2018; Gunn, 1944). Bilirubin metabolism and toxicity has been considerably investigated and revealed by studying this *in vivo* model. Gunn rats showed comparable phenotypes to CNS such as life-long non-hemolytic unconjugated hyperbilirubinemia, abnormalities in cerebellum, and hearing impairments. Nevertheless, they are not identical with the human system as unlike CNS patients, Gunn rats reach adulthood and persists fertility (Bortolussi & Muro, 2020).

Genetic modification and manipulation in mouse genome with constitutive and conditional knock-in or knockout have been performed to investigate more BIND associated disease aspects (Bortolussi & Muro, 2020; Rice & Shapiro, 2008; Schiavon et al., 2018). Thus, a UGT1a-null mouse model has been established as another popular *in vivo* model, which can mimic CNS more aggressively with complete *UGT1A1* absence. This mutant mouse model manifests neurological damage more aggravatedly, however, they die within 11 days post-birth, making this model inconvenient to investigate the long-term neurological damage in bilirubin encephalopathy (Nguyen et al., 2008). The correlation between increased UCB levels and neurological damage has been investigated and shown using these *in vivo* models.

As only BF can cross the BBB, thus being the key player to cause BIND, it is crucial to inspect specifically BF induced responses in the neuronal cells. Even though the *in vivo* models have kept on rolling bilirubin neurotoxicity research with invaluable discoveries, the pathology and mechanism in human brain still remains an open question. Therefore, human cell-derived *in vitro* model systems and tissue derived organotypic *ex vivo* cultures have been employed to obtain more insights into the molecular basic of the disease resembling to the human system (Bortolussi & Muro, 2020; Brites, 2012; Calligaris et al., 2009; Chang et al., 2009; Dal Ben et al., 2017). 2D cell culture systems can be used to study cellular responses and bioactivities upon BF treatment in biochemical and biophysical directions (Duval et al., 2017). Hippocampal neurons have been the most commonly used *in vitro* neuro-cellular model to study bilirubin induced responses in neuronal cells, whereas immortalized cell lines such as human neuroblastoma cell lines and human U87 astrocytoma cells have extensively been used to explore bilirubin neurotoxicity. Additionally, primary cultures such as neurons, astrocytes, oligodendrocytes, microglia, endothelial cells, and embryonic fibroblasts obtained from rodents, and tissue slices such as hippocampal slices or post-mortem tissue sections have also

been used to study BIND *in vitro* (Figure 4) (Bortolussi & Muro, 2020). iPSC derived neuronal cultures such as neurons, astrocytes, oligodendrocytes, and co-cultures of the neural populations can be employed as a potential 2D system to study BF induced effects. Exposing different neural cell types to different concentrations and duration to BF is one of the key methods in exploring BIND. Despite of revealing valuable information on BIND toxicity, 2D models lack the complex cytoarchitecture, morphology, and physiological resemblance of a whole tissue.

To gain a better understanding of BIND pathophysiology and to develop clinical therapeutics and therapies, it is important to establish a human system-based model which can closely recapitulate the main characteristics of BIND. In this regard, iPSC-derived 3D culture models such as spheroids or organoids can be a potential appliance to study different biological, pathological, and physiological processes. Thus, the lack of *in vivo*-like responses in 2D systems can be resolved by incorporating another dimension. Addition of extracellular matrix results in 3D cultures, which remarkably impacts the cellular fate considering proliferation, differentiation, mechano-response, and cell viability (Bonnier et al., 2015; Duval et al., 2017). Compared to other *in vitro* models, iPSC-derived 3D brain organoids mimic the developing human brain and the neural environment better, considering the possibilities to achieve specific incorporated brain regions (such as choroid plexus, hippocampus, forebrain, hindbrain, midbrain, and BBB) in those organoids to facilitate the understanding of disease mechanism, toxicological studies, drug mechanism and customized medication (Edmondson et al., 2014; Liu et al., 2018; Martins et al., 2022; Nascimento et al., 2019; Qian et al., 2016).

Human brain organoids have already been employed to model a variety of neurological disorders such as microcephaly, Timothy syndrome, and Nijmegen breakage syndrome, as well as brain tumors such as gliomas and medulloblastoma (Birey et al., 2017; Goranci-Buzhala et al., 2020; Lancaster et al., 2013; Martins et al., 2022; Sidhaye & Knoblich, 2021; van Essen et al., 2024). This model has already shown its potential as an efficient and valid platform for studying human brain development and associated neurological disorders. Reviewing the existing BIND models as well as the possible application of brain organoids, the further goal extended to establish a CNS model manifesting BIND with emerging iPSC-derived 3D brain organoids (Koo et al., 2019). Eventually, successful modelling of BIND using brain organoids will enhance the knowledge and understanding of BIND etiology and its pathology in the human CNS[#], which will aid the future drug development and clinical applications.

4.2 Modelling Crigler-Najjar syndrome using hiPSC-derived cortical organoids to investigate BF-induced neurotoxicity

Severe hyperbilirubinemia due to a deficient bilirubin conjugation mechanism can progress into kernicterus or bilirubin encephalopathy (BIND) (Gazzin & Tiribelli, 2011). CNS is a rare hereditary hyperbilirubinemic condition, consisting mutation in the UGT1A1 encoding gene resulting in defective UGT1A1 enzymatic activity, and existing models mentioned in chapter 1.2.8, 3.1, and 4.1 cannot precisely recapitulate the human condition. Therefore, this work aimed to establish a human-derived potential 3D *in vitro* UGT1A1 mutation harbouring CNS model, to investigate BF-induced effects in the developing human brain.

In this study, a healthy individual- and a CNS patient-derived iPSCs were differentiated into self-patterned 3D cortical organoids and the neural features of the generated cortical organoids were confirmed with the presence of neuronal markers MAP2 (microtubule-associated protein 2), DCX (doublecortin), and TUJ1 (beta-3-tubulin) expression (Bohndorf et al., 2017; Graffmann et al., 2021). To confirm that organoids generated from the CNS patient iPSCs harboured the UGT1A1 mutation, which is a crucial feature for modelling CNS, iPSCs were also differentiated to hepatocyte-like cells which retained defective UGT1A1 expression. BIND was induced in day 20 cortical organoids (both cell lines) with 200 nM BF exposure for 72 h. Analyses at 24 and 72 h post-treatment showed increased mRNA expression and secretion levels of the pro-inflammatory cytokines IL-6, IL-8, and TNF-α along with other pro- and anti-inflammatory cytokines indicating the onset or initiation of BF-induced neuro-inflammation in the cortical organoids of both cell lines. During brain injury, nerve cell responses are significantly regulated by cytokines, and BF enhances cytokine release to cause bilirubin neurotoxicity (Allan & Rothwell, 2001; Palmela et al., 2011). Although microglia is the primary immune cell type for the CNS[#], previous studies reported neurons also secrete inflammatory cytokines (in lower level) such as IL-6, TNF- α, and IL-1β (Fernandes et al., 2006; Gazzin & Tiribelli, 2011). 24 h post BF treatment, the patient-organoids showed increased IL- 6 and IL-8 mRNA expression and protein secretion, which decreased at 72 h. Secretome analysis revealed that secretion levels of anti-inflammatory proteins: IL-10 and IL-13 were enhanced at 72 h, which might suppress IL-6 and IL-8 secretion at 72 h mimicking the *in vivo* like cellular defence mechanism after BF induced cellular stress (Zhang & An, 2007). Furthermore, increased IL-1β secretion was observed only in patient organoids at 24 h, whereas IL-1ra (IL-1 receptor antagonist) secretion was increased at 72 h for both healthy- and patient-organoids.

Since IL-1ra is a natural IL-1β inhibitor and has anti-inflammatory effects, elevated IL-1ra level might have antagonized cytokine-mediated inflammatory responses to recommence the normal condition at 72 h (Jeanjean et al., 1995; Schweizer et al., 1988). Pro- and anti-inflammatory cytokine expression profiles upon BF treatment pointed towards initiation of BF-induced inflammatory responses at 24 h in the patient organoids and thus earlier than in the healthy organoids where inflammation initiated at 72 h. It gradually decreased to normal levels in patient organoids at 72 h establishing homeostasis. In parallel, in the healthy organoids elevated *IL-8* mRNA expression was observed only at 24 h upon BF stimulation, while IL-8 protein secretion was increased only at 72 h. Contrarily, IL-6 protein secretion levels were increased at both time points, however *IL-6* mRNA expression was enhanced only at 72 h after BF treatment. Additionally, TNF-*α* showed a slight increase both in secretome and mRNA expression only in the patient-organoids. The observed pattern of mRNA expression and protein secretion in our data induced a slight temporal shift in mRNA and protein expression as an indication of distinct cellular response to stress to induce inflammation in the CNS[#]. Although BF treatment instigated inflammatory response in the patient organoids earlier (at 24 h) than in the healthy organoids, the overall secretome profile indicated profound neuro-inflammation upon BF exposure in both healthy and diseased organoids by portraying a pro-inflammatory CNS[#] environment with variable cytokine secretion. While healthy organoids showed inflammatory response at 72 h, the inflammatory response in the patient organoids decreased at that time point compared to the observation at 24 h which can be interpreted as cellular defence upon BF-induced stress in these organoids.

A global overview of the molecular effects of BF was assessed in this study with microarray-based transcriptome analysis. KEGG-associated pathway analysis based on the uniquely expressed gene sets upon BF treatment in both healthy- and patient- organoids (compared to their corresponding controls) commonly showed activation of the cytokine–cytokine receptor interaction, calcium-signalling pathway, MAPK signalling, and neuroactive ligand-receptor interaction. These pathways and associated GO-BP (Gene Ontology-biological process) terms were not activated in the healthy organoids at 24 h, rather only at 72 h, indicating a delayed initiation of inflammation in the healthy organoids. Contrarily, in the patient-organoids, BF treatment activated those mentioned pathways at both 24 h and 72 h, implying patient organoids to show an accelerated response to instigate inflammatory response upon BF exposure (Bassani et al., 2015). The initiation of inflammation in the patient organoids were

further confirmed with increased mRNA expression of associated genes such as *TNFSF12* (TNF superfamily member 12), *AZI2* (5-azacytidine induced 2), and *MyD88* (myeloid differentiation primary response protein) and activation of NFκB, PI3K, and chemokine signalling pathways according to GO-BP terms (Bassani et al., 2015; Bayer & Alcaide, 2021; Fukasaka et al., 2013; Kim et al., 2004). Furthermore, GO-BP terms analyses of the uniquely expressed gene sets showed that at 72 h treated conditions BF activated positive regulation of NFκB transcription factor activity (*AR*, *TRADD*, and *RPS6KA4*) in the patient organoids and NLRP3 (NLR family pyrin domain-containing 3) inflammasome complex assembly (*GBP5* and *NLRP3*) in the healthy organoids. Additionally, GO-BP terms of the common gene sets (between control and treated conditions) demonstrated differential upregulation of neurodevelopmental pathways in both healthy and patient organoids at 72 h post-BF treatment.

In KEGG pathway analysis of the common set of genes, BF treated healthy organoids showed upregulation of DNA damage-repair related pathways such as p53 signalling, Fanconi anemia pathway and homologous recombination at 24 h, while these pathways were downregulated in the patient organoids at the same time point. DNA damage-repair and apoptosis-associated genes: *p53* (tumor protein P53), *BCL2* (B-cell lymphoma 2), *ATM* (ataxia telangiectasia mutated), *ATR* (ataxia telangiectasia and Rad3-related protein), *CHEK1* (checkpoint kinase 1), and *CHEK2* also showed increased mRNA expression in the BF treated healthy organoids compared to the patient organoids. 24 h post treatment, both BF treated organoids (healthy and patient) demonstrated increased cell death. Healthy organoids showed higher apoptotic markers (TUNEL and cleaved caspase 3) *and* γH2AX expression levels than the patient organoids, whereas necroptosis associated genes (*XIAP*, *TRAF2*, *TRAF5*, *STAT1*, *STAT2*, *STAT3*, *STAT4*, *JAK2*, *BIRC3*, *BIRC5*, and *BIRC6*) were upregulated in the patient organoids, indicating rescued apoptosis but necroptosis mediated enhanced inflammatory responses (Duodu et al., 2022; Lalani et al., 2018; Perner et al., 2019; Vucic, 2018). In brief, healthy organoids responded with enhanced apoptotic cell death and DNA damage-repair-related gene expression at 24 h upon BF exposure, and later followed into activation of inflammatory-related pathways at 72 h. In contrast to the healthy organoids, patient organoids did not show increased DNA damage-repair mechanisms, rather leaned towards instigating inflammatory responses at 24 h, which further reduced at 72 h.

In summary, a novel human iPSC-derived 3D CNS model was successfully generated confirming initiation of neuro-inflammatory responses upon BF treatment with activation of

inflammation associated pathways and increased pro-inflammatory cytokine expressions. The patient organoids initiated inflammation at 24 h upon BF exposure, which then decreased at 72 h, whereas the healthy organoids showed enhanced cell death and DNA damage-repair related gene expression at 24 h post-BF treatment and then the activation of inflammatory-related pathways at 72 h. Conversely, the patient organoids did not manifest increased DNA damage and repair-related gene expression upon BF treatment, but increased cell death was observed at 24 h BF treated condition. Although both healthy and patient organoids manifested BF-induced inflammatory responses, they indicated a switch or shift in the initiation of inflammation and other cascade of cellular events such as cell death and DNA damage-repair after treating with BF. This model held some limitations with the lack of appropriate immune responsive cells, more neural cell types, and BBB. Further improvement (such as: controlled fluidic flow, better nutrient and oxygen delivery to cells, more cell maturation, incorporation of vascularization, and immune cells) can make this model more closely human recapitulating system (Andrews & Kriegstein, 2022; Hofer & Lutolf, 2021; Huang et al., 2021). Nevertheless, the established CNS model can be applied to study the etiology of BIND kernicterus. The hiPSC-derived CNS organoid model also pertains great potential with its applicability towards BIND-associated toxicological studies, drug screening, treatments, and therapies.

4.3 Modelling cerebral malaria using hiPSC-derived neuronal culture to investigate HMZ-induced effects on neurons

Malaria caused by *Plasmodium falciparum* infection is a public health concern, while it can lead to severe neurological complications encompassing cerebral malaria (CM). Among many of CM manifestations, impaired consciousness with coma is the most severe, while 30% surviving patients end up with neurological sequelae, exerting influence on life quality (Idro et al., 2010; Oluwayemi et al., 2013; "Severe malaria," 2014; Weiss et al., 2019). CM etiology is under-investigated, yet it is known that malaria pigment or malaria toxin- known as hemozoin (HMZ), is the principle to the *P.falciparum* pathogenesis. By releasing HMZ, *P.falciparum* can induce severe damage to neurons (Karikari et al., 2021; Polimeni & Prato, 2014). *Plasmodium* parasite doesn’t enter the brain itself, rather stays inside cerebral erythrocytes and causes BBB disruption by aggravating RBC-cytoadherence with endothelial

cells lining the BBB (Mehra et al., 2021; Schiess et al., 2020). However, depending on the model system, BBB disruption severity in CM is variable (Elsheikha & Khan, 2010; Medana & Turner, 2006; Polimeni & Prato, 2014). CM affected brain samples are difficult to obtain, making it difficult to investigate the neuro-pathogenesis of CM and the resulting neurological sequelae (Mehra et al., 2021; Schiess et al., 2020). Considering the challenges in CM investigation and the limitations of an appropriate human based experimental model for *P. falciparum* accompanied CM mentioned in paragraph 1.3.4 and 3.3, it is essential to emerge new models of CM. In this regard, human iPSCs can be used as a relevant potential tool in modelling CM *in vitro*. Hence, the aim of this study was particularly to investigate HMZ- induced cellular and molecular responses in hiPSC-derived 2D neuronal culture as an *in vitro* model of CM.

iPSCs (UM51 and B4) from two healthy ethnically diverse males were used to differentiate into 2D neuronal cultures up to day 16 (Bohndorf et al., 2017; Wang & Adjaye, 2011). Then CM was induced in those neuronal cultures using 20 µM HMZ for 48 h. Experimental and clinical malaria manifest accumulation of HMZ into tissues as a common feature, which was mimicked in iPSC-derived neuronal cultures with HMZ deposition as brown crystals inside or around the neurons (Eugenin et al., 2019; Frita et al., 2012). Neuronal identity was confirmed with the neuronal marker expressions (Beta-3-tubulin, microtubule associated protein Tau, and MAP2) in both control and HMZ treated neuronal cultures. Secretome analysis at 48 h post treatment of UM51 neuronal cultures indicated HMZ induced inflammatory response in treated neurons with an increased IL-1β, IL-8, IL-16, IFN-γ, PDGFB (platelet derived growth factor subunit B), MIF (macrophage migration inhibitory factor), MCP-1 (monocyte chemotactic protein-1), and VCAM-1 (vascular cell adhesion molecule 1) secretion. Neuro-inflammation is reported to be one of the CM-induced effects and IL-1β, IL-6, IL-8, IFN-γ, TNF-α, PECAM-1 (platelet and endothelial cell adhesion molecule 1), VCAM-1, and ICAM-1 (intercellular adhesion molecule 1) are some notable associated markers to that (Akide Ndunge et al., 2022; Brown et al., 1999; Newton & Krishna, 1998). On one hand, former studies suggested enhanced pro-inflammatory cytokines and inflammation associated proteins such as IL-8, MCP-1, IL-1β, and IL-16 to play crucial roles in CM patients to develop neurocognitive, neurodegenerative, and psychiatric disorders (Cheng et al., 2023; Di Rosa et al., 2006; Pawlowski et al., 2014). On the other hand, reduced secretion of anti-inflammatory IL-4 and IL-13 in the treated cells also indicated that HMZ induced an inflammatory response, as

continued upregulation of pro-inflammatory cytokines and insufficient production of anti-inflammatory cytokines are the features of CM pathogenesis (Waknine-Grinberg et al., 2010). Additionally, elevated secretion of the brain-derived neurotrophic factor- BDNF could be a cellular response to HMZ-induced inflammatory environment, since elevated BDNF has been reported to aid faster recovery from coma in CM patient and it plays a protective role against neuronal damage (Calabrese et al., 2014; McDonald et al., 2017). Using the identified up-and down- regulated secreted proteins upon HMZ exposure, metascape-based analysis showed enrichment of malaria, inflammatory processes, and MAPK cascade associated proteins. This observation affirmed that HMZ can activate malaria infection associated cellular processes in 2D neuronal cultures without the presence of the parasite and this hiPSC-derived *in vitro* CM model is applicable to study CM pathogenesis. Furthermore, KEGG analysis also showed malaria, MAPK signalling, neurodegeneration, and AD as associated upregulated pathways, while apoptosis and p53 signalling pathways were downregulated. On the other hand, observed downregulated pathways could potentially be a counteraction of the increased BDNF expression (both in mRNA and protein secretion), as BDNF decreases apoptosis by lowering p53 and active Caspase-3 expression in astrocytes (Harbuzariu et al., 2019; Saba et al., 2018). Furthermore, mRNA expression analysis in both cell lines based on genes associated with the upregulated KEGG pathways namely: *BDNF, CCL2 (MCP-1), PECAM1, PDGFB,* and *VEGFA (*vascular endothelial growth factor A*)*, showed an enhanced mRNA expression with the exception of the angiogenic factors, *PDGFB* and *VEGFA*, although PDGFB and VEGF were elevated in the secretome analysis. Additionally, upregulation of pro-inflammatory cytokines *TNF-α* and *IL-8* were observed in both neuronal cultures (UM51 and B4), and *IL-6* only in the UM51 neurons. *BDNF* also showed enhanced mRNA expression in both cell lines. Observed alteration in mRNA expression and protein secretion of IL-6, TNF-α, PDGFB, and VEGF could be an outcome of poor correlation between mRNA and protein synthesis (Liu et al., 2016). Overall, these observations from chemo- and cytokines represent HMZ induced inflammatory response in 2D neuronal cultures associated to CM pathogenesis.

Eventually, HMZ-induced inflammation resulted in DNA damage in the neuronal cultures of both cell lines with significant increase in γH2AX levels (Mah et al., 2010). Further analysis of DNA damage-repair and cell cycle checkpoint markers demonstrated a significant increase in mRNA expression of *ATM*, *ATR*, *CHEK1,* and *CHEK2* in both cultures, but more evidently in UM51 neurons (Harris & Levine, 2005). However, p53 transcripts were downregulated in both

cultures on mRNA level, while slightly increased on protein level. MDM2 (mouse double minute 2 homolog) is a negative regulator of p53, and FAS is a downstream target of p53 (Koster et al., 2011). Both MDM2 and FAS showed decreased mRNA and protein expression in both neuronal cultures upon HMZ treatment. Aligning with the data from KEGG analysis, the observed data from the downstream target analyses indicated the p53 pathway to be downregulated and not to be involved in stress response in this experimental setup. Additionally, total p38-MAPK protein level was increased in both cell lines, although phosphorylated p38-MAPK expression was not significantly altered upon HMZ exposure. This pointed towards p38 pathway activation in response to HMZ in the neuronal cultures. As previous studies showed upregulation of p38-MAPK in *P. falciparum* infected patient's peripheral blood mononuclear cells and p38-MAPK gets activated in response to DNA damage via ATM, these observations point p38-MAPK to be involved in alleviating cellular response to *P. falciparum* and HMZ (Hu, 2013; Polimeni et al., 2012).

Overall, this study provided insights into the involved molecules and pathways that mediate neuronal response to HMZ. It was demonstrated that HMZ-induced inflammatory response is a key cellular response in neuronal cultures which consequently caused DNA damage to the neurons. An inflammatory environment with pro- and anti-inflammatory chemo- and cytokine modulation in the neuronal cultures upon HMZ treatment was shown, whereas IL-16 seemed to be uniquely associated with CM. The basic cellular model used in this study can further be improved with hiPSC-derived brain organoids comprising astrocytes, microglia, oligodendrocytes, and vascular units which could help solving some of the mentioned limitations of the system and could model CM pathogenesis in a more human recapitulating system. Nevertheless, human iPSC-derived 2D neuronal cultures can be used as a robust CM model to study the pathogenesis, toxicological studies, drug testing, and therapies.

5. Conclusion

The current knowledge on CNS and CM pathogenesis is still limited. Most of the existing research has been performed in animal models, which carry interspecies differences. This thesis provides insights into how human iPSC-derived 2D and 3D neuronal models can serve as prospective platforms for investigating the etiology underlying BIND kernicterus and CM. Firstly, an elaborated assessment of the existing and emerging BIND models gave an explicit depiction of the current state of the art, advancements, and challenges faced by various models in disease modelling. Concomitantly, the possibilities to employ hiPSC-derived 3D brain organoids as a potential tool for research and future clinical applications with toxicological studies, drug screening, and therapeutics development were also discussed. In this thesis, CNS and CM were successfully modelled along with gaining deeper understanding of the disease mechanisms utilizing hiPSC-derived neurons and brain organoids. In the cortical organoid model of CNS, BF stimulated neuro-inflammation for both healthy and patient organoids, however the patient organoids instigated earlier inflammatory response than the healthy organoids. Additionally, the findings revealed molecular insights into BF-induced neuro-inflammation with the activation of distinct inflammatory pathways and genes resulting in cell death, DNA damage-repair, or inflammation. It was also demonstrated that another toxin- HMZ induced inflammatory responses in a comparable manner to clinical *falciparum* malaria in the hiPSC-derived neuronal culture model of CM, confirming this model to be an alternative to rodent experimental models of CM. CM modelling also unveiled HMZ exposure to activate molecules and pathways similar to that observed in CM along with causing DNA damage to the neurons. Besides, both CNS and CM models showed a profound inflammatory environment in the neurons of the developing human brain with the pro- and anti-inflammatory chemo- and cytokine profiles.

Taken together, both 2D and 3D approaches of iPSC-application in disease modelling have shown an improvement to the existing encephalopathy models with regards to investigating brain dysfunction *in vitro*. Additionally, this thesis provides more insights into BIND kernicterus and CM etiology on a cellular and molecular level, emphasizing that human iPSC-derived 3D brain organoid model and 2D neuronal cultures can serve as prospective platforms for studying distinct brain dysfunction and associated neurological disorders.

6. References

Abu-Dawud, R., Graffmann, N., Ferber, S., Wruck, W., & Adjaye, J. (2018). Pluripotent stem cells: induction and self-renewal. *Philos Trans R Soc Lond B Biol Sci*, *373*(1750). https://doi.org/10.1098/rstb.2017.0213

Adams, Y., & Jensen, A. R. (2022). Cerebral malaria - modelling interactions at the blood-brain barrier in vitro. *Dis Model Mech*, *15*(7). https://doi.org/10.1242/dmm.049410

Afanasyeva, T. A. V., Corral-Serrano, J. C., Garanto, A., Roepman, R., Cheetham, M. E., & Collin, R. W. J. (2021). A look into retinal organoids: methods, analytical techniques, and applications. *Cell Mol Life Sci*, *78*(19-20), 6505-6532. https://doi.org/10.1007/s00018-021-03917-4

Ahdab-Barmada, M. (2000). *The neuropathology of kernicterus: definitions and debate* (W. J. F. Maisels M. J., In Neonatal Jaundice, Ed.). Harwood Academic Publishers.

Ahdab-Barmada, M., & Moossy, J. (1984). The neuropathology of kernicterus in the premature neonate: diagnostic problems. *J Neuropathol Exp Neurol*, *43*(1), 45-56. https://doi.org/10.1097/00005072-198401000-00004

Akide Ndunge, O. B., Kilian, N., & Salman, M. M. (2022). Cerebral Malaria and Neuronal Implications of Plasmodium Falciparum Infection: From Mechanisms to Advanced Models. *Adv Sci (Weinh)*, *9*(36), e2202944. https://doi.org/10.1002/advs.202202944

Albrecht-Schgoer, K., Lackner, P., Schmutzhard, E., & Baier, G. (2022). Cerebral Malaria: Current Clinical and Immunological Aspects. *Front Immunol*, *13*, 863568. https://doi.org/10.3389/fimmu.2022.863568

Allan, S. M., & Rothwell, N. J. (2001). Cytokines and acute neurodegeneration. *Nat Rev Neurosci*, *2*(10), 734-744. https://doi.org/10.1038/35094583

Almeqdadi, M., Mana, M. D., Roper, J., & Yilmaz, O. H. (2019). Gut organoids: mini-tissues in culture to study intestinal physiology and disease. *Am J Physiol Cell Physiol*, *317*(3), C405-C419. https://doi.org/10.1152/ajpcell.00300.2017

Ambrosino, G., Varotto, S., Strom, S. C., Guariso, G., Franchin, E., Miotto, D., Caenazzo, L., Basso, S., Carraro, P., Valente, M. L., D'Amico, D., Zancan, L., & D'Antiga, L. (2005). Isolated hepatocyte transplantation for Crigler-Najjar syndrome type 1. *Cell Transplant*, *14*(2-3), 151-157. https://doi.org/10.3727/000000005783983250

Amin, S. B., Prinzing, D., & Myers, G. (2009). Hyperbilirubinemia and language delay in premature infants. *Pediatrics*, *123*(1), 327-331. https://doi.org/10.1542/peds.2007-3723

Amin, S. B., Smith, T., & Timler, G. (2019). Developmental influence of unconjugated hyperbilirubinemia and neurobehavioral disorders. *Pediatr Res*, *85*(2), 191-197. https://doi.org/10.1038/s41390-018-0216-4

Amini, N., Vousooghi, N., Soleimani, M., Samadikuchaksaraei, A., Akbari, M., Safakheil, H., Atafimanesh, P., Shahbazi, A., Brouki Milan, P., Ramezani, S., Mozafari, M., & Joghataei, M. T. (2017). A new rat model of neonatal bilirubin encephalopathy (kernicterus). *J Pharmacol Toxicol Methods*, *84*, 44-50. https://doi.org/10.1016/j.vascn.2016.10.002

Amino, R., Menard, R., & Frischknecht, F. (2005). In vivo imaging of malaria parasites--recent advances and future directions. *Curr Opin Microbiol*, *8*(4), 407-414. https://doi.org/10.1016/j.mib.2005.06.019

Andrews, M. G., & Kriegstein, A. R. (2022). Challenges of Organoid Research. *Annu Rev Neurosci*, *45*, 23-39. https://doi.org/10.1146/annurev-neuro-111020-090812

Auclair, C., Hakim, J., Boivin, P., Troube, H., & Boucherot, J. (1976). Bilirubin and paranitrophenol glucuronyl transferase activities of the liver in patients with Gilbert's syndrome An attempt at a biochemical breakdown of the Gilbert's syndrome. *Enzyme*, *21*(2), 97-107. https://doi.org/10.1159/000458848

Aziz, S., Kotal, P., Leroy, P., Servaes, R., Eggermont, E., & Fevery, J. (2001). Bilirubin-IXalpha and -IXbeta pigments, coproporphyrins and bile acids in meconium and stools from full-term and preterm neonates during the first month of life. *Acta Paediatr*, *90*(1), 81-87. https://doi.org/10.1080/080352501750064923

Bassani, T. B., Vital, M. A., & Rauh, L. K. (2015). Neuroinflammation in the pathophysiology of Parkinson's disease and therapeutic evidence of anti-inflammatory drugs. *Arq Neuropsiquiatr*, *73*(7), 616-623. https://doi.org/10.1590/0004-282X20150057

Bayer, A. L., & Alcaide, P. (2021). MyD88: At the heart of inflammatory signaling and cardiovascular disease. *J Mol Cell Cardiol*, *161*, 75-85. https://doi.org/10.1016/j.yjmcc.2021.08.001

Beattie, R., & Hippenmeyer, S. (2017). Mechanisms of radial glia progenitor cell lineage progression. *FEBS Lett*, *591*(24), 3993-4008. https://doi.org/10.1002/1873-3468.12906

Bergmann, S., Lawler, S. E., Qu, Y., Fadzen, C. M., Wolfe, J. M., Regan, M. S., Pentelute, B. L., Agar, N. Y. R., & Cho, C. F. (2018). Blood-brain-barrier organoids for investigating the permeability of CNS therapeutics. *Nat Protoc*, *13*(12), 2827-2843. https://doi.org/10.1038/s41596-018-0066-x

Bhandari, J., Thada, P. K., & Yadav, D. (2024). Crigler-Najjar Syndrome. In *StatPearls*. https://www.ncbi.nlm.nih.gov/pubmed/32965842

Bhutani, V. K., Zipursky, A., Blencowe, H., Khanna, R., Sgro, M., Ebbesen, F., Bell, J., Mori, R., Slusher, T. M., Fahmy, N., Paul, V. K., Du, L., Okolo, A. A., de Almeida, M. F., Olusanya, B. O., Kumar, P., Cousens, S., & Lawn, J. E. (2013). Neonatal hyperbilirubinemia and Rhesus disease of the newborn: incidence and impairment estimates for 2010 at regional and global levels. *Pediatr Res*, *74 Suppl 1*(Suppl 1), 86-100. https://doi.org/10.1038/pr.2013.208

Birey, F., Andersen, J., Makinson, C. D., Islam, S., Wei, W., Huber, N., Fan, H. C., Metzler, K. R. C., Panagiotakos, G., Thom, N., O'Rourke, N. A., Steinmetz, L. M., Bernstein, J. A., Hallmayer, J., Huguenard, J. R., & Pasca, S. P. (2017). Assembly of functionally integrated human forebrain spheroids. *Nature*, *545*(7652), 54-59. https://doi.org/10.1038/nature22330

Birraux, J., Menzel, O., Wildhaber, B., Jond, C., Nguyen, T. H., & Chardot, C. (2009). A step toward liver gene therapy: efficient correction of the genetic defect of hepatocytes isolated from a patient with Crigler-Najjar syndrome type 1 with lentiviral vectors. *Transplantation*, *87*(7), 1006-1012. https://doi.org/10.1097/TP.0b013e31819ca245

Bohndorf, M., Ncube, A., Spitzhorn, L. S., Enczmann, J., Wruck, W., & Adjaye, J. (2017). Derivation and characterization of integration-free iPSC line ISRM-UM51 derived from SIX2-positive renal cells isolated from urine of an African male expressing the CYP2D6 *4/*17 variant which confers

intermediate drug metabolizing activity. *Stem Cell Res*, *25*, 18-21. https://doi.org/10.1016/j.scr.2017.10.004

Bonnier, F., Keating, M. E., Wróbel, T. P., Majzner, K., Baranska, M., Garcia-Munoz, A., Blanco, A., & Byrne, H. J. (2015). Cell viability assessment using the Alamar blue assay: a comparison of 2D and 3D cell culture models. *Toxicol In Vitro*, *29*(1), 124-131. https://doi.org/10.1016/j.tiv.2014.09.014

Bortolussi, G., Baj, G., Vodret, S., Viviani, G., Bittolo, T., & Muro, A. F. (2014). Age-dependent pattern of cerebellar susceptibility to bilirubin neurotoxicity in vivo in mice. *Dis Model Mech*, *7*(9), 1057-1068. https://doi.org/10.1242/dmm.016535

Bortolussi, G., & Muro, A. F. (2018). Advances in understanding disease mechanisms and potential treatments for Crigler–Najjar syndrome. *Expert Opinion on Orphan Drugs*, *6*(7), 425-439. https://doi.org/10.1080/21678707.2018.1495558

Bortolussi, G., & Muro, A. F. (2020). Experimental models assessing bilirubin neurotoxicity. *Pediatr Res*, *87*(1), 17-25. https://doi.org/10.1038/s41390-019-0570-x

Bortolussi, G., Zentilin, L., Baj, G., Giraudi, P., Bellarosa, C., Giacca, M., Tiribelli, C., & Muro, A. F. (2012). Rescue of bilirubin-induced neonatal lethality in a mouse model of Crigler-Najjar syndrome type I by AAV9-mediated gene transfer. *FASEB J*, *26*(3), 1052-1063. https://doi.org/10.1096/fj.11-195461

Bozhilov, Y. K., Hsu, I., Brown, E. J., & Wilkinson, A. C. (2023). In Vitro Human Haematopoietic Stem Cell Expansion and Differentiation. *Cells*, *12*(6). https://doi.org/10.3390/cells12060896

Bras, J., Henriques, D., Moreira, R., Santana, M. M., Silva-Pedrosa, R., Adao, D., Braz, S., Alvaro, A. R., de Almeida, L. P., & Mendonca, L. S. (2022). Establishment and characterization of human pluripotent stem cells-derived brain organoids to model cerebellar diseases. *Sci Rep*, *12*(1), 12513. https://doi.org/10.1038/s41598-022-16369-y

Brites, D. (2011). Bilirubin injury to neurons and glial cells: new players, novel targets, and newer insights. *Semin Perinatol*, *35*(3), 114-120. https://doi.org/10.1053/j.semperi.2011.02.004

Brites, D. (2012). The evolving landscape of neurotoxicity by unconjugated bilirubin: role of glial cells and inflammation. *Front Pharmacol*, *3*, 88. https://doi.org/10.3389/fphar.2012.00088

Brites, D., & Fernandes, A. (2015). Bilirubin-induced neural impairment: a special focus on myelination, age-related windows of susceptibility and associated co-morbidities. *Semin Fetal Neonatal Med*, *20*(1), 14-19. https://doi.org/10.1016/j.siny.2014.12.002

Brito, M. A., Pereira, P., Barroso, C., Aronica, E., & Brites, D. (2013). New autopsy findings in different brain regions of a preterm neonate with kernicterus: neurovascular alterations and up-regulation of efflux transporters. *Pediatr Neurol*, *49*(6), 431-438. https://doi.org/10.1016/j.pediatrneurol.2013.08.020

Brown, H., Turner, G., Rogerson, S., Tembo, M., Mwenechanya, J., Molyneux, M., & Taylor, T. (1999). Cytokine expression in the brain in human cerebral malaria. *J Infect Dis*, *180*(5), 1742-1746. https://doi.org/10.1086/315078

Cai, J. S., & Chen, J. H. (2014). The mechanism of enterohepatic circulation in the formation of gallstone disease. *J Membr Biol*, *247*(11), 1067-1082. https://doi.org/10.1007/s00232-014-9715-3

Calabrese, F., Rossetti, A. C., Racagni, G., Gass, P., Riva, M. A., & Molteni, R. (2014). Brain-derived neurotrophic factor: a bridge between inflammation and neuroplasticity. *Front Cell Neurosci*, *8*, 430. https://doi.org/10.3389/fncel.2014.00430

Calligaris, R., Bellarosa, C., Foti, R., Roncaglia, P., Giraudi, P., Krmac, H., Tiribelli, C., & Gustincich, S. (2009). A transcriptome analysis identifies molecular effectors of unconjugated bilirubin in human neuroblastoma SH-SY5Y cells. *BMC Genomics*, *10*, 543. https://doi.org/10.1186/1471-2164-10-543

Calligaris, S., Cekic, D., Roca-Burgos, L., Gerin, F., Mazzone, G., Ostrow, J. D., & Tiribelli, C. (2006). Multidrug resistance associated protein 1 protects against bilirubin-induced cytotoxicity. *FEBS Lett*, *580*(5), 1355-1359. https://doi.org/10.1016/j.febslet.2006.01.056

Camp, J. G., Badsha, F., Florio, M., Kanton, S., Gerber, T., Wilsch-Brauninger, M., Lewitus, E., Sykes, A., Hevers, W., Lancaster, M., Knoblich, J. A., Lachmann, R., Paabo, S., Huttner, W. B., & Treutlein, B. (2015). Human cerebral organoids recapitulate gene expression programs of fetal neocortex development. *Proc Natl Acad Sci U S A*, *112*(51), 15672-15677. https://doi.org/10.1073/pnas.1520760112

Canals, I., Quist, E., & Ahlenius, H. (2021). Transcription Factor-Based Strategies to Generate Neural Cell Types from Human Pluripotent Stem Cells. *Cell Reprogram*, *23*(4), 206-220. https://doi.org/10.1089/cell.2021.0045

Canu, G., Minucci, A., Zuppi, C., & Capoluongo, E. (2013). Gilbert and Crigler Najjar syndromes: an update of the UDP-glucuronosyltransferase 1A1 (UGT1A1) gene mutation database. *Blood Cells Mol Dis*, *50*(4), 273-280. https://doi.org/10.1016/j.bcmd.2013.01.003

Carey, R., & Balisteri, W. (2011). *Inherited deficient conjugation of bilirubin (familial nonhemolytic unconjugated hyperbilirubinemia)* (S. B. Kliegman RM, Schol NF, St Geme III JW, Behrman RE in Nelson Textbook of Pediatrics, Ed. 19th ed.). Philadelphia: Elsevier.

Carter, J. A., Mung'ala-Odera, V., Neville, B. G., Murira, G., Mturi, N., Musumba, C., & Newton, C. R. (2005). Persistent neurocognitive impairments associated with severe falciparum malaria in Kenyan children. *J Neurol Neurosurg Psychiatry*, *76*(4), 476-481. https://doi.org/10.1136/jnnp.2004.043893

Chang, F. Y., Lee, C. C., Huang, C. C., & Hsu, K. S. (2009). Unconjugated bilirubin exposure impairs hippocampal long-term synaptic plasticity. *PLoS One*, *4*(6), e5876. https://doi.org/10.1371/journal.pone.0005876

Chang, T., Zheng, W., Tsark, W., Bates, S., Huang, H., Lin, R. J., & Yee, J. K. (2011). Brief report: phenotypic rescue of induced pluripotent stem cell-derived motoneurons of a spinal muscular atrophy patient. *Stem Cells*, *29*(12), 2090-2093. https://doi.org/10.1002/stem.749

Cheng, X., Xie, Y., Wang, A., Zhu, C., Yan, F., Pei, W., & Zhang, X. (2023). Correlation between elevated serum interleukin-1beta, interleukin-16 levels and psychiatric symptoms in patients with schizophrenia at different stages. *BMC Psychiatry*, *23*(1), 396. https://doi.org/10.1186/s12888-023-04896-5

Ciarpella, F., Zamfir, R. G., Campanelli, A., Ren, E., Pedrotti, G., Bottani, E., Borioli, A., Caron, D., Di Chio, M., Dolci, S., Ahtiainen, A., Malpeli, G., Malerba, G., Bardoni, R., Fumagalli, G., Hyttinen, J., Bifari, F., Palazzolo, G., Panuccio, G., . . . Decimo, I. (2021). Murine cerebral organoids develop network of functional neurons and hippocampal brain region identity. *iScience*, *24*(12), 103438. https://doi.org/10.1016/j.isci.2021.103438

Collaud, F., Bortolussi, G., Guianvarc'h, L., Aronson, S. J., Bordet, T., Veron, P., Charles, S., Vidal, P., Sola, M. S., Rundwasser, S., Dufour, D. G., Lacoste, F., Luc, C., Wittenberghe, L. V., Martin, S., Le Bec, C., Bosma, P. J., Muro, A. F., Ronzitti, G., . . . Mingozzi, F. (2019). Preclinical Development of an AAV8-hUGT1A1 Vector for the Treatment of Crigler-Najjar Syndrome. *Mol Ther Methods Clin Dev*, *12*, 157-174. https://doi.org/10.1016/j.omtm.2018.12.011

Corro, C., Novellasdemunt, L., & Li, V. S. W. (2020). A brief history of organoids. *Am J Physiol Cell Physiol*, *319*(1), C151-C165. https://doi.org/10.1152/ajpcell.00120.2020

CRIGLER-NAJJAR SYNDROME. Retrieved 29 April, 2024 from http://criglernajjar.altervista.org/tre.htm

Dal Ben, M., Bottin, C., Zanconati, F., Tiribelli, C., & Gazzin, S. (2017). Evaluation of region selective bilirubin-induced brain damage as a basis for a pharmacological treatment. *Sci Rep*, *7*, 41032. https://doi.org/10.1038/srep41032

Dani, C., Pratesi, S., Ilari, A., Lana, D., Giovannini, M. G., Nosi, D., Buonvicino, D., Landucci, E., Bani, D., Mannaioni, G., & Gerace, E. (2019). Neurotoxicity of Unconjugated Bilirubin in Mature and Immature Rat Organotypic Hippocampal Slice Cultures. *Neonatology*, *115*(3), 217-225. https://doi.org/10.1159/000494101

de Wert, G., & Mummery, C. (2003). Human embryonic stem cells: research, ethics and policy. *Hum Reprod*, *18*(4), 672-682. https://doi.org/10.1093/humrep/deg143

Di Rosa, M., Dell'Ombra, N., Zambito, A. M., Malaguarnera, M., Nicoletti, F., & Malaguarnera, L. (2006). Chitotriosidase and inflammatory mediator levels in Alzheimer's disease and cerebrovascular dementia. *Eur J Neurosci*, *23*(10), 2648-2656. https://doi.org/10.1111/j.1460-9568.2006.04780.x

Dorovini-Zis, K., Prameya, R., & Bowman, P. D. (1991). Culture and characterization of microvascular endothelial cells derived from human brain. *Lab Invest*, *64*(3), 425-436. https://www.ncbi.nlm.nih.gov/pubmed/2002659

Drews, K., Jozefczuk, J., Prigione, A., & Adjaye, J. (2012). Human induced pluripotent stem cells--from mechanisms to clinical applications. *J Mol Med (Berl)*, *90*(7), 735-745. https://doi.org/10.1007/s00109-012-0913-0

Dunst, J., Kamena, F., & Matuschewski, K. (2017). Cytokines and Chemokines in Cerebral Malaria Pathogenesis. *Front Cell Infect Microbiol*, *7*, 324. https://doi.org/10.3389/fcimb.2017.00324

Duodu, P., Sosa, G., Canar, J., Chhugani, O., & Gamero, A. M. (2022). Exposing the Two Contrasting Faces of STAT2 in Inflammation. *J Interferon Cytokine Res*, *42*(9), 467-481. https://doi.org/10.1089/jir.2022.0117

Duval, K., Grover, H., Han, L. H., Mou, Y., Pegoraro, A. F., Fredberg, J., & Chen, Z. (2017). Modeling Physiological Events in 2D vs. 3D Cell Culture. *Physiology (Bethesda)*, *32*(4), 266-277. https://doi.org/10.1152/physiol.00036.2016

Edmondson, R., Broglie, J. J., Adcock, A. F., & Yang, L. (2014). Three-dimensional cell culture systems and their applications in drug discovery and cell-based biosensors. *Assay Drug Dev Technol*, *12*(4), 207-218. https://doi.org/10.1089/adt.2014.573

Elsheikha, H. M., & Khan, N. A. (2010). Protozoa traversal of the blood-brain barrier to invade the central nervous system. *FEMS Microbiol Rev*, *34*(4), 532-553. https://doi.org/10.1111/j.1574-6976.2010.00215.x

Encephalopathy. (2023). Cleveland Clinic. Retrieved 28 April, 2024 from https://my.clevelandclinic.org/health/diseases/encephalopathy

Ennever, J. F., Costarino, A. T., Polin, R. A., & Speck, W. T. (1987). Rapid clearance of a structural isomer of bilirubin during phototherapy. *J Clin Invest*, *79*(6), 1674-1678. https://doi.org/10.1172/JCI113006

Erkkinen, M. G., & Berkowitz, A. L. (2019). A Clinical Approach to Diagnosing Encephalopathy. *Am J Med*, *132*(10), 1142-1147. https://doi.org/10.1016/j.amjmed.2019.07.001

Erlinger, S., Arias, I. M., & Dhumeaux, D. (2014). Inherited disorders of bilirubin transport and conjugation: new insights into molecular mechanisms and consequences. *Gastroenterology*, *146*(7), 1625-1638. https://doi.org/10.1053/j.gastro.2014.03.047

Erratum. (2015). *Organogenesis*, *11*(2), 93. https://doi.org/10.1080/15476278.2015.1063374

Eugenin, E. A., Martiney, J. A., & Berman, J. W. (2019). The malaria toxin hemozoin induces apoptosis in human neurons and astrocytes: Potential role in the pathogenesis of cerebral malaria. *Brain Res*, *1720*, 146317. https://doi.org/10.1016/j.brainres.2019.146317

Evans, D. (2007). Neonatal jaundice. *BMJ Clin Evid*, *2007*. https://www.ncbi.nlm.nih.gov/pubmed/19454091

Evans, M. (1981). Origin of mouse embryonal carcinoma cells and the possibility of their direct isolation into tissue culture. *J Reprod Fertil*, *62*(2), 625-631. https://doi.org/10.1530/jrf.0.0620625

Evans, M. J., & Kaufman, M. H. (1981). Establishment in culture of pluripotential cells from mouse embryos. *Nature*, *292*(5819), 154-156. https://doi.org/10.1038/292154a0

Falcao, A. S., Silva, R. F., Vaz, A. R., Silva, S. L., Fernandes, A., & Brites, D. (2013). Cross-talk between neurons and astrocytes in response to bilirubin: early beneficial effects. *Neurochem Res*, *38*(3), 644-659. https://doi.org/10.1007/s11064-012-0963-2

Fargo, M. V., Grogan, S. P., & Saguil, A. (2017). Evaluation of Jaundice in Adults. *Am Fam Physician*, *95*(3), 164-168. https://www.ncbi.nlm.nih.gov/pubmed/28145671

Fernandes, A., Falcao, A. S., Abranches, E., Bekman, E., Henrique, D., Lanier, L. M., & Brites, D. (2009). Bilirubin as a determinant for altered neurogenesis, neuritogenesis, and synaptogenesis. *Dev Neurobiol*, *69*(9), 568-582. https://doi.org/10.1002/dneu.20727

Fernandes, A., Falcao, A. S., Silva, R. F., Gordo, A. C., Gama, M. J., Brito, M. A., & Brites, D. (2006). Inflammatory signalling pathways involved in astroglial activation by unconjugated bilirubin. *J Neurochem*, *96*(6), 1667-1679. https://doi.org/10.1111/j.1471-4159.2006.03680.x

Fernandes, A., Silva, R. F., Falcao, A. S., Brito, M. A., & Brites, D. (2004). Cytokine production, glutamate release and cell death in rat cultured astrocytes treated with unconjugated bilirubin and LPS. *J Neuroimmunol*, *153*(1-2), 64-75. https://doi.org/10.1016/j.jneuroim.2004.04.007

Fevery, J. (2008). Bilirubin in clinical practice: a review. *Liver Int*, *28*(5), 592-605. https://doi.org/10.1111/j.1478-3231.2008.01716.x

Fevery, J., Van de Vijver, M., Michiels, R., & Heirwegh, K. P. (1977). Comparison in different species of biliary bilirubin-IX alpha conjugates with the activities of hepatic and renal bilirubin-IX alpha-

uridine diphosphate glycosyltransferases. *Biochem J*, *164*(3), 737-746. https://doi.org/10.1042/bj1640737

Fietz, S. A., Kelava, I., Vogt, J., Wilsch-Brauninger, M., Stenzel, D., Fish, J. L., Corbeil, D., Riehn, A., Distler, W., Nitsch, R., & Huttner, W. B. (2010). OSVZ progenitors of human and ferret neocortex are epithelial-like and expand by integrin signaling. *Nat Neurosci*, *13*(6), 690-699. https://doi.org/10.1038/nn.2553

Flaherman, V. J., Kuzniewicz, M. W., Escobar, G. J., & Newman, T. B. (2012). Total serum bilirubin exceeding exchange transfusion thresholds in the setting of universal screening. *J Pediatr*, *160*(5), 796-800 e791. https://doi.org/10.1016/j.jpeds.2011.09.063

Francis, S. E., Sullivan, D. J., Jr., & Goldberg, D. E. (1997). Hemoglobin metabolism in the malaria parasite Plasmodium falciparum. *Annu Rev Microbiol*, *51*, 97-123. https://doi.org/10.1146/annurev.micro.51.1.97

Frankenberg, S. R., de Barros, F. R., Rossant, J., & Renfree, M. B. (2016). The mammalian blastocyst. *Wiley Interdiscip Rev Dev Biol*, *5*(2), 210-232. https://doi.org/10.1002/wdev.220

Frita, R., Carapau, D., Mota, M. M., & Hanscheid, T. (2012). In Vivo Hemozoin Kinetics after Clearance of Plasmodium berghei Infection in Mice. *Malar Res Treat*, *2012*, 373086. https://doi.org/10.1155/2012/373086

Frohlich, E. (2018). Comparison of conventional and advanced in vitro models in the toxicity testing of nanoparticles. *Artif Cells Nanomed Biotechnol*, *46*(sup2), 1091-1107. https://doi.org/10.1080/21691401.2018.1479709

Fujioka, H., Millet, P., Maeno, Y., Nakazawa, S., Ito, Y., Howard, R. J., Collins, W. E., & Aikawa, M. (1994). A nonhuman primate model for human cerebral malaria: rhesus monkeys experimentally infected with Plasmodium fragile. *Exp Parasitol*, *78*(4), 371-376. https://doi.org/10.1006/expr.1994.1040

Fukasaka, M., Ori, D., Kawagoe, T., Uematsu, S., Maruyama, K., Okazaki, T., Kozaki, T., Imamura, T., Tartey, S., Mino, T., Satoh, T., Akira, S., & Takeuchi, O. (2013). Critical role of AZI2 in GM-CSF-induced dendritic cell differentiation. *J Immunol*, *190*(11), 5702-5711. https://doi.org/10.4049/jimmunol.1203155

Fusaki, N., Ban, H., Nishiyama, A., Saeki, K., & Hasegawa, M. (2009). Efficient induction of transgene-free human pluripotent stem cells using a vector based on Sendai virus, an RNA virus that does not integrate into the host genome. *Proc Jpn Acad Ser B Phys Biol Sci*, *85*(8), 348-362. https://doi.org/10.2183/pjab.85.348

Gazzin, S., Jayanti, S., & Tiribelli, C. (2023). Models of bilirubin neurological damage: lessons learned and new challenges. *Pediatr Res*, *93*(7), 1838-1845. https://doi.org/10.1038/s41390-022-02351-x

Gazzin, S., & Tiribelli, C. (2011). Bilirubin-induced neurological damage. *J Matern Fetal Neonatal Med*, *24 Suppl 1*, 154-155. https://doi.org/10.3109/14767058.2011.607590

Giandomenico, S. L., Sutcliffe, M., & Lancaster, M. A. (2021). Generation and long-term culture of advanced cerebral organoids for studying later stages of neural development. *Nat Protoc*, *16*(2), 579-602. https://doi.org/10.1038/s41596-020-00433-w

Gillrie, M. R., & Ho, M. (2017). Dynamic interactions of Plasmodium spp. with vascular endothelium. *Tissue Barriers*, *5*(1), e1268667. https://doi.org/10.1080/21688370.2016.1268667

Goranci-Buzhala, G., Mariappan, A., Gabriel, E., Ramani, A., Ricci-Vitiani, L., Buccarelli, M., D'Alessandris, Q. G., Pallini, R., & Gopalakrishnan, J. (2020). Rapid and Efficient Invasion Assay of Glioblastoma in Human Brain Organoids. *Cell Rep*, *31*(10), 107738. https://doi.org/10.1016/j.celrep.2020.107738

Gordon, A., Yoon, S. J., Tran, S. S., Makinson, C. D., Park, J. Y., Andersen, J., Valencia, A. M., Horvath, S., Xiao, X., Huguenard, J. R., Pasca, S. P., & Geschwind, D. H. (2021). Long-term maturation of human cortical organoids matches key early postnatal transitions. *Nat Neurosci*, *24*(3), 331-342. https://doi.org/10.1038/s41593-021-00802-y

Gotz, M., & Huttner, W. B. (2005). The cell biology of neurogenesis. *Nat Rev Mol Cell Biol*, *6*(10), 777-788. https://doi.org/10.1038/nrm1739

Gourley, G. R. (1997). Bilirubin metabolism and kernicterus. *Adv Pediatr*, *44*, 173-229. https://www.ncbi.nlm.nih.gov/pubmed/9265971

Graffmann, N., Martins, S., Ljubikj, T., Matte, J. C., Bohndorf, M., Wruck, W., & Adjaye, J. (2021). Generation of a Crigler-Najjar Syndrome Type I patient-derived induced pluripotent stem cell line CNS705 (HHUUKDi005-A). *Stem Cell Res*, *51*, 102167. https://doi.org/10.1016/j.scr.2021.102167

Gunn, C. K. (1944). Hereditary Acholuric Jaundice in the Rat. *Can Med Assoc J*, *50*(3), 230-237. https://www.ncbi.nlm.nih.gov/pubmed/20323028

Hadjilaou, A., Brandi, J., Riehn, M., Friese, M. A., & Jacobs, T. (2023). Pathogenetic mechanisms and treatment targets in cerebral malaria. *Nat Rev Neurol*, *19*(11), 688-709. https://doi.org/10.1038/s41582-023-00881-4

Hansen, D. V., Lui, J. H., Parker, P. R., & Kriegstein, A. R. (2010). Neurogenic radial glia in the outer subventricular zone of human neocortex. *Nature*, *464*(7288), 554-561. https://doi.org/10.1038/nature08845

Hansen, T. W. R., Maisels, M. J., Ebbesen, F., Vreman, H. J., Stevenson, D. K., Wong, R. J., & Bhutani, V. K. (2020). Sixty years of phototherapy for neonatal jaundice - from serendipitous observation to standardized treatment and rescue for millions. *J Perinatol*, *40*(2), 180-193. https://doi.org/10.1038/s41372-019-0439-1

Harbuzariu, A., Pitts, S., Cespedes, J. C., Harp, K. O., Nti, A., Shaw, A. P., Liu, M., & Stiles, J. K. (2019). Modelling heme-mediated brain injury associated with cerebral malaria in human brain cortical organoids. *Sci Rep*, *9*(1), 19162. https://doi.org/10.1038/s41598-019-55631-8

Harris, S. L., & Levine, A. J. (2005). The p53 pathway: positive and negative feedback loops. *Oncogene*, *24*(17), 2899-2908. https://doi.org/10.1038/sj.onc.1208615

Heirwegh, K. P. M., Van Hees, G.P., Blanckaert, N., Fevery, J., Compernolle, F. . (1976). *Comparative Studies on the Structures of Conjugated Bilirubin-IXα and Changes in Cholestasis.* (Vol. 7). Springer, Boston, MA. https://doi.org/https://doi.org/10.1007/978-1-4615-8900-6_16

Hofer, M., & Lutolf, M. P. (2021). Engineering organoids. *Nat Rev Mater*, *6*(5), 402-420. https://doi.org/10.1038/s41578-021-00279-y

Hoffman, G. E., Hartley, B. J., Flaherty, E., Ladran, I., Gochman, P., Ruderfer, D. M., Stahl, E. A., Rapoport, J., Sklar, P., & Brennand, K. J. (2017). Transcriptional signatures of schizophrenia in hiPSC-derived NPCs and neurons are concordant with post-mortem adult brains. *Nat Commun*, *8*(1), 2225. https://doi.org/10.1038/s41467-017-02330-5

Honar, N., Ghashghaei Saadi, E., Saki, F., Pishva, N., Shakibazad, N., & Hosseini Teshnizi, S. (2016). Effect of Ursodeoxycholic Acid on Indirect Hyperbilirubinemia in Neonates Treated With Phototherapy. *J Pediatr Gastroenterol Nutr*, *62*(1), 97-100. https://doi.org/10.1097/MPG.0000000000000874

Hora, R., Kapoor, P., Thind, K. K., & Mishra, P. C. (2016). Cerebral malaria--clinical manifestations and pathogenesis. *Metab Brain Dis*, *31*(2), 225-237. https://doi.org/10.1007/s11011-015-9787-5

Hu, W. C. (2013). Human immune responses to Plasmodium falciparum infection: molecular evidence for a suboptimal THalphabeta and TH17 bias over ideal and effective traditional TH1 immune response. *Malar J*, *12*, 392. https://doi.org/10.1186/1475-2875-12-392

Huang, H., Guo, M., Liu, N., Zhao, C., Chen, H., Wang, X., Liao, S., Zhou, P., Liao, Y., Chen, X., Lan, X., Chen, J., Xu, D., Li, X., Shi, X., Yu, L., Nie, Y., Wang, X., Zhang, C. E., & Liu, J. (2017). Bilirubin neurotoxicity is associated with proteasome inhibition. *Cell Death Dis*, *8*(6), e2877. https://doi.org/10.1038/cddis.2017.274

Huang, Y., Huang, Z., Tang, Z., Chen, Y., Huang, M., Liu, H., Huang, W., Ye, Q., & Jia, B. (2021). Research Progress, Challenges, and Breakthroughs of Organoids as Disease Models. *Front Cell Dev Biol*, *9*, 740574. https://doi.org/10.3389/fcell.2021.740574

Hwang, N. S., Zhang, C., Hwang, Y. S., & Varghese, S. (2009). Mesenchymal stem cell differentiation and roles in regenerative medicine. *Wiley Interdiscip Rev Syst Biol Med*, *1*(1), 97-106. https://doi.org/10.1002/wsbm.26

Hyman, C. B., Keaster, J., Hanson, V., Harris, I., Sedgwick, R., Wursten, H., & Wright, A. R. (1969). CNS abnormalities after neonatal hemolytic disease or hyperbilirubinemia. A prospective study of 405 patients. *Am J Dis Child*, *117*(4), 395-405. https://doi.org/10.1001/archpedi.1969.02100030397002

Idro, R., Marsh, K., John, C. C., & Newton, C. R. (2010). Cerebral malaria: mechanisms of brain injury and strategies for improved neurocognitive outcome. *Pediatr Res*, *68*(4), 267-274. https://doi.org/10.1203/PDR.0b013e3181eee738

Imaizumi, Y., & Okano, H. (2014). Modeling human neurological disorders with induced pluripotent stem cells. *J Neurochem*, *129*(3), 388-399. https://doi.org/10.1111/jnc.12625

Jawabri, K. H., & Sharma, S. (2024). Physiology, Cerebral Cortex Functions. In *StatPearls*. https://www.ncbi.nlm.nih.gov/pubmed/30860731

Jeanjean, A. P., Moussaoui, S. M., Maloteaux, J. M., & Laduron, P. M. (1995). Interleukin-1 beta induces long-term increase of axonally transported opiate receptors and substance P. *Neuroscience*, *68*(1), 151-157. https://doi.org/10.1016/0306-4522(95)00106-s

John, C. C., Bangirana, P., Byarugaba, J., Opoka, R. O., Idro, R., Jurek, A. M., Wu, B., & Boivin, M. J. (2008). Cerebral malaria in children is associated with long-term cognitive impairment. *Pediatrics*, *122*(1), e92-99. https://doi.org/10.1542/peds.2007-3709

Johnson, L., & Bhutani, V. K. (2011). The clinical syndrome of bilirubin-induced neurologic dysfunction. *Semin Perinatol*, *35*(3), 101-113. https://doi.org/10.1053/j.semperi.2011.02.003

Juopperi, T. A., Kim, W. R., Chiang, C. H., Yu, H., Margolis, R. L., Ross, C. A., Ming, G. L., & Song, H. (2012). Astrocytes generated from patient induced pluripotent stem cells recapitulate features of Huntington's disease patient cells. *Mol Brain*, *5*, 17. https://doi.org/10.1186/1756-6606-5-17

Kadakol, A., Ghosh, S. S., Sappal, B. S., Sharma, G., Chowdhury, J. R., & Chowdhury, N. R. (2000). Genetic lesions of bilirubin uridine-diphosphoglucuronate glucuronosyltransferase (UGT1A1) causing Crigler-Najjar and Gilbert syndromes: correlation of genotype to phenotype. *Hum Mutat*, *16*(4), 297-306. https://doi.org/10.1002/1098-1004(200010)16:4<297::AID-HUMU2>3.0.CO;2-Z

Karikari, A. A., Wruck, W., & Adjaye, J. (2021). Transcriptome-based analysis of blood samples reveals elevation of DNA damage response, neutrophil degranulation, cancer and neurodegenerative pathways in Plasmodium falciparum patients. *Malar J*, *20*(1), 383. https://doi.org/10.1186/s12936-021-03918-5

Karmirian, K., Holubiec, M., Goto-Silva, L., Fernandez Bessone, I., Vitoria, G., Mello, B., Alloatti, M., Vanderborght, B., Falzone, T. L., & Rehen, S. (2023). Modeling Alzheimer's Disease Using Human Brain Organoids. *Methods Mol Biol*, *2561*, 135-158. https://doi.org/10.1007/978-1-0716-2655-9_7

Kato, S., Iwata, O., Yamada, Y., Kakita, H., Yamada, T., Nakashima, H., Sugiura, T., Suzuki, S., & Togari, H. (2020). Standardization of phototherapy for neonatal hyperbilirubinemia using multiple-wavelength irradiance integration. *Pediatr Neonatol*, *61*(1), 100-105. https://doi.org/10.1016/j.pedneo.2019.07.002

Kawai, S., Aikawa, M., Kano, S., & Suzuki, M. (1993). A primate model for severe human malaria with cerebral involvement: Plasmodium coatneyi-infected Macaca fuscata. *Am J Trop Med Hyg*, *48*(5), 630-636. https://doi.org/10.4269/ajtmh.1993.48.630

Kim, H., & Jiang, P. (2021). Generation of human pluripotent stem cell-derived fused organoids with oligodendroglia and myelin. *STAR Protoc*, *2*(2), 100443. https://doi.org/10.1016/j.xpro.2021.100443

Kim, S. H., Kang, Y. J., Kim, W. J., Woo, D. K., Lee, Y., Kim, D. I., Park, Y. B., Kwon, B. S., Park, J. E., & Lee, W. H. (2004). TWEAK can induce pro-inflammatory cytokines and matrix metalloproteinase-9 in macrophages. *Circ J*, *68*(4), 396-399. https://doi.org/10.1253/circj.68.396

Kolios, G., & Moodley, Y. (2013). Introduction to stem cells and regenerative medicine. *Respiration*, *85*(1), 3-10. https://doi.org/10.1159/000345615

Koo, B., Choi, B., Park, H., & Yoon, K. J. (2019). Past, Present, and Future of Brain Organoid Technology. *Mol Cells*, *42*(9), 617-627. https://doi.org/10.14348/molcells.2019.0162

Koster, R., Timmer-Bosscha, H., Bischoff, R., Gietema, J. A., & de Jong, S. (2011). Disruption of the MDM2-p53 interaction strongly potentiates p53-dependent apoptosis in cisplatin-resistant human testicular carcinoma cells via the Fas/FasL pathway. *Cell Death Dis*, *2*(4), e148. https://doi.org/10.1038/cddis.2011.33

Kuenzle, C. C. (1970). Bilirubin conjugates of human bile. Nuclear-magnetic-resonance, infrared and optical spectra of model compounds. *Biochem J*, *119*(3), 395-409. https://doi.org/10.1042/bj1190395

Labrune, P., Myara, A., Hadchouel, M., Ronchi, F., Bernard, O., Trivin, F., Chowdhury, N. R., Chowdhury, J. R., Munnich, A., & Odievre, M. (1994). Genetic heterogeneity of Crigler-Najjar syndrome type I: a study of 14 cases. *Hum Genet*, *94*(6), 693-697. https://doi.org/10.1007/BF00206965

Labrune, P., & Odievre, M. (1992). [Toward a treatment of Crigler-Najjar syndrome?]. *Arch Fr Pediatr*, *49*(5), 467-468. https://www.ncbi.nlm.nih.gov/pubmed/1530446 (Vers un traitement de la maladie de Crigler-Najjar?)

Lalani, A. I., Zhu, S., Gokhale, S., Jin, J., & Xie, P. (2018). TRAF molecules in inflammation and inflammatory diseases. *Curr Pharmacol Rep*, *4*(1), 64-90. https://doi.org/10.1007/s40495-017-0117-y

Lancaster, M. A., & Knoblich, J. A. (2014). Organogenesis in a dish: modeling development and disease using organoid technologies. *Science*, *345*(6194), 1247125. https://doi.org/10.1126/science.1247125

Lancaster, M. A., Renner, M., Martin, C. A., Wenzel, D., Bicknell, L. S., Hurles, M. E., Homfray, T., Penninger, J. M., Jackson, A. P., & Knoblich, J. A. (2013). Cerebral organoids model human brain development and microcephaly. *Nature*, *501*(7467), 373-379. https://doi.org/10.1038/nature12517

Levine, R. L., Fredericks, W. R., & Rapoport, S. I. (1985). Clearance of bilirubin from rat brain after reversible osmotic opening of the blood-brain barrier. *Pediatr Res*, *19*(10), 1040-1043. https://doi.org/10.1203/00006450-198510000-00019

Li, M. L., Aggeler, J., Farson, D. A., Hatier, C., Hassell, J., & Bissell, M. J. (1987). Influence of a reconstituted basement membrane and its components on casein gene expression and secretion in mouse mammary epithelial cells. *Proc Natl Acad Sci U S A*, *84*(1), 136-140. https://doi.org/10.1073/pnas.84.1.136

Liu, C., Oikonomopoulos, A., Sayed, N., & Wu, J. C. (2018). Modeling human diseases with induced pluripotent stem cells: from 2D to 3D and beyond. *Development*, *145*(5). https://doi.org/10.1242/dev.156166

Liu, S., Helen A, R., Elena, M. M. R., Ivan, K., Alejo, J. N.-H., Noel, B., Simon, L., & study., D. a. F. P. (2023). IPSC-derived neurons with amyloid-β treatment reflect features of Alzheimer's disease patients. *Alzheimer's & Dementia*. https://doi.org/ https://doi.org/10.1002/alz.065060

Liu, Y., Beyer, A., & Aebersold, R. (2016). On the Dependency of Cellular Protein Levels on mRNA Abundance. *Cell*, *165*(3), 535-550. https://doi.org/10.1016/j.cell.2016.03.014

Logan, S., Arzua, T., Canfield, S. G., Seminary, E. R., Sison, S. L., Ebert, A. D., & Bai, X. (2019). Studying Human Neurological Disorders Using Induced Pluripotent Stem Cells: From 2D Monolayer to 3D Organoid and Blood Brain Barrier Models. *Compr Physiol*, *9*(2), 565-611. https://doi.org/10.1002/cphy.c180025

London, I. M., West, R., Shemin, D., & Rittenberg, D. (1950). On the origin of bile pigment in normal man. *J Biol Chem*, *184*(1), 351-358. https://www.ncbi.nlm.nih.gov/pubmed/15422003

Luo, C., Lancaster, M. A., Castanon, R., Nery, J. R., Knoblich, J. A., & Ecker, J. R. (2016). Cerebral Organoids Recapitulate Epigenomic Signatures of the Human Fetal Brain. *Cell Rep*, *17*(12), 3369-3384. https://doi.org/10.1016/j.celrep.2016.12.001

Mah, L. J., El-Osta, A., & Karagiannis, T. C. (2010). gammaH2AX: a sensitive molecular marker of DNA damage and repair. *Leukemia*, *24*(4), 679-686. https://doi.org/10.1038/leu.2010.6

Marchetto, M. C., Brennand, K. J., Boyer, L. F., & Gage, F. H. (2011). Induced pluripotent stem cells (iPSCs) and neurological disease modeling: progress and promises. *Hum Mol Genet*, *20*(R2), R109-115. https://doi.org/10.1093/hmg/ddr336

Martins, S., Erichsen, L., Datsi, A., Wruck, W., Goering, W., Chatzantonaki, E., de Amorim, V. C. M., Rossi, A., Chrzanowska, K. H., & Adjaye, J. (2022). Impaired p53-Mediated DNA Damage Response Contributes to Microcephaly in Nijmegen Breakage Syndrome Patient-Derived Cerebral Organoids. *Cells*, *11*(5). https://doi.org/10.3390/cells11050802

Marton, R. M., Miura, Y., Sloan, S. A., Li, Q., Revah, O., Levy, R. J., Huguenard, J. R., & Pasca, S. P. (2019). Differentiation and maturation of oligodendrocytes in human three-dimensional neural cultures. *Nat Neurosci*, *22*(3), 484-491. https://doi.org/10.1038/s41593-018-0316-9

McDonagh, A. F., & Assisi, F. (1972). The ready isomerization of bilirubin IX- in aqueous solution. *Biochem J*, *129*(3), 797-800. https://doi.org/10.1042/bj1290797

McDonald, C. R., Conroy, A. L., Hawkes, M., Elphinstone, R. E., Gamble, J. L., Hayford, K., Namasopo, S., Opoka, R. O., Liles, W. C., & Kain, K. C. (2017). Brain-derived Neurotrophic Factor Is Associated With Disease Severity and Clinical Outcome in Ugandan Children Admitted to Hospital With Severe Malaria. *Pediatr Infect Dis J*, *36*(2), 146-150. https://doi.org/10.1097/INF.0000000000001382

McKinney, C. E. (2017). Using induced pluripotent stem cells derived neurons to model brain diseases. *Neural Regen Res*, *12*(7), 1062-1067. https://doi.org/10.4103/1673-5374.211180

Medana, I. M., Day, N. P., Hien, T. T., Mai, N. T., Bethell, D., Phu, N. H., Farrar, J., Esiri, M. M., White, N. J., & Turner, G. D. (2002). Axonal injury in cerebral malaria. *Am J Pathol*, *160*(2), 655-666. https://doi.org/10.1016/S0002-9440(10)64885-7

Medana, I. M., & Turner, G. D. (2006). Human cerebral malaria and the blood-brain barrier. *Int J Parasitol*, *36*(5), 555-568. https://doi.org/10.1016/j.ijpara.2006.02.004

Mehra, A., Balaji, S. N., & Trivedi, V. (2021). Hemozoin is a potential threat in cerebral malaria pathology through the induction of RBC-EC cytoadherence. *Acta Trop*, *217*, 105867. https://doi.org/10.1016/j.actatropica.2021.105867

Memon, N., Weinberger, B. I., Hegyi, T., & Aleksunes, L. M. (2016). Inherited disorders of bilirubin clearance. *Pediatr Res*, *79*(3), 378-386. https://doi.org/10.1038/pr.2015.247

Miranda, A. S., Brant, F., Rocha, N. P., Cisalpino, D., Rodrigues, D. H., Souza, D. G., Machado, F. S., Rachid, M. A., Teixeira, A. L., Jr., & Campos, A. C. (2013). Further evidence for an anti-inflammatory role of artesunate in experimental cerebral malaria. *Malar J*, *12*, 388. https://doi.org/10.1186/1475-2875-12-388

Mishra, S. K., & Newton, C. R. (2009). Diagnosis and management of the neurological complications of falciparum malaria. *Nat Rev Neurol*, *5*(4), 189-198. https://doi.org/10.1038/nrneurol.2009.23

Misra, U. K., Kalita, J., Prabhakar, S., Chakravarty, A., Kochar, D., & Nair, P. P. (2011). Cerebral malaria and bacterial meningitis. *Ann Indian Acad Neurol*, *14*(Suppl 1), S35-39. https://doi.org/10.4103/0972-2327.83101

Miura, Y., Li, M. Y., Birey, F., Ikeda, K., Revah, O., Thete, M. V., Park, J. Y., Puno, A., Lee, S. H., Porteus, M. H., & Pasca, S. P. (2020). Generation of human striatal organoids and cortico-striatal assembloids from human pluripotent stem cells. *Nat Biotechnol*, *38*(12), 1421-1430. https://doi.org/10.1038/s41587-020-00763-w

Mohamad Fawzi Mahomoodally, J. T. L. (2022). *Antioxidants Effects in Health, Chapter2.1 - Bilirubin*. Elsevier,. https://doi.org/https://doi.org/10.1016/B978-0-12-819096-8.00021-5

Moore, L. R., Fujioka, H., Williams, P. S., Chalmers, J. J., Grimberg, B., Zimmerman, P. A., & Zborowski, M. (2006). Hemoglobin degradation in malaria-infected erythrocytes determined from live cell magnetophoresis. *FASEB J*, *20*(6), 747-749. https://doi.org/10.1096/fj.05-5122fje

Morris, B. H., Oh, W., Tyson, J. E., Stevenson, D. K., Phelps, D. L., O'Shea, T. M., McDavid, G. E., Perritt, R. L., Van Meurs, K. P., Vohr, B. R., Grisby, C., Yao, Q., Pedroza, C., Das, A., Poole, W. K., Carlo, W. A., Duara, S., Laptook, A. R., Salhab, W. A., . . . Network, N. N. R. (2008). Aggressive vs. conservative phototherapy for infants with extremely low birth weight. *N Engl J Med*, *359*(18), 1885-1896. https://doi.org/10.1056/NEJMoa0803024

Nascimento, J. M., Saia-Cereda, V. M., Sartore, R. C., da Costa, R. M., Schitine, C. S., Freitas, H. R., Murgu, M., de Melo Reis, R. A., Rehen, S. K., & Martins-de-Souza, D. (2019). Human Cerebral Organoids and Fetal Brain Tissue Share Proteomic Similarities. *Front Cell Dev Biol*, *7*, 303. https://doi.org/10.3389/fcell.2019.00303

Ndreu, A., Hajdari, D., Ndoni, A., Shkurti, K., Kraja, D., Como, N., Bino, S., Gjermeni, N., Domi, R., & Mingomataj, E. C. (2016). Epidemiological, clinical and therapeutic aspects of cerebral malaria imported in Albania. *J Infect Dev Ctries*, *10*(2), 190-194. https://doi.org/10.3855/jidc.6321

Newman, T. B., Wu, Y. W., Kuzniewicz, M. W., Grimes, B. A., & McCulloch, C. E. (2018). Childhood Seizures After Phototherapy. *Pediatrics*, *142*(4). https://doi.org/10.1542/peds.2018-0648

Newton, C. R., & Krishna, S. (1998). Severe falciparum malaria in children: current understanding of pathophysiology and supportive treatment. *Pharmacol Ther*, *79*(1), 1-53. https://doi.org/10.1016/s0163-7258(98)00008-4

Nguyen, L., Wruck, W., Erichsen, L., Graffmann, N., & Adjaye, J. (2022). The Nephrotoxin Puromycin Aminonucleoside Induces Injury in Kidney Organoids Differentiated from Induced Pluripotent Stem Cells. *Cells*, *11*(4). https://doi.org/10.3390/cells11040635

Nguyen, N., Bonzo, J. A., Chen, S., Chouinard, S., Kelner, M. J., Hardiman, G., Belanger, A., & Tukey, R. H. (2008). Disruption of the ugt1 locus in mice resembles human Crigler-Najjar type I disease. *J Biol Chem*, *283*(12), 7901-7911. https://doi.org/10.1074/jbc.M709244200

Olivier, M., Van Den Ham, K., Shio, M. T., Kassa, F. A., & Fougeray, S. (2014). Malarial pigment hemozoin and the innate inflammatory response. *Front Immunol*, *5*, 25. https://doi.org/10.3389/fimmu.2014.00025

Oluwayemi, I. O., Brown, B. J., Oyedeji, O. A., & Oluwayemi, M. A. (2013). Neurological sequelae in survivors of cerebral malaria. *Pan Afr Med J*, *15*, 88. https://doi.org/10.11604/pamj.2013.15.88.1897

Ormel, P. R., Vieira de Sa, R., van Bodegraven, E. J., Karst, H., Harschnitz, O., Sneeboer, M. A. M., Johansen, L. E., van Dijk, R. E., Scheefhals, N., Berdenis van Berlekom, A., Ribes Martinez, E., Kling, S., MacGillavry, H. D., van den Berg, L. H., Kahn, R. S., Hol, E. M., de Witte, L. D., & Pasterkamp, R. J. (2018). Microglia innately develop within cerebral organoids. *Nat Commun*, *9*(1), 4167. https://doi.org/10.1038/s41467-018-06684-2

Pais, T. F., & Penha-Goncalves, C. (2023). In vitro model of brain endothelial cell barrier reveals alterations induced by Plasmodium blood stage factors. *Parasitol Res*, *122*(3), 729-737. https://doi.org/10.1007/s00436-023-07782-x

Palmela, I., Cardoso, F. L., Bernas, M., Correia, L., Vaz, A. R., Silva, R. F., Fernandes, A., Kim, K. S., Brites, D., & Brito, M. A. (2011). Elevated levels of bilirubin and long-term exposure impair human brain microvascular endothelial cell integrity. *Curr Neurovasc Res*, *8*(2), 153-169. https://doi.org/10.2174/156720211795495358

Pandey, A. V., & Tekwani, B. L. (1996). Formation of haemozoin/beta-haematin under physiological conditions is not spontaneous. *FEBS Lett*, *393*(2-3), 189-193. https://doi.org/10.1016/0014-5793(96)00881-2

Pasca, A. M., Sloan, S. A., Clarke, L. E., Tian, Y., Makinson, C. D., Huber, N., Kim, C. H., Park, J. Y., O'Rourke, N. A., Nguyen, K. D., Smith, S. J., Huguenard, J. R., Geschwind, D. H., Barres, B. A., & Pasca, S. P. (2015). Functional cortical neurons and astrocytes from human pluripotent stem cells in 3D culture. *Nat Methods*, *12*(7), 671-678. https://doi.org/10.1038/nmeth.3415

Pawlowski, T., Radkowski, M., Malyszczak, K., Inglot, M., Zalewska, M., Jablonska, J., & Laskus, T. (2014). Depression and neuroticism in patients with chronic hepatitis C: correlation with peripheral blood mononuclear cells activation. *J Clin Virol*, *60*(2), 105-111. https://doi.org/10.1016/j.jcv.2014.03.004

Pellegrini, L., Bonfio, C., Chadwick, J., Begum, F., Skehel, M., & Lancaster, M. A. (2020). Human CNS barrier-forming organoids with cerebrospinal fluid production. *Science*, *369*(6500). https://doi.org/10.1126/science.aaz5626

Penney, J., Ralvenius, W. T., & Tsai, L. H. (2020). Modeling Alzheimer's disease with iPSC-derived brain cells. *Mol Psychiatry*, *25*(1), 148-167. https://doi.org/10.1038/s41380-019-0468-3

Percario, S., Moreira, D. R., Gomes, B. A., Ferreira, M. E., Goncalves, A. C., Laurindo, P. S., Vilhena, T. C., Dolabela, M. F., & Green, M. D. (2012). Oxidative stress in malaria. *Int J Mol Sci*, *13*(12), 16346-16372. https://doi.org/10.3390/ijms131216346

Perner, F., Perner, C., Ernst, T., & Heidel, F. H. (2019). Roles of JAK2 in Aging, Inflammation, Hematopoiesis and Malignant Transformation. *Cells*, *8*(8). https://doi.org/10.3390/cells8080854

Plasmodium. (2024). In T. E. o. E. Britannica (Ed.), *Encyclopedia Britannica*.

Polimeni, M., & Prato, M. (2014). Host matrix metalloproteinases in cerebral malaria: new kids on the block against blood-brain barrier integrity? *Fluids Barriers CNS*, *11*(1), 1. https://doi.org/10.1186/2045-8118-11-1

Polimeni, M., Valente, E., Aldieri, E., Khadjavi, A., Giribaldi, G., & Prato, M. (2012). Haemozoin induces early cytokine-mediated lysozyme release from human monocytes through p38 MAPK- and NF-kappaB-dependent mechanisms. *PLoS One*, *7*(6), e39497. https://doi.org/10.1371/journal.pone.0039497

Pomeshchik, Y., Klementieva, O., Gil, J., Martinsson, I., Hansen, M. G., de Vries, T., Sancho-Balsells, A., Russ, K., Savchenko, E., Collin, A., Vaz, A. R., Bagnoli, S., Nacmias, B., Rampon, C., Sorbi, S., Brites, D., Marko-Varga, G., Kokaia, Z., Rezeli, M., . . . Roybon, L. (2023). Human iPSC-Derived Hippocampal Spheroids: An Innovative Tool for Stratifying Alzheimer Disease Patient-Specific Cellular Phenotypes and Developing Therapies. *Stem Cell Reports*, *18*(5), 1244-1245. https://doi.org/10.1016/j.stemcr.2023.04.009

Postels, D. G., & Birbeck, G. L. (2013). Cerebral malaria. *Handb Clin Neurol*, *114*, 91-102. https://doi.org/10.1016/B978-0-444-53490-3.00006-6

Practice parameter: management of hyperbilirubinemia in the healthy term newborn. American Academy of Pediatrics. Provisional Committee for Quality Improvement and Subcommittee on Hyperbilirubinemia. (1994). *Pediatrics*, *94*(4 Pt 1), 558-565. https://www.ncbi.nlm.nih.gov/pubmed/7755691

Pranty, A. I., Shumka, S., & Adjaye, J. (2022). Bilirubin-Induced Neurological Damage: Current and Emerging iPSC-Derived Brain Organoid Models. *Cells*, *11*(17). https://doi.org/10.3390/cells11172647

Qaisiya, M., Brischetto, C., Jasprova, J., Vitek, L., Tiribelli, C., & Bellarosa, C. (2017). Bilirubin-induced ER stress contributes to the inflammatory response and apoptosis in neuronal cells. *Arch Toxicol*, *91*(4), 1847-1858. https://doi.org/10.1007/s00204-016-1835-3

Qian, X., Nguyen, H. N., Song, M. M., Hadiono, C., Ogden, S. C., Hammack, C., Yao, B., Hamersky, G. R., Jacob, F., Zhong, C., Yoon, K. J., Jeang, W., Lin, L., Li, Y., Thakor, J., Berg, D. A., Zhang, C., Kang, E., Chickering, M., . . . Ming, G. L. (2016). Brain-Region-Specific Organoids Using Mini-bioreactors for Modeling ZIKV Exposure. *Cell*, *165*(5), 1238-1254. https://doi.org/10.1016/j.cell.2016.04.032

Radlovic, N. (2014). Hereditary hyperbilirubinemias. *Srp Arh Celok Lek*, *142*(3-4), 257-260. https://doi.org/10.2298/sarh1404257r

Radu, P., & Atsmon, J. (2001). Gilbert's syndrome--clinical and pharmacological implications. *Isr Med Assoc J*, *3*(8), 593-598. https://www.ncbi.nlm.nih.gov/pubmed/11519385

Ramakrishnan, N., Bittar, K., & Jialal, I. (2024). Impaired Bilirubin Conjugation. In *StatPearls*. https://www.ncbi.nlm.nih.gov/pubmed/29494090

Ratajczak, M. Z., Zuba-Surma, E., Kucia, M., Poniewierska, A., Suszynska, M., & Ratajczak, J. (2012). Pluripotent and multipotent stem cells in adult tissues. *Adv Med Sci*, *57*(1), 1-17. https://doi.org/10.2478/v10039-012-0020-z

Rawat, V., Bortolussi, G., Gazzin, S., Tiribelli, C., & Muro, A. F. (2018). Bilirubin-Induced Oxidative Stress Leads to DNA Damage in the Cerebellum of Hyperbilirubinemic Neonatal Mice and Activates DNA Double-Strand Break Repair Pathways in Human Cells. *Oxid Med Cell Longev*, *2018*, 1801243. https://doi.org/10.1155/2018/1801243

Renia, L., Howland, S. W., Claser, C., Charlotte Gruner, A., Suwanarusk, R., Hui Teo, T., Russell, B., & Ng, L. F. (2012). Cerebral malaria: mysteries at the blood-brain barrier. *Virulence*, *3*(2), 193-201. https://doi.org/10.4161/viru.19013

Rice, A. C., & Shapiro, S. M. (2008). A new animal model of hemolytic hyperbilirubinemia-induced bilirubin encephalopathy (kernicterus). *Pediatr Res*, *64*(3), 265-269. https://doi.org/10.1203/PDR.0b013e31817d9be0

Riemens, R. J. M., Kenis, G., & van den Beucken, T. (2020). Human-induced pluripotent stem cells as a model for studying sporadic Alzheimer's disease. *Neurobiol Learn Mem*, *175*, 107318. https://doi.org/10.1016/j.nlm.2020.107318

Ritter, J. K., Crawford, J. M., & Owens, I. S. (1991). Cloning of two human liver bilirubin UDP-glucuronosyltransferase cDNAs with expression in COS-1 cells. *J Biol Chem*, *266*(2), 1043-1047. https://www.ncbi.nlm.nih.gov/pubmed/1898728

Rodrigues, C. M., Sola, S., Silva, R. F., & Brites, D. (2002). Aging confers different sensitivity to the neurotoxic properties of unconjugated bilirubin. *Pediatr Res*, *51*(1), 112-118. https://doi.org/10.1203/00006450-200201000-00020

Rossant, J., & Tam, P. P. (2009). Blastocyst lineage formation, early embryonic asymmetries and axis patterning in the mouse. *Development*, *136*(5), 701-713. https://doi.org/10.1242/dev.017178

Russo, F. B., Cugola, F. R., Fernandes, I. R., Pignatari, G. C., & Beltrao-Braga, P. C. (2015). Induced pluripotent stem cells for modeling neurological disorders. *World J Transplant*, *5*(4), 209-221. https://doi.org/10.5500/wjt.v5.i4.209

Saba, J., Turati, J., Ramirez, D., Carniglia, L., Durand, D., Lasaga, M., & Caruso, C. (2018). Astrocyte truncated tropomyosin receptor kinase B mediates brain-derived neurotrophic factor anti-apoptotic effect leading to neuroprotection. *J Neurochem*, *146*(6), 686-702. https://doi.org/10.1111/jnc.14476

Sakaguchi, H., Kadoshima, T., Soen, M., Narii, N., Ishida, Y., Ohgushi, M., Takahashi, J., Eiraku, M., & Sasai, Y. (2015). Generation of functional hippocampal neurons from self-organizing human embryonic stem cell-derived dorsomedial telencephalic tissue. *Nat Commun*, *6*, 8896. https://doi.org/10.1038/ncomms9896

Sarasua, S. M., Dwivedi, A., Boccuto, L., Chen, C. F., Sharp, J. L., Rollins, J. D., Collins, J. S., Rogers, R. C., Phelan, K., & DuPont, B. R. (2014). 22q13.2q13.32 genomic regions associated with severity of speech delay, developmental delay, and physical features in Phelan-McDermid syndrome. *Genet Med*, *16*(4), 318-328. https://doi.org/10.1038/gim.2013.144

Schauer, R., Stangl, M., Lang, T., Zimmermann, A., Chouker, A., Gerbes, A. L., Schildberg, F. W., & Rau, H. G. (2003). Treatment of Crigler-Najjar type 1 disease: relevance of early liver transplantation. *J Pediatr Surg*, *38*(8), 1227-1231. https://doi.org/10.1016/s0022-3468(03)00273-2

Schiavon, E., Smalley, J. L., Newton, S., Greig, N. H., & Forsythe, I. D. (2018). Neuroinflammation and ER-stress are key mechanisms of acute bilirubin toxicity and hearing loss in a mouse model. *PLoS One*, *13*(8), e0201022. https://doi.org/10.1371/journal.pone.0201022

Schiess, N., Villabona-Rueda, A., Cottier, K. E., Huether, K., Chipeta, J., & Stins, M. F. (2020). Pathophysiology and neurologic sequelae of cerebral malaria. *Malar J*, *19*(1), 266. https://doi.org/10.1186/s12936-020-03336-z

Schweizer, A., Feige, U., Fontana, A., Muller, K., & Dinarello, C. A. (1988). Interleukin-1 enhances pain reflexes. Mediation through increased prostaglandin E2 levels. *Agents Actions*, *25*(3-4), 246-251. https://doi.org/10.1007/BF01965025

Seubert, J. M., Darmon, A. J., El-Kadi, A. O., D'Souza, S. J., & Bend, J. R. (2002). Apoptosis in murine hepatoma hepa 1c1c7 wild-type, C12, and C4 cells mediated by bilirubin. *Mol Pharmacol*, *62*(2), 257-264. https://doi.org/10.1124/mol.62.2.257

Severe falciparum malaria. World Health Organization, Communicable Diseases Cluster. (2000). *Trans R Soc Trop Med Hyg*, *94 Suppl 1*, S1-90. https://www.ncbi.nlm.nih.gov/pubmed/11103309

Severe malaria. (2014). *Trop Med Int Health*, *19 Suppl 1*, 7-131. https://doi.org/10.1111/tmi.12313_2

Shapiro, S. M. (2003). Bilirubin toxicity in the developing nervous system. *Pediatr Neurol*, *29*(5), 410-421. https://doi.org/10.1016/j.pediatrneurol.2003.09.011

Sidhaye, J., & Knoblich, J. A. (2021). Brain organoids: an ensemble of bioassays to investigate human neurodevelopment and disease. *Cell Death Differ*, *28*(1), 52-67. https://doi.org/10.1038/s41418-020-0566-4

Sierra-Sanchez, A., Ordonez-Luque, A., Espinosa-Ibanez, O., Ruiz-Garcia, A., & Arias-Santiago, S. (2018). Epithelial In vitro Differentiation of Mesenchymal Stem Cells. *Curr Stem Cell Res Ther*, *13*(6), 409-422. https://doi.org/10.2174/1574888X13666180501120416

Simian, M., & Bissell, M. J. (2017). Organoids: A historical perspective of thinking in three dimensions. *J Cell Biol*, *216*(1), 31-40. https://doi.org/10.1083/jcb.201610056

Singh, A., & Jialal, I. (2021). Unconjugated Hyperbilirubinemia. In *StatPearls*. StatPearls Publishing Copyright © 2021, StatPearls Publishing LLC.

Sloan, S. A., Andersen, J., Pasca, A. M., Birey, F., & Pasca, S. P. (2018). Generation and assembly of human brain region-specific three-dimensional cultures. *Nat Protoc*, *13*(9), 2062-2085. https://doi.org/10.1038/s41596-018-0032-7

Smits, L. M., Reinhardt, L., Reinhardt, P., Glatza, M., Monzel, A. S., Stanslowsky, N., Rosato-Siri, M. D., Zanon, A., Antony, P. M., Bellmann, J., Nicklas, S. M., Hemmer, K., Qing, X., Berger, E., Kalmbach, N., Ehrlich, M., Bolognin, S., Hicks, A. A., Wegner, F., . . . Schwamborn, J. C. (2019). Modeling Parkinson's disease in midbrain-like organoids. *NPJ Parkinsons Dis*, *5*, 5. https://doi.org/10.1038/s41531-019-0078-4

Song, S., Hu, Y., Gu, X., Si, F., & Hua, Z. (2014). A novel newborn rat kernicterus model created by injecting a bilirubin solution into the cisterna magna. *PLoS One*, *9*(5), e96171. https://doi.org/10.1371/journal.pone.0096171

Sorrentino, D., & Berk, P. D. (1988). Mechanistic aspects of hepatic bilirubin uptake. *Semin Liver Dis*, *8*(2), 119-136. https://doi.org/10.1055/s-2008-1040533

Sticova, E., & Jirsa, M. (2013). New insights in bilirubin metabolism and their clinical implications. *World J Gastroenterol*, *19*(38), 6398-6407. https://doi.org/10.3748/wjg.v19.i38.6398

Stoddard-Bennett, T., & Reijo Pera, R. (2019). Treatment of Parkinson's Disease through Personalized Medicine and Induced Pluripotent Stem Cells. *Cells*, *8*(1). https://doi.org/10.3390/cells8010026

Strassburg, C. P. (2010). Hyperbilirubinemia syndromes (Gilbert-Meulengracht, Crigler-Najjar, Dubin-Johnson, and Rotor syndrome). *Best Pract Res Clin Gastroenterol*, *24*(5), 555-571. https://doi.org/10.1016/j.bpg.2010.07.007

Strauss, K. A., Ahlfors, C. E., Soltys, K., Mazareigos, G. V., Young, M., Bowser, L. E., Fox, M. D., Squires, J. E., McKiernan, P., Brigatti, K. W., Puffenberger, E. G., Carson, V. J., & Vreman, H. J. (2020). Crigler-Najjar Syndrome Type 1: Pathophysiology, Natural History, and Therapeutic Frontier. *Hepatology*, *71*(6), 1923-1939. https://doi.org/10.1002/hep.30959

Takahashi, K., Tanabe, K., Ohnuki, M., Narita, M., Ichisaka, T., Tomoda, K., & Yamanaka, S. (2007). Induction of pluripotent stem cells from adult human fibroblasts by defined factors. *Cell*, *131*(5), 861-872. https://doi.org/10.1016/j.cell.2007.11.019

Takahashi, K., & Yamanaka, S. (2006). Induction of pluripotent stem cells from mouse embryonic and adult fibroblast cultures by defined factors. *Cell*, *126*(4), 663-676. https://doi.org/10.1016/j.cell.2006.07.024

Thomson, J. A., Itskovitz-Eldor, J., Shapiro, S. S., Waknitz, M. A., Swiergiel, J. J., Marshall, V. S., & Jones, J. M. (1998). Embryonic stem cell lines derived from human blastocysts. *Science*, *282*(5391), 1145-1147. https://doi.org/10.1126/science.282.5391.1145

Tian, Z., Yu, T., Liu, J., Wang, T., & Higuchi, A. (2023). Introduction to stem cells. *Prog Mol Biol Transl Sci*, *199*, 3-32. https://doi.org/10.1016/bs.pmbts.2023.02.012

Tietze, K. J. (2012). *Clinical Skills for Pharmacists* (3 ed.). Elsevier. https://shop.elsevier.com/books/clinical-skills-for-pharmacists/tietze/978-0-323-07738-5

Tomaskovic-Crook, E., Guerrieri-Cortesi, K., & Crook, J. M. (2021). Induced pluripotent stem cells for 2D and 3D modelling the biological basis of schizophrenia and screening possible therapeutics. *Brain Res Bull*, *175*, 48-62. https://doi.org/10.1016/j.brainresbull.2021.07.004

Tongren, J. E., Yang, C., Collins, W. E., Sullivan, J. S., Lal, A. A., & Xiao, L. (2000). Expression of proinflammatory cytokines in four regions of the brain in Macaque mulatta (rhesus) monkeys infected with Plasmodium coatneyi. *Am J Trop Med Hyg*, *62*(4), 530-534. https://doi.org/10.4269/ajtmh.2000.62.530

Torres, A. E., Lyons, A. B., Hamzavi, I. H., & Lim, H. W. (2021). Role of phototherapy in the era of biologics. *J Am Acad Dermatol*, *84*(2), 479-485. https://doi.org/10.1016/j.jaad.2020.04.095

Tsang, S. H., & Sharma, T. (2018). Glossary of Relevant Genetic and Molecular/Cell Biology. *Adv Exp Med Biol*, *1085*, 23-28. https://doi.org/10.1007/978-3-319-95046-4_7

Tung, T. C., & Ku, S. H. (1944). Experimental studies on the development of the pronephric duct in anuran embryos. *J Anat*, *78*(Pt 1-2), 52-57. https://www.ncbi.nlm.nih.gov/pubmed/17104942

Urich, E., Patsch, C., Aigner, S., Graf, M., Iacone, R., & Freskgard, P. O. (2013). Multicellular self-assembled spheroidal model of the blood brain barrier. *Sci Rep*, *3*, 1500. https://doi.org/10.1038/srep01500

Valentim, M. (2018). Cerebral malaria. *Journal of Neurology & Stroke*, *8*(4). https://doi.org/10.15406/jnsk.2018.08.00313

van der Heyde, H. C., Nolan, J., Combes, V., Gramaglia, I., & Grau, G. E. (2006). A unified hypothesis for the genesis of cerebral malaria: sequestration, inflammation and hemostasis leading to microcirculatory dysfunction. *Trends Parasitol*, *22*(11), 503-508. https://doi.org/10.1016/j.pt.2006.09.002

Van Der Veere, C. N., Schoemaker, B., Bakker, C., Van Der Meer, R., Jansen, P. L., & Elferink, R. P. (1996). Influence of dietary calcium phosphate on the disposition of bilirubin in rats with unconjugated hyperbilirubinemia. *Hepatology*, *24*(3), 620-626. https://doi.org/10.1002/hep.510240326

van Essen, M. J., Apsley, E. J., Riepsaame, J., Xu, R., Northcott, P. A., Cowley, S. A., Jacob, J., & Becker, E. B. E. (2024). PTCH1-mutant human cerebellar organoids exhibit altered neural development

and recapitulate early medulloblastoma tumorigenesis. *Dis Model Mech*, *17*(2). https://doi.org/10.1242/dmm.050323

van Hensbroek, M. B., Palmer, A., Jaffar, S., Schneider, G., & Kwiatkowski, D. (1997). Residual neurologic sequelae after childhood cerebral malaria. *J Pediatr*, *131*(1 Pt 1), 125-129. https://doi.org/10.1016/s0022-3476(97)70135-5

van Veelen, C. W., Verbiest, H., Vlug, A. M., Rijksen, G., & Staal, G. E. (1978). Isozymes of pyruvate kinase from human brain, meningiomas, and malignant gliomas. *Cancer Res*, *38*(12), 4681-4687. https://www.ncbi.nlm.nih.gov/pubmed/214230

Vaz, A. R., Silva, S. L., Barateiro, A., Falcão, A. S., Fernandes, A., Brito, M. A., & Brites, D. (2011). Selective vulnerability of rat brain regions to unconjugated bilirubin. *Mol Cell Neurosci*, *48*(1), 82-93. https://doi.org/10.1016/j.mcn.2011.06.008

Vitek, L., & Ostrow, J. D. (2009). Bilirubin chemistry and metabolism; harmful and protective aspects. *Curr Pharm Des*, *15*(25), 2869-2883. https://doi.org/10.2174/138161209789058237

Volpe, J. J. (1981). Neurology of the newborn. *Major Probl Clin Pediatr*, *22*, 1-648. https://www.ncbi.nlm.nih.gov/pubmed/7022034

Vucic, D. (2018). XIAP at the crossroads of cell death and inflammation. *Oncotarget*, *9*(44), 27319-27320. https://doi.org/10.18632/oncotarget.25363

Wah, S. T., Hananantachai, H., Kerdpin, U., Plabplueng, C., Prachayasittikul, V., & Nuchnoi, P. (2016). Molecular basis of human cerebral malaria development. *Trop Med Health*, *44*, 33. https://doi.org/10.1186/s41182-016-0033-6

Waknine-Grinberg, J. H., McQuillan, J. A., Hunt, N., Ginsburg, H., & Golenser, J. (2010). Modulation of cerebral malaria by fasudil and other immune-modifying compounds. *Exp Parasitol*, *125*(2), 141-146. https://doi.org/10.1016/j.exppara.2010.01.005

Wang, L., Schlagal, C. R., Gao, J., Hao, Y., Dunn, T. J., McGrath, E. L., Labastida, J. A., Yu, Y., Feng, S. Q., Liu, S. Y., & Wu, P. (2018). Oligodendrocyte differentiation from human neural stem cells: A novel role for c-Src. *Neurochem Int*, *120*, 21-32. https://doi.org/10.1016/j.neuint.2018.07.006

Wang, Y., & Adjaye, J. (2011). A cyclic AMP analog, 8-Br-cAMP, enhances the induction of pluripotency in human fibroblast cells. *Stem Cell Rev Rep*, *7*(2), 331-341. https://doi.org/10.1007/s12015-010-9209-3

Watchko, J. F. (2006). Kernicterus and the molecular mechanisms of bilirubin-induced CNS injury in newborns. *Neuromolecular Med*, *8*(4), 513-529. https://doi.org/10.1385/NMM:8:4:513

Watchko, J. F., & Tiribelli, C. (2013). Bilirubin-induced neurologic damage--mechanisms and management approaches. *N Engl J Med*, *369*(21), 2021-2030. https://doi.org/10.1056/NEJMra1308124

Weiss, D. J., Lucas, T. C. D., Nguyen, M., Nandi, A. K., Bisanzio, D., Battle, K. E., Cameron, E., Twohig, K. A., Pfeffer, D. A., Rozier, J. A., Gibson, H. S., Rao, P. C., Casey, D., Bertozzi-Villa, A., Collins, E. L., Dalrymple, U., Gray, N., Harris, J. R., Howes, R. E., . . . Gething, P. W. (2019). Mapping the global prevalence, incidence, and mortality of Plasmodium falciparum, 2000-17: a spatial and temporal modelling study. *Lancet*, *394*(10195), 322-331. https://doi.org/10.1016/S0140-6736(19)31097-9

Weiss, P., & Taylor, A. C. (1960). Reconstitution of Complete Organs from Single-Cell Suspensions of Chick Embryos in Advanced Stages of Differentiation. *Proc Natl Acad Sci U S A*, *46*(9), 1177-1185. https://doi.org/10.1073/pnas.46.9.1177

Weksler, B. B., Subileau, E. A., Perriere, N., Charneau, P., Holloway, K., Leveque, M., Tricoire-Leignel, H., Nicotra, A., Bourdoulous, S., Turowski, P., Male, D. K., Roux, F., Greenwood, J., Romero, I. A., & Couraud, P. O. (2005). Blood-brain barrier-specific properties of a human adult brain endothelial cell line. *FASEB J*, *19*(13), 1872-1874. https://doi.org/10.1096/fj.04-3458fje

White, N. J., Turner, G. D., Medana, I. M., Dondorp, A. M., & Day, N. P. (2010). The murine cerebral malaria phenomenon. *Trends Parasitol*, *26*(1), 11-15. https://doi.org/10.1016/j.pt.2009.10.007

Wilson, H. V. (1907). A New Method by Which Sponges May Be Artificially Reared. *Science*, *25*(649), 912-915. https://doi.org/10.1126/science.25.649.912

Xia, Y., Sancho-Martinez, I., Nivet, E., Rodriguez Esteban, C., Campistol, J. M., & Izpisua Belmonte, J. C. (2014). The generation of kidney organoids by differentiation of human pluripotent cells to ureteric bud progenitor-like cells. *Nat Protoc*, *9*(11), 2693-2704. https://doi.org/10.1038/nprot.2014.182

Xu, Y., Zhao, J., Ren, Y., Wang, X., Lyu, Y., Xie, B., Sun, Y., Yuan, X., Liu, H., Yang, W., Fu, Y., Yu, Y., Liu, Y., Mu, R., Li, C., Xu, J., & Deng, H. (2022). Derivation of totipotent-like stem cells with blastocyst-like structure forming potential. *Cell Res*, *32*(6), 513-529. https://doi.org/10.1038/s41422-022-00668-0

Yoon, S. J., Elahi, L. S., Pasca, A. M., Marton, R. M., Gordon, A., Revah, O., Miura, Y., Walczak, E. M., Holdgate, G. M., Fan, H. C., Huguenard, J. R., Geschwind, D. H., & Pasca, S. P. (2019). Reliability of human cortical organoid generation. *Nat Methods*, *16*(1), 75-78. https://doi.org/10.1038/s41592-018-0255-0

Yu, J., Vodyanik, M. A., Smuga-Otto, K., Antosiewicz-Bourget, J., Frane, J. L., Tian, S., Nie, J., Jonsdottir, G. A., Ruotti, V., Stewart, R., Slukvin, II, & Thomson, J. A. (2007). Induced pluripotent stem cell lines derived from human somatic cells. *Science*, *318*(5858), 1917-1920. https://doi.org/10.1126/science.1151526

Yueh, M. F., Chen, S., Nguyen, N., & Tukey, R. H. (2017). Developmental, Genetic, Dietary, and Xenobiotic Influences on Neonatal Hyperbilirubinemia. *Mol Pharmacol*, *91*(5), 545-553. https://doi.org/10.1124/mol.116.107524

Zahmatkesh, E., Khoshdel-Rad, N., Mirzaei, H., Shpichka, A., Timashev, P., Mahmoudi, T., & Vosough, M. (2021). Evolution of organoid technology: Lessons learnt in Co-Culture systems from developmental biology. *Dev Biol*, *475*, 37-53. https://doi.org/10.1016/j.ydbio.2021.03.001

Zapata Zapata, C. H., & Blair Trujillo, S. (2003). Cerebral malaria. *Iatreia*, *16*(3), 202-216. https://doi.org/https://doi.org/10.17533/udea.iatreia.4003

Zecevic, N., Chen, Y., & Filipovic, R. (2005). Contributions of cortical subventricular zone to the development of the human cerebral cortex. *J Comp Neurol*, *491*(2), 109-122. https://doi.org/10.1002/cne.20714

Zhang, C., Cao, J., Li, X., Xu, H., Wang, W., Wang, L., Zhao, X., Li, W., Jiao, J., Hu, B., Zhou, Q., & Zhao, T. (2016). Treatment of multiple sclerosis by transplantation of neural stem cells derived from

induced pluripotent stem cells. *Sci China Life Sci*, *59*(9), 950-957. https://doi.org/10.1007/s11427-016-0114-9

Zhang, J. M., & An, J. (2007). Cytokines, inflammation, and pain. *Int Anesthesiol Clin*, *45*(2), 27-37. https://doi.org/10.1097/AIA.0b013e318034194e

Zhang, W., Jiang, J., Xu, Z., Yan, H., Tang, B., Liu, C., Chen, C., & Meng, Q. (2023). Microglia-containing human brain organoids for the study of brain development and pathology. *Mol Psychiatry*, *28*(1), 96-107. https://doi.org/10.1038/s41380-022-01892-1

Zhao, Z., Chen, X., Dowbaj, A. M., Sljukic, A., Bratlie, K., Lin, L., Fong, E. L. S., Balachander, G. M., Chen, Z., Soragni, A., Huch, M., Zeng, Y. A., Wang, Q., & Yu, H. (2022). Organoids. *Nat Rev Methods Primers*, *2*. https://doi.org/10.1038/s43586-022-00174-y

Zhong, X., Gutierrez, C., Xue, T., Hampton, C., Vergara, M. N., Cao, L. H., Peters, A., Park, T. S., Zambidis, E. T., Meyer, J. S., Gamm, D. M., Yau, K. W., & Canto-Soler, M. V. (2014). Generation of three-dimensional retinal tissue with functional photoreceptors from human iPSCs. *Nat Commun*, *5*, 4047. https://doi.org/10.1038/ncomms5047

Zhou, W., & Freed, C. R. (2009). Adenoviral gene delivery can reprogram human fibroblasts to induced pluripotent stem cells. *Stem Cells*, *27*(11), 2667-2674. https://doi.org/10.1002/stem.201

7. Appendix

7.1 Oral presentation

Abida Islam Pranty, Wasco Wruck, and James Adjaye. Modelling bilirubin-induced neuro-inflammation using hiPSC-derived Cortical Organoid Model of Crigler-Najjar Syndrome. London Stem Cell Network, 7th Annual Symposium in London, England, 2024.

7.2 Poster presentations

1. **Abida Islam Pranty**, Wasco Wruck, and James Adjaye. Modelling bilirubin-induced neuro-inflammation using hiPSC-derived Cortical Organoid Model of Crigler-Najjar Syndrome. London Stem Cell Network, 7th Annual Symposium in London, England, 2024.

2. **Abida Islam Pranty**, Wasco Wruck, and James Adjaye. Modelling of bilirubin-induced neuroinflammation using hiPSC-derived brain organoids. ISSCR Annual meeting 2023, Boston, USA, 2023.

3. **Abida Islam Pranty**, Wasco Wruck, and James Adjaye. Modelling of bilirubin-induced neuroinflammation using hiPSC-derived brain organoids. 11th International Meeting, Stem Cell Network North Rhein-Westphalia, Aachen, Germany, 2023.

4. **Abida Islam Pranty**, Wasco Wruck, and James Adjaye. Modelling of bilirubin-induced neuroinflammation using hiPSC-derived brain organoids. 10th GSCN Conference, Münster, Germany, 2022.

5. **Abida Islam Pranty**, Wasco Wruck, and James Adjaye. Modelling of bilirubin-induced neuroinflammation using hiPSC-derived brain organoids. Tübingen Stem cells for Disease Modelling and Regeneration, Tübingen, Germany, 2022.

6. **Abida Islam Pranty**, Wasco Wruck, and James Adjaye. Modelling of bilirubin-induced neuroinflammation using hiPSC-derived brain organoids. 13th Internal Meeting, Stem Cell Network North Rhein-Westphalia, Herne, Germany, 2022.

7.3 Journal article

Identification of novel evolutionarily conserved genes and pathways in human and mouse musculoskeletal progenitors

Saravanan S[1], #, Devika A. S[1], #, **Abida Islam Pranty**[4], Shaji R. V[2], Raghu Bhushan[3], James Adjaye[4, 5]*, Smita Sudheer[1], *

BioRxiv (2024)

Abstract:

The axial skeletal system and skeletal muscles of the vertebrates arise from somites, the blocks of tissues flanking both sides of the neural tube. The progenitors of Somites, called the Presomitic Mesoderm (PSM) reside at the posterior end of a developing embryo. Most of our understanding about these two early developmental stages comes from the studies on chick and mouse, and in the recent past, there have been a few studies on human. Here, we have analysed and compared the RNA-sequencing data of PSM and somite tissues from Mouse and Human. The functional and pathway enrichment analysis identified the key Hub-genes that are evolutionarily conserved in the PSM and the somites of both the organisms that include 23 multifunctional genes likely to be associated with different developmental disorders in humans. Our analysis revealed that NOTCH, WNT, MAPK, BMP, Calcium, ErbB, cGMP-PKG, RAS and RAP1 signaling pathways are conserved in both human and mouse during the development of PSM and Somites. Furthermore, we validated the expression of representative conserved candidates in the hESCs-derived PSM and somite cells (NOG, BMP2, BMP7, BMP5, HES5 and MEF2C). Taken together, our study identifies putative gene interactions and pathways that are conserved across the mouse and human genomes, which may potentially have crucial roles in human PSM and somite development.

Author Contribution: 10%

A.I.P. reviewed and edited the manuscript.

Status: Submitted to *BMC Genomics* Journal (under revision).

Pre-print available in the open access pre-print repository *BioRxiv* (doi.org/10.1101/2024.03.14.584954).

Identification of novel evolutionarily conserved genes and pathways in human and mouse musculoskeletal progenitors

Saravanan S[1, #], Devika A. S[1, #], Abida Islam Pranty[4], Shaji R. V[2], Raghu Bhushan[3], James Adjaye[4, 5]*, Smita Sudheer[1, *]

[1]Department of Genomic Science, Central University of Kerala, Tejaswini Hills, Periye. P. O, Kasaragod District, Kerala - 671316, India

[2]The Centre for Stem Cell Research (CSCR), a unit of the Institute for Stem Cell Science and Regenerative Medicine (inStem), Vellore, India

[3]Yenepoya Research Center, Yenepoya (Deemed to be) University, University Road, Deralakatte, Mangalore 575018, Karnataka, India

[4]Institute for Stem Cell Research and Regenerative Medicine, Medical Faculty, Heinrich-Heine University, 40225 Düsseldorf, Germany

[5]University College London –EGA Institute for Women's Health, Zayed Centre for Research into Rare Diseases in Children (ZCR). 20 Guilford Street, London WC1N 1DZ

[#] Equal contribution

*Corresponding Authors

James Adjaye: james.adjaye@med.uni-duesseldorf.de

Smita Sudheer: smitasudheer@cukerala.ac.in

Abstract

The axial skeletal system and skeletal muscles of the vertebrates arise from somites, the blocks of tissues flanking both sides of the neural tube. The progenitors of Somites, called the Presomitic Mesoderm (PSM) reside at the posterior end of a developing embryo. Most of our understanding about these two early developmental stages comes from the studies on chick and mouse, and in the recent past, there have been a few studies on human. Here, we have analysed and compared the RNA-sequencing data of PSM and somite tissues from Mouse and Human. The functional and pathway enrichment analysis identified the key Hub-genes that are evolutionarily conserved in the PSM and the somites of both the organisms that include 23 multifunctional genes likely to be associated with different developmental disorders in humans. Our analysis revealed that NOTCH, WNT, MAPK, BMP, Calcium, ErbB, cGMP-PKG, RAS and RAP1 signaling pathways are conserved in both human and mouse during the development of PSM and Somites. Furthermore,

we validated the expression of representative conserved candidates in the hESCs-derived PSM and somite cells (*NOG*, *BMP2*, *BMP7*, *BMP5*, *HES5* and *MEF2C*). Taken together, our study identifies putative gene interactions and pathways that are conserved across the mouse and human genomes, which may potentially have crucial roles in human PSM and somite development.

Introduction

Gastrulation initiates with the formation of the primitive node and the primitive streak (PS), which allows the rearrangement of epiblast cells, eventually giving rise to the mesoderm and the endoderm lineages. Presomitic mesoderm (PSM), the progenitors of somites that give rise to the axial skeletal system and skeletal muscles, originates in the PS and resides in the posterior end of a developing embryo [1]. The expression of the T-Box Transcription factors, Brachyury (*T*) [2], *Tbx6* [3] and Mesogenin 1 (*Msgn1*) [4,5] and the oscillation of clock genes involved in the segmentation clock are the hallmarks of PSM [4,6]. According to the regulated activity of two independent gene regulatory networks, known as the segmentation clock and the wavefront phenomenon, the mesenchymal PSM cells form new pairs of somites in the anterior end of the PSM [7–9]. The differentiation occurs from the anterior to posterior direction, while the migration of progenitor cells occurs in the posterior to anterior direction. During this process, the pre-segmented PSM remains in the caudal region, and the segmented PSM resides in the rostral region, dividing the PSM into the posterior PSM and the anterior PSM respectively.

Somites pinch off from the rostral end of the PSM in response to the signaling pathways involved in the clock and wavefront phenomenon. The mutually antagonistic activity of the FGF and the retinoic acid (RA) signaling gradients involved in the wavefront model creates a zone of determination where the mesenchymal PSM cells become compacted to form somitomeres [10–12]. These somitomeres undergo mesenchymal to epithelial transition to form somites, with an outer epithelial layer and an inner mesenchymal core. The exposure of various signaling pathways from the surrounding cells induces the differentiation of the nascent somites into the ventromedial sclerotome and the dorsolateral dermomyotome [13,14]. The *Pax1* and *Pax9* positive sclerotome differentiates into the vertebral column and intervertebral disc, where the *Pax3* and *Pax7* positive dermomyotome develops into the skeletal muscle and dermis.

Here, we have analysed the *in vivo*-derived whole transcriptome data of human and mouse PSM and Somites and identified the evolutionarily conserved known and putative signalling pathways

and hub genes, that could potentially have crucial roles in the development of these cell types and their descendants.

Results

Putative regulatory hub genes of mouse interact with the PSM markers, T and MSGN1 and are involved in the signalling pathways, Rap1, PI3K-AKT, MAPK, Hippo, RAS, WNT

Publicly available data of PSM and somites from the mouse E8.25 embryonic stage embryos (E-MTAB-6155) [15] was utilized to find out the hub-genes involved in the PSM and somites. Principal Component Analysis (PCA) of the differentially regulated genes shows that, the posterior PSM (PSM1, PSM2 and PSM3) were clustered together and segregated from the anterior PSM (PSM4 and (PSM5) and somites (Figure 1. a). The most posterior part of the PSM (PSM1) and the somites are the most variant in this trajectory (Figure 1. a).

We performed weighted correlation network analysis (WGCNA) with the differentially expressed genes (DEGs) and selected three clusters (Black cluster, Red cluster and Yellow cluster), based on the presence of known markers of PSM and Somites in these clusters. Gene regulatory networks (GRN) were constructed using STRING, visualized using Cytoscape and hub-genes were identified (Figure 1. b – d, Table S1) [16–18]. Hub-genes are the genes with high connectivity or correlation in a module. Based on the expression of the hub genes, the selected clusters were identified to represent the most posterior end of the PSM (PSM1) (black cluster: the naïve PSM cluster), the anterior-most part of the PSM (PSM5) (red cluster: the mature PSM-Somite cluster) and the Somites (yellow cluster: the mature Somite cluster) (Figure 1. b-e, Table S1). Chip-seq data available from the previously reported studies clearly shows that the candidates in the identified Hub-genes interact with the PS and the PSM markers, T and MSGN1 [4,19] which validates our predictions. Based on this, the pan-mesoderm marker, *T* [19] interacts with some of the Naïve PSM cluster genes (*Bmp4*, *Fbln2*, *Fgf17*, *Fgf8*, *Hhex*, *Msx2* and *Wnt3a*), the Mature PSM-somite cluster genes (*Cdc25b*, *Epas1*, *Epha1*, *Meox1*, *Prkcz* and *Sox18*) and the mature Somite cluster genes (*Cck* and *Foxc1*) (Figure 1. c-e, Table S1). The PSM marker, *MSGN1* [4] interacts with several genes from the three identified Hub-gene clusters: *Fbln2*, *Gata4*, *Myl7*, *Tbx3*, *Gata6* and *Slit1* (Naïve PSM cluster), *Atp8a1*, *Epas1*, *Sparc*, *Flt1*, *Dach1*, *Epha1*, *Fgfr2*, *Msi1*, *Pax3*, *Plcb4* and *Rhof* (Mature PSM-Somite cluster),

Eya1, *Foxc1*, *Myl1*, *Rhobtb1*, *Six1*, *Ahsg*, *Blnk*, *Fkbp5*, *Gucy1a3*, *Magi3*, *Tbxa2r*, *Tubb4a*, *Wnt2b* (Somite cluster) (Figure 1. c-e, Table S1).[3,17].

The functional enrichment analysis of the identified Hub-genes shows that, these genes are important for species-specific DNA-binding, multicellular organism development, transcription factor activity, transcription factor complex activity, cell differentiation, etc. (Figure 1. f, Table S1). The pathway enrichment analysis indicates the involvement of the Hub-genes in various signaling pathways such as Rap1, PI3K-AKT, MAPK, Hippo, RAS, WNT (Figure 1. g, Table S1), which are important for the development and further differentiation of PSM.

T, SALL4 and LEF1 among the hub genes interacting with the PSM markers, TBX6 and MSGN1 and the conservation of Calcium signalling in human somite development

The whole transcriptome dataset of human PSM, somites and developed somites from human embryos of age 4.5–5 weeks of gestation (GSE90876) [20] was used for the identification of DEGs and Hub-genes involved in the development of human musculoskeletal progenitors. The cluster dendrogram indicates the developmental progression of musculoskeletal progenitors from PSM to somites and further into developed Somites (Figure 2. a).

DEGs were subjected to WGCNA clustering, and two clusters were selected (Yellow cluster and Brown cluster), in which the known markers of PSM and somites were clustered (Figure S2). The members of yellow and brown clusters represent the upregulated genes in PSM and in somites respectively (Figure 2. b – d, Table S2). The Hub-genes in the yellow cluster (PSM cluster) contains the PSM markers *TBX6* and *MSGN1* and important genes such as *T*, *MESP2*, *CYP26A1*, *HES7*, *WNT8A*, *SALL4*, *LEF1*, etc. which are expressed or involved in the development of mesoderm or PSM (Figure 2. c, Table S2) [3,5,21–24]. In mouse, SALL4 is important for the maintenance of neuromesodermal progenitors and the proper development of PSM cells [25]. The SALL4 knockout negatively effects the expression of PSM associated genes *T*, *Lef1*, *Msgn1* and *Hes7* [25], and our analysis shows its probable conservation in human somitogenesis. The Hub-genes identified from the brown cluster (Somite cluster) contains somite-associated genes such as *FOXC1*, *MEF2C*, *MYOG*, *PAX7*, etc. (References) (Figure 2. d, Table S2).

The functional enrichment analysis shows that the PSM and Somite Hub-gene clusters are involved in embryo development, transcription regulator activity, embryonic morphogenesis,

species-specific DNA-binding, protein-DNA complex, structural constituent of muscles, etc. (Figure 2. e, Table S2). The pathway enrichment analysis indicates the role of the predicted Hub-genes in various signaling pathways such as WNT, MAPK, Calcium, Hippo, PI3K-AKT and Rap1 which have crucial roles in musculoskeletal progenitor development (Figure 2. f, Table S2). The importance of Calcium signalling in somitogenesis has been deciphered in Zebra fish [26,27]. Calcium signalling is downstream of FGF signalling [28,29], having a prime role in PSM development [26,27,30]. Till date, there is no direct evidence of the involvement of Ca signalling in mouse and human, however, the appearance of Ca signalling genes among the hub genes shows its possible role in human and mouse somitogenesis.

Muscle development genes and the signalling pathways, NOTCH, WNT, MAPK, Calcium, ErbB, cGMP-PKG, RAS and RAP1 are evolutionarily conserved in somitogenesis of mouse and human

To identify the evolutionarily conserved genes involved in mouse and human musculoskeletal progenitor development, the differentially expressed genes (DEGs) between mouse and human were compared (Figure 3. a). A total of 1670 genes were commonly regulated in both the organisms (Figure 3. a, Table S3). Further, the functional enrichment analysis of these 1670 genes in human and mouse databases reveals that the genes are involved in various biological processes such as, Striated muscle tissue development (*DKK1*, *BMP2*, *NOG*, *KLF4*, *BMP7*, *BMP5, T*, *Bmp7*, *Dll1*, *Nog*, *Bmp5*, *Mef2c*), skeletal muscle tissue development (*DLL1*, *DKK1*, *KLF5, Mef2c*, *Dkk1*, *Dll1*), muscle tissue development (*DKK1*, *BMP2*, *NOG*, *KLF4*, *BMP7*, *BMP5, T*, *Bmp7*, *Dll1*, *Nog*, *Bmp5*, *Mef2c*), muscle organ development (*DKK1*, *BMP2*, *TCF15, Mef2c*, *Tcf15*, *Dkk1*, *Nog*), embryonic organ development (*PAX8*, *MEF2C, Cdx4*, *Cdx2*, *Nog*, *Bmp5*, *Dll1*, *Pax8*, *Zic3*) and anterior/posterior pattern specification (*MESP2*, *CDX4*, *MSGN1*, *TBX6*, *CDX2*, *BMP2*, *HES5, Cdx4*, *Cdx2*, *Msgn1*, *Tbx6*, *T*, *Dkk1*, *Zic3*, *Meox1*, *Tcf15*, *Bmp2*, *Hes7*, *Nog*) (Figure 3. a, Table S4). By analysing the list of genes under various biological processes in mouse and human, we found that most of these genes have important roles in the induction of PSM, somitogenesis and the maturation of somites [31–34].

Pathway enrichment analysis was carried out for the commonly regulated 1670 genes and pathway interaction network was constructed with the most significant signaling pathways that were common for both the organisms (Figure 3. c-d, Table S4). The commonly regulated pathways include NOTCH, WNT, MAPK, Calcium, ErbB, cGMP-PKG, RAS and RAP1

signaling. In a developing embryo, FGF, WNT and NOTCH signaling pathways (Figure 3. c-d) interact with *T*, *Tbx6* and *Msgn1* and promotes the differentiation and maintenance of musculoskeletal progenitor [5,35–38]. RAS-MAPK/ERK1/2 signaling cascade is an effector of FGF pathway, important for early embryonic development [39,40]. FGF signaling is involved in somitogenesis and is highly active in the posterior side of a developing embryo which maintains a crosstalk with WNT and NOTCH signaling pathways to sustain the progenitor population in the tail bud [41–45]. Transcriptome data of known and putative clock genes involved in somitogenesis shows that the genes involved in MAPK (*PDGFA*, *NFATC1*, *TGFA*, *DUSP4* and *EFNA1*), RAS (*EFNA1*, *PDGFA*, *TGFA*, *BDNF* and *Foxo4*), RAP-1 (*EFNA1*, *VAV2* and *PDGFA*), WNT (*NFATC1*, *WNT11*, *DKK1*), NOTCH (*Hes5*, *Hes1*, *Dll1*) signaling pathways oscillate during somitogenesis (Figure 3. c-d, Table S4) [32]. In addition to this, calcium, ErbB and cGMP-PKG signaling pathways are important for gastrulation in embryos, differentiation of mesodermal lineages and somitogenesis (Figure 3. c-d, Table S4) [26,27,46–49]. Taken together, from this analysis, we have identified putative genes, pathways, and pathway interaction networks, which are probably conserved among mouse and human skeletal progenitors.

Evolutionarily conserved multifunctional genes involved in the musculoskeletal progenitor development

Evolutionarily conserved multifunctional genes were predicted based on the functional and pathway enrichment analysis of the common 1670 genes identified from the DEGs of mice and humans (Figure 4. e-f, Table S5).

Multifunctional genes are the genes that are associated with more than one function and/or signaling pathway. Such genes tend to be more conserved and associated with human disorders [50]. The identification of multifunctional genes can help us better understand the molecular and functional organization of a cell type. From the gene enrichment analysis of the commonly regulated evolutionarily conserved 1670 genes, 23 multifunctional genes were identified (Figure 4. e-f, Table S5).

To validate the expression of the identified 23 multifunctional genes, human Pluripotent Stem Cells (hPSCs) were differentiated into musculoskeletal progenitors (PS, PSM and somites) (Figure 4. a). The hESCs-induced PS (*EOMES* and *T*: Figure S4 A), PSM (*T*, *TBX6* and

MSGN1: Figure 4. b, d, Figure S4 A) and Somites (*MEOX1*, *MESP2*, *RIPPLY1* and *DLL1*: Figure 4. c, Figure S4. B) were marked and validated by the expression of their representative markers.

From the identified multifunctional genes, the expressions of 8 genes (*ZIC3*, *NOG*, *BMP2*, *BMP7*, *HES5*, *GLI1*, *BMP5* and *MEF2C*) were validated in the hPSC-derived PSM and somite cells (Figure 4. e-g, Table S5). *Hes5*, *Zic3*, *Zic2* and *Foxo4* are important for mesoderm and neural differentiation (Figure 4. e-g, Table S5) [51–54]. *HES5*, *ZIC3* and *Zic2* have a crucial role in the migration of PS cells during gastrulation and in the segmentation clock, the gene regulatory network involved in somitogenesis (Figure 4. e-g, Table S5) [32,52–54]. MEF2C, a member of the MEF2 transcription factor family which regulates several skeletal muscle-specific genes is an early marker for somitogenesis (Figure 4. e-g, Table S5) [55]. *GLI1* (Figure 4. e-g, Table S5), an intracellular signaling transducer, and a transcriptional effector of the Sonic hedgehog (Shh) signaling pathway, is expressed in the neural tube and paraxial mesoderm in the developing embryo (Figure 4. e-g, Table S5) [56]. The BMP and FGF signaling pathways act antagonistic to each other in the developing embryo during PS formation and BMP signaling is important for somite maturation [57]. The members of the BMP signalling, *NOG*, *BMP2*, *BMP7* and *BMP5* were part of the multifunctional genes, and they were also expressed in the hPSC-derived musculoskeletal progenitors (PS, PSM and somites) (Figure 4. e-g, Table S5). The dysregulation of several of the identified multifunctional genes such as *GLI1, HES5, NOG*, *BMP2*, *BMP7*, *BMP5, MEF2C* have implications in the human musculoskeletal developmental disorders, muscular dystrophy, Osteochondrodysplasias and Spondylocostal dysplasia (Figure 4. h, Table S5). Taken together, we have identified evolutionarily conserved multifunctional genes that are regulated during the development of human musculoskeletal progenitors (PS, PSM and somites), with crucial roles in development, having possible implications for human skeletal developmental disorders.

Discussion

In post-implantation embryos, the crosstalk between several gene regulatory networks promotes the differentiation of PSM into somites, the progenitors of the musculoskeletal tissue. The majority of our understanding about PSM and somites comes from the studies on Zebra fish, chick and mouse and there have been only a few studies on human. Therefore, we set out to identify the

evolutionarily conserved genes in human PSM and Somites, by analysing and comparing the whole transcriptome data from these two tissues of human with mouse (E 8.25) and human (4.5–5 weeks of gestation) [15,20]. Here, we identified known and putative genes (hub-genes), signalling pathways and interactions in the human musculoskeletal progenitors, PSM and somites. Finally, our analysis led to the identification of evolutionarily conserved multifunctional genes which have been reported to have implications in human skeletal muscle developmental disorders, such as muscular dystrophy, Osteochondrodysplasias and Spondylocostal dysplasia (Table S5).

In the developing blastula, the crosstalk between BMP, WNT and NODAL signaling creates an anterior–posterior gradient of NODAL and WNT signaling in the epiblast which results in the localized expression of the pan-mesodermal marker *T* and the formation of PS [43,58–61]. The high concentration of Wnt3a in the PS and the tail bud regulates the expression of Fgf8 and promotes epithelial mesenchymal transition (EMT) in the progenitor cells [62,63]. FGF pathway components *Fgf3*, *Fgf4*, *Fgf8* and *Fgf17* are expressed in the tail bud, the mRNA of Fgf3, Fgf8 and Fgf17 creates posterior to anterior gradient with in the PSM and Fgf4 is localized in anterior part of the PSM [45,64–66]. The progenitor cells in the tail bud undergoes EMT and moves from the posterior to anterior end of the embryo according to the gradient created by FGF8 and FGF4 thus helps in the axial elongation in embryos [67,68]. In developing embryo, WNT and FGF signaling pathway acts antagonistic to retinoic acid (RA) pathway by inducing the expression of retinoic acid-metabolizing (inactivating) enzyme CYP26a1 in the posterior PSM [45,69,70].

WNT and FGF signaling pathways promotes the expression of paraxial mesoderm specific genes, *T*, *Tbx6* and *Msgn1* [71–73]. The elevated level of T in PSM cells regulates the expression of Wnt3a and Cyp26a1 in the posterior end [74]. WNT and FGF signaling pathway together with CYP26a1 limits the concentration of RA in the posterior end and creates an anterior to posterior gradient of RA signaling in developing embryo and helps in the migration of PSM cell towards anterior end [45,69,70,75,76]. The reduced activity of FGF pathway from posterior to anterior end created by the opposing activity of RA signaling pathway negatively affects the expression of *Snai* genes in anterior PSM and promotes the expression of integrins or cadherins [42,77,78]. During somitogenesis, Wnt3a act upstream of *Fgf8*, *Dll1*, and *Ctnnb1* components of FGF, NOTCH and WNT signaling pathways respectively and also promotes the expression of negative regulators of the WNT signaling pathway, *Axin2* and *Dkk1* [41]. FGF and NOTCH signaling maintain their oscillations

during somitogenesis by promotes the expression of ERK inhibitors *Dusp4*, *Dusp6*, and *Spry2* and the transcriptional repressor, *Hes7* [6,79–83]. The oscillatory activity of the genes involved in these signaling pathways together creates a zone which promoter the formation the new pair of somites called the determination front characterized by the expression of (Mesp2, Pax3, Foxc1/2, and Meox1/2) [43]. The PSM marker TBX6 together with NOTCH signaling pathway promotes the expression of *Mesp2* in the anterior side of the determination front and creates a positive and negative regulatory loop between TBX6, MESP2 and the NOTCH ligand, Dll1 [10,84–87]. *Pax3*, the marker of segmented mesoderm is regulated by the transcription factors MESP2 and PARAXIS expressed in anterior PSM [88]. The WNT ligands WNT3A, WNT7A and WNT8C secreted from the neighbouring tissues also promotes the expression of Pax3 and Pax7 in developing dermomyotome [89,90].

A comparative approach was used to identify the common DEGs involved in the development of paraxial mesoderm in mouse and human. The gene enrichment analysis indicates that the identified genes were involved in skeletal muscle development and in the signaling pathways involved in this process. The pathway interaction network constricted with the evolutionarily conserved genes includes NOTCH, WNT, MAPK, Calcium, ErbB, cGMP-PKG, RAS and RAP1 Signaling pathways shows the crosstalk between these genes during musculoskeletal development. FGF and WNT signaling pathway collectively regulates the convergent extension (CE) or the cell movement during gastrulation. CE helps in the body axis elongation and the morphogenesis in developing embryos [91]. ErbB signaling pathway is an upstream regulator of PI3K and FGF signaling pathway and its effector, RAS-MAPK/ERK1/2 signaling pathway [49,92]. In gastrulating embryo, ErbB signaling pathway regulates CE through MAPK and PI3K signaling pathway [49]. RAS-MAPK/ERK1/2 and protein kinase C (PKC)/Ca^{2+} signaling pathways, the downstream effectors of FGF signaling pathway. Sprouty and Spred, proteins which modulates the protein kinase C (PKC)/Ca^{2+} and RAS-MAPK/ERK1/2 signaling pathways respectively [28,29,93]. During early gastrulation, Sprouty inhibits protein kinase C (PKC)/Ca^{2+} signaling pathway, hence the RAS-MAPK/ERK1/2 signaling pathway will be active and helps in cell movement in mesoderm formation [28,29,93]. Alternatively, Spred inhibits RAS-MAPK/ERK1/2 signaling pathway during mid to late gastrulation and turns the activity of FGF pathway through protein kinase C (PKC)/Ca^{2+}, which helps in the morphogenesis [28,93].

The evolutionarily conserved multifunctional genes identified to be conserved in both mouse and human are involved in several biological, cellular, and molecular functions. Most of them are known to be involved in the development of paraxial mesoderm and in the regulation or regeneration of skeletal muscles and its progenitors [94–99]. The dysregulation of these genes may cause developmental or functional impairments of musculoskeletal system. NOTCH and BMP/NODAL/ACTIVIN/TGFβ signaling pathways have crucial roles in the formation, maintenance, and differentiation of musculoskeletal and neuronal progenitors. The abnormalities in these signaling pathways lead to several musculoskeletal and neuromuscular impairments such as osteochondrodysplasia, spondylocostal dysplasia, spinal and bulbar muscular atrophy, etc. [52,100–102]. The identified multifunctional genes such as *MEF2C*, *MECOM*, *ZIC2*, *GLI1*, *FOXO1*, *KLF4* are involved in the normal development and differentiation of musculoskeletal progenitors and their developmental impairments by interacting with various signaling pathways or involved in the transcription of lineage specific markers [103–116]. Taken together, the Hub-genes and multifunctional genes identified from the musculoskeletal progenitors of mouse and human are involved in the development and differentiation of paraxial mesoderm. Among the multifunctional genes, we have identified 23 genes conserved between human and mouse, that are crucial for embryonic development, interact with several signaling pathways and when dysregulated, lead to skeletal developmental disorders.

Materials and Methods

Data collection for meta-analysis

The whole transcriptome data of PSM and somites from the mouse embryos (E 8.25) were obtained from the ArrayExpress database [117,118]. The gene expression of posterior to anterior PSM and somites from four different mouse embryos (E-MTAB-6155) (https://www.ebi.ac.uk/arrayexpress/experiments/E-MTAB-6155/samples/?query=presomitic+mesoderm or https://www.ebi.ac.uk/biostudies/arrayexpress/studies/E-MTAB-6155) were considered for this study (Ibarra-Soria et al., 2018). In mouse, the RNA sequencing data of PSM were obtained from the five individual segments from the left and right sides of posterior to anterior axis within the tail bud region [15](Ibarra-Soria et al., 2018). Gene expression data of human PSM and somites were

obtained from Gene Expression Omnibus (GEO) [119]. The human RNA sequencing data were obtained from PSM, somites and developed somites from two different human embryos of age 4.5–5 weeks of gestation (GSE90876) (https://www.ncbi.nlm.nih.gov/geo/query/acc.cgi?acc=GSE90876) [20]. The Human and Mouse whole genome and Gene transfer file (GTF) files were collected from the NCBI database.

Quality Check and Mapping of RNA seq data

FASTQC Version 0.11.5 was used to find out the GC content, total sequence length, and the base sequence quality of each sample. Unlike the original article [20], for indexing the human genome we used HISAT2 (Version 2.1.0) [120]. The Mapping of the indexed Mouse and Human genome was also carried out by HISAT2. Cufflinks (Version 2.2.1) [121] used to assembles the transcripts for the RNA-seq samples, where we have found out the FPKM (Fragments per Kilobase of exon per million mapped fragments) for each sample.

Principle component analysis (PCA) and hierarchical clustering

Principle component analysis (PCA) was done using R package, in which the similarities and dissimilarities between the samples and its replicates were plotted. Using FPKM values, the hierarchical clustering analysis was conducted to show the similar gene expression status of the samples using R packages.

Differential expression analysis

To find out the differently expressed genes involved in musculoskeletal progenitor development, we used DESeq (Version 1.26.0). Using the raw read counts, the gene expression between samples were identified and filtered based on P-value < 0.05 and the upregulated and downregulated genes were filtered with a threshold of the log2 fold change ≥ 1 and ≤ -1 respectively.

Co-expression Network Construction

Using DEGs identified from the human and mouse data sets, weighted gene co-expression network analysis (WGCNA) with R packages (Version 1.70.3) was performed to find out the modules cluster of genes that are highly correlated. The modules with genes clustered along with the known markers of musculoskeletal progenitors were considered for the further analysis.

Identification of Hub-genes and Functional Annotation

Hub-genes are the genes which shows high connectivity or correlation between the genes in the candidate module. To identify the hub-genes, a protein-protein interaction network (PPI) was constricted with search tool for the retrieval of interacting genes (STRING) [16,122] and visualized using Cytoscape (Version 3.8.2) [17]. The hub-genes used for the PPI were selected based on "OR" condition on Betweenness >10, closeness <0.001, and Degree >2. The functional enrichment analysis was performed using the Database for Annotation, Visualization, and Integrated Discovery (DAVID) [123].

Heat map and plot construction

The expression status of each gene in each sample were represented in heatmap constricted using Gplot (R package, Version 3.1.3). The circus plot representing the involvement of hub-genes in various signaling pathways and the bubble plot were generated with GOplot (R package, Version 1.0.2). The bubble plot representing the functional enrichment analysis was constructed against the genes counts and the p-values of each identified function.

Pathway interaction network construction

Functional and pathway enrichment analysis were performed for evolutionarily conserved genes identified from mouse and human using ClusterProfiler (R package, Version 3.14.3) (https://bioconductor.org/packages/release/bioc/html/clusterProfiler.html). The representatives of functional enrichment analysis were visualized using dotplot. The results obtained from pathway enrichment analysis was represented as pathway interaction network using cnetplot.

Maintenance and Differentiation of human pluripotent stem cells (hPSCs):

The human embryonic stem cell (hESCs) (BJNhem19 (JNCASRe001-A)) line was procured from Jawaharlal Nehru Centre for Advanced Scientific Research (JNCASR), India. The human-induced pluripotent stem cell (hiPSCs) (D14C2) line was a kind gift from Dr. R. V. Shaji, Centre for Stem Cell Research, (CSCR), InStem, India. hESCs and hiPSC was maintained on vitronectin (VTN) (Gibco, A14700) in presence of Essential 8™ (E8) Medium (Gibco, A1517001). The cells were

routinely passaged in 1:6 ratio in every 4 days using 0.5 mM EDTA (Gibco, 15575020) solution during maintenance.

For PS induction, hESCs were exposed to CHIR99021 (CH), inhibitor of GSK-3β for 24 hours and marked by the expression of *EOMES* and *T* (Figure 4. a, Figure S4 A). After PS induction, the cells were exposed to CH (GSK-3β inhibitor), SB431542 (SB) (ALK 4/5/7 inhibitor) and bFGF (C/S/F) for 4 days and detected the expression of PSM markers *TBX6* and *MSGN1* together with the pan-mesodermal marker T (Figure 4. a-b, Figure S4 A). Due to C/S/F treatment for 4 days, the expression the endoderm marker *EOMES* were downregulated, and the expression of pan-mesodermal marker *T* remains unaffected (Figure S4. A). PSM was further differentiated to somites using FGFR inhibitor PD173074 (PD) and WNT pathway inhibitor XAV939 (XAV) [32] and confirmed by the expression of *MEOX1*, *MESP2*, *RIPPLY1* and TCF15/PARAXIS (Figure 4. a, c, Figure S4. B).

Real-Time PCR analysis

Total RNA was isolated using QIAzol Lysis Reagent (QIAGEN, 79306) according to manufactures' instruction, followed by quantification using NanoDrop Spectrophotometer (Thermo Fisher Scientific). Reverse transcription was performed with the iScriptTM cDNA Synthesis Kit (Bio-Rad, 1708891). Quantitative Real-Time PCR (qRT-PCR) was done using PowerUp™ SYBR™ Green Master Mix (2X) (Applied Biosystems, A25776) with gene-specific primers (Table S6) in a thermal cycler (Roche Light Cycler 480). Data was analysed using the ddCt method, with the house-keeping gene, *ACTB*.

Data availability

All data utilized for this study are publicly available data sets from previous publications (E-MTAB-6155, GSE90876)[15,20]. The data that supports the findings of this study are available within this manuscript and in supplementary documents.

List of Figures

Figure 1. Gene expression and regulation in the mouse PSM and somites (a) PCA of mouse PSM from posterior to anterior axis (PSM 1 to PSM5) and somites. Hub-genes were identified from the gene regulatory network analysis of the selected WGCNA clusters (b) Heatmap showing the expression status of Hub-genes identified from the selected clusters (c) Naïve PSM cluster (Black (Figure S1)) (d) Mature PSM-Somites cluster (Red (Figure S1)) and (e)

Somites cluster (Yellow (Figure S1)). Functional enrichment analysis of the Hub-genes shows their involvement in different (f) biological, cellular and molecular functions and in (g) signaling pathways

Figure 2. Gene expression and regulation in the human PSM and somites (a) Cluster dendrogram of human PSM, somites and developed somites. From the Gene regulatory network analysis of selected WGCNA clusters, Hub-genes were identified (b) Heatmap indicating the expression status of Hub-genes identified from the selected clusters (c) PSM cluster (Yellow (Figure S2)) (d) Somite cluster (Brown (Figure S2)). Functional enrichment analysis of the Hub-genes shows their involvement in different (e) biological, cellular and molecular functions and in (f) signaling pathways

Figure 3. Evolutionarily conserved gene and pathway interaction network (a) Venn diagram of mouse and human DEGs, (b) Biological process for evolutionarily conserved genes in human, (c) Pathway interaction network of evolutionarily conserved genes in mouse, (d) Pathway interaction network of evolutionarily conserved genes in human

Figure 4. Evolutionarily conserved multifunctional genes and its validation using *in vitro* derived musculoskeletal progenitors from hESCs (a) schematic representation of *in vitro* derived musculoskeletal progenitors from hESCs (b-c) RT-qPCR of PSM and somite markers of indicated samples. Data are Mean ± s.d., n=2, (d) Immunocytochemistry image of T and TBX6 in indicated samples, (e-f) Heatmap showing the expression status of the predicted evolutionarily conserved multifunctional genes in (e) mouse and (f) human (g) RT-qPCR validation of the predicted evolutionarily conserved multifunctional genes in *in vitro* derived human musculoskeletal progenitors. Data are Mean ± s.d., n=2, (h) Heatmap represents the involvement of multifunctional genes in indicated developmental impairments based on their corresponding evident score. Graphs shown in (b-c) and (g) are representatives of two independent technical replicates.

List of supplementary tables

Table S1: Hub-genes; List of Hub-genes identified as Naïve PSM cluster, Mature PSM-Somite cluster and the Somite cluster – Include the details of GRN, pathway and functional enrichment analysis

Table S2: Hub-genes; List of Hub-genes identified as Naïve PSM cluster, Mature PSM-Somite cluster and the Somite cluster – Include the details of GRN, pathway and functional enrichment analysis

Table S3: List of commonly regulated genes in Mouse and Human

Table S4: Pathway and functional enrichment analysis of commonly regulated genes in Mouse and Human

Table S5: List of Evolutionarily conserved multifunctional genes and their involvement in developmental impairments

Table S6: List of Primers

References

1 Bénazéraf B, Pourquié O. Formation and segmentation of the vertebrate body axis. *Annu Rev Cell Dev Biol* 2013; **29**: 1–26.
2 Herrmann BG, Labeit S, Poustka A, King TR, Lehrach H. Cloning of the T gene required in mesoderm formation in the mouse. *Nature* 1990; **343**: 617–622.
3 Chapman DL, Agulnik I, Hancock S, Silver LM, Papaioannou VE. Tbx6, a mouse T-Box gene implicated in paraxial mesoderm formation at gastrulation. *Dev Biol* 1996; **180**: 534–542.
4 Chalamalasetty RB, Garriock RJ, Dunty WCJ, Kennedy MW, Jailwala P, Si H *et al.* Mesogenin 1 is a master regulator of paraxial presomitic mesoderm differentiation. *Development* 2014; **141**: 4285–4297.
5 Wittler L, Shin E, Grote P, Kispert A, Beckers A, Gossler A *et al.* Expression of Msgn1 in the presomitic mesoderm is controlled by synergism of WNT signalling and Tbx6. *EMBO Rep* 2007; **8**: 784–789.
6 Hubaud A, Pourquié O. Signalling dynamics in vertebrate segmentation. *Nat Rev Mol Cell Biol* 2014; **15**: 709–721.
7 Cooke J, Zeeman EC. A clock and wavefront model for control of the number of repeated structures during animal morphogenesis. *J Theor Biol* 1976; **58**: 455–476.
8 Pourquié O. Vertebrate somitogenesis. *Annu Rev Cell Dev Biol* 2001; **17**: 311–350.
9 Aulehla A, Herrmann BG. Segmentation in vertebrates: clock and gradient finally joined. *Genes Dev* 2004; **18**: 2060–2067.
10 Oginuma M, Niwa Y, Chapman DL, Saga Y. Mesp2 and Tbx6 cooperatively create periodic patterns coupled with the clock machinery during mouse somitogenesis. *Development* 2008; **135**: 2555 LP – 2562.
11 Moreno TA, Kintner C. Regulation of segmental patterning by retinoic acid signaling during Xenopus somitogenesis. *Dev Cell* 2004; **6**: 205–218.
12 Dubrulle J, McGrew MJ, Pourquié O. FGF signaling controls somite boundary position and regulates segmentation clock control of spatiotemporal Hox gene activation. *Cell* 2001; **106**: 219–232.
13 Christ B, Huang R, Scaal M. Amniote somite derivatives. *Dev Dyn* 2007; **236**: 2382–2396.

14 Yusuf F, Brand-Saberi B. The eventful somite: patterning, fate determination and cell division in the somite. *Anat Embryol (Berl)* 2006; **211 Suppl**: 21–30.
15 Ibarra-Soria X, Jawaid W, Pijuan-Sala B, Ladopoulos V, Scialdone A, Jörg DJ *et al.* Defining murine organogenesis at single-cell resolution reveals a role for the leukotriene pathway in regulating blood progenitor formation. *Nat Cell Biol* 2018; **20**: 127–134.
16 Szklarczyk D, Gable AL, Lyon D, Junge A, Wyder S, Huerta-Cepas J *et al.* STRING v11: Protein-protein association networks with increased coverage, supporting functional discovery in genome-wide experimental datasets. *Nucleic Acids Res* 2019; **47**. doi:10.1093/nar/gky1131.
17 Shannon P, Markiel A, Ozier O, Baliga NS, Wang JT, Ramage D *et al.* Cytoscape: A software Environment for integrated models of biomolecular interaction networks. *Genome Res* 2003; **13**. doi:10.1101/gr.1239303.
18 Doncheva NT, Morris JH, Gorodkin J, Jensen LJ. Cytoscape StringApp: Network Analysis and Visualization of Proteomics Data. *J Proteome Res* 2019; **18**. doi:10.1021/acs.jproteome.8b00702.
19 Koch F, Scholze M, Wittler L, Schifferl D, Sudheer S, Grote P *et al.* Antagonistic Activities of Sox2 and Brachyury Control the Fate Choice of Neuro-Mesodermal Progenitors. *Dev Cell* 2017; **42**: 514-526.e7.
20 Xi H, Fujiwara W, Gonzalez K, Jan M, Liebscher S, Van Handel B *et al.* In Vivo Human Somitogenesis Guides Somite Development from hPSCs. *Cell Rep* 2017; **18**: 1573–1585.
21 Cunningham TJ, Kumar S, Yamaguchi TP, Duester G. Wnt8a and Wnt3a cooperate in the axial stem cell niche to promote mammalian body axis extension. *Dev Dyn* 2015; **244**: 797–807.
22 Tsankov AM, Gu H, Akopian V, Ziller MJ, Donaghey J, Amit I *et al.* Transcription factor binding dynamics during human ES cell differentiation. *Nature* 2015; **518**: 344–349.
23 Wilkinson DG, Bhatt S, Herrmann BG. Expression pattern of the mouse T gene and its role in mesoderm formation. *Nature* 1990; **343**: 657–659.
24 Tani S, Chung U-I, Ohba S, Hojo H. Understanding paraxial mesoderm development and sclerotome specification for skeletal repair. *Exp Mol Med* 2020; **52**: 1166–1177.
25 Tahara N, Kawakami H, Chen KQ, Anderson A, Peterson MY, Gong W *et al.* Sall4 regulates neuromesodermal progenitors and their descendants during body elongation in mouse embryos. *Development (Cambridge)* 2019; **146**. doi:10.1242/DEV.177659.
26 Webb SE, Miller AL. Calcium signalling during zebrafish embryonic development. BioEssays. 2000; **22**. doi:10.1002/(SICI)1521-1878(200002)22:2<113::AID-BIES3>3.0.CO;2-L.
27 Créton R, Speksnijder JE, Jaffe LF. Patterns of free calcium in zebrafish embryos. *J Cell Sci* 1998; **111**. doi:10.1242/jcs.111.12.1613.
28 Sivak JM, Petersen LF, Amaya E. FGF signal interpretation is directed by sprouty and spred proteins during mesoderm formation. *Dev Cell* 2005; **8**. doi:10.1016/j.devcel.2005.02.011.
29 Nutt SL, Dingwell KS, Holt CE, Amaya E. Xenopus sprouty2 inhibits FGF-mediated gastrulation movements but does not affect mesoderm induction and patterning. *Genes Dev* 2001; **15**. doi:10.1101/gad.191301.
30 Slusarski DC, Pelegri F. Calcium signaling in vertebrate embryonic patterning and morphogenesis. Dev Biol. 2007; **307**. doi:10.1016/j.ydbio.2007.04.043.

31 Diaz-Cuadros M, Wagner DE, Budjan C, Hubaud A, Tarazona OA, Donelly S *et al.* In vitro characterization of the human segmentation clock. *Nature* 2020; **580**: 113–118.

32 Matsuda M, Yamanaka Y, Uemura M, Osawa M, Saito MK, Nagahashi A *et al.* Recapitulating the human segmentation clock with pluripotent stem cells. *Nature* 2020; **580**: 124–129.

33 Chu L-F, Mamott D, Ni Z, Bacher R, Liu C, Swanson S *et al.* An In Vitro Human Segmentation Clock Model Derived from Embryonic Stem Cells. *Cell Rep* 2019; **28**: 2247-2255.e5.

34 van den Brink SC, Alemany A, van Batenburg V, Moris N, Blotenburg M, Vivié J *et al.* Single-cell and spatial transcriptomics reveal somitogenesis in gastruloids. *Nature* 2020. doi:10.1038/s41586-020-2024-3.

35 Nowotschin S, Ferrer-Vaquer A, Concepcion D, Papaioannou VE, Hadjantonakis A-K. Interaction of Wnt3a, Msgn1 and Tbx6 in neural versus paraxial mesoderm lineage commitment and paraxial mesoderm differentiation in the mouse embryo. *Dev Biol* 2012; **367**: 1–14.

36 Chalamalasetty RB, Dunty WCJ, Biris KK, Ajima R, Iacovino M, Beisaw A *et al.* The Wnt3a/β-catenin target gene Mesogenin1 controls the segmentation clock by activating a Notch signalling program. *Nat Commun* 2011; **2**: 390.

37 Hofmann M, Schuster-Gossler K, Watabe-Rudolph M, Aulehla A, Herrmann BG, Gossler A. WNT signaling, in synergy with T/TBX6, controls Notch signaling by regulating Dll1 expression in the presomitic mesoderm of mouse embryos. *Genes Dev* 2004; **18**. doi:10.1101/gad.1248604.

38 White PH, Farkas DR, Chapman DL. Regulation of Tbx6 expression by Notch signaling. *Genesis* 2005; **42**: 61–70.

39 Hardy KM, Yatskievych TA, Konieczka J, Bobbs AS, Antin PB. FGF signalling through RAS/MAPK and PI3K pathways regulates cell movement and gene expression in the chicken primitive streak without affecting E-cadherin expression. *BMC Dev Biol* 2011; **11**. doi:10.1186/1471-213X-11-20.

40 Lunn JS, Fishwick KJ, Halley PA, Storey KG. A spatial and temporal map of FGF/Erk1/2 activity and response repertoires in the early chick embryo. *Dev Biol* 2007; **302**. doi:10.1016/j.ydbio.2006.10.014.

41 Aulehla A, Wehrle C, Brand-Saberi B, Kemler R, Gossler A, Kanzler B *et al.* Wnt3a plays a major role in the segmentation clock controlling somitogenesis. *Dev Cell* 2003; **4**: 395–406.

42 Ciruna B, Rossant J. FGF Signaling Regulates Mesoderm Cell Fate Specification and Morphogenetic Movement at the Primitive Streak. *Dev Cell* 2001; **1**: 37–49.

43 Chal J, Pourquié O. Making muscle: skeletal myogenesis in vivo and in vitro *Development* 2017; **144**: 2104 LP – 2122.

44 Yamaguchi TP, Harpal K, Henkemeyer M, Rossant J. Fgfr-1 Is Required for Embryonic Growth and Mesodermal Patterning During Mouse Gastrulation. *Genes Dev* 1994; **8**: 3032–3044.

45 Wahl MB, Deng C, Lewandoski M, Pourquié O. FGF signaling acts upstream of the NOTCH and WNT signaling pathways to control segmentation clock oscillations in mouse somitogenesis. *Development* 2007; **134**: 4033–4041.

46 Mujoo K, Krumenacker JS, Murad F. Nitric oxide-cyclic GMP signaling in stem cell differentiation. Free Radic Biol Med. 2011; **51**. doi:10.1016/j.freeradbiomed.2011.09.037.

47 Cazzato D, Assi E, Moscheni C, Brunelli S, de Palma C, Cervia D *et al.* Nitric oxide drives embryonic myogenesis in chicken through the upregulation of myogenic differentiation factors. *Exp Cell Res* 2014; **320**. doi:10.1016/j.yexcr.2013.11.006.

48 Nie S, Chang C. Regulation of Xenopus gastrulation by ErbB signaling. *Dev Biol* 2007; **303**. doi:10.1016/j.ydbio.2006.10.039.

49 Nie S, Chang C. PI3K and Erk MAPK mediate ErbB signaling in Xenopus gastrulation. *Mech Dev* 2007; **124**. doi:10.1016/j.mod.2007.07.005.

50 Pritykin Y, Ghersi D, Singh M. Genome-Wide Detection and Analysis of Multifunctional Genes. *PLoS Comput Biol* 2015; **11**. doi:10.1371/journal.pcbi.1004467.

51 Vilchez D, Boyer L, Lutz M, Merkwirth C, Morantte I, Tse C *et al.* FOXO4 is necessary for neural differentiation of human embryonic stem cells. *Aging Cell* 2013; **12**. doi:10.1111/acel.12067.

52 Dunwoodie SL, Clements M, Sparrow DB, Sa X, Conlon RA, Beddington RSP. Axial skeletal defects caused by mutation in the spondylocostal dysplasia/pudgy gene Dll3 are associated with disruption of the segmentation clock within the presomitic mesoderm. Development. 2002; **129**. doi:10.1242/dev.129.7.1795.

53 Sutherland MJ, Wang S, Quinn ME, Haaning A, Ware SM. Zic3 is required in the migrating primitive streak for node morphogenesis and left-right patterning. *Hum Mol Genet* 2013; **22**. doi:10.1093/hmg/ddt001.

54 Inoue T, Ota M, Mikoshiba K, Aruga J. Zic2 and Zic3 synergistically control neurulation and segmentation of paraxial mesoderm in mouse embryo. *Dev Biol* 2007; **306**. doi:10.1016/j.ydbio.2007.04.003.

55 Ticho BS, Stainier DYR, Fishman MC, Breitbart RE. Three zebrafish MEF2 genes delineate somitic and cardiac muscle development in wild-type and mutant embryos. *Mech Dev* 1996; **59**. doi:10.1016/0925-4773(96)00601-6.

56 Murashima A, Akita H, Okazawa M, Kishigami S, Nakagata N, Nishinakamura R *et al.* Midline-derived shh regulates mesonephric tubule formation through the paraxial mesoderm. *Dev Biol* 2014; **386**. doi:10.1016/j.ydbio.2013.12.026.

57 Miura S, Davis S, Klingensmith J, Mishina Y. BMP signaling in the epiblast is required for proper recruitment of the prospective paraxial mesoderm and development of the somites. *Development* 2006; **133**. doi:10.1242/dev.02552.

58 Shahbazi MN, Zernicka-Goetz M. Deconstructing and reconstructing the mouse and human early embryo. *Nat Cell Biol* 2018; **20**: 878–887.

59 Yamamoto M, Saijoh Y, Perea-Gomez A, Shawlot W, Behringer RR, Ang S-L *et al.* Nodal antagonists regulate formation of the anteroposterior axis of the mouse embryo. *Nature* 2004; **428**: 387–392.

60 Arnold SJ, Robertson EJ. Making a commitment: Cell lineage allocation and axis patterning in the early mouse embryo. *Nat Rev Mol Cell Biol* 2009; **10**: 91–103.

61 Rivera-Pérez JA, Magnuson T. Primitive streak formation in mice is preceded by localized activation of Brachyury and Wnt3. *Dev Biol* 2005; **288**: 363–371.

62 Takada S, Stark KL, Shea MJ, Vassileva G, McMahon JA, McMahon AP. Wnt-3a regulates somite and tailbud formation in the mouse embryo. *Genes Dev* 1994; **8**. doi:10.1101/gad.8.2.174.

63 Sun X, Meyers EN, Lewandoski M, Martin GR. Targeted disruption of Fgf8 causes failure of cell migration in the gastrulating mouse embryo. *Genes Dev* 1999; **13**: 1834–1846.

64 Crossley PH, Martin GR. The mouse Fgf8 gene encodes a family of polypeptides and is expressed in regions that direct outgrowth and patterning in the developing embryo. *Development* 1995; **121**. doi:10.1242/dev.121.2.439.

65 Maruoka Y, Ohbayashi N, Hoshikawa M, Itoh N, Hogan BL m., Furuta Y. Comparison of the expression of three highly related genes, Fgf8, Fgf17 and Fgf18, in the mouse embryo. *Mech Dev* 1998; **74**. doi:10.1016/S0925-4773(98)00061-6.

66 Niswander L, Martin GR. Fgf-4 expression during gastrulation, myogenesis, limb and tooth development in the mouse. *Development* 1992; **114**. doi:10.1242/dev.114.3.755.

67 Yang X, Dormann D, Münsterberg AE, Weijer CJ. Cell movement patterns during gastrulation in the chick are controlled by positive and negative chemotaxis mediated by FGF4 and FGF8. *Dev Cell* 2002; **3**. doi:10.1016/S1534-5807(02)00256-3.

68 Boulet AM, Capecchi MR. Signaling by FGF4 and FGF8 is required for axial elongation of the mouse embryo. *Dev Biol* 2012; **371**: 235–245.

69 Diez del Corral R, Storey KG. Opposing FGF and retinoid pathways: a signalling switch that controls differentiation and patterning onset in the extending vertebrate body axis. *Bioessays* 2004; **26**: 857–869.

70 Kudoh T, Wilson SW, Dawid IB. Distinct roles for Fgf, Wnt and retinoic acid in posteriorizing the neural ectoderm. *Development* 2002; **129**: 4335–4346.

71 Yamaguchi TP, Takada S, Yoshikawa Y, Wu N, McMahon AP. T (Brachyury) is a direct target of Wnt3a during paraxial mesoderm specification. *Genes Dev* 1999; **13**: 3185–3190.

72 Wittler L, Shin EH, Grote P, Kispert A, Beckers A, Gossler A *et al.* Expression of Msgn1 in the presomitic mesoderm is controlled by synergism of WNT signalling and Tbx6. *EMBO Rep* 2007; **8**: 784–789.

73 Sudheer S, Liu J, Marks M, Koch F, Anurin A, Scholze M *et al.* Different Concentrations of FGF Ligands, FGF2 or FGF8 Determine Distinct States of WNT-Induced Presomitic Mesoderm. *Stem Cells* 2016; **34**. doi:10.1002/stem.2371.

74 Martin BL, Kimelman D. Brachyury establishes the embryonic mesodermal progenitor niche. *Genes Dev* 2010; **24**: 2778–2783.

75 Aulehla A, Pourquié O. Signaling gradients during paraxial mesoderm development. *Cold Spring Harb Perspect Biol* 2010; **2**: a000869.

76 Aulehla A, Wiegraebe W, Baubet V, Wahl MB, Deng C, Taketo M *et al.* A beta-catenin gradient links the clock and wavefront systems in mouse embryo segmentation. *Nat Cell Biol* 2008; **10**: 186–193.

77 Dale JK, Malapert P, Chal J, Vilhais-Neto G, Maroto M, Johnson T *et al.* Oscillations of the snail genes in the presomitic mesoderm coordinate segmental patterning and morphogenesis in vertebrate somitogenesis. *Dev Cell* 2006; **10**: 355–366.

78 Rifes P, Carvalho L, Lopes C, Andrade RP, Rodrigues G, Palmeirim I *et al.* Redefining the role of ectoderm in somitogenesis: a player in the formation of the fibronectin matrix of presomitic mesoderm. *Development* 2007; **134**: 3155–3165.

79 Yabe T, Takada S. Molecular mechanism for cyclic generation of somites: Lessons from mice and zebrafish. *Dev Growth Differ* 2016; **58**: 31–42.

80 Bessho Y, Hirata H, Masamizu Y, Kageyama R. Periodic repression by the bHLH factor Hes7 is an essential mechanism for the somite segmentation clock. *Genes Dev* 2003; **17**: 1451–1456.

81 Matsumiya M, Tomita T, Yoshioka-Kobayashi K, Isomura A, Kageyama R. ES cell-derived presomitic mesoderm-like tissues for analysis of synchronized oscillations in the segmentation clock. *Development* 2018; **145**. doi:10.1242/dev.156836.

82 Niwa H, Ogawa K, Shimosato D, Adachi K. A parallel circuit of LIF signalling pathways maintains pluripotency of mouse ES cells. *Nature* 2009; **460**: 118–122.

83 Harima Y, Kageyama R. Oscillatory links of Fgf signaling and Hes7 in the segmentation clock. *Curr Opin Genet Dev* 2013; **23**: 484–490.

84 Oginuma M, Takahashi Y, Kitajima S, Kiso M, Kanno J, Kimura A *et al.* The oscillation of Notch activation, but not its boundary, is required for somite border formation and rostral-caudal patterning within a somite. *Development* 2010; **137**: 1515–1522.

85 Saga Y. Segmental border is defined by the key transcription factor Mesp2, by means of the suppression of Notch activity. *Dev Dyn* 2007; **236**: 1450–1455.

86 Sasaki N, Kiso M, Kitagawa M, Saga Y. The repression of Notch signaling occurs via the destabilization of mastermind-like 1 by Mesp2 and is essential for somitogenesis. *Development* 2011; **138**: 55–64.

87 Yasuhiko Y, Haraguchi S, Kitajima S, Takahashi Y, Kanno J, Saga Y. Tbx6-mediated Notch signaling controls somite-specific Mesp2 expression. *Proc Natl Acad Sci U S A* 2006; **103**: 3651–3656.

88 Takahashi Y, Takagi A, Hiraoka S, Koseki H, Kanno J, Rawls A *et al.* Transcription factors Mesp2 and Paraxis have critical roles in axial musculoskeletal formation. *Developmental Dynamics* 2007; **236**. doi:10.1002/dvdy.21178.

89 Tajbakhsh S, Borello U, Vivarelli E, Kelly R, Papkoff J, Duprez D *et al.* Differential activation of Myf5 and MyoD by different Wnts in explants of mouse paraxial mesoderm and the later activation of myogenesis in the absence of Myf5. *Development* 1998; **125**: 4155–4162.

90 Ikeya M, Takada S. Wnt signaling from the dorsal neural tube is required for the formation of the medial dermomyotome. *Development* 1998; **125**: 4969–4976.

91 Wallingford JB, Fraser SE, Harland RM. Convergent extension: The molecular control of polarized cell movement during embryonic development. Dev Cell. 2002; **2**. doi:10.1016/S1534-5807(02)00197-1.

92 Schlessinger J. SH2/SH3 signaling proteins. *Curr Opin Genet Dev* 1994; **4**. doi:10.1016/0959-437X(94)90087-6.

93 Dorey K, Amaya E. FGF signalling: diverse roles during early vertebrate embryogenesis. *Development* 2010; **137**: 3731–3742.

94 Lee H-J, Göring W, Ochs M, Mühlfeld C, Steding G, Paprotta I *et al.* Sox15 Is Required for Skeletal Muscle Regeneration. *Mol Cell Biol* 2004; **24**. doi:10.1128/mcb.24.19.8428-8436.2004.

95 Meeson AP, Shi X, Alexander MS, Williams RS, Allen RE, Jiang N *et al.* Sox15 and Fhl3 transcriptionally coactivate Foxk1 and regulate myogenic progenitor cells. *EMBO Journal* 2007; **26**. doi:10.1038/sj.emboj.7601635.

96 van Nes J, de Graaff W, Lebrin F, Gerhard M, Beck F, Deschamps J. The Cdx4 mutation affects axial development and reveals an essential role of Cdx genes in the ontogenesis of the placental labyrinth in mice. *Development* 2006; **133**. doi:10.1242/dev.02216.

97 Pan H, Gustafsson MK, Aruga J, Tiedken JJ, Jennifer JC, Emerson CP. A role for Zic1 and Zic2 in Myf5 regulation and somite myogenesis. *Dev Biol* 2011; **351**. doi:10.1016/j.ydbio.2010.12.037.

98 Odaka YS, Tohmonda T, Toyoda A, Aruga J. An Evolutionarily Conserved Mesodermal Enhancer in Vertebrate Zic3. *Sci Rep* 2018; **8**. doi:10.1038/s41598-018-33235-y.

99 Reshef R, Maroto M, Lassar AB. Regulation of dorsal somitic cell fates: BMPs and Noggin control the timing and pattern of myogenic regulator expression. *Genes Dev* 1998; **12**: 290–303.

100 Kondo N, Tohnai G, Sahashi K, Iida M, Kataoka M, Nakatsuji H *et al.* DNA methylation inhibitor attenuates polyglutamine-induced neurodegeneration by regulating Hes5. *EMBO Mol Med* 2019; **11**. doi:10.15252/emmm.201708547.

101 Long F, Shi H, Li P, Guo S, Ma Y, Wei S *et al.* A SMOC2 variant inhibits BMP signaling by competitively binding to BMPR1B and causes growth plate defects. *Bone* 2021; **142**. doi:10.1016/j.bone.2020.115686.

102 Gomez-Puerto MC, Iyengar PV, García de Vinuesa A, ten Dijke P, Sanchez-Duffhues G. Bone morphogenetic protein receptor signal transduction in human disease. Journal of Pathology. 2019; **247**. doi:10.1002/path.5170.

103 Ma X, Su P, Yin C, Lin X, Wang X, Gao Y *et al.* The roles of foxo transcription factors in regulation of bone cells function. Int J Mol Sci. 2020; **21**. doi:10.3390/ijms21030692.

104 Sanchez AMJ, Candau RB, Bernardi H. FoxO transcription factors: Their roles in the maintenance of skeletal muscle homeostasis. Cellular and Molecular Life Sciences. 2014; **71**. doi:10.1007/s00018-013-1513-z.

105 Teixeira CC, Liu Y, Thant LM, Pang J, Palmer G, Alikhani M. Foxo1, a novel regulator of osteoblast differentiation and skeletogenesis. *Journal of Biological Chemistry* 2010; **285**. doi:10.1074/jbc.M109.079962.

106 Yu S, Guo J, Sun Z, Lin C, Tao H, Zhang Q *et al.* BMP2-dependent gene regulatory network analysis reveals Klf4 as a novel transcription factor of osteoblast differentiation. *Cell Death Dis* 2021; **12**. doi:10.1038/s41419-021-03480-7.

107 Lyu Y, Nakano K, Davis RR, Tepper CG, Campbell M, Izumiya Y. ZIC2 Is Essential for Maintenance of Latency and Is a Target of an Immediate Early Protein during Kaposi's Sarcoma-Associated Herpesvirus Lytic Reactivation. *J Virol* 2017; **91**. doi:10.1128/jvi.00980-17.

108 Salhotra A, Shah HN, Levi B, Longaker MT. Mechanisms of bone development and repair. Nat Rev Mol Cell Biol. 2020; **21**. doi:10.1038/s41580-020-00279-w.

109 Juneja SC, Vonica A, Zeiss C, Lezon-Geyda K, Yatsula B, Sell DR *et al.* Deletion of mecom in mouse results in early-onset spinal deformity and osteopenia. *Bone* 2014; **60**. doi:10.1016/j.bone.2013.11.020.

110 Dey BK, Mueller AC, Dutta A. Long non-coding rnas as emerging regulators of differentiation, development, and disease. Transcription. 2014; **5**. doi:10.4161/21541272.2014.944014.

111 Piasecka A, Sekrecki M, Szcześniak MW, Sobczak K. MEF2C shapes the microtranscriptome during differentiation of skeletal muscles. *Sci Rep* 2021; **11**. doi:10.1038/s41598-021-82706-2.

112 Chen X, Gao B, Ponnusamy M, Lin Z, Liu J. MEF2 signaling and human diseases. Oncotarget. 2017; **8**. doi:10.18632/oncotarget.22899.

113 Arnold MA, Kim Y, Czubryt MP, Phan D, McAnally J, Qi X *et al.* MEF2C Transcription Factor Controls Chondrocyte Hypertrophy and Bone Development. *Dev Cell* 2007; **12**. doi:10.1016/j.devcel.2007.02.004.

114 Kan C, Chen L, Hu Y, Ding N, Li Y, McGuire TL *et al.* Gli1-labeled adult mesenchymal stem/progenitor cells and hedgehog signaling contribute to endochondral heterotopic ossification. *Bone* 2018; **109**. doi:10.1016/j.bone.2017.06.014.
115 Park HL, Bai C, Platt KA, Matise MP, Beeghly A, Hui CC *et al.* Mouse Gli1 mutants are viable but have defects in SHH signaling in combination with a Gli2 mutation. *Development* 2000; **127**. doi:10.1242/dev.127.8.1593.
116 Houtmeyers R, Souopgui J, Tejpar S, Arkell R. The ZIC gene family encodes multi-functional proteins essential for patterning and morphogenesis. Cellular and Molecular Life Sciences. 2013; **70**. doi:10.1007/s00018-013-1285-5.
117 Rocca-Serra P, Brazma A, Parkinson H, Sarkans U, Shojatalab M, Contrino S *et al.* ArrayExpress: A public database of gene expression data at EBI. *C R Biol* 2003; **326**. doi:10.1016/j.crvi.2003.09.026.
118 Sarkans U, Füllgrabe A, Ali A, Athar A, Behrangi E, Diaz N *et al.* From ArrayExpress to BioStudies. *Nucleic Acids Res* 2021; **49**. doi:10.1093/nar/gkaa1062.
119 Barrett T, Wilhite SE, Ledoux P, Evangelista C, Kim IF, Tomashevsky M *et al.* NCBI GEO: Archive for functional genomics data sets - Update. *Nucleic Acids Res* 2013; **41**. doi:10.1093/nar/gks1193.
120 Kim D, Paggi JM, Park C, Bennett C, Salzberg SL. Graph-based genome alignment and genotyping with HISAT2 and HISAT-genotype. *Nat Biotechnol* 2019; **37**. doi:10.1038/s41587-019-0201-4.
121 Trapnell C, Williams BA, Pertea G, Mortazavi A, Kwan G, Van Baren MJ *et al.* Transcript assembly and quantification by RNA-Seq reveals unannotated transcripts and isoform switching during cell differentiation. *Nat Biotechnol* 2010; **28**: 511–515.
122 Szklarczyk D, Franceschini A, Wyder S, Forslund K, Heller D, Huerta-Cepas J *et al.* STRING v10: Protein-protein interaction networks, integrated over the tree of life. *Nucleic Acids Res* 2015; **43**. doi:10.1093/nar/gku1003.
123 Dennis G, Sherman BT, Hosack DA, Yang J, Gao W, Lane HC *et al.* DAVID: Database for Annotation, Visualization, and Integrated Discovery. *Genome Biol* 2003; **4**. doi:10.1186/gb-2003-4-9-r60.

Acknowledgements

This work was supported by the Department of Science and Technology/ Science and Engineering Research Board (DST/SERB) (ECR/2017/001216), Indian Council of Medical Research (ICMR) (2019-3008/SCR/ADHOC/BMS) and the Council of Scientific & Industrial Research (CSIR) (09/1108(13739)/2022-EMR-1), New Delhi, India.

J.A. acknowledges the medical faculty of Heinrich Heine University for financial support.

Authors' contributions

SA.S, D.A.S. designed the study with SM.S, performed the experiments, analysed, and interpreted data. SA.S processed the RNA sequencing data. S.R.V gifted the iPSCs. SA.S and D.A.S. wrote the manuscript and composed the figures. A.I.P, R.B, J.A and SM.S reviewed and edited the

manuscript. SM.S conceptualised and supervised the work, acquired funding. SM.S and J.A: final approval of the manuscript.

Competing interests

The authors declare that they have no competing interests.

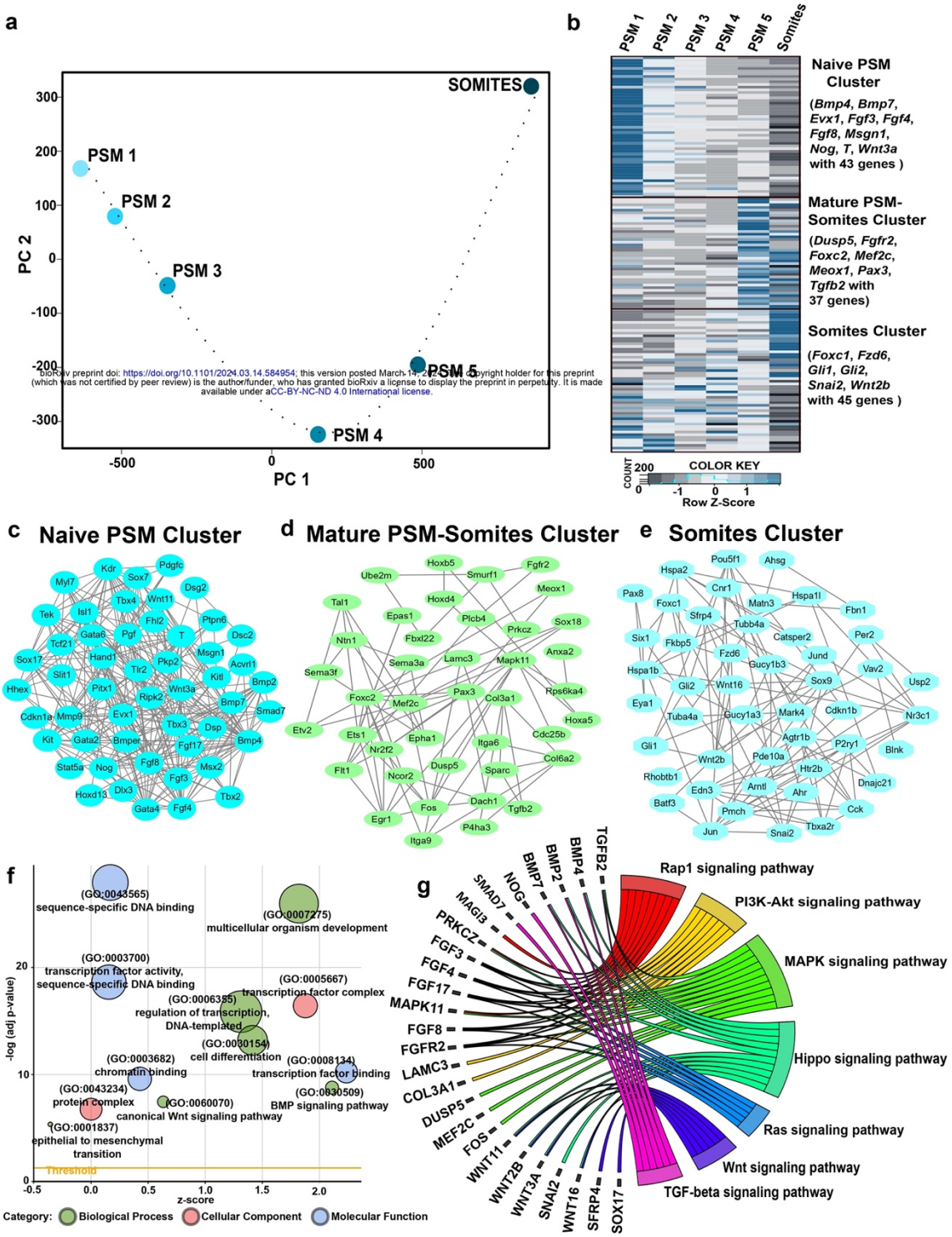

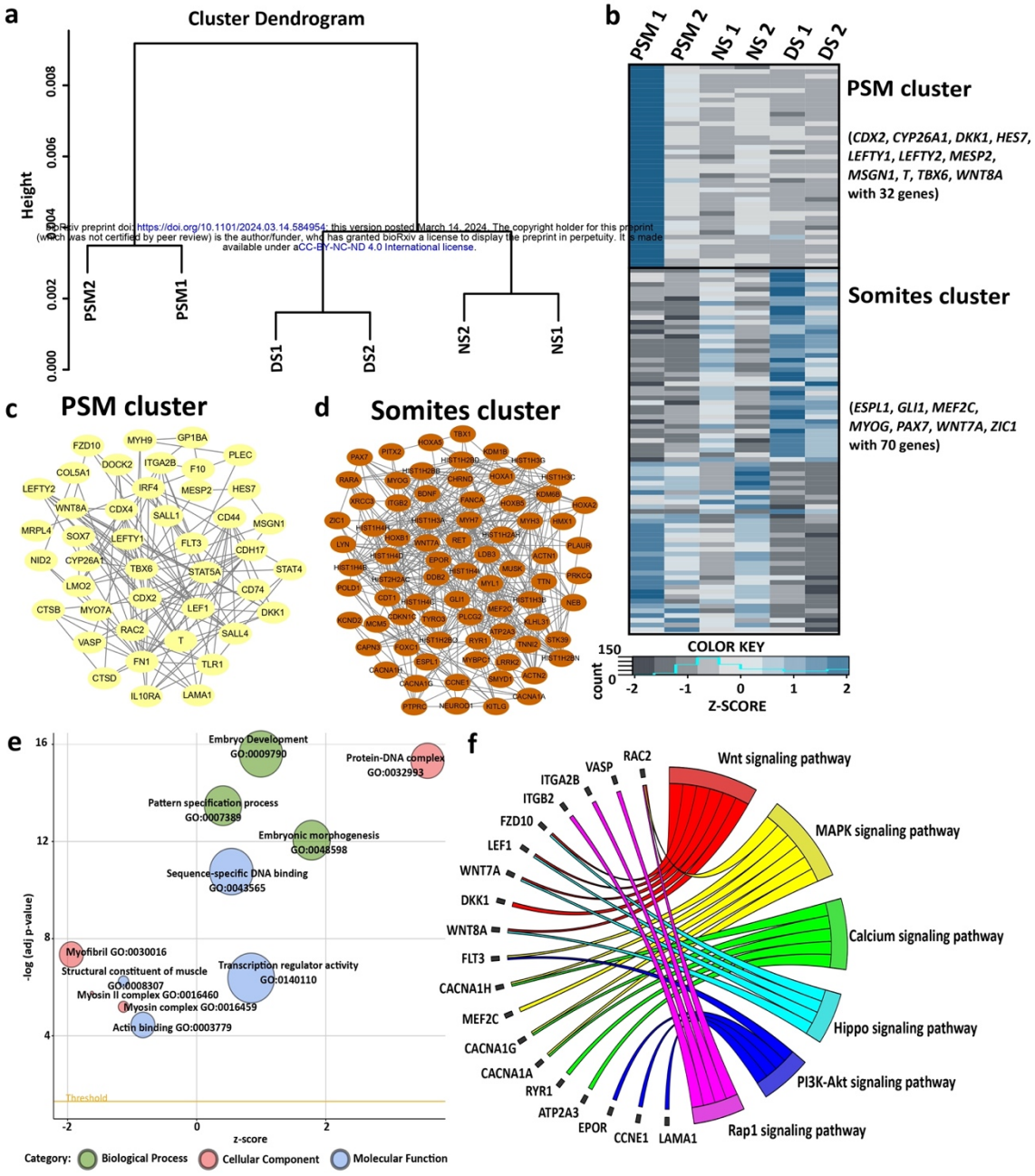

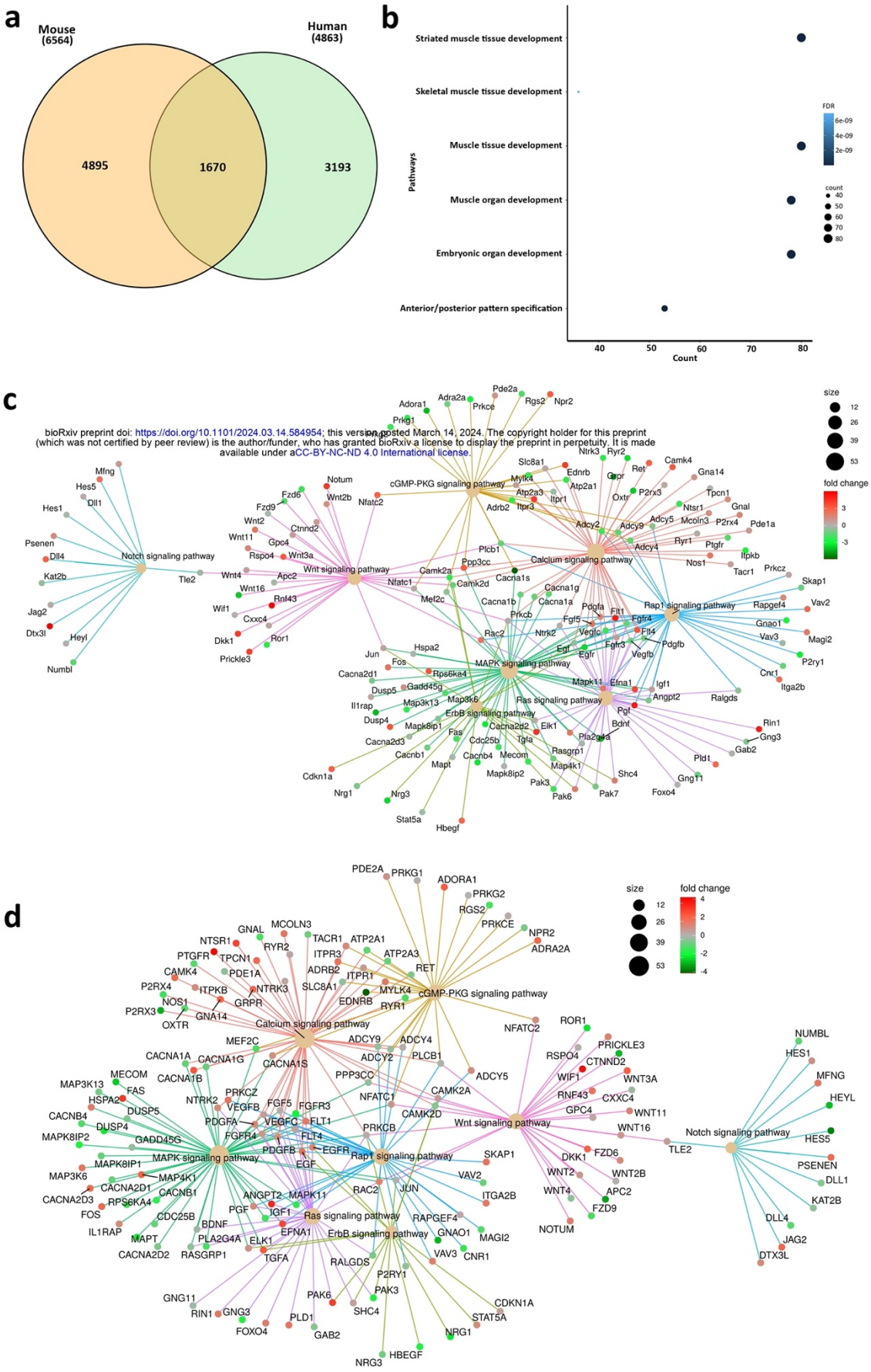

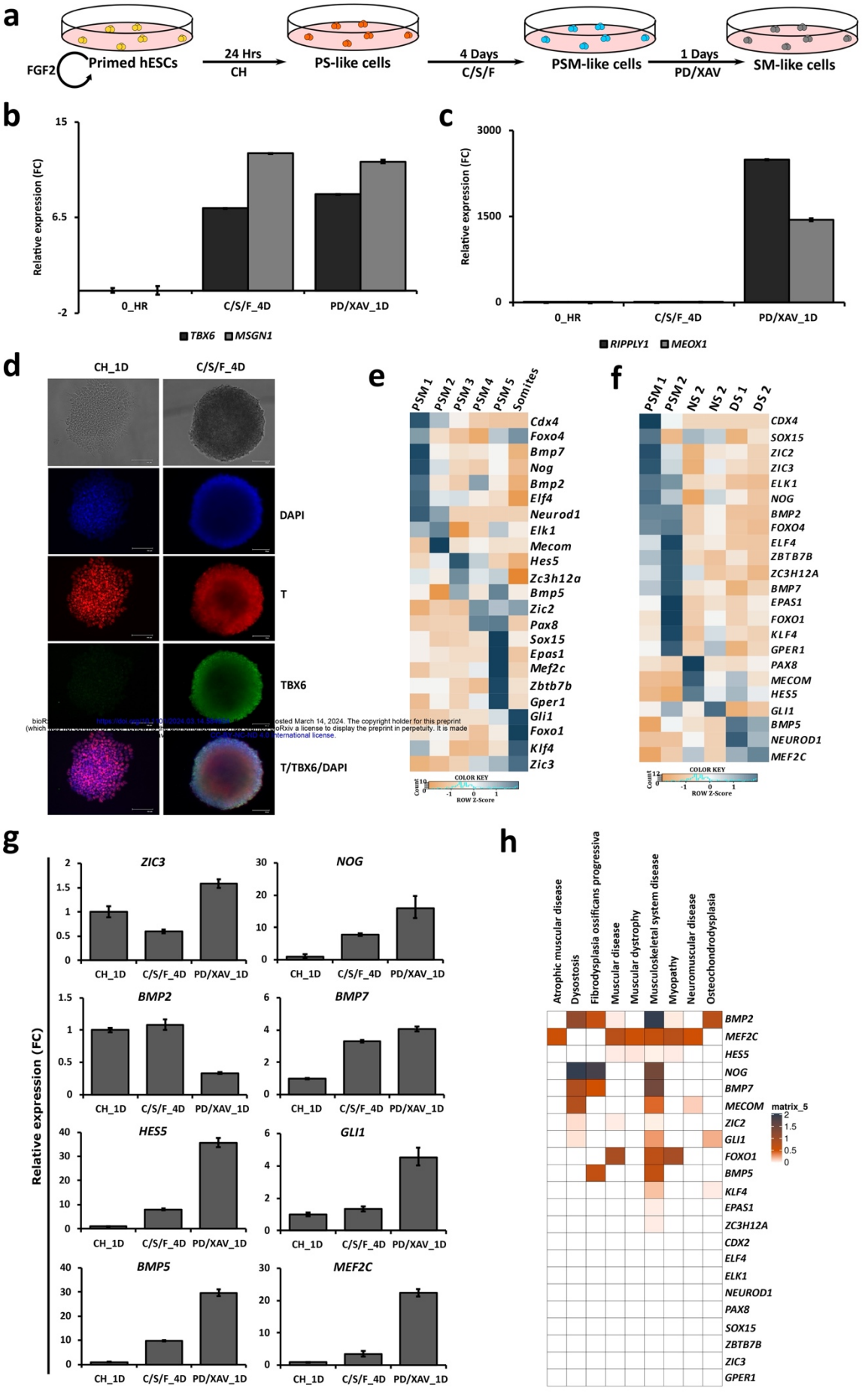
a
FGF2
Primed hESCs
24 Hrs
CH
PS-like cells
4 Days
C/S/F
PSM-like cells
1 Days
PD/XAV
SM-like cells
b
Relative expression (FC)
TBX6
MSGN1
0_HR
C/S/F_4D
PD/XAV_1D
c
Relative expression (FC)
RIPPLY1
MEOX1
d
CH_1D
C/S/F_4D
DAPI
T
TBX6
T/TBX6/DAPI
e
PSM1
PSM2
PSM3
PSM4
PSM5
Somites
Cdx4
Foxo4
Bmp7
Nog
Bmp2
Elf4
Neurod1
Elk1
Mecom
Hes5
Zc3h12a
Bmp5
Zic2
Pax8
Sox15
Epas1
Mef2c
Zbtb7b
Gper1
Gli1
Foxo1
Klf4
Zic3
COLOR KEY
ROW Z-Score
f
PSM1
PSM2
NS2
NS2
DS1
DS2
CDX4
SOX15
ZIC2
ZIC3
ELK1
NOG
BMP2
FOXO4
ELF4
ZBTB7B
ZC3H12A
BMP7
EPAS1
FOXO1
KLF4
GPER1
PAX8
MECOM
HES5
GLI1
BMP5
NEUROD1
MEF2C
COLOR KEY
ROW Z-Score
g
Relative expression (FC)
ZIC3
NOG
BMP2
BMP7
HES5
GLI1
BMP5
MEF2C
CH_1D
C/S/F_4D
PD/XAV_1D
h
Atrophic muscular disease
Dysostosis
Fibrodysplasia ossificans progressiva
Muscular disease
Muscular dystrophy
Musculoskeletal system disease
Myopathy
Neuromuscular disease
Osteochondrodysplasia
BMP2
MEF2C
HES5
NOG
BMP7
MECOM
ZIC2
GLI1
FOXO1
BMP5
KLF4
EPAS1
ZC3H12A
CDX2
ELF4
ELK1
NEUROD1
PAX8
SOX15
ZBTB7B
ZIC3
GPER1
matrix_5

Statutory Declaration

Ich, Abida Islam Pranty, versichere an Eides Statt, dass die Dissertation von mir selbständig und ohne unzulässige fremde Hilfe unter Beachtung der „Grundsätze zur Sicherung guter wissenschaftlicher Praxis an der Heinrich-Heine-Universität Düsseldorf“ erstellt worden ist.

Diese Arbeit wurde noch nicht in gleicher oder ähnlicher Form bei einer Prüfungsstelle eingereicht und ist ebenso nicht veröffentlicht worden. Die Dissertation wurde ebenfalls nicht, auch nicht auszugsweise, in einer anderen Prüfung oder als Studienleistung verwendet.

Ort, Datum: ..... Unterschrift: .....

Abida Islam Pranty